Duke Power Company
Oconee Nuclear Station

Reactor Vessel
Pressurized Thermal Shock Evaluation

January 1982

DPC-RS-1001

DUKE POWER COMPANY

OCONEE NUCLEAR STATION

Reactor Vessel

Pressurized Thermal Shock Evaluation

January 1982

DPC-RS-1001

Duke Power Company
Oconee Nuclear Station

Reactor Vessel
Pressurized Thermal Shock Evaluation

TABLE OF CONTENTS

TABLE OF CONTENTS (cont'd)

TABLE OF CONTENTS (cont'd)

TABLE OF CONTENTS (cont'd)

LIST OF TABLES

LIST OF FIGURES

LIST OF FIGURES (cont'd)

LIST OF FIGURES (cont'd)

LIST OF FIGURES (cont'd)

1.0 INTRODUCTION

1.0 INTRODUCTION

1.1 Background

The ability of the reactor pressure vessel to maintain its integrity is an important factor in ensuring the safety of the primary system in light water reactors. The beltline region of the reactor vessel is most the critical region of the vessel because it is exposed to neutron irradiation. The general effects of fast neutron irradiation on the mechanical properties of such low-alloy ferritic steels as SA302B, Code Case 1339, used in the fabrication of the Oconee 1 reactor vessel are well characterized and documented in the literature. The low-alloy ferritic steels used in the beltline region of reactor vessels exhibit an increase in ultimate and yield strength properties with a corresponding decrease in ductility after irradiation. In reactor pressure vessel steels, the most significant mechanical property change is the reduction in toughness which decreases the margin to fracture accompanied by a reduction in the upper shelf impact strength.

Appendix G to 10 CFR 50, "Fracture Toughness Requirements," specifies minimum fracture toughness requirements for the ferritic materials of the pressure-retaining components of the reactor coolant pressure boundary (RCPB) of water-cooled power reactors and provides specific guidelines for determining the pressure-temperature limitations on operation of the RCPB. The toughness and operational requirements are specified to provide adequate safety margins during any condition of normal operation, including anticipated operational occurrence and system hydrostatic tests, to which the pressure boundary may be subjected over its service lifetime. Although the requirements of Appendix G 10 CFR 50 became effective on August 13, 1973, the requirements are applicable to all boiling and pressurized water-cooled nuclear power reactors, including those under construction or in operation on the effective date.

Appendix H to 10 CFR 50, "Reactor Vessel Materials Surveillance Program Requirements," defines the material surveillance program required to monitor changes in the fracture toughness properties of ferritic materials in the reactor vessel beltline region of water-cooled reactors resulting from exposure to neutron irradiation and the thermal environment. Fracture toughness test data are obtained from material specimens withdrawn periodically from the reactor vessel. These data will permit determination of the conditions under which the vessel can be operated with adequate safety margins against fracture throughout its service life. Allowable pressure-temperature limits are established for normal heatup, cooldown, and hydrostatic test. These are vessel specific and included in the Oconee Technical Specification as a limiting condition for operation.

In 1977, Duke, in cooperation with B&W, and the owners of other B&W 177 fuel assembly plants, implemented an integrated reactor vessel materials surveillance programs to obtain data on materials used in the construction of the vessels. This program was evaluated by the Staff and approved for implementation by license amendments 50-269/44, 50-270/44, and 50-287/41 dated July 14, 1977. Concurrent with this effort to obtain irradiated materials data, tasks were initiated to address the drop in upper shelf energy, to refine neutron fluence calculations, and to characterize the chemistry of 177-FA reactor vessel beltline weld. An initial report of the results of these efforts, entitled "Irradiated-Induced Reduction in Charpy Upper-Shelf Energy of Reactor Vessel Welds," was submitted for Staff review in March 1981.[1] This program is ongoing with tasks planned into 1995.

During the past two years, concerns over reactor vessel integrity during moderate frequency events have been expressed. One of the required actions following the Three Mile Island, Unit 2, accident in March 1979, was the evaluation of reactor vessel brittle fracture during recovery from a small break LOCA with extended loss of feedwater. A generic and bounding analysis was performed and submitted to the NRC in January 1981.[2] At the time of the submittal, Duke realized the conservatisms which existed and the need to perform further evaluations using realistic assumptions appropriate to the plant design.

In March 1981, the first of several industry/NRC meetings to discuss the issue of reactor vessel integrity following postulated overcooling transients as well as small break LOCA thermal shock was held. Following this initial meeting, a second meeting was held in April 1981 where the Staff requested specific submittals which were made in May.[3,4] In July and September, the Staff was briefed on our plans to address the issue of pressurized reactor vessel thermal shock and the schedule for completion.

Finally, during July and August 1981, a 10-year inservice inspection was conducted on the Oconee 1 reactor vessel. The results of this examination were submitted to the NRC in December 1981[5] and indicated that the vessel was free of service induced flaw indications. All indications were not only less than the ASME code allowable, but also less than the flaw sizes critical to the thermal shock issue. This examination provides added assurance of the integrity of the Oconee 1 reactor vessel during postulated overcooling transients.

1.2 Investigations

This report provides an extensive evaluation of the pressurized reactor vessel thermal shock concern for several transients as specifically applied to the Oconee 1 reactor vessel. Several engineering disciplines, codes, and programs are required to completely evaluate the concern. To assist in understanding the flow of analytical information among the various engineering disciplines, Figure 1.2-1 is provided. The following paragraphs provide summary discussions which are keyed to sections of the report.

The evaluation of pressurized reactor vessel thermal shock can be broken into five broad engineering areas:

Transient Analysis
Heat Transfer/Mixing
Vessel Materials
Fracture Mechanics
Probabilistic Analysis

The transient analyses are conducted to develop bulk fluid temperature and pressure responses and flow conditions for postulated transients. An important factor to be included in this output for use in heat transfer calculations is the reactor coolant system flow rate. HPI flowrate is also important in the SBLOCA analyses. With these outputs, detailed analyses of mixing in the cold leg and reactor vessel downcomer are conducted and then used, along with RCS flowrate, to calculate the heat removal from the reactor vessel wall. The temperature gradients through the wall are determined for specific locations as a function of time. The materials of the beltline region of the vessel, including the base metal, welds, and heat affected zones are affected to varying degrees by not only temperature, but also the neutron fluence at the specific location. With the materials properties properly established, the fracture mechanics analyses are conducted, the results of which provide the operational limit for the specific vessel. In parallel with these efforts, a probabilistic analysis was conducted to establish the estimated frequency of occurrence of selected postulated transients.

Chapter 2.0 provides information for overcooling transients resulting from postulated secondary system upsets. Chapter 3.0 provides similar the transient analysis for a typical small break LOCA and the supporting justification for the assumptions used.

Chapter 4.0 provides the analysis of fluid mixing in the RCS cold leg and the vessel downcomer under various flow regimes - forced flow, natural circulation flow, and zero loop flow for each of the transients of interest. Chapter 5.0 provides the analysis of the wall film heat transfer coefficient, considering the flow conditions, for each transient of interest. With the heat transfer coefficient and wall surface temperature determined, the temperature gradient is established.

Chapter 6.0 provides the vessel specific material properties that are used in the fracture mechanical analyses. The properties have been obtained through the integrated vessel materials surveillance program alluded to previously. Chapter 7.0 provides the reactor vessel fluence determination for each weld in the vessel beltline region. The fluence

data was obtained and analytical techniques developed through the vessel materials program previously mentioned. With the materials properties and fluence values thus obtained, Chapter 8.0 provides the details of the methods and results of the fracture mechanics analyses for the selected transients. The final analytical section, Chapter 9.0, provides an in-depth analysis of the frequency of postulated event sequences. The objective of this section is to put into perspective the frequency of occurrence of several thermal shock sequences. Chapter 10.0 provides the summary and conclusions of the results of our efforts to date.

FIGURE 1.2--1

PRESSURIZED THERMAL SHOCK ANALYTICAL PROGRAM

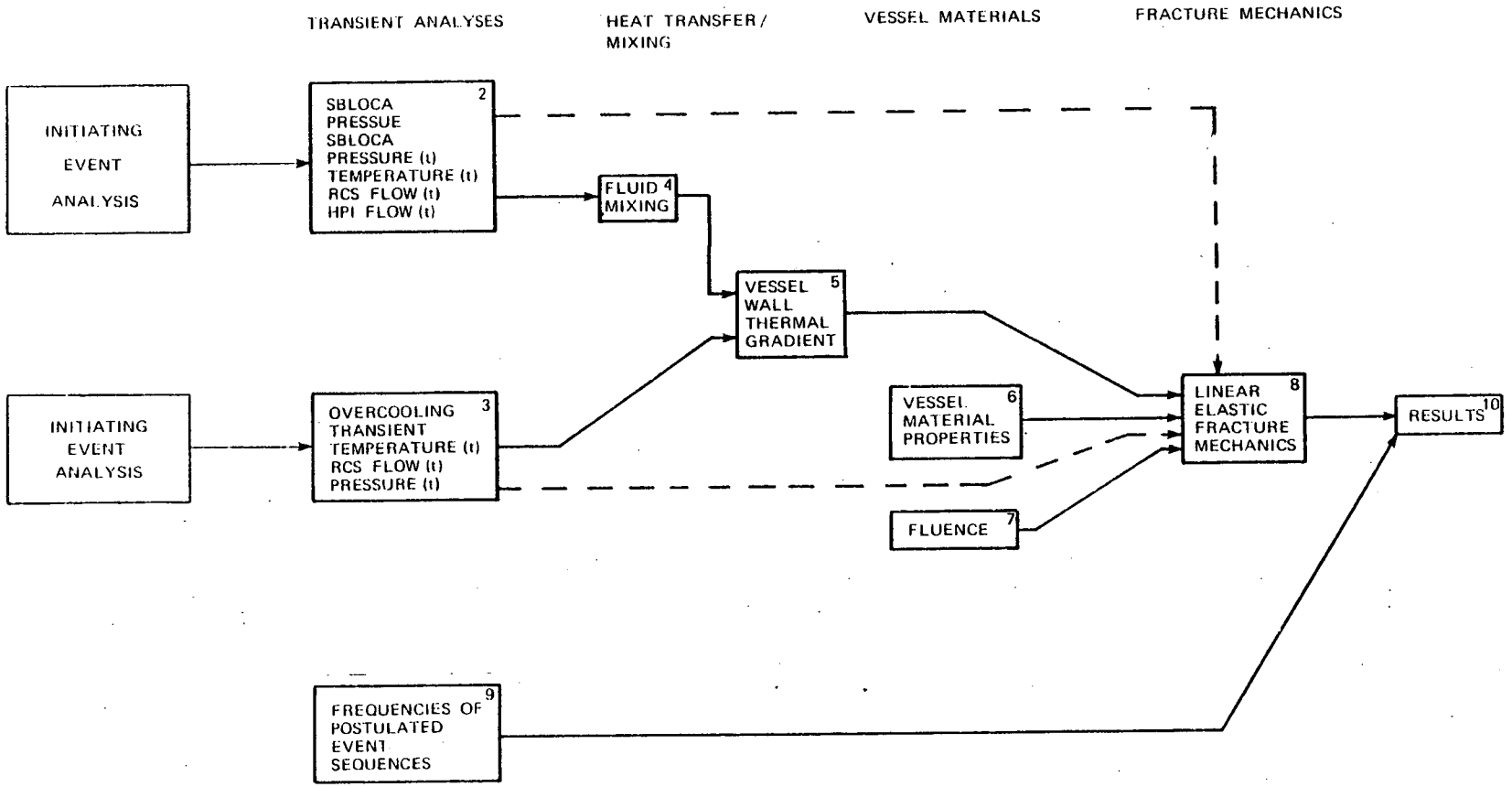

2.0 OVERCOOLING TRANSIENT ANALYSES

2.0 OVERCOOLING TRANSIENT ANALYSES

2.1 Introduction

2.1.1 Overview of Plant Systems

The Oconee Nuclear Station is a three unit 2568 MWt B&W lowered loop design. The Reactor Coolant System (RCS) configuration (Figure 2.1-1) is a two-loop, four cold leg design utilizing the B&W once-through steam generator (OTSG). Plant control is by the Integrated Control System (ICS), which matches reactor power and feedwater flow to the electrical generation demand. Plant transients are mitigated by the Reactor Protective System (RPS) and the Engineered Safety Feature System (ESFS) which, if necessary, actuates the Emergency Core Cooling System (ECCS) for long term core subcriticality and decay heat removal.

The ECCS includes the High Pressure Injection System (HPIS), the passive Core Flood Tank System (CFTS), and the Low Pressure Injection System (LPIS). The HPIS, which also provides reactor coolant pump seal injection and normal makeup and letdown control, consists of three pumps injecting into four cold leg locations (Figure 2.1-2). The HPI pumps are actuated on low RCS pressure at 1500 psig, and have a combined flow rate as shown in Figure 2.1-3. Two of the three pumps are normally aligned to the A loop. The two passive CFT's have a liquid volume of 1010 ft^3 each and inject through two core flood lines to the reactor vessel downcomer. Injection begins when the RCS pressure decreases below the 600 psig nitrogen overpressure in the tank. The LPIS consists of two pumps that are actuated on low RCS pressure at 500 psig and inject through the core flood lines to the reactor vessel downcomer. Although the LPIS is actuated at 500 psig, the pump shutoff head prevents injection until the RCS pressure decreases below 200 psig, so that the LPI is not functional for non-LOCA transients. RCS pressure control is accomplished by the pressurizer spray (200 gpm), the pressurizer heaters (1638 kW), the pressurizer relief valve (1-3/32 inch ID), and two pressurizer safety valves (1-4/5 inch ID).

Feedwater is delivered from the condenser hotwell to the steam generators by three hotwell pumps, three condensate booster pumps, and two turbine-driven main feedwater pumps. A closed secondary cycle of two trains of six stages of feedwater heaters is utilized (Figure 2.1-4). The Emergency Feedwater System (EFWS) consists of two motor-driven and one turbine-driven pump. One motor-driven pump is dedicated to each steam generator and the turbine-driven pump is shared. Steam generator pressure control is performed by the Turbine Bypass System (TBS), which is part of the ICS, and the main steam code safety relief valves. Each steam generator is equipped with two turbine bypass valves with 12.5% total steam relief capacity, and eight safety valves with 58.5% total steam relief capacity.

2.1.2 Overview of Overcooling Transient Scenarios

An overcooling transient is considered to be a sequence of operating events which lead to exceeding the 100°F/hr cooldown rate limit. For non-LOCA transients, this situation can only evolve from an increase in primary to secondary heat transfer, an injection of cold water into the RCS, or a combination of the two events. Primary to secondary heat transfer will increase due to a reduction in steam generator pressure which causes a decrease in secondary temperature, and hence an increase in the primary to secondary ΔT. Primary to secondary heat transfer will also increase due to an increase in feedwater flow or a decrease in feedwater temperature, both of which effectively increase the ΔT and/or increase the overall heat transfer coefficient in the steam generator. An injection of cold water into the RCS can occur by delivery from the HPIS, CFTS, and the LPIS. These systems are most likely to be actuated in the event of a transient which depressurizes the RCS below their respective acutation setpoints. The injection rates will be highest at low RCS backpressures.

2.1.2.1 Based on the above cooldown initiating processes, the plant systems have been evaluated to identify potential overcooling transient precursor events. Steam generator pressure could decrease as a result of the following:

1. A steam system pipe break.
2. Excessive steam flow through the TBS.
3. Excessive steam flow through the main steam code safety relief valves.
4. Excessive auxiliary steam demand (main feedwater pump turbines, EFW pump turbine, condensate steam air ejectors, turbine gland seal steam, etc.).
5. Excessive main feedwater or EFW delivery.

2.1.2.2 Excessive feedwater flow or feedwater temperature reduction could occur as a result of the following:

1. Failure of feedwater control valves.
2. Failure of the ICS to match feedwater flow to reactor power, electrical generation demand, and BTU availability.
3. Loss of feedwater heaters or heater system upset.
4. Failure of the ICS to control steam generator level.
5. Failure of the EFWS to control steam generator level upon actuation of the EFWS.

Based on an assessment of the initiating event and the relative severity of the overcooling, the spectrum of scenarios can be classified into three general categories. The first category is steam generator overfeeds. The second category is TBS failures which include small steam line breaks and steam leaks up to approximately 0.40 ft^2 break area or 25% steam flow. The third category is large steam line breaks, which includes feedwater pipe breaks between the steam generator and the check valve.

2.1.2.3 A description of the normal and expected response of the systems important to overcooling transients is presented in the following paragraphs:

1. Main Feedwater and Condensate Systems - The Main Feedwater System (MFWS) is designed to deliver the correct feedwater flowrate to each steam generator as demanded by the ICS to meet the generated electrical demand. The feedwater demand is cross-limited to reactor power to prevent a mismatch of greater than 5%. Feedwater is limited by the BTU limit which determines the maximum feedwater flow based on RCS flow, hot leg temperature, feedwater temperature, and steam generator pressure. The BTU limit assures sufficient superheating of the generated steam by limiting overfeeding of the steam generators. Feedwater is also limited by the high steam generator level limit to 85% on the operating range level. In addition, if either steam generator reaches 90% level, both MFW pumps trip. Both MFW pumps trip on loss of ICS power as a result of the steam generator level transmitters failing high. A minimum level of 2 ft startup range with reactor coolant pumps on, or 50% operating range with all four reactor coolant pumps tripped is the most downstream feedwater control variable. If all four reactor coolant pumps trip, the ICS transfers main feedwater from the main feedwater header to the auxiliary feedwater header to promote natural circulation. Flow through the auxiliary header is limited by hydraulic losses to much lower flowrates than the normal flowpath. The MFW pumps also trip on low suction pressure at 235 psig. The Condensate System (CS) delivers from the condenser hotwell to the MFWS. The hotwell pumps trip on low hotwell level at 6 inches. Condensate booster pumps trip on low suction pressure at 16 psig, and have a shutoff head of approximately 550 psig.

2. Emergency Feedwater System - The EFW pumps are actuated by MFW pump trip as indicated by low MFW pump discharge pressure at 750 psig or low MFW pump turbine oil pressure.

The EFWS valves do not open and initiate delivery of feedwater until steam generator level decreases below the minimum level setpoints corresponding to reactor coolant pumps on or off. The EFW pumps deliver through the auxiliary feedwater header. The EFWS is safety grade and independent of the ICS.

3. Turbine Bypass System - The TBS normally functions as a steam relief flowpath when steam generator pressure exceeds the turbine header pressure setpoint by +50 psi. Following a reactor trip, the TBS setpoint automatically transfers from +50 psi to +125 psi (1010 psig), and controls steam generator pressure to the setpoint. On loss of ICS power, the TB valves fail closed.

4. High Pressure Injection System - On the low RCS pressure ESFS actuation at 1500 psig, all three HPI pumps are actuated. Full flow continues until operator action occurs.

2.1.2.4 Overcooling transients are identified by alarms and panel indications which alert the operator and clearly identify the symptoms of the transient. Primary system alarms actuated would include:

Reactor trip on turbine trip
Reactor trip on pressure - temperature
Reactor trip on low pressure - 1800 psig
Reactor trip on high flux - 105.5%
Low T-ave - 574°F (579°F)
ΔT-cold mismatch - ±5°F
Low pressure - 2055 psig (2155 psig)
Low-low pressure - 1850 psig
Low pressurizer level - 200 inches (220 inches)
Low-low pressurizer level - 80 inches
High flux - 102%
Rod withdrawal limit - 103%

ESFS actuation - 1500 psig

RCS approaching saturated conditions

Secondary system alarms actuated include:

Turbine trip

Turbine in manual

ICS tracking

Large MW error

Low turbine header pressure - 835 psig (885 psig)

Low MFW pump discharge pressure - 900 psig (1050 psig)

High steam generator level - 82% (60%)

Both MFW pumps trip

Feedwater error cross limit

BTU limit

Nominal operating conditions are indicated in parentheses.

Based on these alarms and the available instrumentation, the operator would respond as directed by training and procedures. Current procedures require the reactor coolant pumps to be tripped on low RCS pressure ESFS actuation at 1500 psig, as a mitigative operator action for SBLOCA. For severe overcooling transients, the initial transient response is dominated by a rapid depressurization of the RCS, which is similar to the SBLOCA response. Since both transients respond similarly in the initial phase, the operator will immediately trip the reactor coolant pumps on ESFS actuation for overcooling transients. In the procedures, overcooling transients (steam supply system rupture) are identified by symptoms of rapidly decreasing steam generator pressure, RCS cold leg temperatures, RCS pressure, and possible automatic initiation of HPI. If the operator determines that an overcooling transient, rather than a SBLOCA, has occurred, his immediate instructions are to isolate feedwater to the affected steam generator. Engineered safety features (i.e., HPIS) are not to be overridden unless continued operation will result in unsafe plant conditions or will threaten vessel integrity. The

pressure-temperature curve (Figure 2.1-5) is referenced to assess the acceptable operating conditions. Subsequent operator actions are to assure that the unaffected steam generator is controlling at the natural circulation setpoint, and that the RCS is 50°F subcooled on the Subcooled Margin Monitor. Once the RCS is 50°F subcooled, one reactor coolant pump in each loop is to be restarted. The HPI pumps are to remain in operation until either:

1. Both LPI pumps are in operation and have been delivering >1000 gpm each for at least 20 minutes.

2. All hot and cold leg temperatures are at least 50°F subcooled. The degree of subcooling is to be limited by the pressure-temperature curve (Figure 2.1-5).

3. Operator action must be taken to prevent an unsafe condition.

2.1.2.5 The previous paragraphs have identified the types of overcooling transients which can be initiated in an Oconee type plant, and also discuss the normal and expected response of the systems important to an overcooling event. The operator will be alerted by a sequence of alarms from which the source of the overcooling can be identified and will result in appropriate operator actions as specified in the plant procedures. These procedures specify immediate isolation of the overcooling source, and tripping of all reactor coolant pumps on low RCS pressure ESFS actuation. One reactor coolant pump in each loop will be restarted when a 50°F subcooled margin has been attained. The HPIS will not be throttled until the 50°F subcooled margin has been attained, and then only when long term cooling has been established, or to prevent an unsafe system condition. The pressure-temperature cooldown limit curve provides guidance to the operator to prevent thermal shock of the reactor vessel.

2.2 Overcooling Transient Experience

A detailed review of the operating history of Oconee has resulted in the identification of events which have resulted in exceeding the cooldown rate limit of 100°F/hr, as well as identifying those events which could have led to exceeding the cooldown rate limit if not mitigated by automatic plant controls and protective functions, or operator action. A review of the operating history of other B&W plants was not undertaken due to the plant specific nature of overcooling transients, although the types of transients experienced are expected to have been similar. An evaluation of the applicability of the Rancho Seco event of March 20, 1978 to Oconee is included. For the purposes of this report, a normal and controlled cooldown which slightly exceeded the 100°F/hr limit is not considered to be of interest.

Event 1: Unit 1 - May 5, 1973

This event occurred during pre-commercial testing and includes several system responses and operator actions which are atypical of current operation. From an initial power level of 18%, a CS upset resulted in a trip of both MFW pumps. A manual trip of the reactor followed at 30 seconds. The TBS on SG A was in manual due to controller problems and SG B was in automatic pressure control. Since TB valves on SG A remained partially open following reactor trip on loss of feedwater, SG A essentially boiled dry. Both SG pressures decreased to 700 psig. The EFW pump (only one turbine-driven pump at this time) was not in automatic control and did not start. Three minutes after trip the MFWS was manually restored and an overfeed of both SG's occurred. The combination of low SG pressure and overfeed, along with a low decay heat level, resulted in a minimum RCS pressure of 1330 psig, and a minimum temperature of approximately 500°F. The normal post-trip temperature is 550°F. System conditions stabilized within 15 minutes.

Event 2: Unit 2 - January 4, 1974

A loss of offsite power from an initial power level of 75% resulted in a reactor trip, RC pump trip, and MFW pump trip. The EFW pump (one turbine-driven pump) initiated fill of the SG's to 95% SG level as originally designed for natural circulation. An auxiliary steam demand of 80,000 lb/hr was being supplied to the auxiliary steam header. These conditions caused reductions in T-cold(A) from 562°F to 422°F, and T-cold(B) from 562°F to 426.5°F in the first hour. These are cooldown rates of 140°F/hr and 135.5°F/hr respectively. This transient was the first operational occurrence of natural circulation in a B&W plant. The excessive cooldown rates necessitated a reduction in the natural circulation setpoint from 95% to 50% on the steam generator level operating range.

Event 3: Unit 2 - July 11, 1974

A loss of ICS power from an initial power level of 80% resulted in a reactor trip and a loss of normal feedwater control whereby feedwater was delivered through both the main and auxiliary feedwater headers. In addition, the pressurizer relief valve apparently failed open on the loss of ICS power. This is not the current failure mode, which is to fail closed on loss of ICS power. Approximately 20 to 30 seconds following trip, the system had depressurized to 1550 psig and the HPIS was actuated. ICS power was manually restored in 30 to 45 seconds and the system returned to normal pressure within 3 to 4 minutes. The minimum RCS temperature was 515°F, and the minimum pressure 1450 psig.

Event 4: Unit 2 - September 10, 1974

From an initial power level of 80%, a partial failure of the turbine header pressure signal to the ICS caused the TB valves on SG A to fail open. The ICS responded to the reduction in electrical generation by withdrawing rods to meet the megawatt demand. The operator was alerted to the situation and, after identifying that the TB

valves were functioning incorrectly, manually isolated the valves. The faulty electronic component was replaced and the TBS returned to normal. A slight reduction in T-ave resulted which contributed to a small increase in reactor power. The unit remained on line.

Event 5: Unit 2 - September 17, 1974

Following a reactor trip from 100% power, the ICS did not successfully runback feedwater. The moderate overfeed resulted in a high SG level trip of both MFW pumps at 220 seconds. The EFW pump (one turbine-driven pump) was actuated. The transient resulted in a minimum RCS temperature of 547°F, and a minimum pressure of 1700 psig.

Event 6: Unit 2 - March 7, 1975

At an initial power level of 15%, feedwater control began the normal switch from the startup control valve to the main control valve. As the B main block valve opened, an overfeed of SG B occurred which was terminated by the high SG level trip of the MFW pump. RCS pressure decreased to 1925 psig, at which time the operator manually tripped the reactor. The subsequent investigation identified that the MFW control valve B was stuck open. The valve was repaired. The RCS temperature decreased only slightly.

Event 7: Unit 3 - April 30, 1975

During a loss of load test from 100% power, the ICS runback of main feedwater was too slow and resulted in a high SG level trip of both MFW pumps. In addition, one main steam code safety valve did not reseat until 850 psig (normal reseat pressure 1000 psig). RCS pressure decreased to 1575 psig, and a minimum temperature of 540°F resulted.

Event 8: Unit 3 - May 25, 1975

From an initial power level of 100%, a blown fuse in the power supply to a solenoid valve on the air supply to the TB valves on SG A resulted in the valves failing open. The ICS responded by increasing feedwater flow and withdrawing rods. The reduction in T-ave resulted in an increase in reactor power, and a trip on high flux occurred. The turbine bypass valves were isolated at approximately 20-25 minutes following trip. Pressurizer level decreased to 25 inches, and the resulting minimum temperature was 485°F.

Event 9: Unit 3 - June 13, 1975

During a normal shutdown from 100% power, an RCS pressure spike occurred at 19% power due to manual pressure control of the SG's. The pressurizer relief valve opened at 2267 psig and failed to reseat. The reactor tripped on low RCS pressure 80 seconds later. HPI was actuated on low RCS pressure at 1500 psig 209 seconds after the relief valve failed, the block valve was manually closed 25 minutes following relief valve failure, and the RCS pressure bottomed out at 720 psig. The transient was under control 28 minutes after relief valve failure with the RCS temperature at 510°F. A normal cooldown then followed.

Event 10: Unit 3 - July 13, 1975

From an initial power level of 80%, a transistor failure in the TBS caused the TB valves on SG B to fail open. The ICS responded by withdrawing rods. Reactor power increased in response to the rod motion and the decrease in T-ave. The operator promptly identified the open TB valves and manually isolated them. The unit remained on line.

Event 11: Unit 1 - August 14, 1976

During three pump operation at 75% power, an asymmetric rod position alarm initiated a runback to 60% power. Soon afterward, control rod group 6 dropped into the core due to a rod drive problem. The operator assumed manual control of feedwater during the ensuing power increase. Difficulty with feedwater in manual control resulted in an overfeed of SG A, and tripped the MFW pumps and the turbine. The reactor subsequently tripped on high pressure. No cooldown occurred.

Event 12: Unit 1 - December 14, 1978

From an initial power level of 98%, a short in the ICS T-ave recorder incorrectly transmitted a low T-ave signal resulting in rod withdrawal. The operator noticed power increasing and assumed manual rod control. With T-ave control by rods defeated, the ICS transferred T-ave control to the MFWS which resulted in a reduction in feedwater flow. The operator recognized T-hot increasing with decreasing feedwater flow and assumed manual control of feedwater. The reactor tripped on high temperature. Feedwater was increased rapidly, and the resulting high discharge pressure tripped both pumps. The EFW pump (one turbine-driven pump) was actuated 7 seconds later, and was stopped 21 seconds later when the MFW pumps were reset and started. SG levels continued to decrease until SG A reached 6 inches and SG B boiled dry. Recognizing the loss of SG level, the operators proceeded to feed both SG's through the auxiliary headers, and restored SG A to 80 inches and SG B to 30 inches. The EFW pump was started to help feed SG B. In response to the refilling of the SG's, RCS pressure rapidly decreased resulting in HPIS actuation and a minimum pressure of 1450 psig. Both MFW pumps then tripped on low vacuum, and the EFW pump was then aligned to feed both SG's. RCS temperature reached a minimum of 500°F.

Event 13: Unit 3 - November 10, 1979

From an initial power level of 99%, a false signal tripped the hotwell pumps which tripped one of the three condensate booster pumps. This initiated a reactor runback on low feedwater flow. The runback was unsuccessful, and the reactor tripped on high pressure at 55 seconds. A loss of ICS power occurred at 115 seconds . This resulted in a trip of both MFW pumps, and actuation of all three EFW pumps. The loss of ICS power caused an extensive loss of instrumentation. RCS wide range pressure was unaffected. All three HPI pumps were put in operation. ICS powered was restored at 223 seconds. At that time RCS pressure was 1675 psig and increasing, and pressurizer level was 20 inches and increasing. The RCS temperature was 525°F. On restoration of ICS power, the TB valves partially opened. Auxiliary steam was being supplied from this unit at that time. Both SG's were near boiled dry conditions. Approximately 10 minutes after transient initiation, the level in SG B increased abruptly following startup of one hotwell pump and one booster pump. SG pressure was 400 psig. As a result of these steam generator conditions, the RCS temperature decreased to 420°F in 20 minutes. This is a cooldown of 115°F, which exceeds the cooldown limit of 100°F/hr. At 31 minutes following transient initiation, the auxiliary steam flowpath and the TB valves were isolated. A return to hot shutdown conditions proceeded normally.

Event 14: Unit 2 - January 30, 1980

Following a reactor trip from 89% power, the operator recognized that the ICS was not decreasing feedwater flow rapidly enough, as indicated by SG level. Although manual control of feedwater was attempted, a high SG level trip of both MFW pumps occurred. The RCS temperature decreased to 540°F.

Event 15: Unit 3 - March 14, 1980

Following a reactor trip from 100% power, the ICS failed to runback feedwater as designed due to a wiring problem and calibration

error. The subsequent overfeed of SG A tripped both MFW pumps on high SG level. The RCS temperature decreased to 546°F.

Event 16: Unit 1 - May 4, 1981

From an initial power level of 100%, the SG A pressure input to the ICS drifted high causing the TB valves on SG A to open. The resulting steam leak caused a 12.5% decrease in electrical generation. The ICS responded by withdrawing rods until inhibited by high flux at 103% power. The unit remained on line. RCS temperature decreased by 4°F.

A summary of the sixteen events detailed above is given in Table 2.2-1. The operating history includes a variety of initiating failures which resulted in the potential for overcooling by two mechanisms, SG overfeed and TBS failures. No steam line breaks have been experienced. In the 23 years of accumulated operating experience, a total of 186 reactor trips have occurred as of August 1981. Following each trip not initiated by a loss of feedwater, the ICS initiated a main feedwater runback, nine of which were not successful, due to a slow runback or a failure to maintain the runback, which subsequently resulted in an overfeed of one or both SG's at a reduced flow rate. All nine overfeed events were successfully terminated by the high SG level trip of both MFW pumps, and in all cases the resulting RCS cooldown was insignificant. The one EFW overfeed occurred due to the original SG level setpoint for natural circulation which, as a result of the event, has since been reduced. Two events had potential for overcooling due to a loss of inventory through the pressurizer relief valve. Of the six TBS failure events, there were no instances where the TB valves on both SG's failed full open. If all four valves were open, it was a result of the operator manually throttling the valves to a partially open position. Three of the six TBS failures, each of which was a complete failure of both valves on one SG, did not even result in a reactor trip due to automatic ICS response and operator action. Failure of a main steam code safety relief valve to reseat contributed only minimally to one event when the reseat occurred 150 psig below the normal reseat pressure. In almost all events operator response was very

prompt and appropriate. In the remaining events operator response was sufficiently prompt to prevent an excessive cooldown. Operator error was infrequent and not severe.

Of the sixteen events only two exceeded the 100°F/hr cooldown limit. Both events are precluded in the future by implemented design changes. Event 2 (140°F/hr) resulted in a reduction of the SG level setpoint for natural circulation. The likelihood of Event 13 (115°F/hr) recurring is very low due to the upgrade in ICS power supplies, increased operator awareness as a result of operating experience and review of similar events, and the development of an emergency procedure specific to the event.

Based on a review of the Rancho Seco transient of March 20, 1978, it can be concluded that an overcooling event of this type has an extremely low probability of occurrence at Oconee. This assessment results from the recognition that several key system responses which caused the overcooling were plant specific to Rancho Seco. These responses will not occur at Oconee. The key Rancho Seco specific features which existed at the time of event were as follows:

1. Auxiliary feedwater controlled by the ICS.
2. Auxiliary feedwater bypass valves go to full open position on low RCS pressure ESFS actuation.
3. No high SG level trip of the MFW pumps.

The following Oconee specific features preclude a transient such as the Rancho Seco event:

1. EFWS is safety grade and independent of the ICS.
2. High SG level of trip of MFW pumps.
3. Highly reliable ICS power supplies.
4. Redundant computer display groups for monitoring RCS conditions.

5. Subcooled Margin Monitor.
6. Emergency procedure for loss of ICS power.
7. Operating experience gained promotes prompt and positive operator action.

A detailed review of the operating history at Oconee shows that there does not exist a record of severe or frequent overcooling events. The existing mitigating equipment and systems design, some of which include modifications which have been implemented as a result of operating experience, sufficiently mitigate the frequency and the severity of those overcooling events which have a reasonable probability of occurrence. Transients similar to the Rancho Seco event are precluded from occurrence by plant specific Oconee features.

2.3 Plant Features and Evaluations Concerning Overcooling Transients

Based on the types of overcooling transients which potentially can occur and the history of overcooling transients or precursors which have occurred, several plant modifications have been implemented. In addition, several plant features not specifically designed to mitigate overcooling do in fact help perform that function. Evaluations have also been performed to identify precursor events and to provide operator guidance for dealing with overcooling events.

The plant features which aid in the mitigation of overcooling transients include:

1. High steam generator level trip of both MFW pumps.
2. Reduction in the steam generator level setpoint for natural circulation from 95% to 50% on the operating range.
3. Upgraded the redundancy of ICS power supplies to reduce the likelihood of off-normal control system responses and incorrect instrumentation indications.
4. Safety grade EFWS and control.

5. Subcooled Margin Monitor to provide additional information on RCS conditions.
6. Upgraded control room instrumentation displays for monitoring key system parameters.

The transient performance of the ICS assuming failures in ICS inputs, and outputs and functions has been a concern for overcooling transients. This concern has been addressed in the B&W topical report, "Integrated Control System Reliability Analysis," BAW-1564. This report is a thorough failure modes and effects analysis of the ICS. It identifies the potential overcooling event precursors within the ICS and the trends of the RCS response to the assumed failure.

2.4 Overcooling Transient Analyses

2.4.1 Selection of Overcooling Transients

In order to perform a comprehensive evaluation of potential overcooling transient scenarios, a set of thirteen cases were selected for detailed thermal hydraulic simulations. This set consists of three SG overfeed transients, seven TBS failure initiated transients, and three steam line break transients. It is obvious that an infinite number of scenarios can be constructed from different combinations of assumptions of the initiating event, systems response, equipment availability, and operator action. The cases selected are considered to be bounding based on the assumptions incorporated into each analysis. The expected system responses for similar cases have been compared to identify what assumptions lead to a bounding analysis. The cases selected are much more severe than any transients experienced to date, and based on current plant specific features and normal operator actions as specified in plant procedures, are expected to be much more severe than any transients which might potentially occur in the future.

The assumptions made in the analyses regarding system and component performance were selected with the intent of maximizing the cooldown rate and the repressurization rate of the RCS. These conditions will result

in maximizing the potential effect of thermal shock. The assumptions are also required to be realistic and within the physical limits of the systems and components. Parameters with some apparent uncertainty were conservatively selected. This approach has resulted in analyses which are realistic for the analytical assumptions utilized, but are conservative and bounding with respect to thermal shock due to the conservatism of the system assumptions.

The response of the operator is a key consideration for overcooling transients. Prompt positive operator action can successfully mitigate all credible overcooling transients. Consistent with the approach of performing realistic simulations based on conservative assumptions, the role of the operator in each transient case has been thoroughly evaluated. Operator action assumed in these analyses are those which are required by the existing procedures and which are consistent with the conventional actions for mitigating the transient. Furthermore, operator action was not assumed to occur unless necessary and reasonable for each specific transient. No credit was taken in any analysis for the operator throttling the HPIS, although all overcooling transients evolve into a normal RCS refill phase where pressurizer level is normally recovered and the RCS has a more than adequate subcooling margin. Current procedures require the operator to promptly trip all reactor coolant pumps on low RCS pressure ESFS actuation. For those transients where this action might occur, cases with and without pump trip were analyzed. For all transients except steam line breaks, no operator action is assumed for 20 minutes with the exception of a possible reactor coolant pump trip. For all steam line breaks, the operator is assumed to isolate all feedwater to the affected SG at 5 minutes. For steam line breaks that included a reactor coolant pump trip, the operator is assumed to restart one pump in each loop on the basis of the recovery of the subcooling margin as required by procedures.

2.4.2 Simulation Model

The overcooling transients were simulated using the RETRAN-Ø2MODØØ1 code developed by EPRI. The code is related to the RELAP4 family of codes and includes many models specifically intended for versatile and

realistic simulation of operational transients in PWR's. The nodalization used for the overcooling simulations is shown in Figure 2.4-1. For transients with loop symmetry a model collapsed to one loop was utilized. Similar plant models have been benchmarked by comparison with actual Oconee plant transient data. The effect of control system responses pertinent to each transient case were included. A non-equilibrium pressurizer (PZR) is used to conservatively predict the repressurization of the system during refill. All interfacing systems, HPIS, CFTS, MFWS, EFWS, CS, TBS, etc., have been modeled using expected plant specific system performance. The analyses required calculation of the MFW temperature following reactor trip as a function of integrated flowrate. The simulation model includes the MFW piping from the MFW control valve to the SG. A calculation of the feedwater temperature from the hotwell to the control valve was undertaken. The feedwater volume between the MFW pumps and the control valve was calculated by geometry. The balance of the inventory between the hotwell and the MFW pumps remained. One half of this volume was assumed to be at the hotwell temperature, and the other half at a linear gradient to the temperature at the MFW pump. This is a very conservative method of representing the MFW temperature reduction following trip, since no credit is taken for energy stored in the feedwater heaters. The resulting total integrated flow - enthalpy table is as follows:

lbs	h
0	441.72
44,000	441.72
79,400	388.15
101,500	388.15
130,000	348.26
232,000	348.26
584,000	60.76

EFW is delivered through the upper auxiliary header. The RETRAN nodalization used cannot handle injecting cold water into a steam filled space, so that EFW is injected into the SG downcomer in the simulation until the SG is flooded by the overfeed. At that time the code switches EFW to the proper geometric elevation. This is conservative since injecting into the downcomer forces the EFW to flow up the full length of the SG tubes, which maximizes heat removal from the RCS. Operator actions are detailed for each case. If the transient initiates at power, a reactor trip at time zero is assumed to minimize the core power generated. Reactor kinetic feedback resulting from the Doppler and moderator coefficients of reactivity was not assumed in order to prevent core heat addition from a return to power condition. Structural metal has been accounted for. Unless specified otherwise, no decay heat is assumed. If decay heat is assumed, a multiplier of 0.5 is applied to the ANS standard. Each case was simulated a minimum of 10 minutes transient time, with the bounding cases run out from 15 to 40 minutes, depending on when the long term trends of the transient were established.

2.4.3 Steam Generator Overfeed Simulation Results

Case 1: Following a reactor trip from full power, the ICS fails to runback MFW and full feedwater flow continues. A high SG level trip of both MFW pumps occurs and actuates the EFW pumps. EFWS level control fails and full EFW flow continues. No operator action, no decay heat, and maximum HPI.

Sequence of Events

Time (sec)	Event Description
0	Reactor trip with ICS failure to runback MFW, full feedwater flow continues.
4	PZR heaters on.
20	PZR heaters isolated on low PZR level.
36	High SG level trip of both MFW pumps.
46	EFWS activates.
140	Loss of PZR level indication.
248	PZR empties for 5 seconds.
250	HPIS actuates (1500 psig).
254	Minimum RCS pressure (1498 psig)
407	PZR level indication regained.
576	SG water solid.
841	PZR heaters on.
871	RCS pressure regained (2155 psig)
884	PZR heaters off.
905	PZR spray begins cycling (2205 psig).
1200	Reactor vessel minimum inlet temperature (424°F).

The minimum reactor vessel downcomer inlet temperature and downcomer pressure transients are shown in Figure 2.4-2. No steam voids develop outside of the pressurizer.

Case 2: From a hot shutdown initial condition, the MFW pump in operation increases to full speed and overfeeds one SG with 90°F feedwater. This could result from a failure in the ICS minimum SG level control and failure of the BTU limiter and high level limiter, or a valve failure. The MFW pump trips on high SG level and actuates the EFW pumps. EFWS level control fails in both SG's. No operator action, 3 MW decay heat, and maximum HPI.

Sequence of Events

Time (sec)	Event Description
0	One MFW pump initiates overfeed of one SG from hot shutdown.
5	PZR heaters on.
19	High SG level trip of both MFW pumps.
29	EFWS actuates.
145	PZR heaters isolated on low PZR level.
440	HPIS actuates, minimum RCS pressure (1500 psig), minimum PZR level (10 inches) on scale.
574	SG water solid.
584	PZR heaters on.
600	RCS pressure (1993 psig) increasing, reactor vessel minimum inlet temperature (478°F).

The minimum reactor vessel downcomer inlet temperature and downcomer pressure transients are shown in Figure 2.4-3. No steam voids develop outside of the pressurizer.

Case 3: Following a reactor trip from full power, the ICS fails to runback MFW to one SG with the other SG in normal ICS control. The BTU limiter, the high SG level limiter, and the high SG level trip fail. The operator trips the reactor coolant pumps on low RCS pressure ESFS actuation. Feedwater is isolated at 20 minutes. Maximum HPI. Decay heat of 0.5 x ANS standard was assumed to show the expected system transient recovery following feedwater isolation.

Sequence of Events

Time (sec)	Event Description
0	Reactor trip with ICS failure to runback MFW to one SG, full feedwater flow continues.
4	PZR heaters on.
24	PZR heaters isolated on low PZR level.
36	High SG level trip fails to trip both MFW pumps.
115	SG water solid.
124	Loss of PZR level indication.
155	HPI actuates (1500 psig).
165	Operator trips reactor coolant pumps, MFW switches to auxiliary header.
190	PZR empties for 10 seconds.
218	Minimum RCS pressure (418 psig).
298	PZR level indication regained.
390	Steam line filled with water.
540	PZR heaters on.
640	RCS pressure returns to normal (2155 psig).
647	PZR heaters off.
830	PZR relief valve begins cycling (2450 psig)
980	MFW temperature (90°F).
1200	MFW isolated.
1260	PZR level returns to normal (220 inches).
1370	Reactor vessel minimum inlet temperature (372°F).
1420	Reactor vessel minimum inlet temperature (392°F).

The minimum reactor vessel downcomer inlet temperature and downcomer pressure transients are shown in Figure 2.4-4. No steam voids develop outside of the pressurizer.

Summary of Steam Generator Overfeed Simulation Results

The results of the three SG overfeed overcooling transients analyzed show that all three cases result in a moderate rate of overcooling. The high SG level trip of both MFW pumps prevents the SG's from overfilling greater than 60% of the available SG fluid volume. Case 3 assumed a failure of the high SG level trip in one SG. In the unlikely event of failure of the high SG level trip of both MFW pumps, one of four actions will result in the transients being no more severe than Case 3. The first action, assumed in Case 3, is the manual trip of the reactor coolant pumps by the operator. The second is manual trip of the MFW pumps. The third is manual isolation of MFW. The fourth is manual control of MFW. Following a reactor trip, one of the parameters most closely monitored by the operator is MFW. Although the necessity of operator action is unlikely, if required it should be prompt and positive.

The SG overfeed scenarios are not representative of the types of overfeed transients experienced at Oconee. They are more severe as a result of the conservative equipment failures and operator actions assumed.

2.4.4 Turbine Bypass Failure Simulation Results

Case 4: Following a reactor trip from full power, the TB valves on one SG fail open. The ICS controls MFW as designed. No operator action, no decay heat, and maximum HPI.

Sequence of Events

Time (sec)	Event Description
0	Reactor trip with TB valves on one SG failing open.
4	PZR heaters on.
26	PZR heaters isolated on low PZR level.
74	Loss of PZR level indication.
100	HPIS actuates (1500 psig).
100	PZR empties.
284	Minimum RCS pressure (871 psig).
284	PZR refilling.
382	PZR level indication regained.
597	PZR heaters on.
600	Reactor vessel minimum inlet temperature (431°F).

The minimum reactor vessel downcomer inlet temperature and downcomer pressure transients are shown in Figure 2.4-5. No steam voids develop outside of the pressurizer.

Case 5: Following a reactor trip from full power, the TB valves on one SG fail open. The ICS fails to run back MFW and full feedwater flow continues. A high SG level trip of both MFW pumps occurs and actuates the EFW pumps. EFWS level control fails in the affectd SG and full EFW flow continues. No operator action, no decay heat, and maximum HPI.

Sequence of Events

Time (sec)	Event Description
0	Reactor trip with TB valves on one SG failing open. Failure of ICS MFW runback.
3	PZR heaters on.
21	PZR heaters isolated on low PZR level.
35	High SG level trip of both MFW pumps.
45	EFWS actuates.
56	Loss of PZR level indication.
77	HPIS actuates (1500 psig).
78	PZR empties.
292	Core flood tank injection begins.
308	Minimum RCS pressure (471 psig).
310	Core flood tank injection ends.
324	PZR refilling.
412	PZR level indication regained.
589	PZR heaters on.
600	Reactor vessel minimum inlet temperature (397°F).

The minimum reactor vessel downcomer inlet temperature and downcomer pressure transients are shown in Figure 2.4-6. No steam voids develop outside of the pressurizer.

Case 6: Following a reactor trip from full power, the TB valves on both SG's fail open. The ICS controls MFW as designed. No operator action, no decay heat, and maximum HPI.

Sequence of Events

Time (sec)	Event Description
0	Reactor trip with TB valves on both SG's failing open.
3	PZR heaters on.
26	PZR heaters isolated on low PZR level.
56	Loss of PZR level indication.
69	HPIS actuates (1500 psig).
103	PZR empties.
103	Hot leg is at saturation conditions.
118	Upper head is at saturation conditions.
122	Upper head returns to subcooled conditions.
218	Core flood tank injection begins.
260	Hot leg returns to subcooled conditions.
280	PZR refilling.
282	Minimum RCS pressure (396 psig).
285	Core flood tank injection ends.
378	PZR level indication regained.
548	PZR heaters on.
600	Reactor vessel minimum inlet temperature (384°F).

The minimum reactor vessel downcomer inlet temperature and downcomer pressure transients are shown in Figure 2.4-7. Although the hot leg and the reactor vessel upper head are at saturation conditions for a period of time, the reactor coolant pumps remain in operation which prevents loss of loop circulation.

Case 7: Following a reactor trip from full power, the TB valves on both SG's fail open. The ICS controls MFW as designed. The operator trips the reactor coolant pumps on low RCS pressure ESFS actuation. No decay heat and maximum HPI.

Sequence of Events

Time (sec)	Event Description
0	Reactor trip with TB valves on both SG's failing open.
3	PZR heaters on.
25	PZR heaters isolated on low PZR level.
55	Loss of PZR level indication.
67	HPIS actuates (1500 psig).
77	Operator trips reactor coolant pumps, MFW switches to auxiliary header.
99	PZR empties.
99	Upper head is at saturation conditions.
206	SG level at natural circulation setpoint.
458	PZR refilling.
469	Upper head returns to subcooled conditions.
474	Minimum RCS pressure (474 psig).
531	PZR level indication regained.
600	Reactor vessel minimum inlet temperature (352°F).

The minimum reactor vessel downcomer inlet temperature and downcomer pressure transients are shown in Figure 2.4-8. Following trip of the reactor coolant pumps the system enters a sustained natural circulation mode of loop circulation.

Case 8: From a hot shutdown initial condition, the TB valves on both SG's fail open. The ICS controls MFW as designed with 90°F feedwater. The operator trips the reactor coolant pumps on low RCS pressure ESFS actuation. Three MW decay heat and maximum HPI.

Sequence of Events

Time (sec)	Event Description
0	TB valves on both SG's fail open at hot shutdown.
6	PZR heaters on.
60	PZR heaters isolated on low PZR level.
96	Loss of PZR level indication.
69	HPIS actuates (1500 psig).
114	PZR empties.
117	HPIS actuates (1500 psig).
127	Operator trips reactor coolant pumps, MFW switches to auxiliary header.
177	SG level at natural circulation setpoint.
181	Core flood tank injection begins.
191	PZR refilling.
192	Minimum RCS pressure (532 psig).
207	Core flood tank injection ends.
354	PZR level indication regained.
525	PZR heaters on.
600	Reactor vessel minimum inlet temperature (308°F).

The minimum reactor vessel downcomer inlet temperature and downcomer pressure transients are shown in Figure 2.4-9. Following trip of the reactor coolant pumps the system enters a sustained natural circulation mode of loop circulation.

Case 9: Following a reactor trip from full power, the TB valves on both SG's fail open. The ICS fails to runback MFW and full feedwater flow continues. A high SG level trip of both MFW pumps occurs and actuates the EFW pumps. EFWS level control functions as designed. At 20 minutes the operator isolates the EFWS. No decay heat and maximum HPI.

Sequence of Events

Time (sec)	Event Description
0	Reactor trip with TB valves on both SG's failing open. Failure of ICS MFW runback.
3	PZR heaters on.
21	PZR heaters isolated on low PZR level.
39	High SG level trip of both MFW pumps.
45	Loss of PZR level indication.
49	EFWS actuates.
62	PZR empties.
62	HPIS actuates (1500 psig).
132	Hot leg is at saturation conditions.
213	Core flood tank injection begins.
254	Hot leg returns to subcooled conditions.
281	PZR refilling.
282	Minimum RCS pressure (389 psig).
283	Core flood tank injection ends.
371	PZR level indication regained.
590	PZR heaters on.
600	Reactor vessel minimum inlet temperature (369°F).
877	PZR level returns to normal (220 inches).
1105	RCS pressure returns to normal (2155 psig).
1107	PZR heaters off.
1113	PZR spray begins cycling (2205 psig).
1200	EFWS isolated.
1417	Reactor vessel minimum inlet temperature (296°F).
1417	PZR water solid.
1428	PZR relief valve begins cycling (2450 psig).
1433	PZR safety valves begin cycling (2500 psig).
1495	SG's boil dry.
1800	Reactor vessel inlet temperature (305°F).

The minimum reactor vessel downcomer inlet temperature and downcomer pressure transients are shown in Figure 2.4-10. Although the hot leg is at saturation conditions for a period of time, the reactor coolant pumps remain in operation which prevents loss of loop circulation. The operator action to isolate the EFWS at 20 minutes terminates the cooldown.

Case 10: Following a reactor trip from full power, the TB valves on both SG's fail open. The ICS fails to runback MFW and full feedwater flow continues. A high SG level trip of both MFW pumps occurs and actuates the EFW pumps. EFW level control functions as designed. The operator trips the reactor coolant pumps on low RCS pressure ESFS actuation. At 20 minutes the operator isolates the turbine bypass and the EFWS. Maximum HPI is assumed. In order to simulate the recovery phase of the transient, a minimal decay heat power of 0.5 times the ANS standard was used.

Sequence of Events

Time (sec)	Event Description
0	Reactor trip with TB valves on both SG's failing open. Failure of ICS MFW runback.
3	PZR heaters on.
23	PZR heaters isolated on low PZR level.
39	High SG level trip of both MFW pumps.
49	EFWS actuates.
50	Loss of PZR level indication.
70	PZR empties.
70	HPIS actuates (1500 psig).
80	Operator trips reactor coolant pumps.
124	Upper head at saturation conditions.
264	SG level at natural circulation setpoint.
381	PZR refilling.
390	Minimum RCS pressure (746 psig).

Sequence of Events

Time (sec)	Event Description
390	Upper head returns to subcooled conditions.
443	PZR level indication regained.
600	Reactor vessel inlet temperature (369°F).
668	PZR heaters on.
1024	PZR level returns to normal (220 inches).
1065	RCS pressure returns to normal (2155 psig).
1070	PZR heaters off.
1167	PZR relief valve begins cycling (2450 psig).
1200	Operator isolates EFWS and TBS.
1355	Reactor vessel minimum inlet temperature (289°F).
1617	PZR safety valves begin cycling (2500 psig).
1634	PZR water solid.
1800	Reactor vessel inlet temperature (302°F).
2400	Reactor vessel inlet temperature (316°F).

The minimum reactor vessel downcomer inlet temperature and downcomer pressure transients are shown in Figure 2.4-11. The temperature assuming no decay heat is also shown. Following trip of the reactor coolant pumps the system enters a sustained natural circulation mode of loop circulation. Although the reactor vessel upper head reaches saturation conditions, the hot leg does not. The operator action to isolate the EFWS and the TBS at 20 minutes terminates the cooldown.

Summary of Turbine Bypass Failure Simulation Results

The results of the seven TBS failure initiated transients analyzed show varying cooldown rates based on the combination of five parameters which determine the system response. The

first parameter is whether the TB valves on one or both SG's fail. It is obvious that the cooldown rate will be greater for the higher steam relief occurring when both SG's are affected. It should be recognized that a failure of all TB valves has not ocurred at Oconee. The second parameter is whether or not the operator trips the reactor coolant pumps. With the pumps tripped the system enters natural circulation. None of the cases analyzed predict an interruption of natural circulation since the hot leg does not reach saturation conditions with the pumps tripped. Due to flashing in the reactor vessel upper head, the pressure responses for the cases with the pumps tripped show higher minimum pressures. The cases with the pumps tripped also result in a larger SG inventory due to the SG level control switching to the higher natural circulation setpoint. This causes an extended cooldown following feedwater isolation while the inventory boils down. The extended cooldown can be terminated by isolation of the TBS. The third parameter is whether the MFWS or the EFWS is delivering the feedwater. The MFWS has more flow capacity but higher fluid temperatures than the EFWS. The fourth parameter is whether the transient initiates from power operation or at hot shutdown. Only Case 8 initiated at hot shutdown. Although Case 8 results in a lower minimum temperature than the corresponding power operation case (Case 7), the concern from the viewpoint of thermal shock is the temperature difference between the reactor vessel and the fluid. Since for the hot shutdown case the vessel is at a lower temperature initially, the temperature difference is less, and is comparable to the cases initiating from power operation. The fifth parameter is the assumptions made concerning operator action. Three types of operator action were assumed. Both sides of the assumption of tripping the reactor coolant pumps were analyzed, and both resulted in similar cooldown rates. Two types of actions were assumed to mitigate the overcooling, the isolation of feedwater to the affected SG and the isolation of the TBS, both occurring no earlier than 20 minutes. Both of these actions are realistically expected

to occur much sooner in response to the alarms actuated as a result of the symptoms of the overcooling accident. No operator action to limit the RCS repressurization by throttling the HPIS was assumed.

The TBS failure initiated transients analyzed are bounded by Case 9 and 10 for the conditions of reactor coolant pumps on and off respectively. The cooldown rates and the pressure responses are similar. No mitigative operator action was assumed until 20 minutes, although under realistic assumptions and based on operating experience, positive operator action would be prompt and effective. The transients analyzed are realistic simulations based on conservative assumptions. The cases analyzed are bounding and much more severe than those transients which have occurred, and are also more severe than those scenarios which have a reasonable probability of occurrence in the future. The cooldown rates resulting from small steam line breaks are bounded by these cases up to a break size of approximately 0.40 ft^2.

2.4.5 Steam Line Break Simulation Results

Case 11: Coincident with a reactor trip from full power, a rupture of a 34 inch main steam line occurs. The unaffected SG is isolated by the fast closing turbine stop valves. The ICS controls MFW as designed. The operator isolates feedwater to the affected SG at 5 minutes. Maximum HPI and no decay heat.

Sequence of Events

Time (sec)	Event Description
0	Reactor trip and steam line break.
1	PZR heaters on.
8	HPIS actuates (1500 psig).
10	PZR heaters isolated on low PZR level.

Sequence of Events

Time (sec)	Event Description
20	Loss of PZR level indication.
25	PZR empties.
34	Upper head at saturation conditions.
57	Affected loop hot leg at saturation conditions.
66	Unaffected loop hot leg at saturation conditions.
70	Upper head returns to subcooled conditions.
88	Unaffected loop hot leg returns to subcooled conditions.
98	Core flood tank injection begins.
109	Affected loop hot leg returns to subcooled conditions.
183	PZR refilling.
250	PZR level indication regained.
271	Minimum RCS pressure (182 psig).
276	Core flood tank injection ends.
300	Operator isolates MFWS.
300	Reactor vessel inlet temperature (312°F).
326	Minimum reactor vessel inlet temperature (303°F).
350	Affected SG boils dry.
379	PZR heaters on.
531	PZR level returns to normal (220 inches).
600	Reactor vessel inlet temperature (329°F).
755	RCS pressure returns to normal (2155 psig).
757	PZR heaters off.
759	PZR spray begins cycling (2205 psig).

Sequence of Events

Time (sec)	Event Description
892	PZR water solid.
900	PZR relief valve begins cycling (2450 psig).
903	PZR safety valves begin cycling (2500 psig).
1200	Reactor vessel inlet temperature (342°F).

The minimum reactor vessel downcomer inlet temperature and downcomer pressure transients are shown in Figure 2.4-12. Although the hot legs are at saturation conditions for a period of time, the reactor coolant pumps remain in operation which prevents loss of loop circulation. The operator action to isolate the feedwater to the affected SG terminates the cooldown.

Case 12: Coincident with a reactor trip from full power, a rupture of a 34 inch main steam line occurs. The unaffected SG is isolated by the fast closing turbine stop valves. The ICS controls MFW as designed. The operator trips the reactor coolant pumps on low RCS pressure ESFS actuation. The operator isolates feedwater to the affected SG at 5 minutes. Maximum HPI is assumed. In order to simulate the recovery phase of the transient, a minimal decay heat power of 0.5 times the ANS standard was used. The operator is also assumed to restart one reactor coolant pump in each loop at 10 minutes. This is the action specified in the procedures once the subcooled margin of 50°F is obtained. For this case that margin occurs at about 7 minutes. The subcooled margin at 10 minutes is greater than 75°F.

Sequence of Events

Time (sec)	Event Description
0	Reactor trip and steam line break.
1	PZR heaters on.
8	HPIS actuates (1500 psig).
10	PZR heaters isolated on low PZR level.
17	Loss of PZR level indication.
18	Operator trips reactor coolant pumps, MFW switches to auxiliary header.
20	PZR empties.
24	Upper head at saturation conditions.
79	Unaffected SG at natural circulation setpoint.
190	Core flood tank injection begins.
198	Unaffected loop hot leg at saturation conditions.
204	Affected loop hot leg at saturation conditions.
288	Affected loop hot leg returns to subcooled conditions.
300	Operator isolates MFWS.
300	Reactor vessel inlet temperature (282°F).
318	Minimum RCS pressure (355 psig).
319	Upper head returns to subcooled conditions.
325	Affected loop hot leg returns to subcooled conditions.
326	Affected SG boils dry.
328	PZR refilling.
344	Core flood tank injection ends.
354	PZR level indication regained.

Sequence of Events

Time (sec)	Event Description
400	Loss of sustained loop circulation.
420	50°F subcooled margin reached.
444	PZR heaters on.
600	Minimum reactor vessel downcomer temperature (228°F).
600	Operator restarts one reactor coolant in each loop.

Note: Times beyond 600 seconds are approximate.

611	PZR level returns to normal (220 inches).
660	Reactor vessel downcomer inlet temperature (345°F).
780	PZR heaters off.
780	RCS pressure returns to normal (2155 psig).
785	PZR spray on (2205 psig).
1000	PZR water solid.
1000	PZR relief valve begins cycling (2450 psig).
1000	PZR safety valves begin cycling (2500 psig).
1200	Reactor vessel downcomer inlet temperature (~354°F).

The minimum reactor vessel downcomer inlet temperature and downcomer pressure transients are shown in Figure 2.4-12. Although the hot legs are at saturation conditions for a period of time, natural circulation is not lost since the hot leg bubble exists for only a short period of time, and is not large enough at the existing high natural circulation flowrates to collect at the top of the hot leg and interrupt circulation. Natural circulation is interrupted at a later time, although the system is subcooled, following isolation of MFW to the affected SG and the resulting loss of heat sink. During the time period following loss of loop circulation and before the operator restarts one

reactor coolant pump in each loop, the HPI injection continues to refill the system. The system becomes stratified with the hotter water in the upper parts of the system, and the cooler water in the lower parts. The system rapidly reaches the 50°F subcooled margin required for restart of the reactor coolant pumps as specified in the procedures. The pumps rapidly mix the system inventory, resulting in a homogeneous system temperature.

Case 13: Coincident with a reactor trip from full power, a rupture of a 34 inch main steam line occurs. The unaffected SG is isolated by the fast closing turbine stop valves. The ICS fails to runback MFW and full flow continues. High SG level in the unaffected SG trips both MFW pumps and actuates the EFW pumps. EFW is delivered at full capacity to the affected SG until isolated by the operator at 5 minutes. Maximum HPI is assumed. In order to simulate the recovery phase of the transient, a minimal decay heat power of 0.5 times the ANS standard was used. The operator is also assumed to restart one reactor coolant pump in each loop at 10 minutes.

Sequence of Events

Time (sec)	Event Description
0	Reactor trip and steam line break. Failure of ICS MFW runback.
1	PZR heaters on.
8	HPIS actuates (1500 psig).
10	PZR heaters isolated on low PZR level.
18	Operator trip reactor coolant pumps, MFW assumed to continue through the MFW nozzle.

Sequence of Events

Time (sec)	Event Description
19	Loss of PZR level indication.
22	PZR empties.
29	Upper head at saturation conditions.
35	High SG level trip of both MFW pumps.
45	EFWS actuates.
136	Unaffected loop hot leg at saturation conditions.
141	Affected loop hot leg at saturation conditions.
155	Loss of natural circulation.
217	Core flood tank injection begins.
270	Affected SG blowdown ends (<10 psig). Boil off of cold feedwater inventory continues.
300	Operator isolates EFWS.
300	Reactor vessel inlet temperature (304°F).
300	Reactor vessel average downcomer temperature (359°F).
336	Minimum RCS pressure (559 psig).
405	Core flood tank injection ends.
410	Natural circulation restarts in affected loop.
420	RCS water solid except PZR, PZR refilling.
420	Reactor vessel inlet temperature (265°F).
420	Reactor vessel average downcomer temperature (306°F).
420	Simulation ended with Case 13 verified to be bounded by Case 12 (evaluation in following paragraph.

The minimum reactor vessel downcomer inlet temperature and downcomer pressure are shown in Figure 2.4-14. Due to a slower RCS cooldown rate than the other steam line break simulation with reactor coolant pumps tripped (Case 12), natural circulation is lost for a period of approximately 4.5 minutes due to bubble formation in both hot legs. CFTS and HPIS injection increase RCS inventory and pressure which collapses the voids at 7 minutes. Natural circulation restarts due to the remaining inventory of cold feedwater slowly boiling off in the affected SG following the end of blowdown. The simulation was terminated at 7 minutes after an evaluation determined that the trends of the transient were established and that the transient was less severe than Case 12. The comparison of the two cases showed that at 7 minutes Case 13 had an RCS average fluid temperature which was 38°F hotter than Case 12.

Summary of Steam Line Break Simulation Results

The results of the three steam line break transients analyzed confirm, as expected, that steam line break scenarios are the most severe overcooling transients. Operator action to isolate feedwater to the affected SG at 5 minutes was assumed. For the case where the operator trips the reactor coolant pumps, the operator is assumed to restart one pump in each loop when the 50°F subcooled margin is reached, but not before 10 minutes. Both of these actions are currently specified in plant procedures. No operator action to limit the RCS repressurization by throttling the HPIS was assumed.

With the reactor coolant pumps tripped, the RCS enters a natural circulation mode. A loss of natural circulation can occur if the fluid in the hot leg flashes and collects as a bubble at the top of the hot leg, thereby blocking flow. A loss of natural circulation can also occur when the affected SG has boiled dry and there is no SG heat removal. If natural circulation is interrupted with cold HPIS flow being injected

into the cold legs, the RCS can become thermally stratified with hot liquid in the upper parts of the system, and the cold HPIS injected liquid in the lower parts of the system. The HPIS will refill the system causing a repressurization and collapse any voids in the system. The system subcooled margin will steadily increase. Natural circulation will then restart if a SG heat removal path exists. If no SG heat removal path exists, loop flow can be established by restarting one reactor coolant pump in each loop as specified in the procedures. Loop circulation will then mix the system fluid inventory to an average temperature and terminate the thermally stratified condition.

Similar to the SBLOCA situation with loss of natural circulation, reactor vessel internals vent valve flow will occur with a sufficient density gradient across the vent valve. The simulations did not allow vent valve flow to occur since the density gradient is driven by the decay heat generated in the core. Vent valve flow would be predicted to occur in Case 12 at 220 seconds, and in Case 13 at 160 seconds. This occurrence would significantly increase the reactor vessel downcomer temperature above the values shown in Figures 2.4-13 and 2.4-14. This represents a major conservatism incorporated into the steam line break analyses.

Although the steam line breaks result in the most severe overcooling transients and require the earliest operator action, operator action is expected to be more prompt than for less severe overcooling transients. This is simply a result of the more severe symptoms associated with the event causing earlier alarm actuation and event recognition. The normal operator actions are not required before an unreasonable timeframe following initiation of the event.

2.4.6 Summary

Oconee plant specific overcooling transients initiated by SG overfeeds, TBS failures, and steam line breaks have been analyzed. The transients were realistically simulated based on a conservative set of assumptions incorporated into each analysis. Therefore, the analysis results are conservative and bounding. Only a limited credit has been taken for operator action as specified in plant procedures, although the operator would be promptly alerted by alarms actuated by the overcooling symptoms. No credit was taken for the operator limiting the RCS repressurization by throttling the HPIS once the subcooling margin is regained.

It should be recognized that the magnitude of the overcooling predicted in the thirteen cases analyzed is much more severe than the overcooling which has occurred in the events which constitute the operating history at Oconee. This is a result of four factors. The first factor is that failure mechanisms with the potential for evolving into overcooling events are infrequent, and those that occur are minor failures compared to the failures assumed in the analyses. The second factor is that the overcooling events are successfully and automatically mitigated by existing plant controls. The third factor is that the operator has responded promptly and positively when required. The fourth factor is the conservative assumptions utilized in the analyses.

Of the overcooling scenarios analyzed, Cases 9, 10, 11, and 12 result in the most severe overcooling of the reactor vessel. Boundary conditions from these cases are utilized for the vessel fracture mechanics evaluation in Chapter 8.0.

Table 2.2-1

Oconee Overcooling Event History

EVENT	UNIT/DATE	OVERCOOLING MECHANISM	AUTOMATIC MITIGATION	OPERATOR ACTION	MIN RCS TEMP (°F)	EVALUATION
1	1/05/73	TBS manually open with subsequent MFW overfeed	None	Failed to isolate TBS, manual overfeed	500	No overcooling resulted Pre-commercial event and not typical of normal operation.
2	2/01/74	High natural circulation setpoint and auxiliary steam load	None	None	422	Cooldown rate 140°F/hr First operating experience with natural circulation, setpoint reduced.
3	2/07/74	Pzr relief valve failed open on loss of ICS power	None	Restored ICS power within one minute	515	No overcooling resulted Pzr relief valve control modified to close on loss of ICS power.
4	2/09/74	Partial TBS failure	ICS controlled transient, unit remained on line	Isolated TBS	Normal	No overcooling resulted Demonstrated capability of ICS to control the transient.
5	2/09/74	Unsuccessful ICS runback of MFW	High SG level trip of both MFW pumps	None	547	No overcooling resulted A moderate transient.
6	2/03/75	Stuck open MFW control valve caused overfeed	High SG level trip of both MFW pumps	None	~540	No overcooling resulted A moderate transient from a low initial power level.
7	3/04/75	Slow ICS runback of MFW. One main steam relief valve reseated low	High SG level trip of both MFW pumps	None	540	No overcooling resulted A moderate transient.
8	3/05/75	Partial TBS failure	ICS control of transient was unsuccessful	Isolated TBS	485	No overcooling resulted

Table 2.2-1 (Cont.)

EVENT	UNIT/DATE	OVERCOOLING MECHANISM	AUTOMATIC MITIGATION	OPERATOR ACTION	MIN RCS TEMP (°F)	EVALUATION
9	3/06/13/75	Pzr relief valve mechanical failure to reseat	None	Pzr relief valve block valve closed	510	No overcooling resulted
10	3/07/13/75	Partial TBS failure	ICS controlled transient, unit remained on line	Isolated TBS	Normal	No overcooling resulted
11	1/08/14/76	Manual MFW overfeed	High SG level trip of both MFW pumps	Manual overfeed	Normal	No overcooling resulted
12	1/12/14/78	Manual MFW and EFW overfeed	None	Manual overfeed	500	No overcooling resulted
13	3/11/10/79	Partial TBS failure. Manual MFW overfeed. Auxiliary steam load	None	Failure to isolate aux steam and TBS. Manual overfeed.	420	Cooldown rate 115°F/hr Demonstrated need to control SG pressure
14	2/01/30/80	Slow ICS runback of MFW	High SG level trip of both MFW pumps	None	540	No overcooling resulted
15	3/03/14/80	Unsuccessful ICS runback of MFW	High SG level trip of both MFW pumps	None	546	No overcooling resulted
16	1/05/04/81	Partial TBS failure	ICS controlled transient, unit remained on line	Isolated TBS	Normal	No overcooling resulted

Figure 2.1-1

Oconee Nuclear Station

Reactor Coolant System

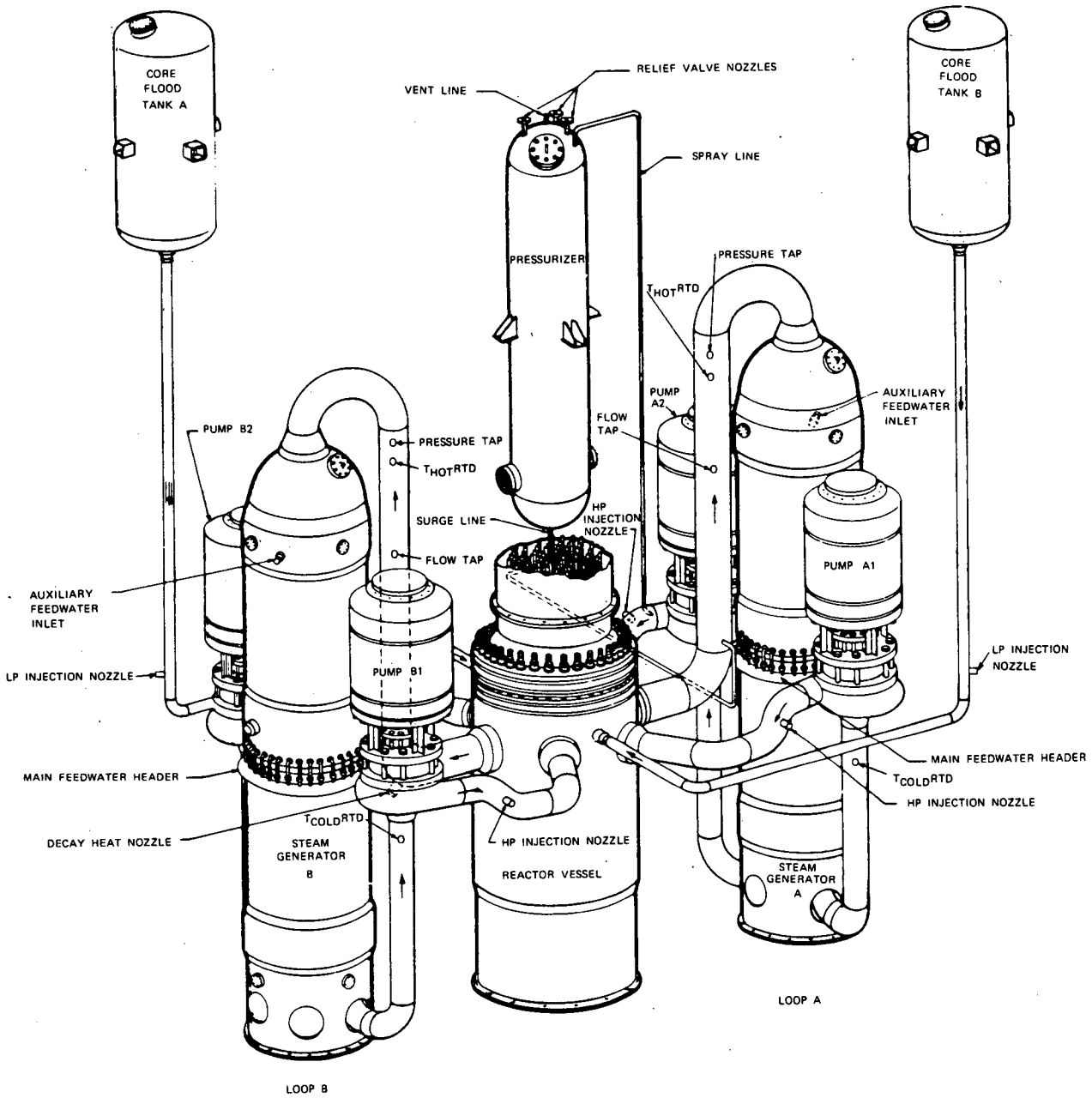

Figure 2.1-2

High Pressure Injection System

Nozzle Geometry

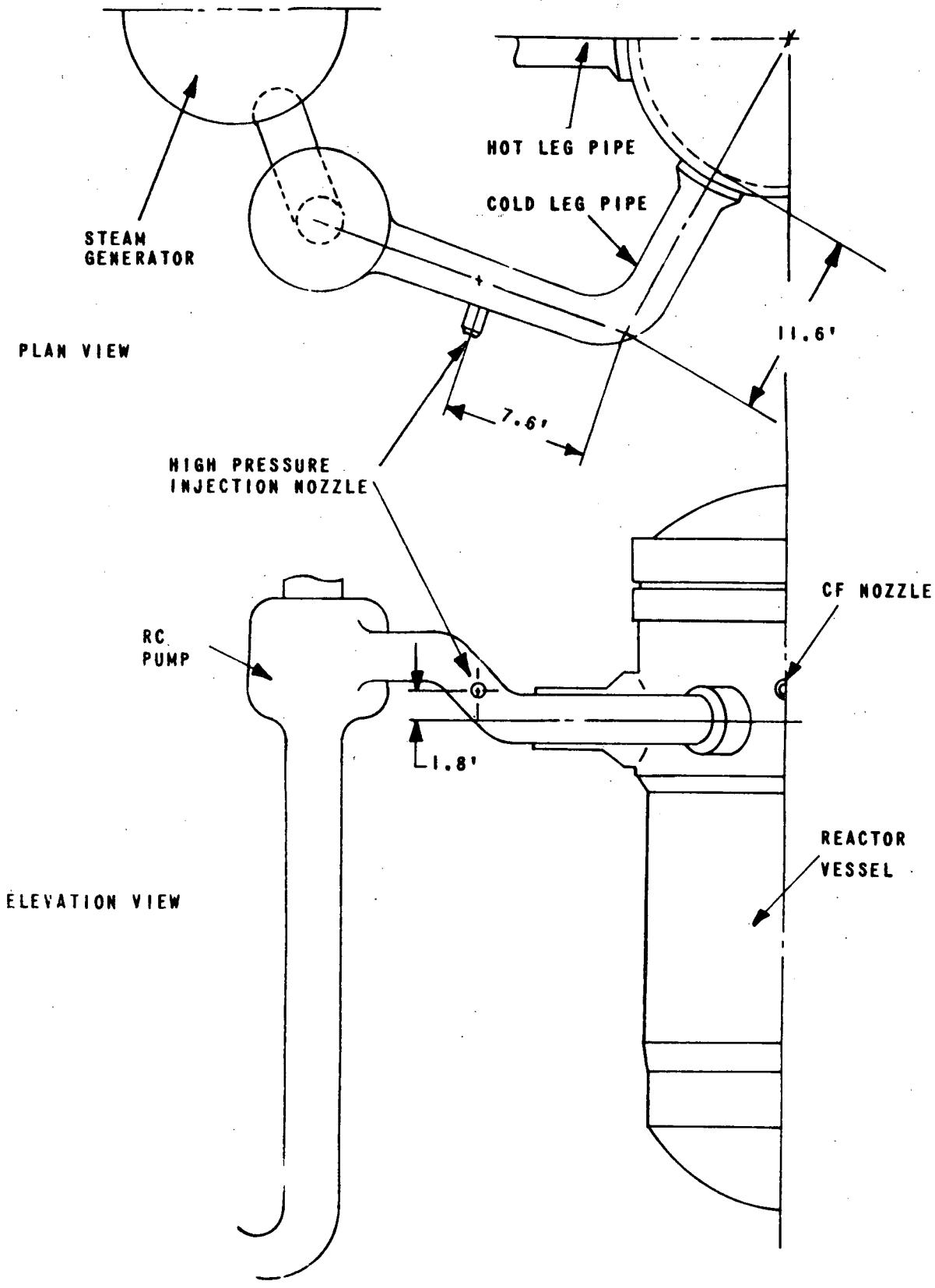

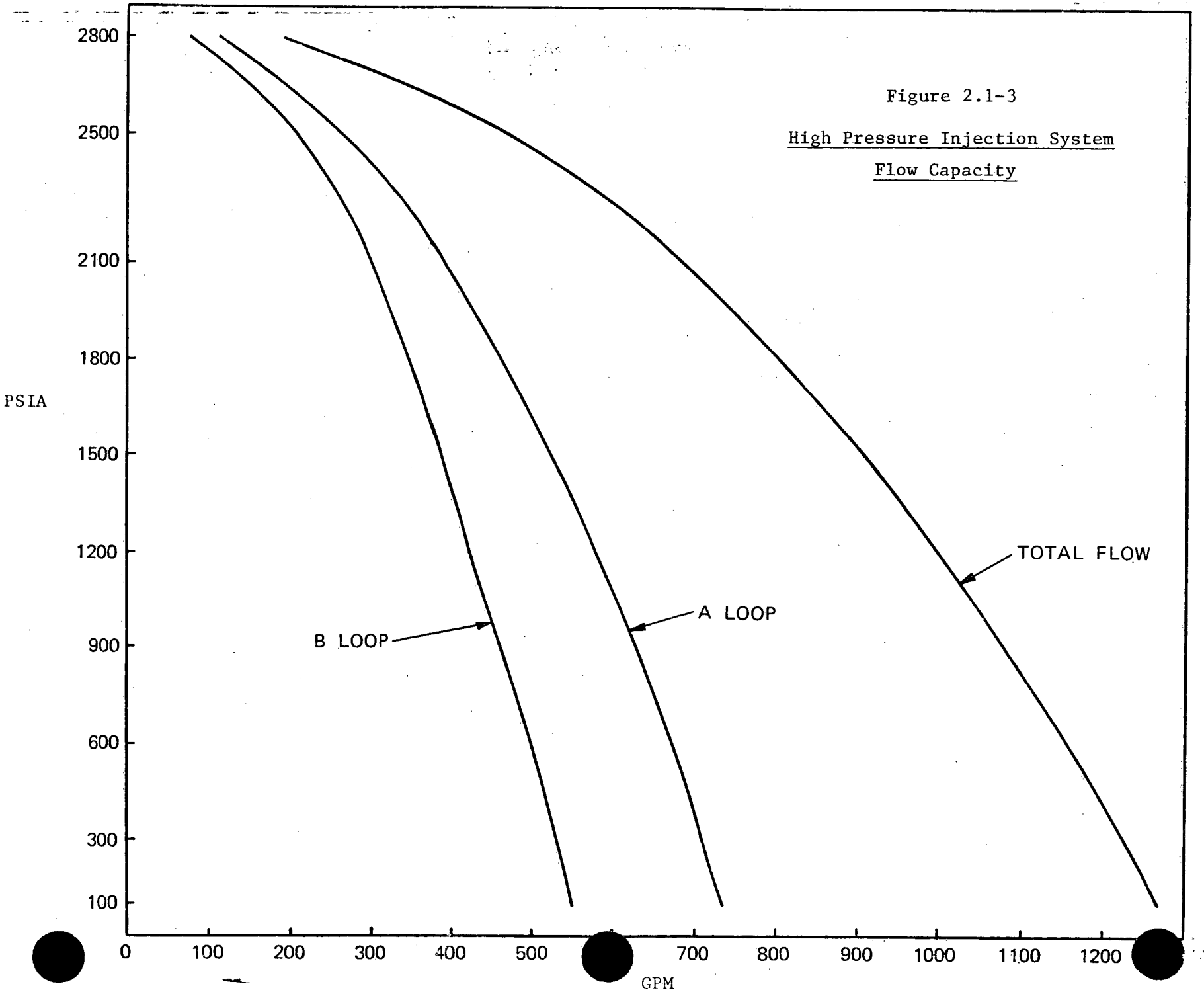

Figure 2.1-3

High Pressure Injection System

Flow Capacity

Figure 2.1-4

Steam and Power Conversion Systems

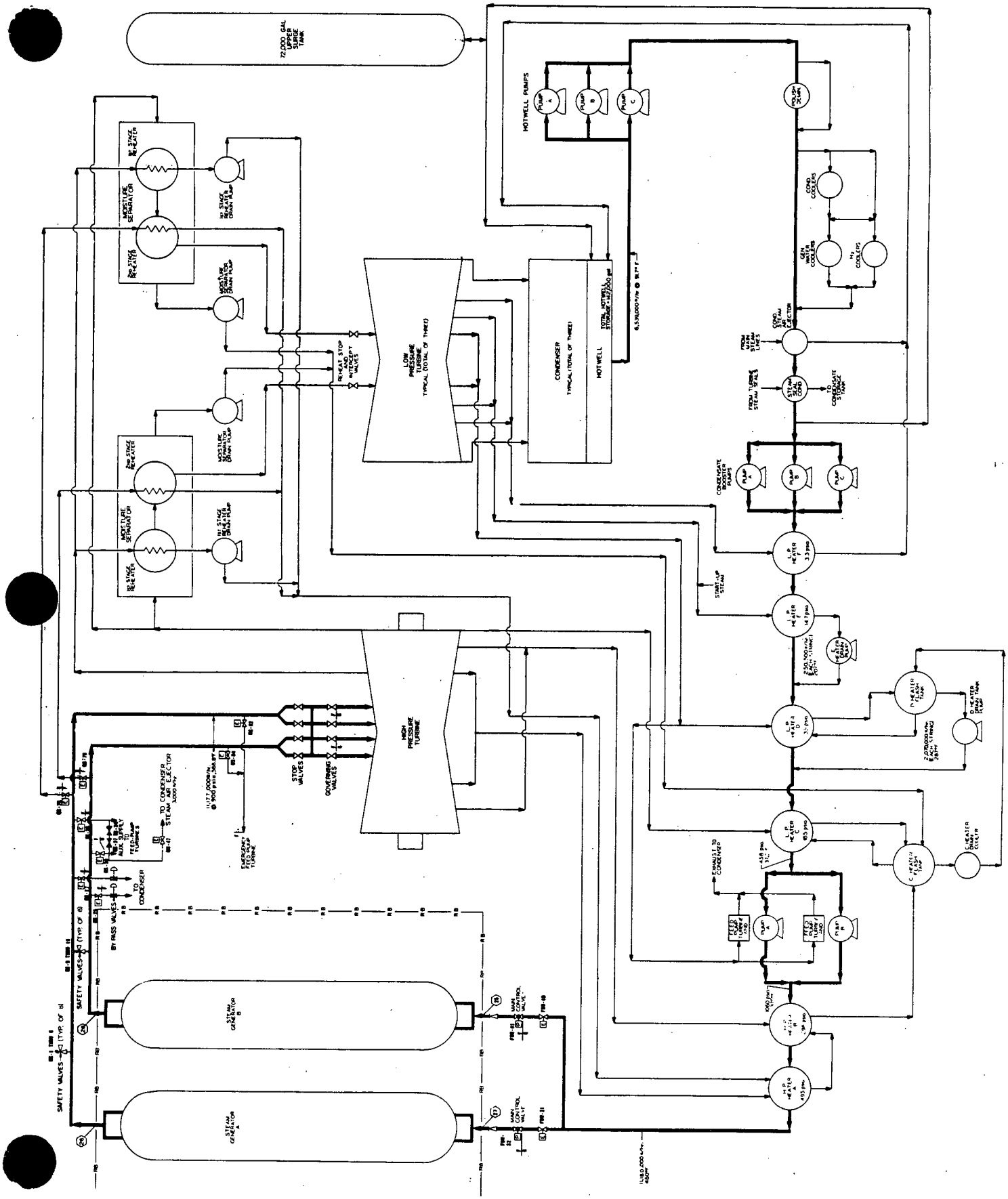

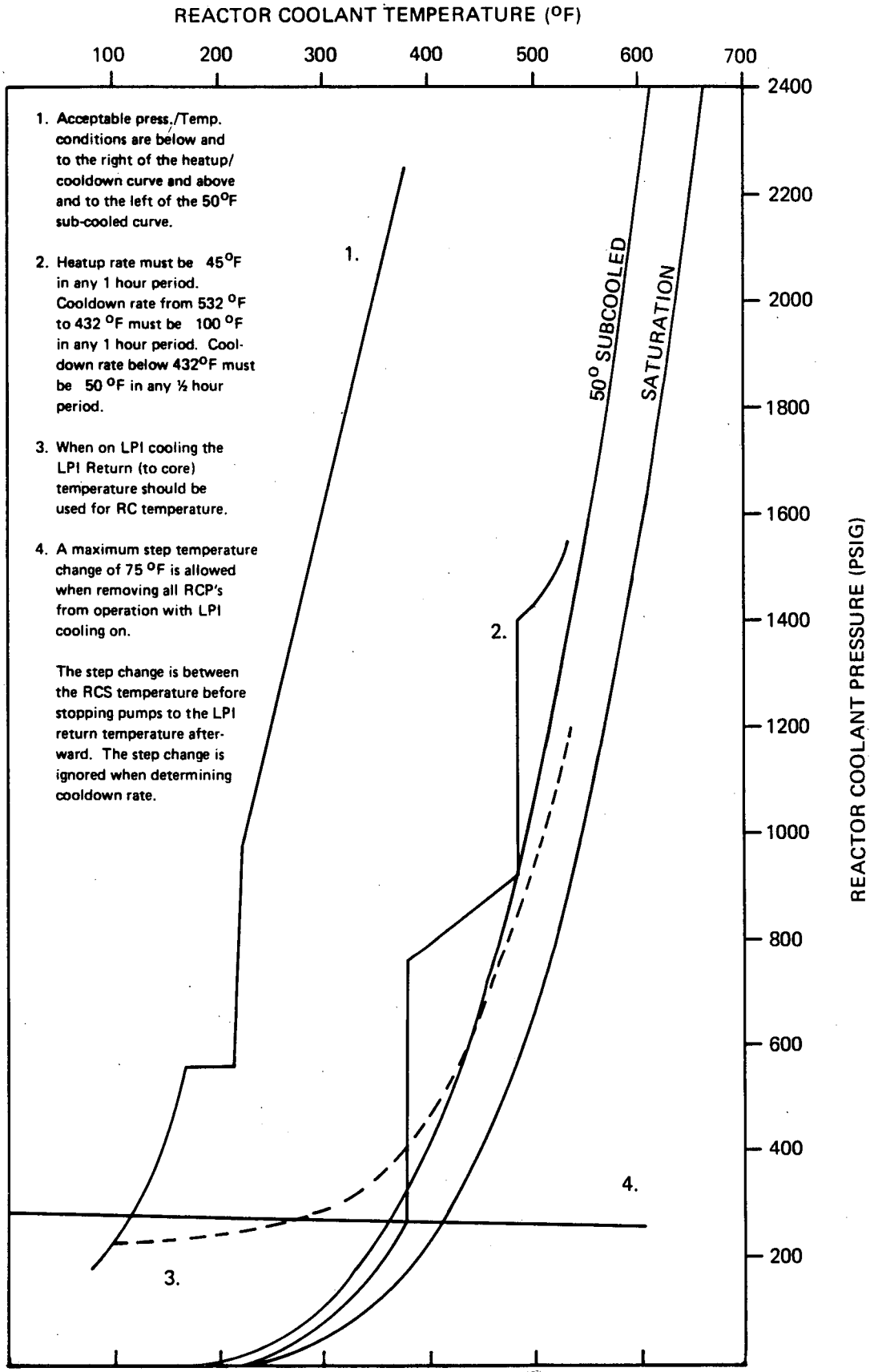

Figure 2.1-5

Cooldown Curve

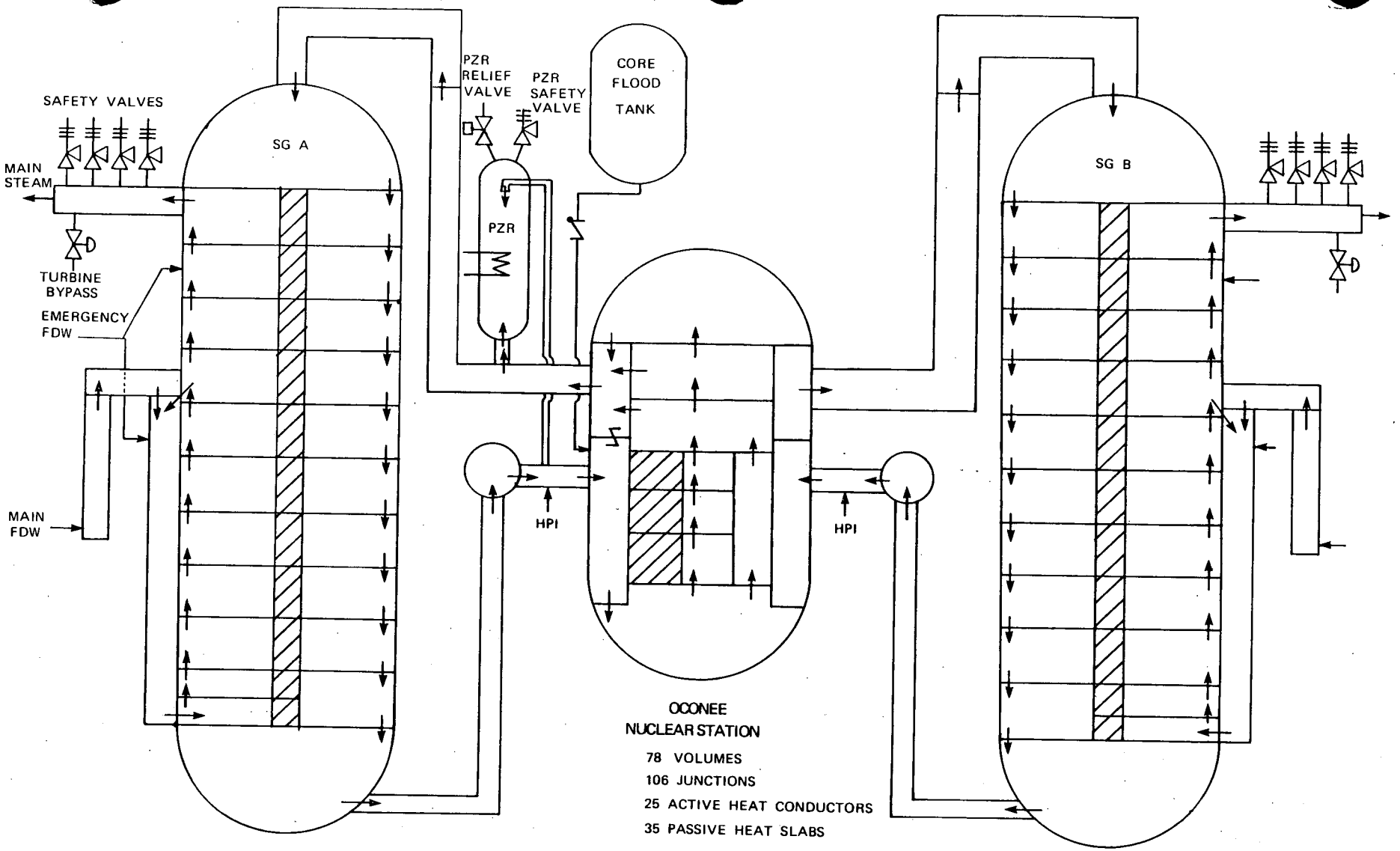

Figure 2.4-1

RETRAN Nodalization

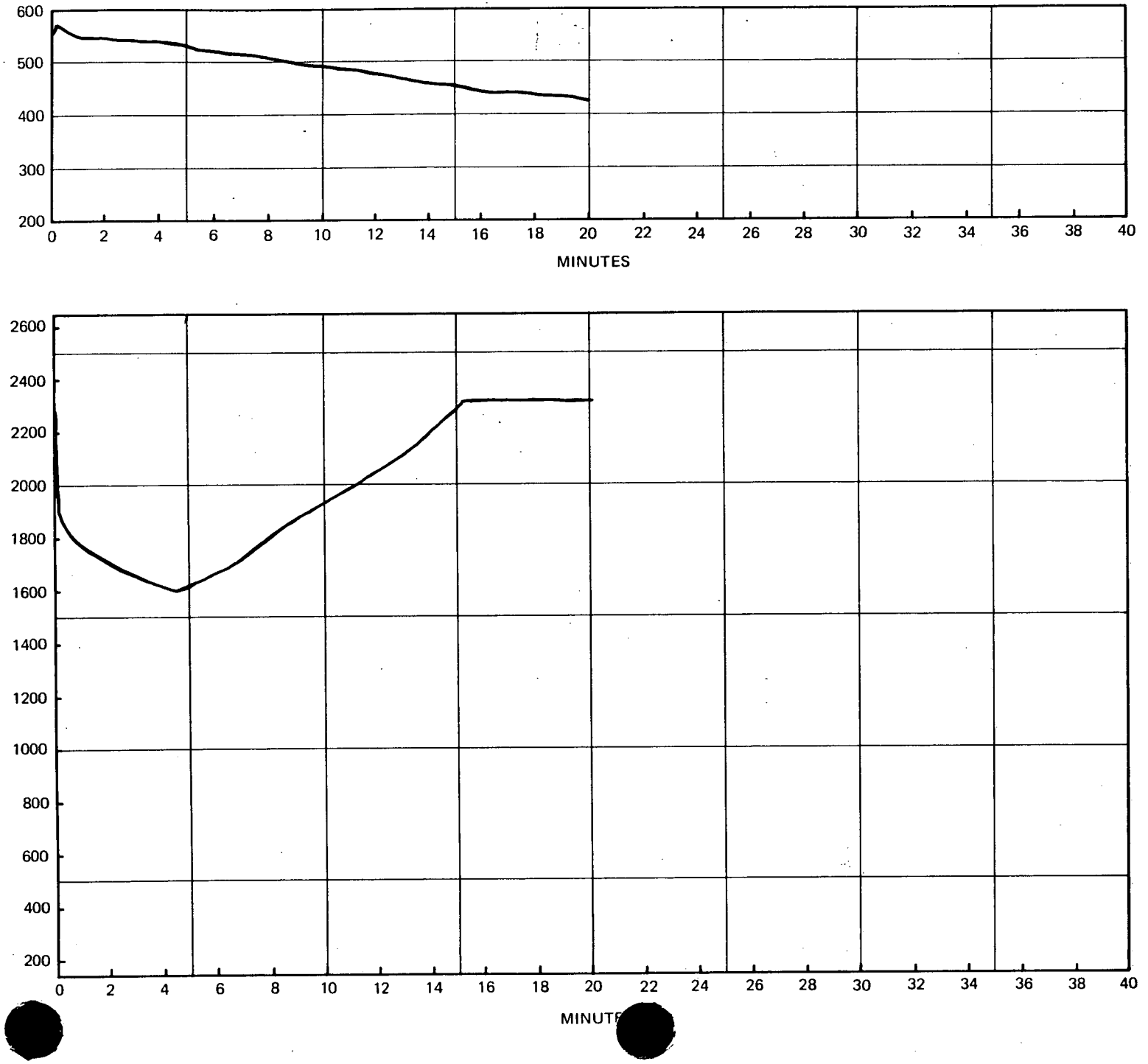

Figure 2.4-2
Overcooling Transient Simulation Results
Case 1 - Steam Generator Overfeed

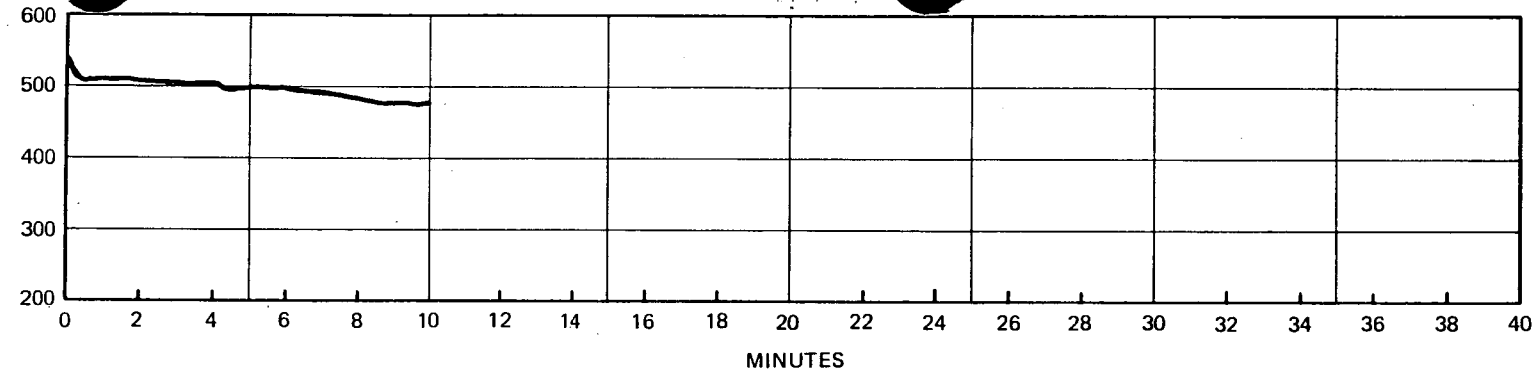

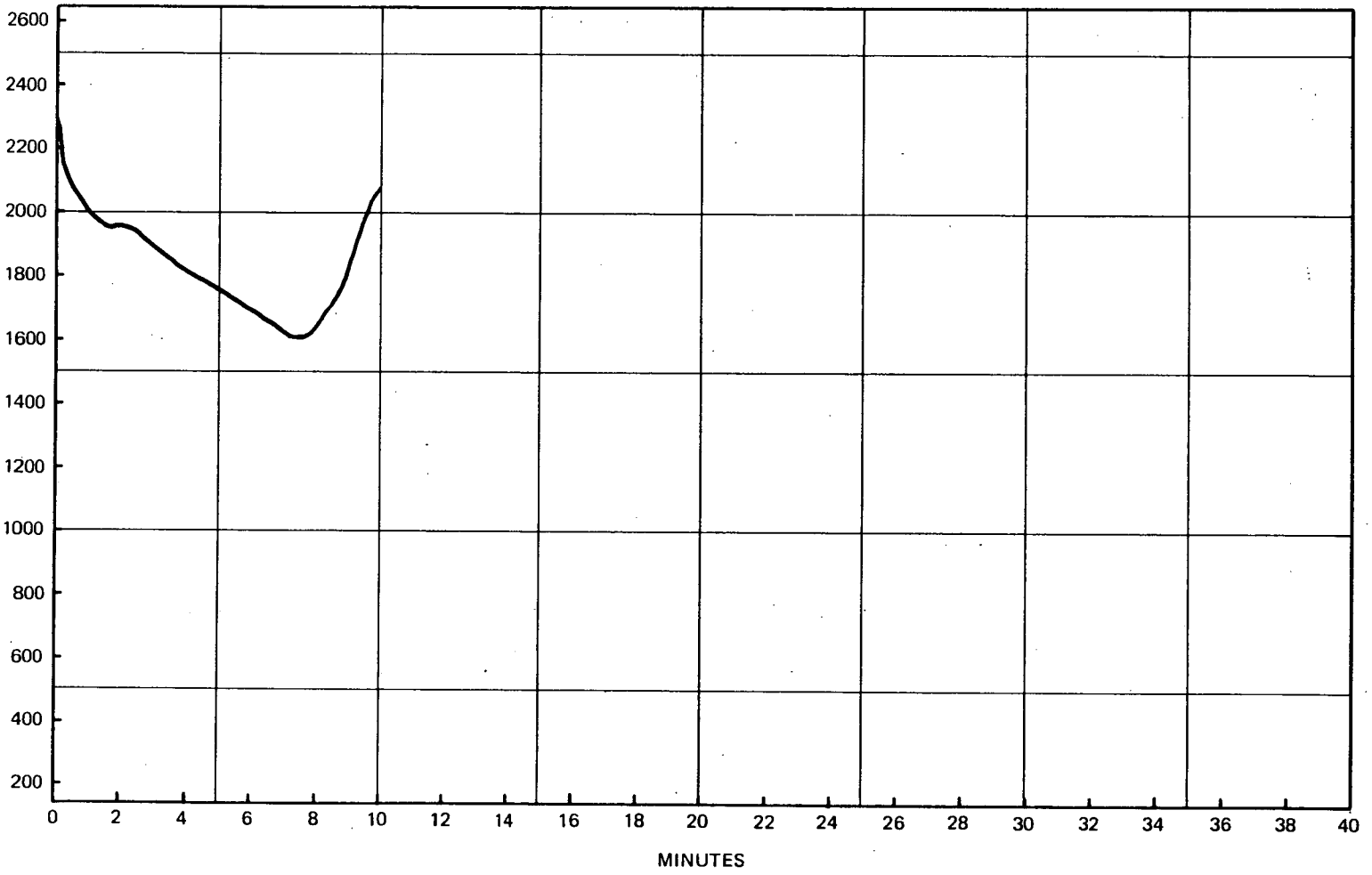

Figure 2.4-3

Overcooling Transient Simulation Results

Case 2 - Steam Generator Overfeed

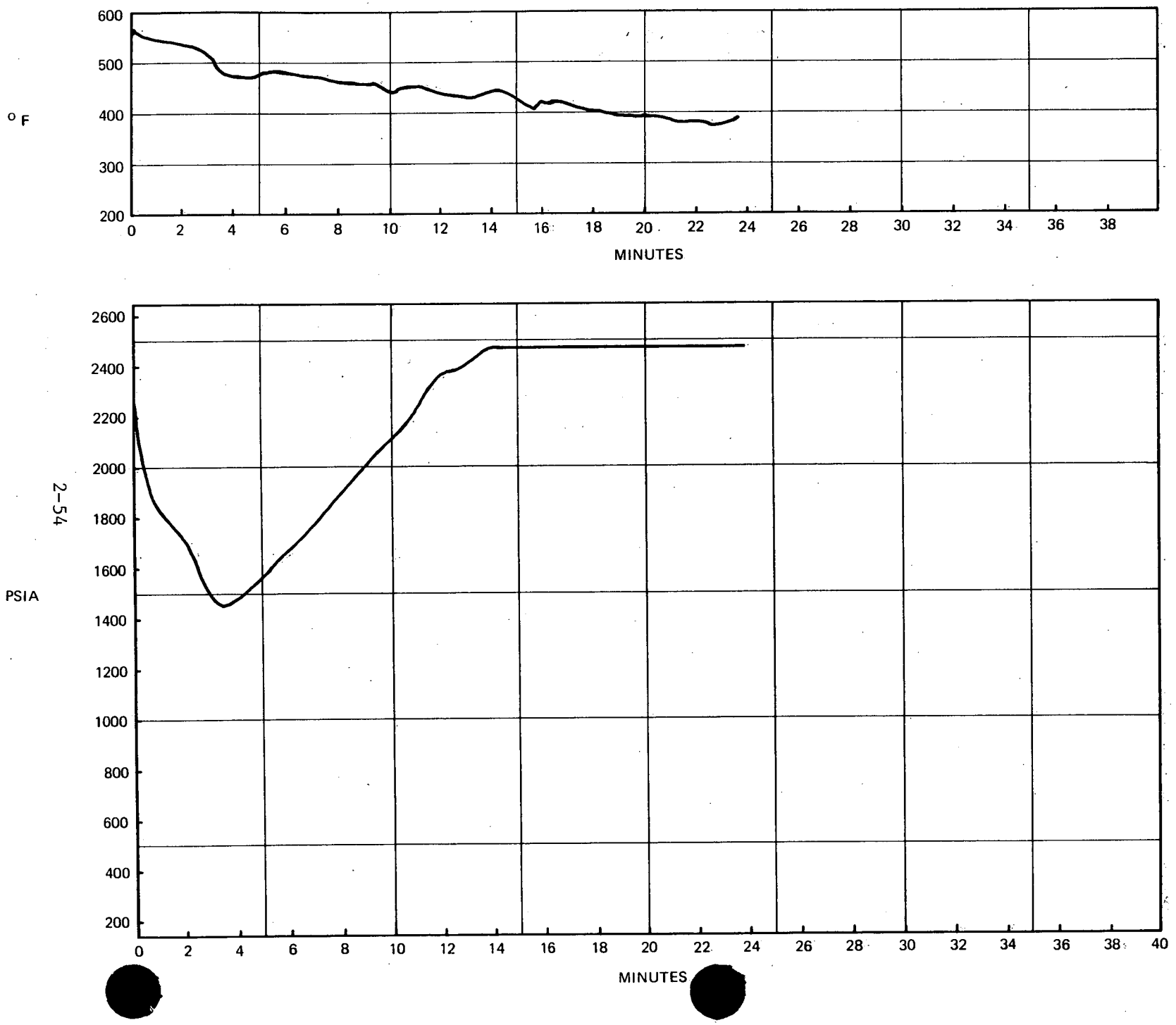

Figure 2.4-4

Overcooling Transient Simulation Results

Case 3 - Steam Generator Overfeed

Figure 2.4-5

Overcooling Transient Simulation Results

Case 4 - Turbine Bypass System Failure

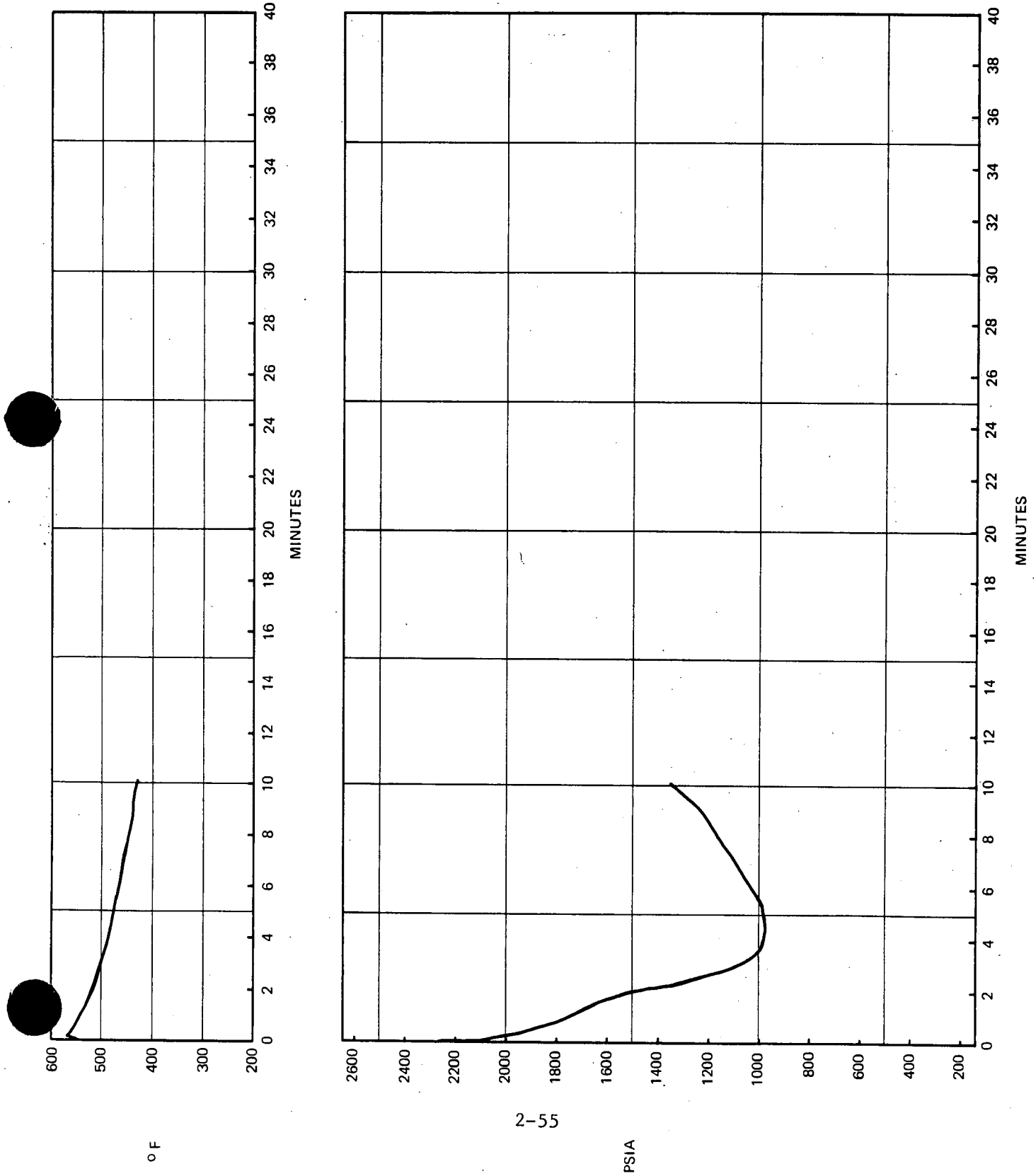

Figure 2.4-6

Overcooling Transient Simulation Results

Case 5 - Turbine Bypass System Failure

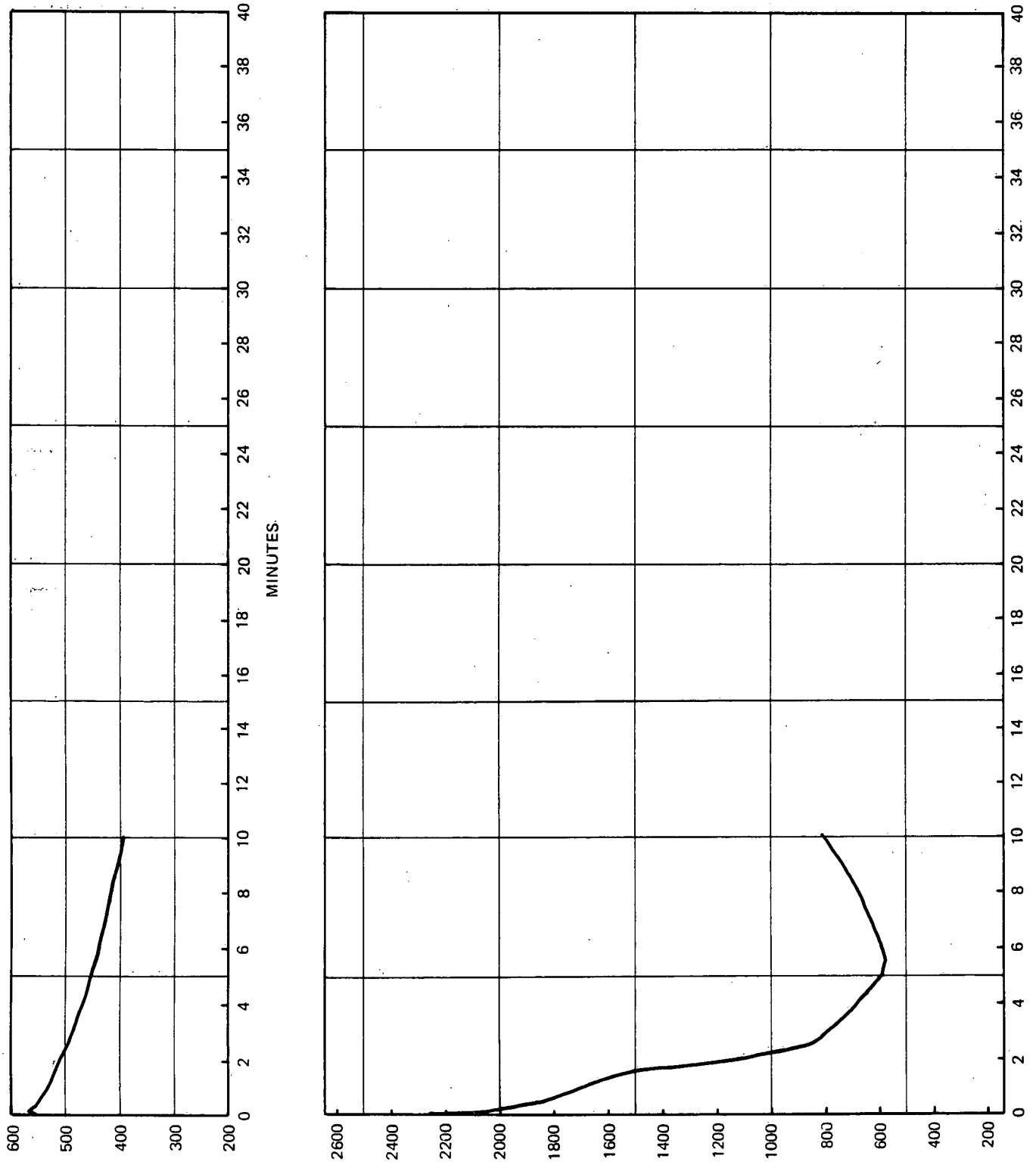

Figure 2.4-7

Overcooling Transient Simulation Results

Case 6 - Turbine Bypass System Failure

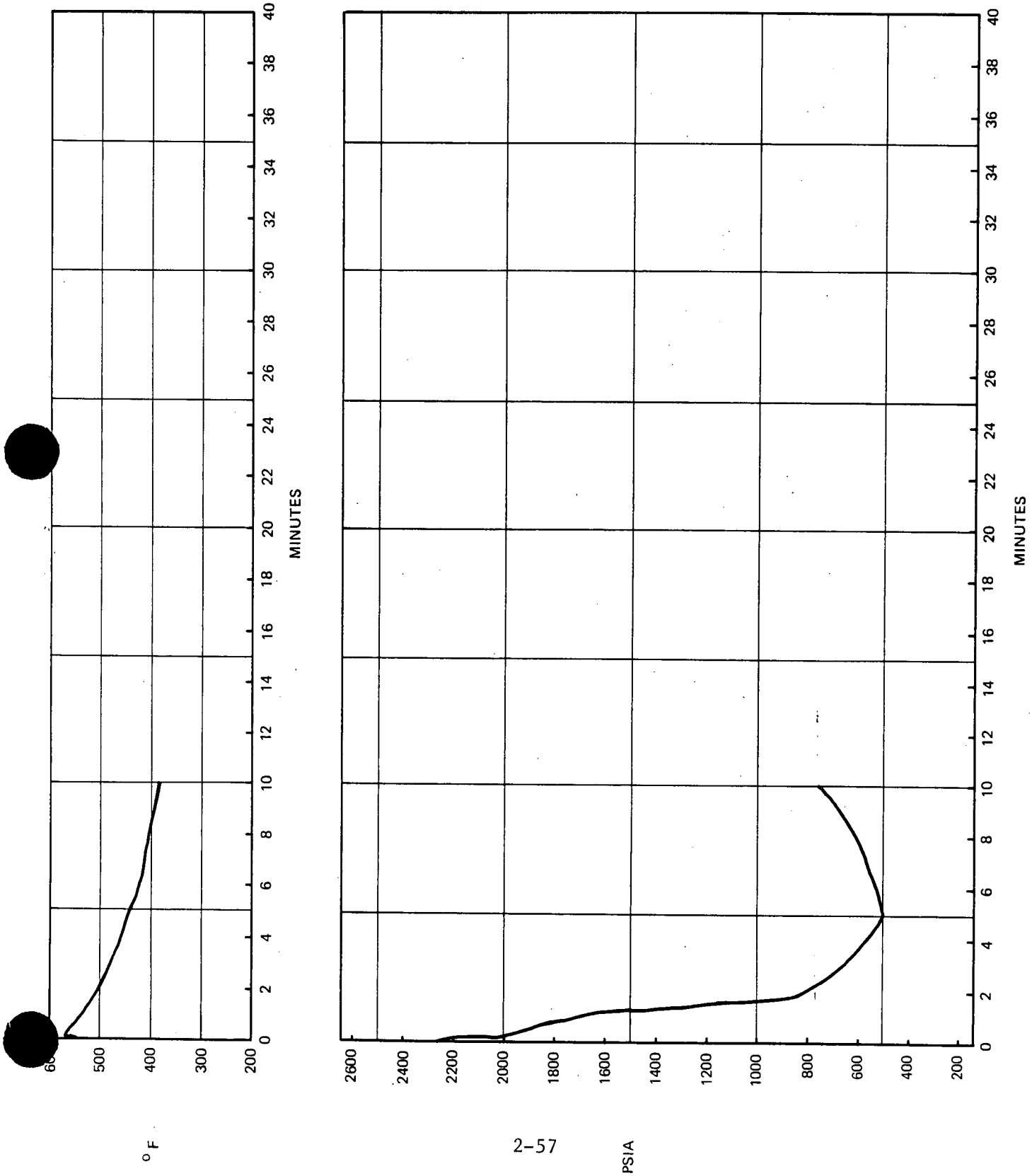

Figure 2.4-8

Overcooling Transient Simulation Results

Case 7 - Turbine Bypass System Failure

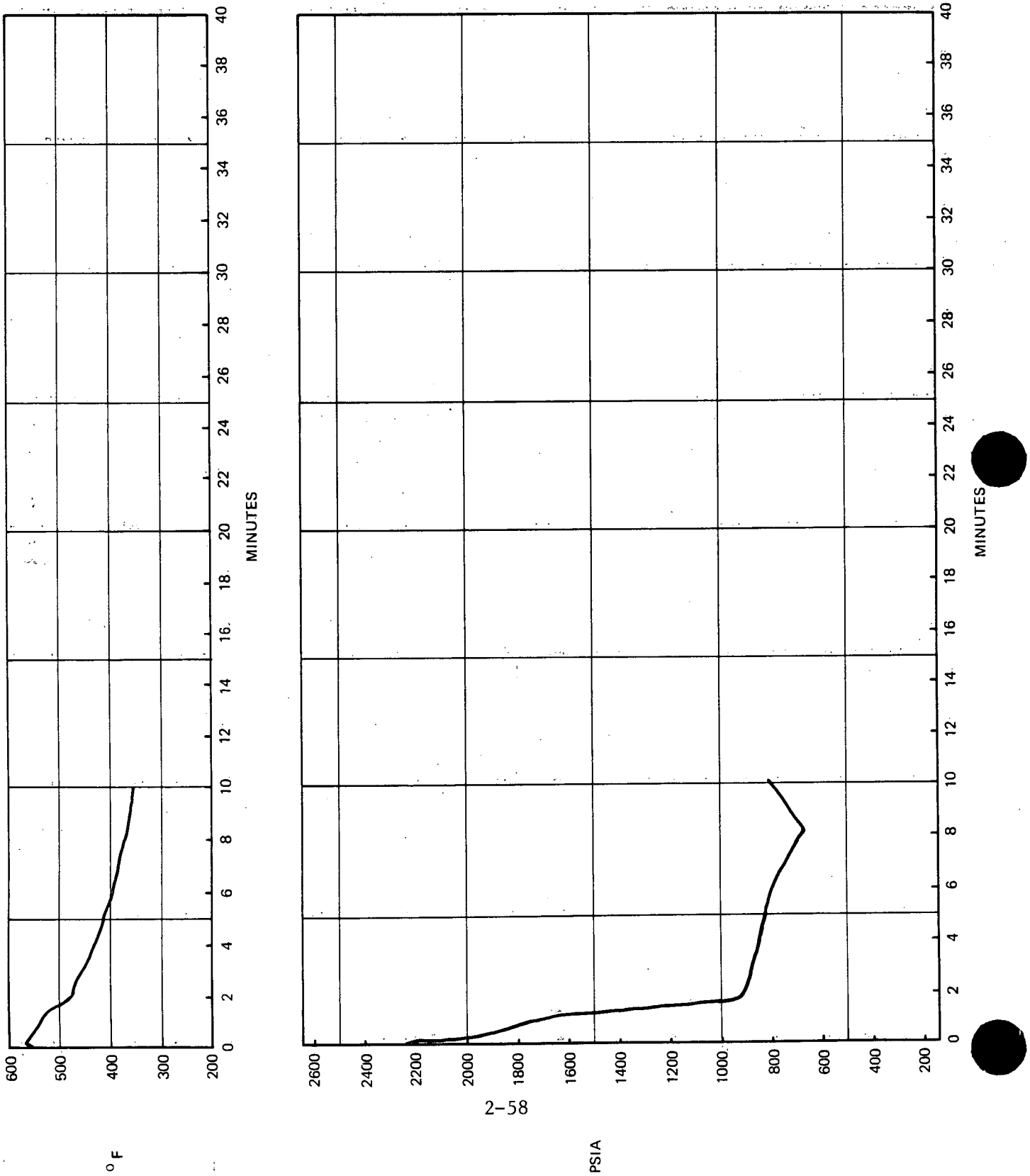

Figure 2.4-9

Overcooling Transient Simulation Results

Case 8 - Turbine Bypass System Failure

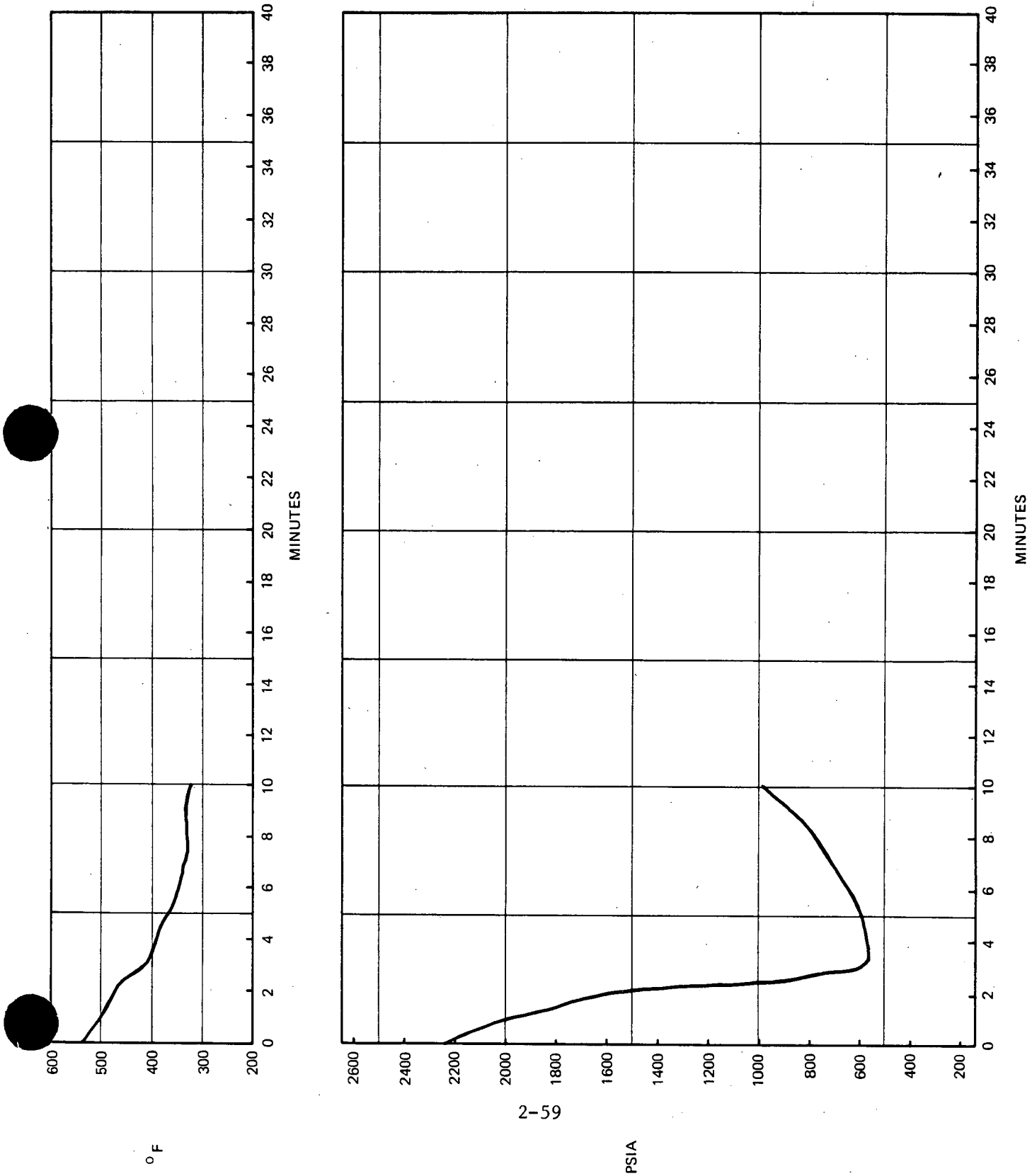

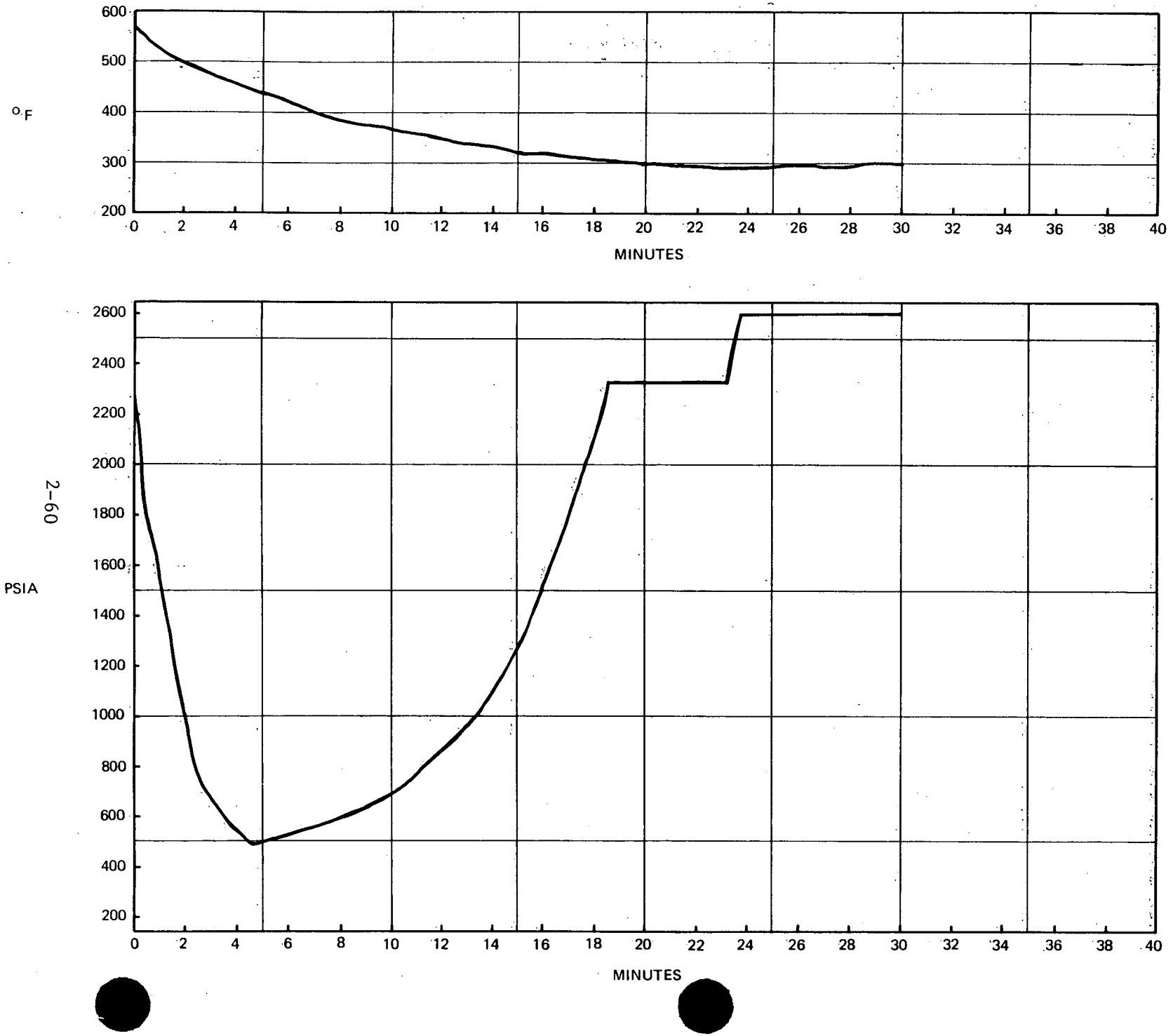

Figure 2.4-10

Overcooling Transient Simulation Results

Case 9 - Turbine Bypass System Failure

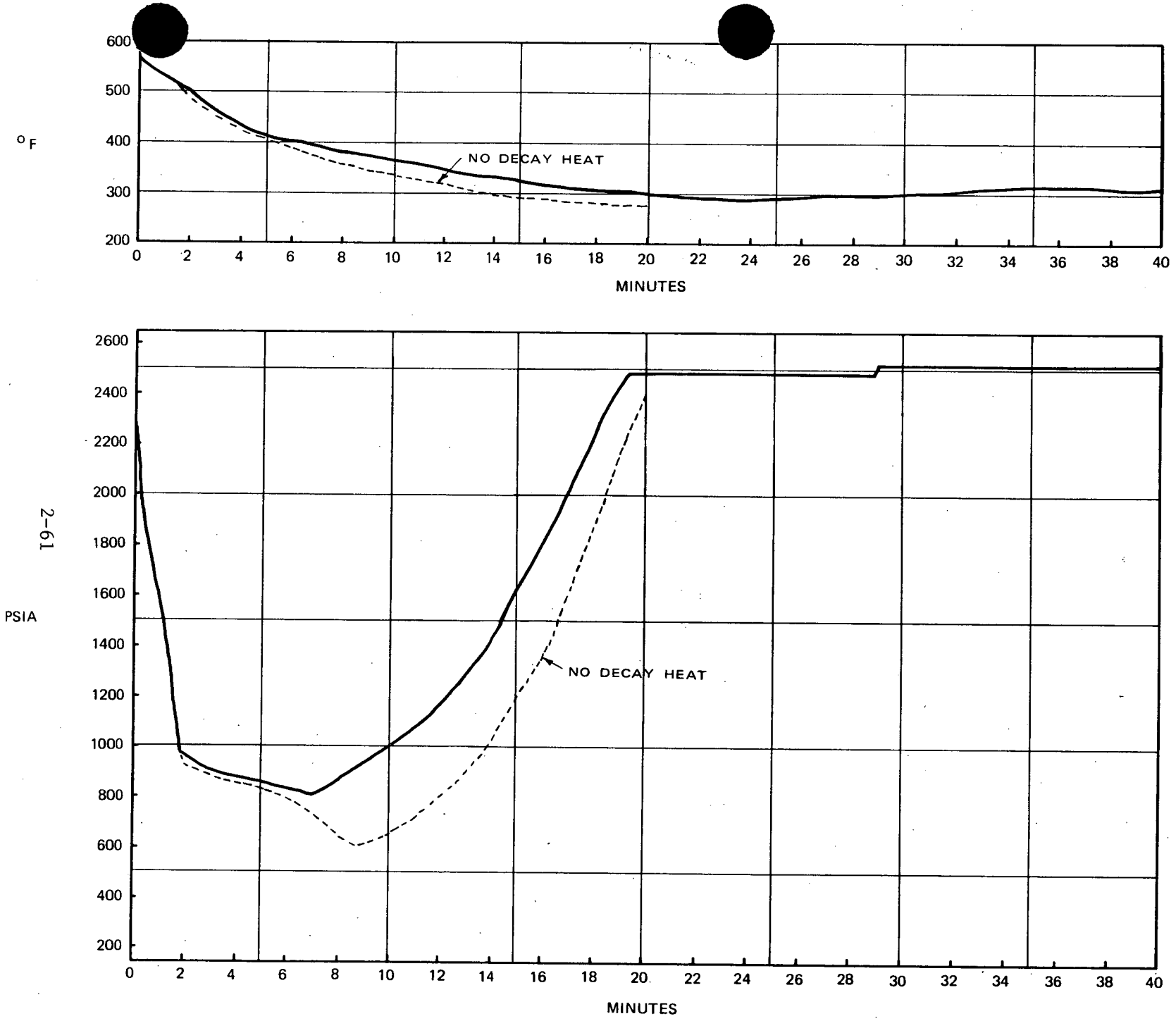

Figure 2.4-11

Overcooling Transient Simulation Results

Case 10 - Turbine Bypass System Failure

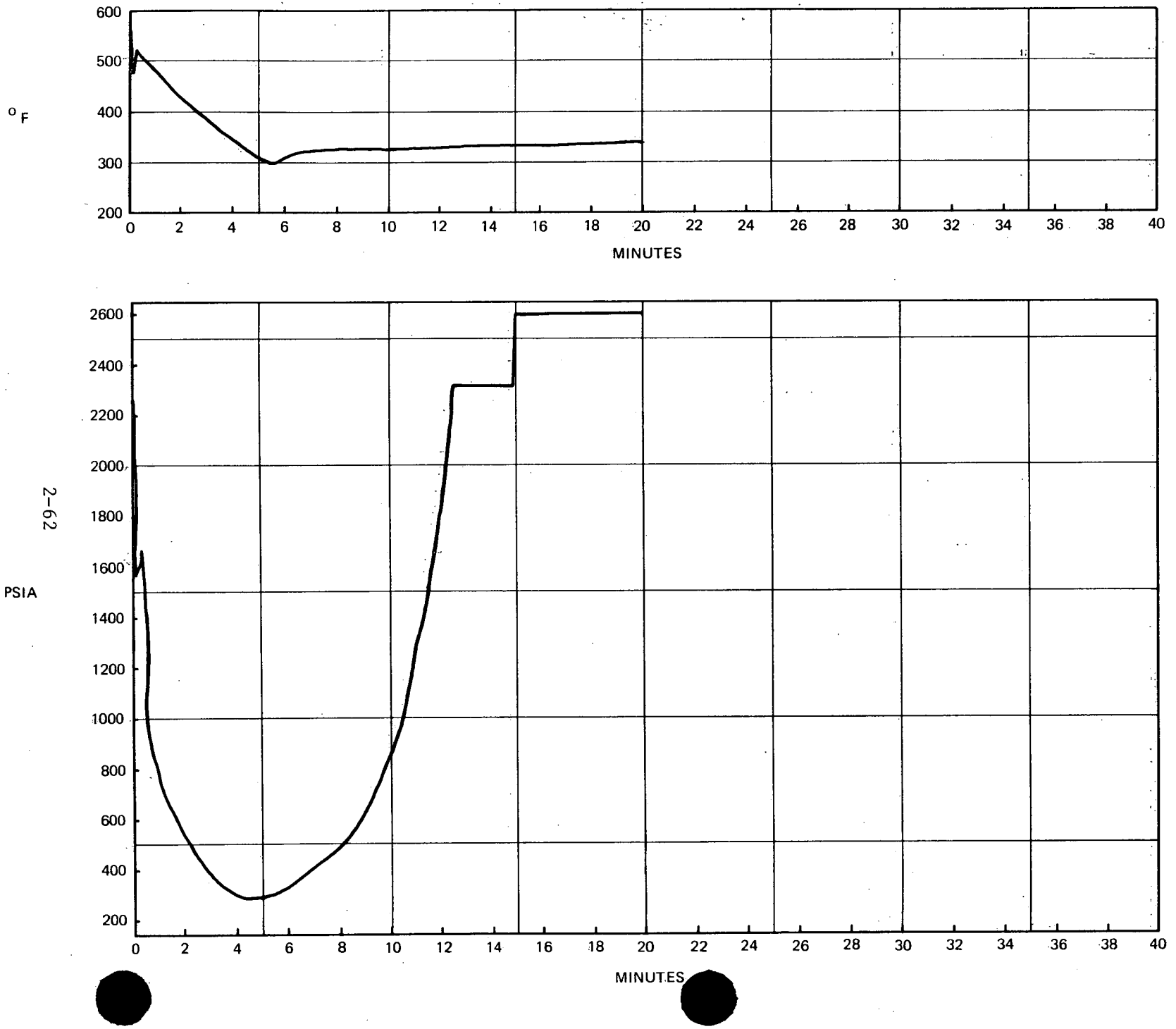

Figure 2.4-12

Overcooling Transient Simulation Results

Case 11 - Steam Line Break

Figure 2.4-13

Overcooling Transient Simulation Results

Case 12 - Steam Line Break

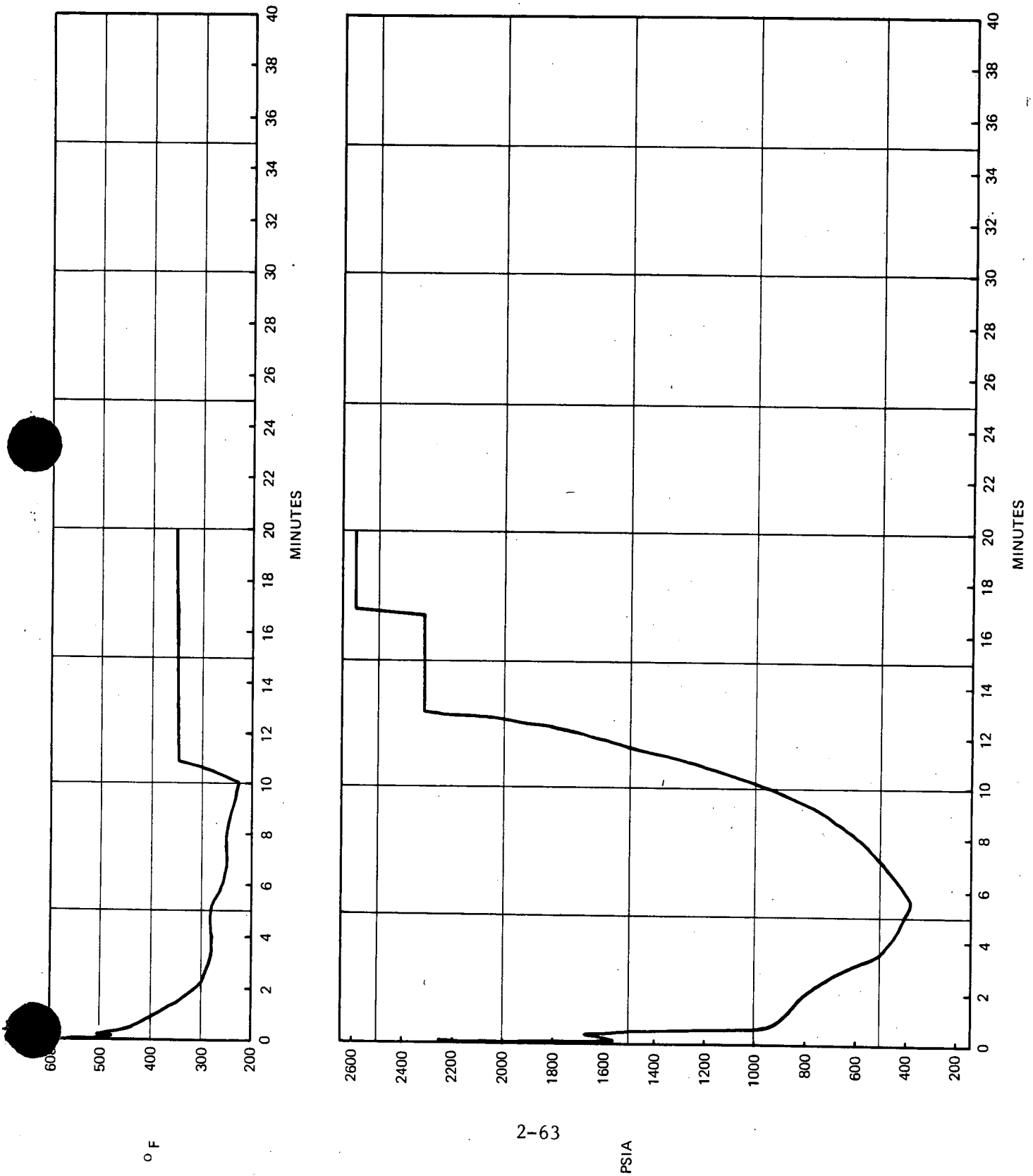

Figure 2.4-14

Overcooling Transient Simulation Results

Case 13 - Steam Line Break

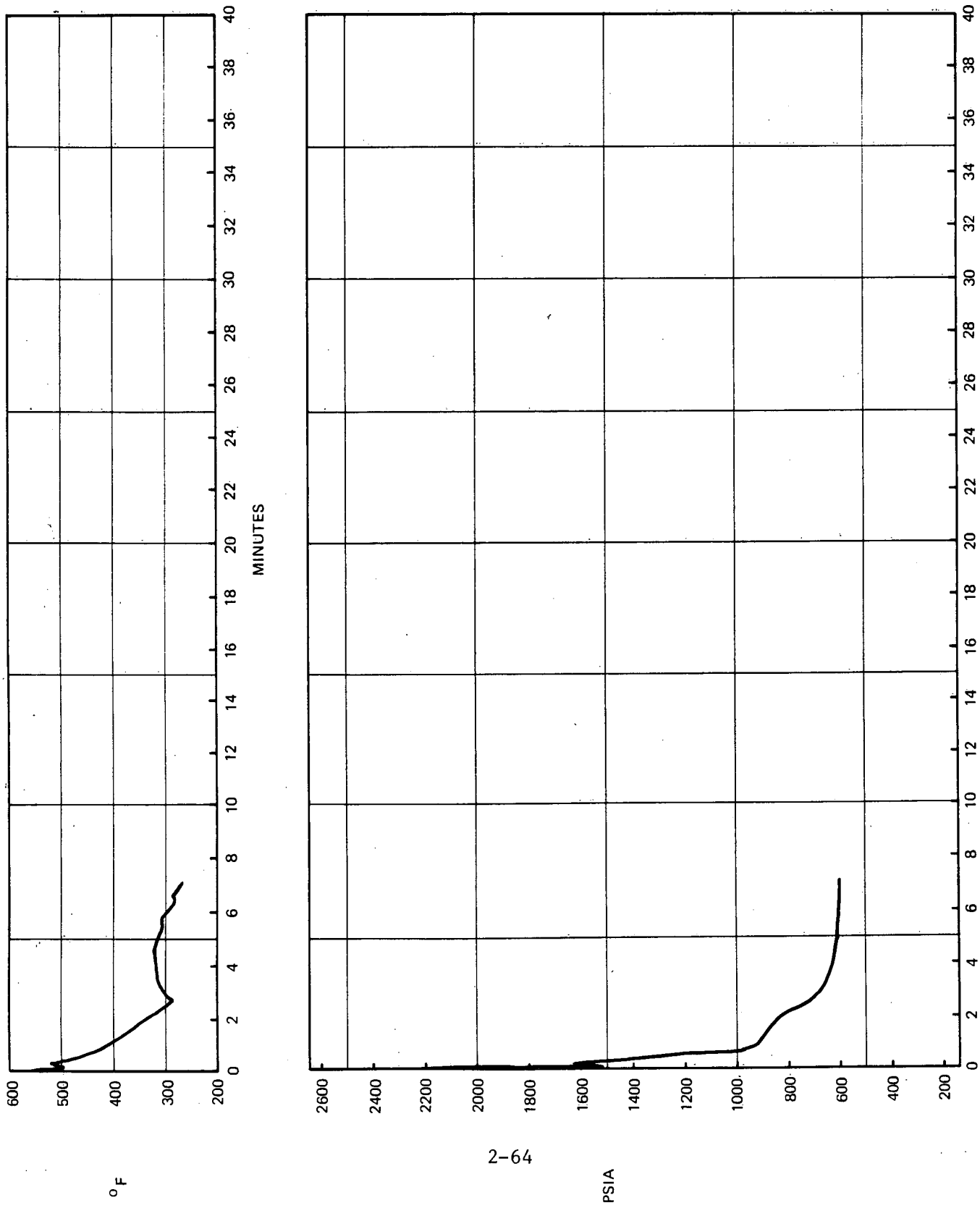

3.0 SMALL BREAK LOCA ANALYSIS

3.0 SMALL BREAK LOCA ANALYSIS

3.1 Introduction

In addition to the potential for reactor vessel thermal shock as a result of overcooling transients, a thermal shock condition can develop following a SBLOCA event. The SBLOCA can be considered to be those pipe breaks or valve failures which result in a loss of RCS inventory at a rate which does not rapidly and completely depressurize the RCS. The SBLOCA is characterized by a slow and sustained system depressurization rather than a violent blowdown typical of larger breaks. The primary safety concern for the SBLOCA is the assurance of long term core cooling. This function is performed by the ECCS for all credible LOCA events. The potential for reactor vessel thermal shock occurs due to the extended delivery of cold ECCS water into the RCS. Since certain SBLOCA events do not completely depressurize the system, the effect of the internal system pressure on the vessel must also be considered. This effect differentiates between the SBLOCA and the larger LOCA from the perspective of thermal shock.

The response of the RCS to a SBLOCA event is determined primarily by the break size. Other factors which affect the system response are the break location, the HPIS capacity, the decay heat power level, SG heat sink availability, and reactor coolant pumps on or off. These factors result in a sequence of events which can be characterized by the following scenario:

Prior to the initiating event, the normal circulation of coolant in the RCS is as shown in Figure 3.1-1. The initiation of the loss of coolant out the break causes a system depressurization which actuates the HPIS at a pressure of 1500 psig. Current operating procedures require the operator to trip all reactor coolant pumps immediately following actuation of the HPIS. If the capacity of the HPI pumps is greater than the break flow, the HPIS will maintain the RCS in a subcooled condition or return the RCS to a subcooled condition. Since the operator has control of system pressure, a controlled shutdown of the plant can be undertaken.

If the capacity of the HPI pumps is insufficient to offset the inventory loss, the RCS will continue to depressurize to a condition where the break flow essentially matches the HPI flow. This situation will be characterized by a nearly steady-state condition that is slowly changing as decay heat decreases. With the reactor coolant pumps tripped and feedwater being delivered to the SG's, a natural circulation mode of loop circulation and core cooling will occur. This mode will continue until such time that the inventory loss and depressurization causes a steam bubble to form at the top of the hot legs, effectively blocking loop flow. With feedwater being delivered to the SG's, a reflux boiling mode occurs until the RCS temperature decreases to less than the SG temperature. Subsequent core cooling is only by once-through HPIS cooling with energy removal out the break. Following loss of natural circulation, the reactor vessel internals vent valves will open once the pressure drop across the valve becomes sufficient. The geometry of the reactor vessel is shown in Figure 3.1-2. An example of the RCS conditions following loss of natural circulation is given in Figure 3.1-3 for the case of a break or valve failure at the top of the pressurizer. With the loss of loop circulation, the cold HPIS injection into the cold legs continues, which results in cold water being delivered into the reactor vessel downcomer. If the RCS pressure decreases below 600 psig, the CFTS also begins injecting cold water directly into the downcomer. The warmer water flowing through the vent valves then mixes with the cooler water flowing from the cold legs in both the cold leg piping and in the downcomer. As a result the reactor vessel wall is then subjected to a spatial and temporal distribution of downcomer water temperature. The resultant temperature gradient in the vessel in combination with the RCS pressure cause the potential for pressurized thermal shock of the vessel.

Current operating procedures require the operator to immediately trip the reactor coolant pumps on the low RCS pressure ESFS actuation. The HPI pumps are to remain in operation until either:

1. Both LPI pumps are in operation and have been delivering >1000 gpm each for at least 20 minutes.

2. All hot and cold leg temperatures are at least 50°F subcooled. The degree of subcooling is to be limited by the pressure-temperature curve (Figure 3.1-4).

3. Operator action must be taken to prevent an unsafe condition.

In summary, the operator guidelines are to throttle HPI to assure a subcooled margin greater than 50°F but limits the subcooled margin where thermal shock becomes a concern. Figure 3.1-4 accounts for the acceptable combination of system pressure and temperature with respect to thermal shock based on near term vessel fluence.

3.2 SBLOCA Selection

Selection of the SBLOCA to be analyzed required an evaluation of the key factors determining the system response. These factors were identified as the break size, break location, HPIS capacity, decay heat power level, SG heat sink availability, and reactor coolant pumps on or off. The effect of each factor on reaching the system conditions most adverse with respect to thermal shock, and the timeframe involved were considered. The basis for selection included the analysis experience gained in the SBLOCA analyses performed in the B&W Topical Report, "Thermal-Mechanical Report - Effect of HPI on Vessel Integrity for Small Break LOCA Event With Extended Loss of Feedwater," BAW-1648.[2]

The break size has been identified as the most important factor since it determines the system pressure response and the rate of loss of RCS inventory. Smaller breaks result in higher system pressures, higher temperatures, and lower HPIS flowrates. A minimum break size threshold for loss of natural circulation exists, for which a smaller break will not evolve into the HPI cooling mode. Larger breaks are bounded by the threshold for which a larger break will result in the RCS completely depressurizing. The break size selected, 0.023 ft^2, corresponds to the flow area of the largest pressurizer safety valve in an Oconee class plant. This size was determined to be in the break size range that

results in the coldest downcomer temperatures without completely depressurizing the RCS. A discharge coefficent of 1.0 was used with the Moody critical flow model.

The break location selected was a break at the top of the pressurizer. For the scenario of interest the system response to a pressurizer break is essentially the same as that of a hot leg break. A cold leg break is less severe for two reasons. Depending on the cold leg break location, some fraction of the HPI injection would be lost out the break, thereby resulting in less cold water being delivered to the vessel. A cold leg break would also result in higher vent valve flow, since the hot fluid leaving the reactor vessel through the outlet nozzles for a pressurizer or hot leg break would flow through the vent valves for a cold leg break.

The HPIS capacity selected is the maximum three pump flow at Oconee. This flowrate bounds all Oconee class plants with the exception of Davis Besse which has significantly higher flow at low RCS pressures. The HPI water is assumed to be at a temperature of 50°F. Operator action to throttle HPI in order to maintain a maximum subcooling margin of 100°F is assumed.

The case analyzed assumes that the reactor trips from full power at time zero. The decay heat power level selected is the ANS standard decay heat power corresponding to a core burnup of 400 EFPD with a multiplier of 1.0.

The availability of a SG heat sink is important only when loop circulation is maintained. For the case analyzed SG heat removal does not affect the system response since natural circulation is lost and not recovered. All feedwater is terminated at time zero.

The reactor coolant pumps are required to be tripped on low RCS pressure ESFS actuation. Since the thermal shock concern occurs following loss of natural circulation, the pumps are tripped at time zero in the analysis in order to accelerate the approach to the loss of natural circulation. No restart of the pumps is assumed.

A summary of the key assumptions in the SBLOCA analysis is given in Table 3.2-1.

3.3 SBLOCA Analysis

The objective of the SBLOCA analysis was to simulate the system response and determine the RCS pressure, HPIS flowrate, vent valve flowrate and temperature, and the timing of significant events. These parameters were then used as boundary conditions for the fluid mixing and fracture mechanics analyses. The simulation consisted of two parts. The first part is a multinode digital simulation performed with the CRAFT code from time zero to the point where the 100°F core outlet temperature subcooling margin was reached. As identified earlier, the system at that point in time is at a nearly steady-state condition. For that reason, a calculation based on the laws of mass and energy conservation in the system is used to continue the simulation. A detailed discussion and justification of this method follows.

3.3.1 CRAFT Simulation Model

The CRAFT nodalization used for the first part of the simulation is shown in Figure 3.3-1. Although the nodalization appears to be rather coarse it is very sufficient for the case being analyzed due to the relatively quiescent nature of the SBLOCA. This was demonstrated by comparison with a 22 node model in BAW-1648, which showed very comparable pressure and temperature results. Both HPIS and CFTS injection are delivered directly to the reactor vessel downcomer. Since the code homogeneously mixes all fluids entering a node, no detailed fluid temperature distribution results can be extracted. The flow components are separately recombined in the mixing analysis.

3.3.2 Steady-State Simulation Model

Under the steady-state assumption, the rate of change of mass (M_{RCS}) and energy (E_{RCS}) in the RCS is zero:

$$\frac{dM_{RCS}}{dt} = \frac{dE_{RCS}}{dt} = 0 \qquad (1)$$

Then the core outlet enthalpy is calculated:

$$h_h = \frac{q}{W_{HPI}} + h_{HPI} \qquad (2)$$

where h_h = core outlet enthalpy (Btu/lbm)

h_{HPI} = enthalpy of HPI water (Btu/lbm)

W_{HPI} = HPI flow (lbm/sec)

q = decay heat (Btu/sec)

The vent valve flow is determined by performing an energy balance in the downcomer region:

$$W_{vv} = W_{HPI} \frac{h_c - h_{HPI}}{h_h - h_c} \qquad (3)$$

where h_c = core inlet enthalpy (Btu/lbm)

W_{vv} = vent valve flow (lbm/sec)

The vent valve flow, which can also be calculated from the elevation pressure drop across the vent valve is given by:

$$W_{vv} = \sqrt{\frac{288\ g_c\ \rho_h\ A^2_{vv}\ \Delta P}{k_{vv}}} = 96.26\ A_{vv} \sqrt{\frac{\rho_h\ \Delta P}{k_{vv}}} \qquad (4)$$

where ρ_h = core outlet density (lbm/ft^3)

A_{vv} = vent valve flow area (ft^2)

k_{vv} = loss coefficient

ΔP = elevation pressure drop (psi)

$= H\ (\rho_c - \rho_h)/144,$

ρ_c = core inlet density (lbm/ft^3)

H = elevation head (ft)

Assuming a system pressure and a downcomer water temperature T_c, the vent valve flow W_{vv} can be calculated using equations 3 and 4. The downcomer water temperature is determined by iterating on the assumed T_c until equations 3 and 4 predict the same vent valve flow.

At steady-state conditions, the relationship of HPI flow to leak flow is defined as:

$$W_L = W_{HPI}\ \frac{\nu_{HPI}}{\nu_L} \qquad (5)$$

where W_L = leak flow (lbm/sec)

W_{HPI} = HPI flow (lbm/sec)

ν_{HPI} = specific volume of HPI (ft^3/lbm)

ν_L = specific volume of core outlet water (ft^3/lbm)

Assuming a system pressure and 100°F subcooling, the leak flow can be calculated by the Moody correlation. Equation 6 is used to determine the HPI flow (W_{HPI}) required to maintain 100°F subcooling. Equation 5 is used as a convergence criterion for determining the system pressure. If W_{HPI} and W_L satisfy the equation, the system pressure is determined, then the equations 3 and 4 are used in the same manner to determine the vent valve flow.

$$q = W_{HPI} (h_p - h_{HPI}) \qquad (6)$$

where q = decay heat rate (Btu/sec)

h_h = enthalpy of core outlet water based on the 100°F subcooled state (Btu/lbm)

h_{HPI} = enthalpy of HPI water (Btu/lbm)

W_{HPI} = HPI flow rate (lbm/sec)

For the steady state analysis, the mixed downcomer temperature was calculated to be equal to the saturation temperature minus 150°F. This value is based on the assumption of 100°F subcooling at the core outlet plus 50°F core ΔT. This steady-state analytical method was benchmarked in BAW-1648 against the craft analysis for the 0.007-ft^2 pressurizer break with no operator action. The results indicate that the steady-state code predicts the downcomer temperature approximately 9% above the

CRAFT prediction. The 9% deviation in the downcomer temperature was used as an adjustment factor for the breaks analyzed in BAW-1648 as well as the present analysis.

3.3.3 SBLOCA Simulation Results

Sequence of Events

Time (min)	Event Description
0	SBLOCA, reactor trip, reactor coolant pump, turbine trip, loss of all feedwater.
0.5	HPIS actuates.
1.5	Core outlet at saturation conditions.
5	SG's boil dry.
10	Core outlet returns to subcooled conditions.
10	Loss of natural circulation.
29	Achieve 50°F subcooled margin at core outlet.
50	Core flood tank injection begins.
93	Achieve 100°F subcooled margin at core outlet, operator throttles HPI to maintain 100°F subcooling.
180	End of simulation.

The results of the SBLOCA analysis are shown in Figures 3.3-2 through 3.3-8. The RCS pressure response shown in Figure 3.3-2 is characterized by a rapid depressurization until the pressurizer goes water solid. A slow rate of depressurization continues for the duration of the transient. The bulk reactor vessel downcomer temperature, Figure 3.3-3, shows the very slow system cooldown typical of the once-through HPI cooling mode. The loss of loop circulation flow is shown in Figure 3.3-4. The HPIS flow, Figure 3.3-5, is a function of RCS pressure until the core outlet temperature achieves the 100°F subcooled margin at

93 minutes. The operator is then assumed to throttle HPI flow to maintain the 100°F margin. As indicated in Figure 3.3-5, the throttling action does not significantly reduce HPI flow, so that the effect of this action is very small. The vent valve flow is shown in Figure 3.3-6. A comparison of vent valve flow to HPI flow indicates a minimum flow ratio of greater than 4 to 1, which emphasizes the strong influence of vent valve flow on the downcomer temperature.

The subcooling margin is shown in Figure 3.3-7. As identified in the previous paragraph, a long period of time is available before operator action would have to be taken. The SBLOCA transient analyzed is shown on a pressure-temperature diagram in Figure 3.3-8. This is the transient progression that an operator would follow using the ATOG approach for handling abnormal transients. The operator would immediately be aware of the rapid loss (90 seconds) of subcooling as the transient goes from point A to saturation at point B. With the HPI system at maximum flow it is not until point C is reached (93 minutes), that any operator action need be taken to throttle HPI flow to meet the requirement to limit core outlet subcooling margin to 100°F.

3.3.4 Summary

The system response to a SBLOCA has been analyzed with a set of assumptions which result in system conditions which have the potential to thermal shock the reactor vessel. Operator action to trip the reactor coolant pumps was assumed as specified in the procedures. This action is adverse from the perspective of thermal shock since thermal mixing of the cold ECCS water with the system inventory is not as efficient with the pumps off. Operator action was also assumed to throttle HPI flow to limit the core outlet subcooling margin to 100°F. The effect of this action is small for the case analyzed and did not occur until 93 minutes following transient initiation. The analysis has resulted in the calculation of the system parameters used for the detailed fluid mixing analysis and the vessel fracture mechanics analysis.

It is apparent that many of the key factors assumed are conservatively bounding. Examples of these are the ECCS water temperature, the maximum HPIS capacity, and the break location. Selection of other parameters, such as break size and decay heat power level, cannot be easily selected in a bounding sense since the effect of each on the system response is very dependent on the other assumptions incorporated in the analysis. An example of this is the effect of break size and decay heat power, along with the HPIS capacity, on the system pressure response. The results of the analysis support the assumptions made in that the RCS does not completely depressurize, which would have occurred for a larger break, and that the vessel temperatures are lower than would result from a smaller break size. The assumption of a lower decay heat power level would result in a faster system cooldown and an earlier timeframe for operator action to throttle the HPIS. The results of the case analyzed show that a substantial period of time for operator action to occur exists. Even with a reduction in the assumed decay heat power level, sufficient time will be available for event diagnosis and positive operator action.

Table 3.2-1

SBLOCA Analysis Assumptions

Break size	0.023 ft^2 (one PZR safety valve)
Break Location	Top of pressurizer
Initial power level	2568 MWt (100% power)
Decay heat	400 EFPD - 1.0 x ANS
HPIS capacity	3 Oconee pumps (Figure 2.1-3)
HPI temperature	50°F
Internals vent valves	All 8 available
Structural metal heat	Yes
Reactor coolant pumps	Tripped at time zero
Feedwater	Terminated at time zero
Operator action	Throttle HPI to limit core outlet subcooling to 100°F

Figure 3.1-1

RCS Flow During Normal System Operation

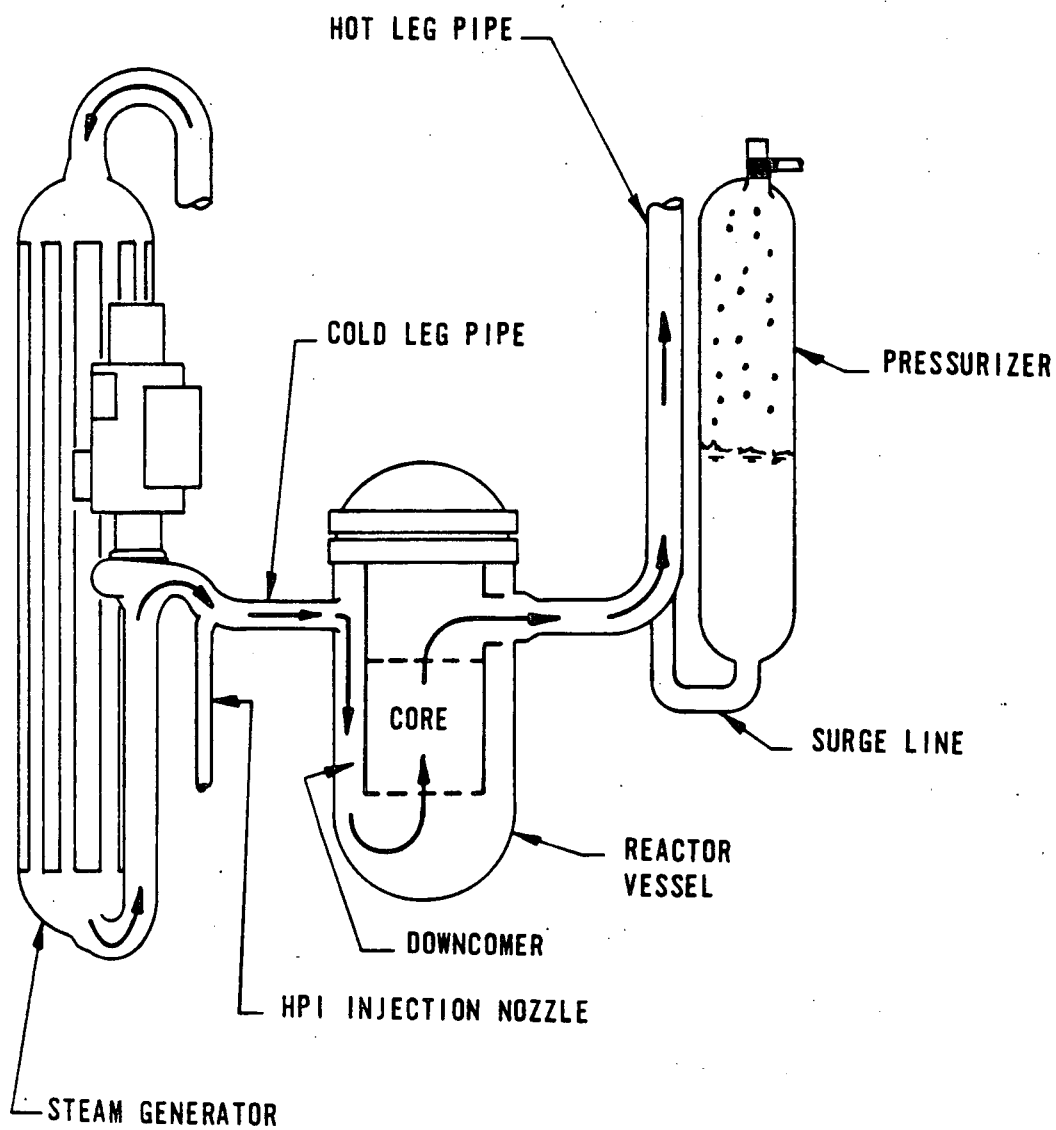

Figure 3.1-2

Reactor Vessel Geometry and Flow During SBLOCA

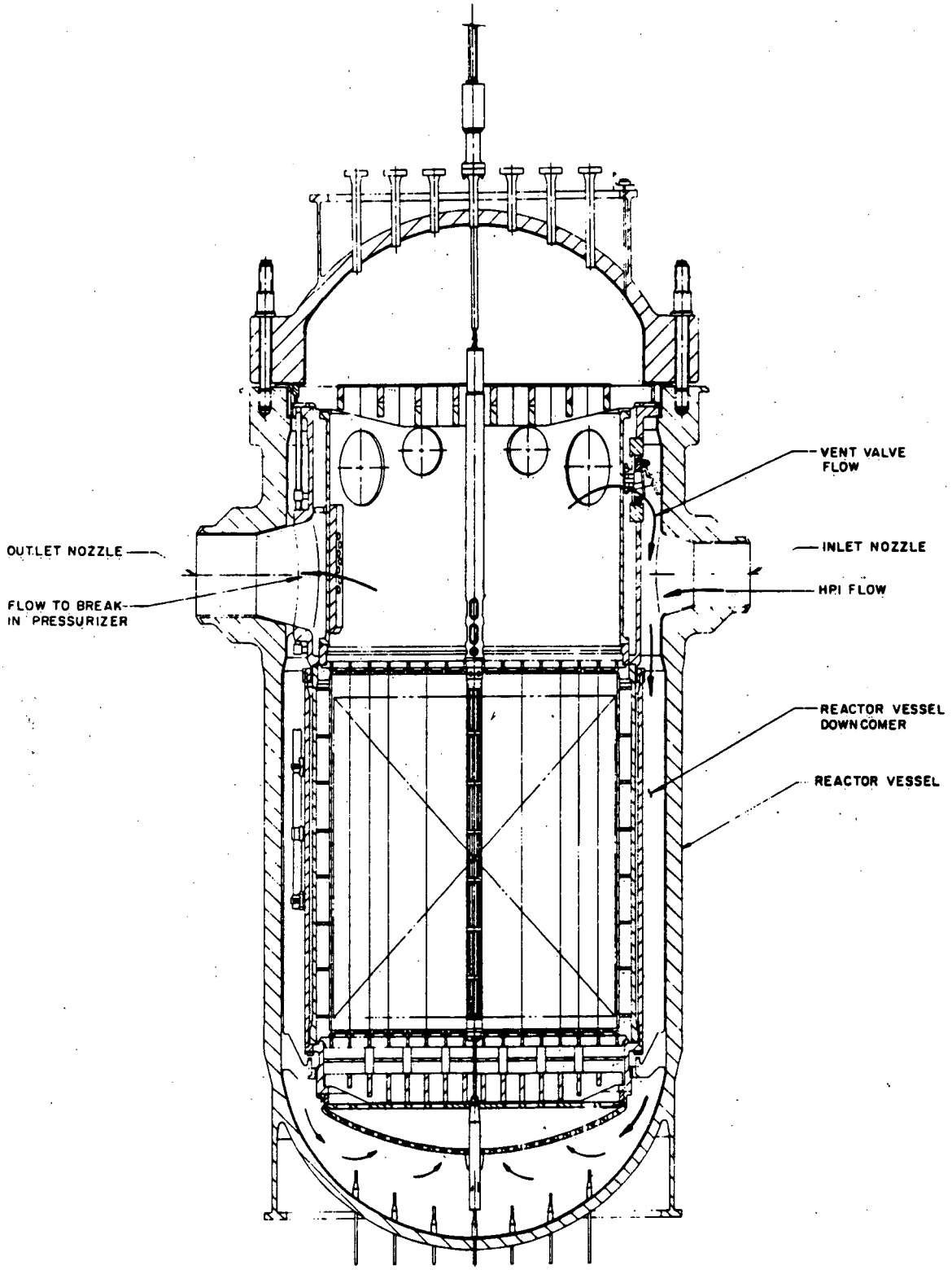

Figure 3.1-3

RCS Conditions During SBLOCA
at the Top of the Pressurizer

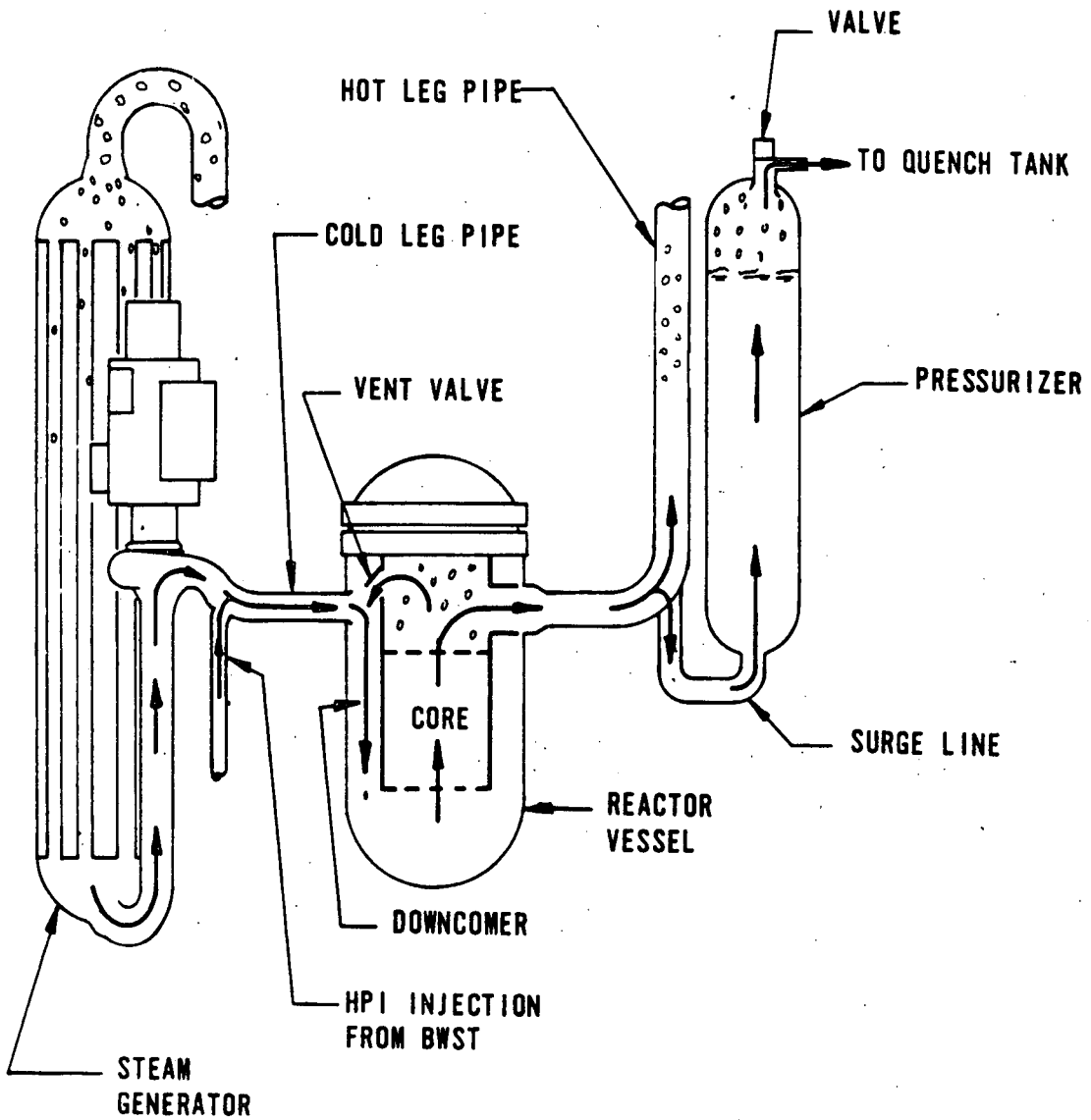

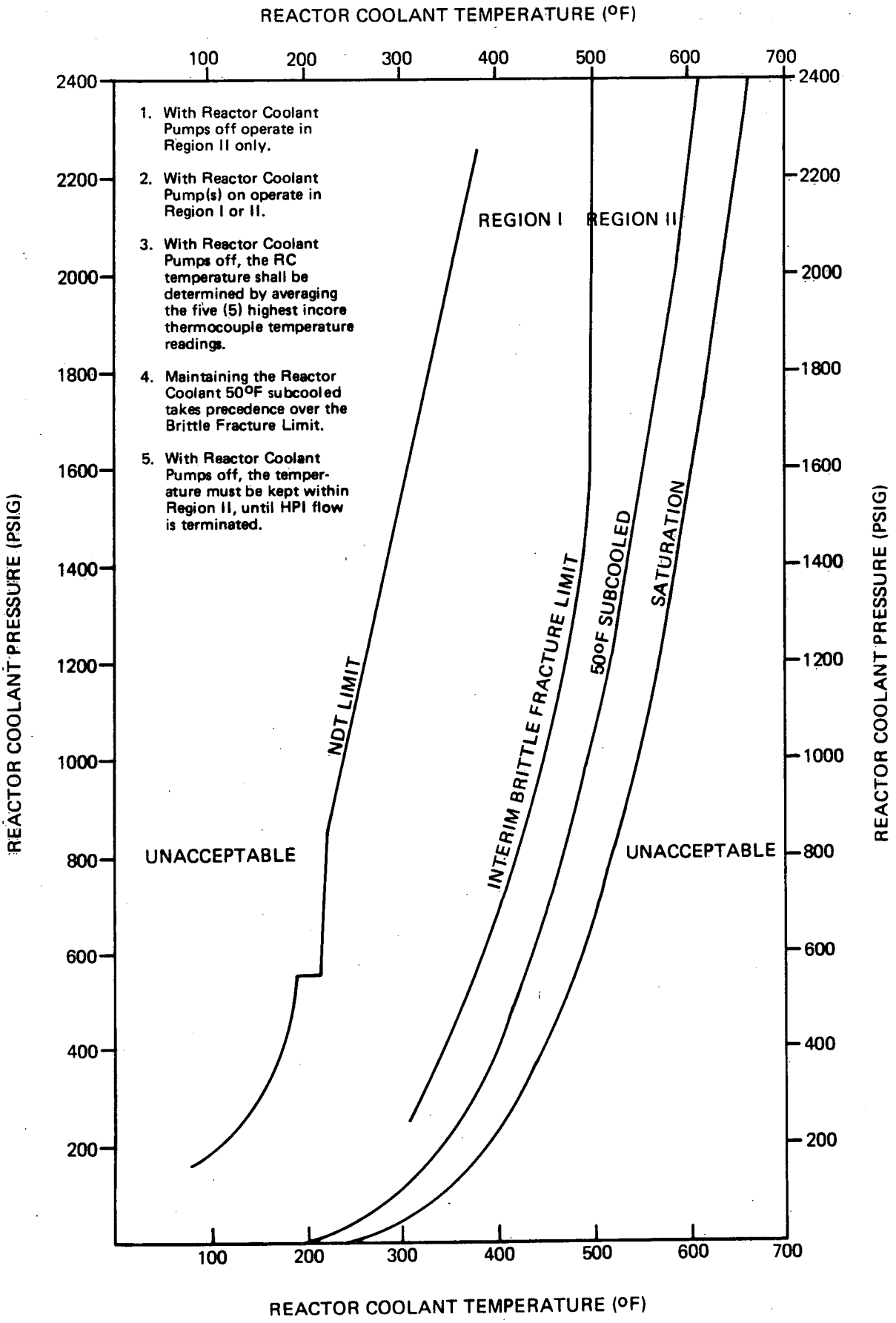

Figure 3.1-4

RCS Pressure-Temperature Curve

Figure 3.3-1

CRAFT Nodalization for SBLOCA

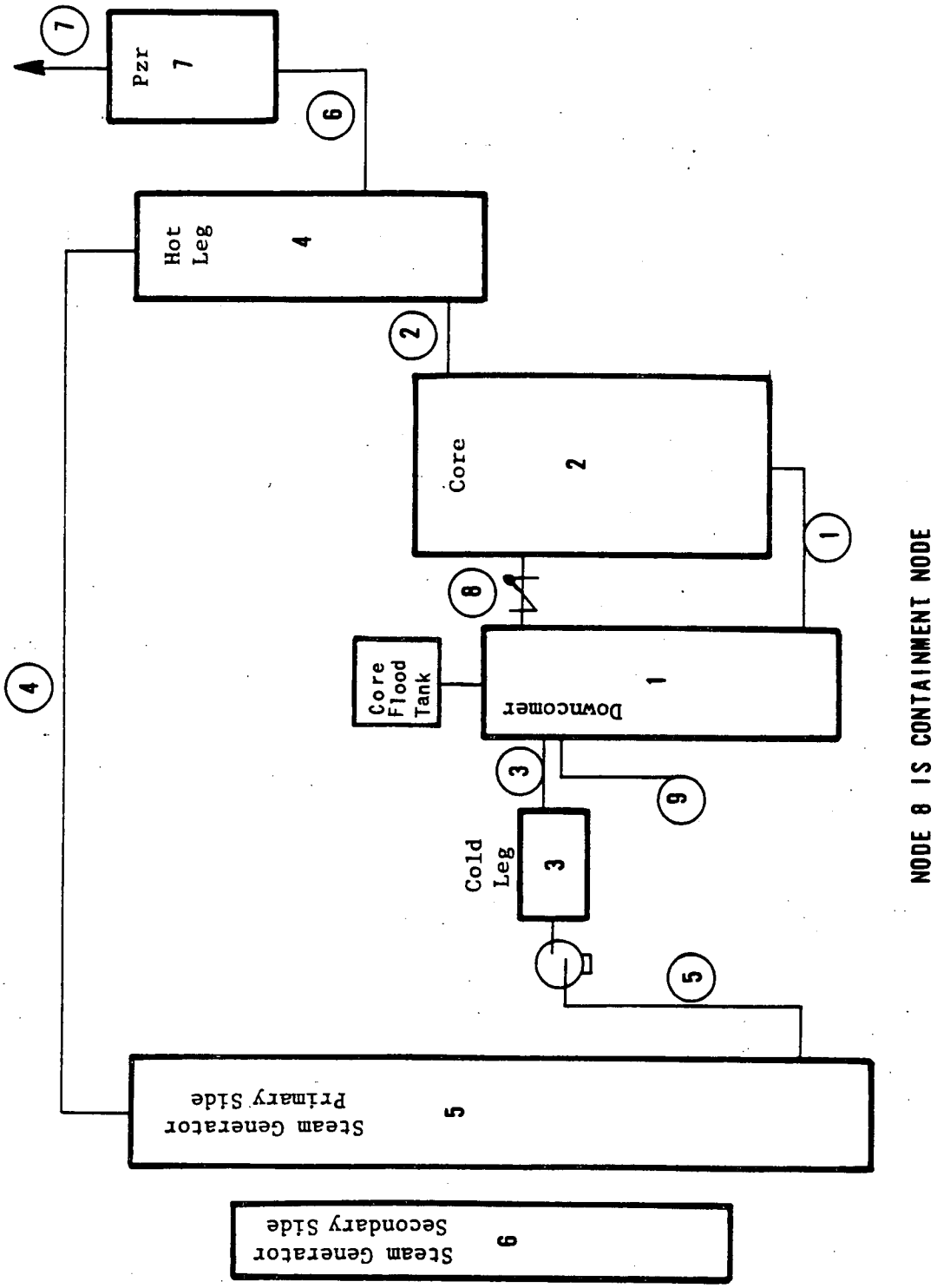

Figure 3.3-2

SBLOCA Simulation Results

Reactor Vessel Pressure

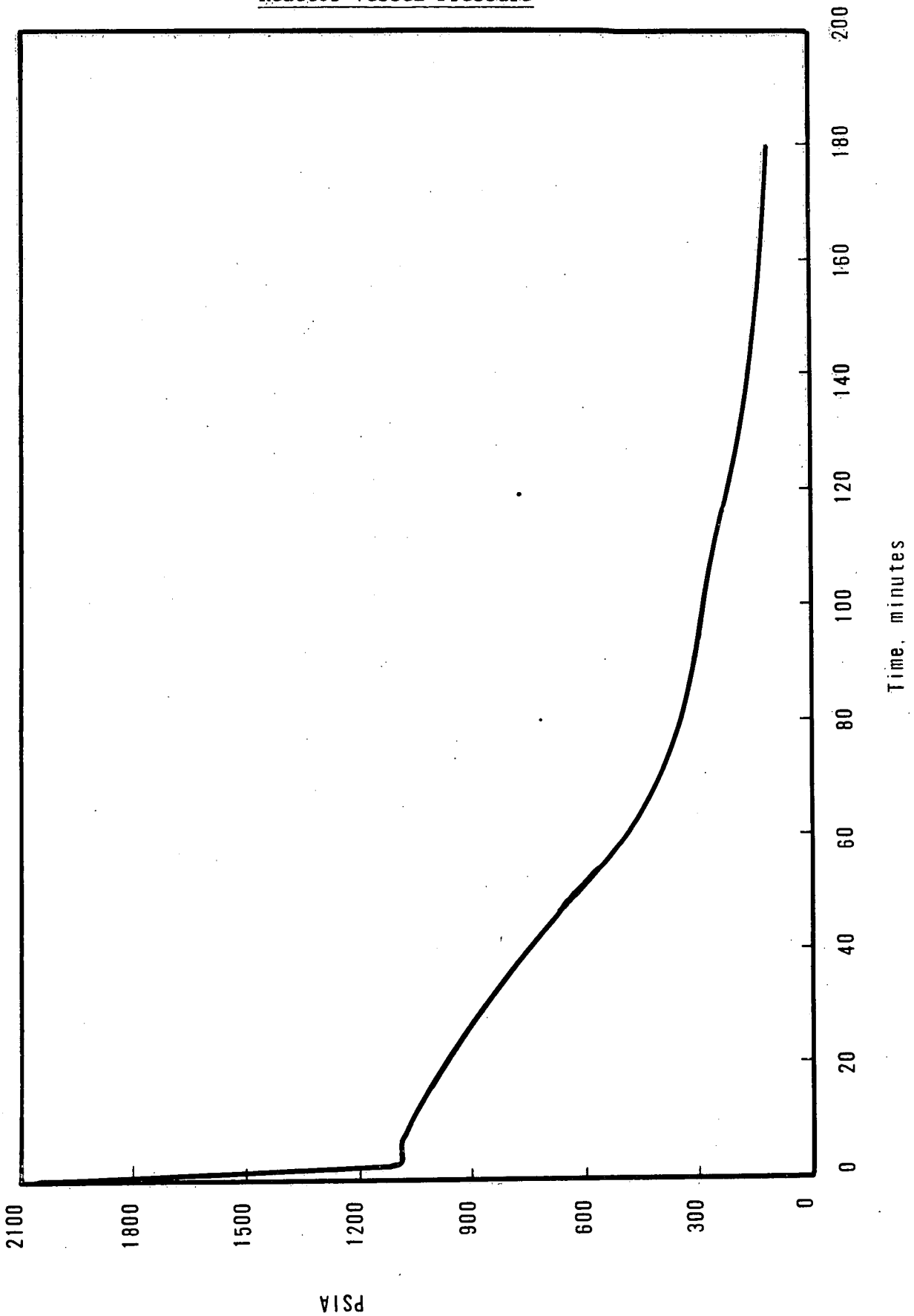

Figure 3.3-3

SBLOCA Simulation Results

Downcomer Temperature

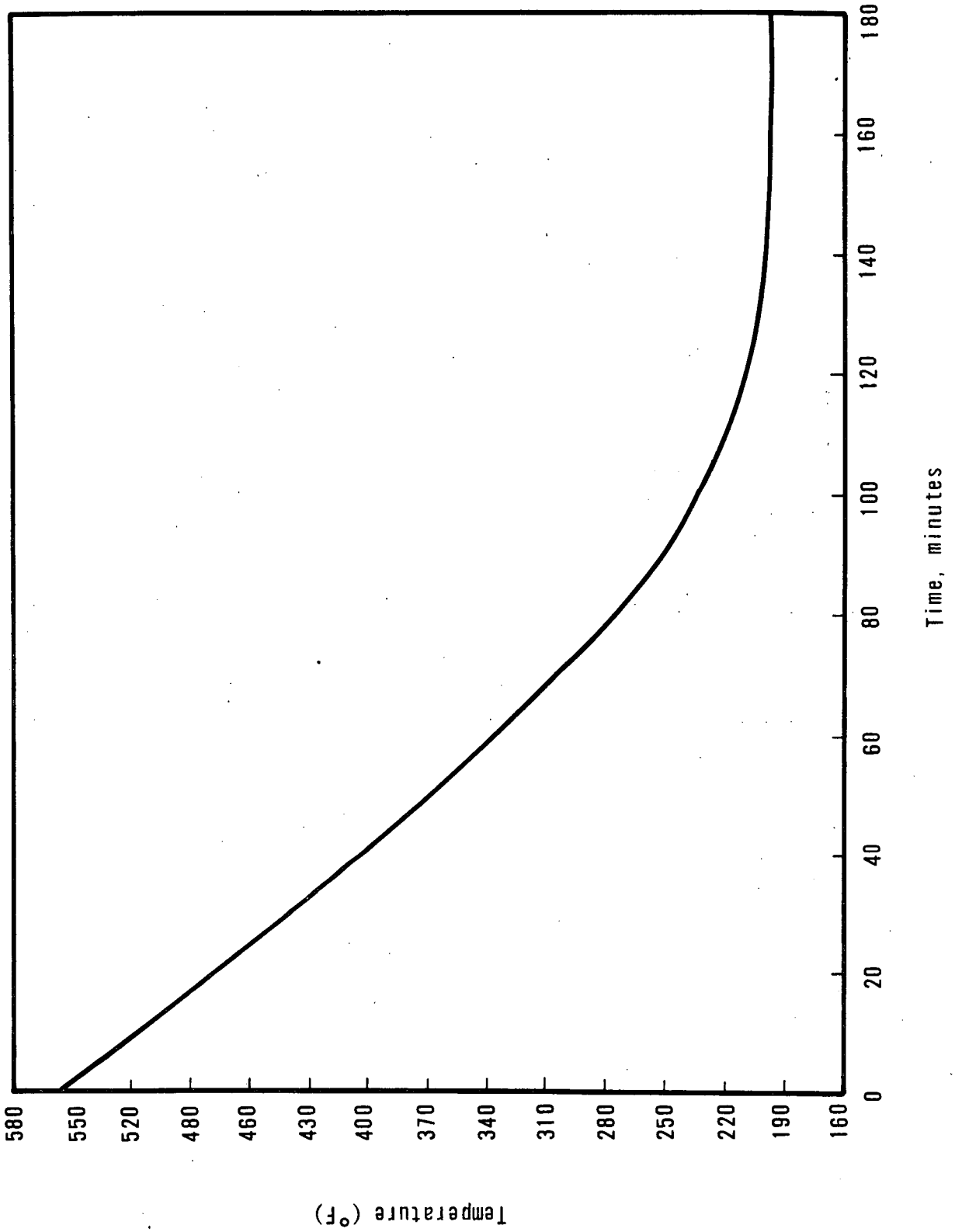

Figure 3.3-4

SBLOCA Simulation Results

RCS Loop Flow

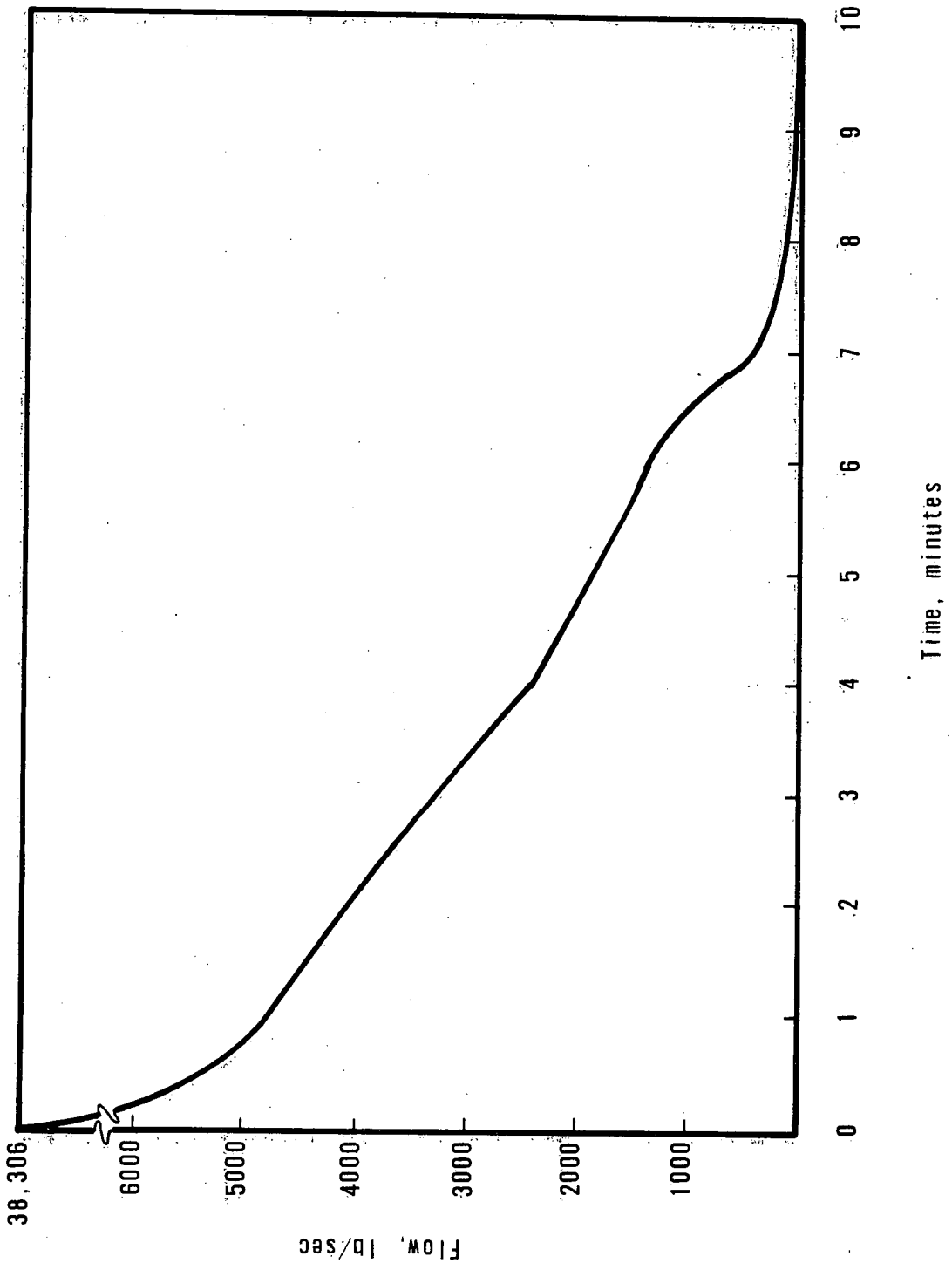

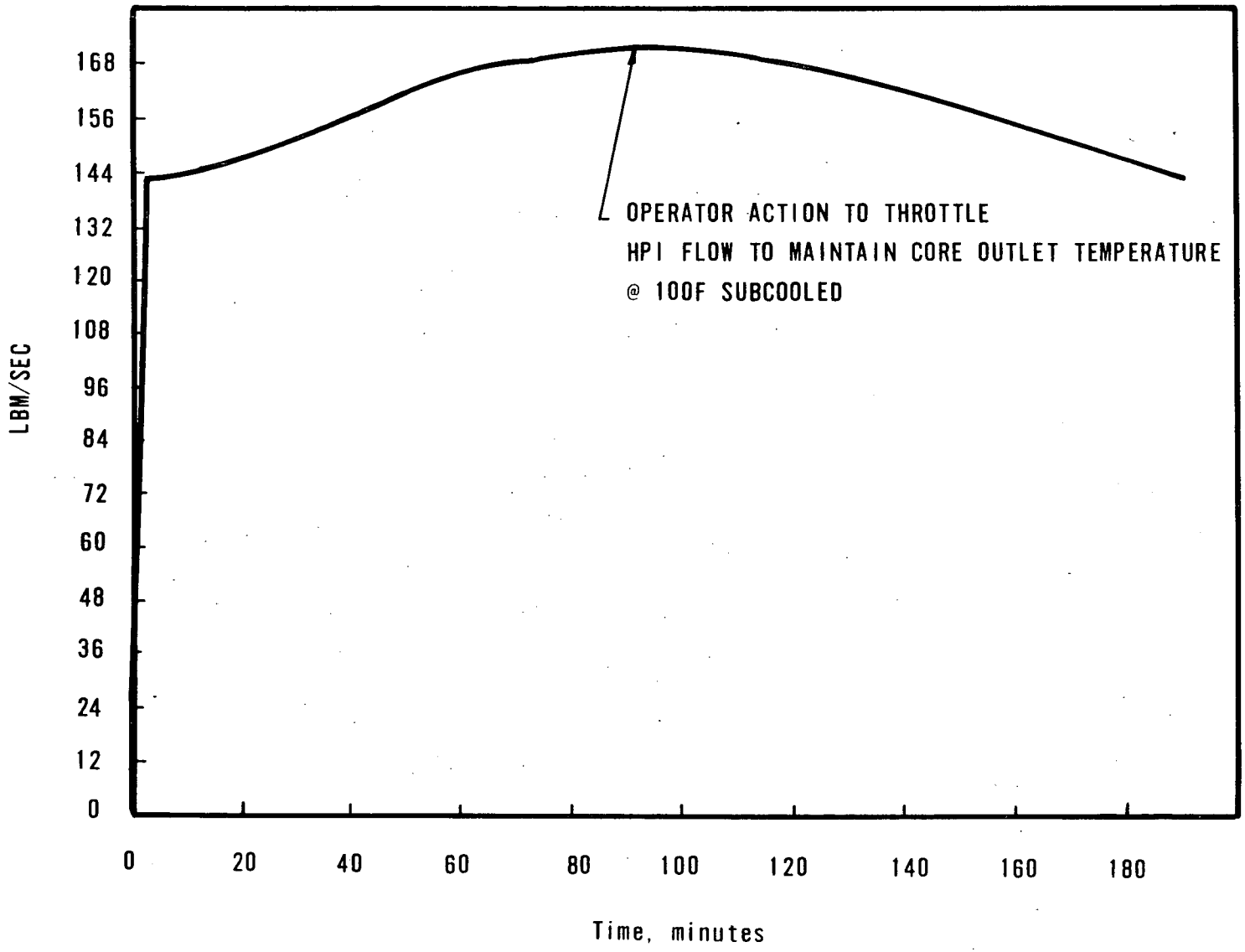

Figure 3.3-5

SBLOCA Simulation Results

HPIS Flow

Figure 3.3-6

SBLOCA Simulation Results

Vent Valve Flow

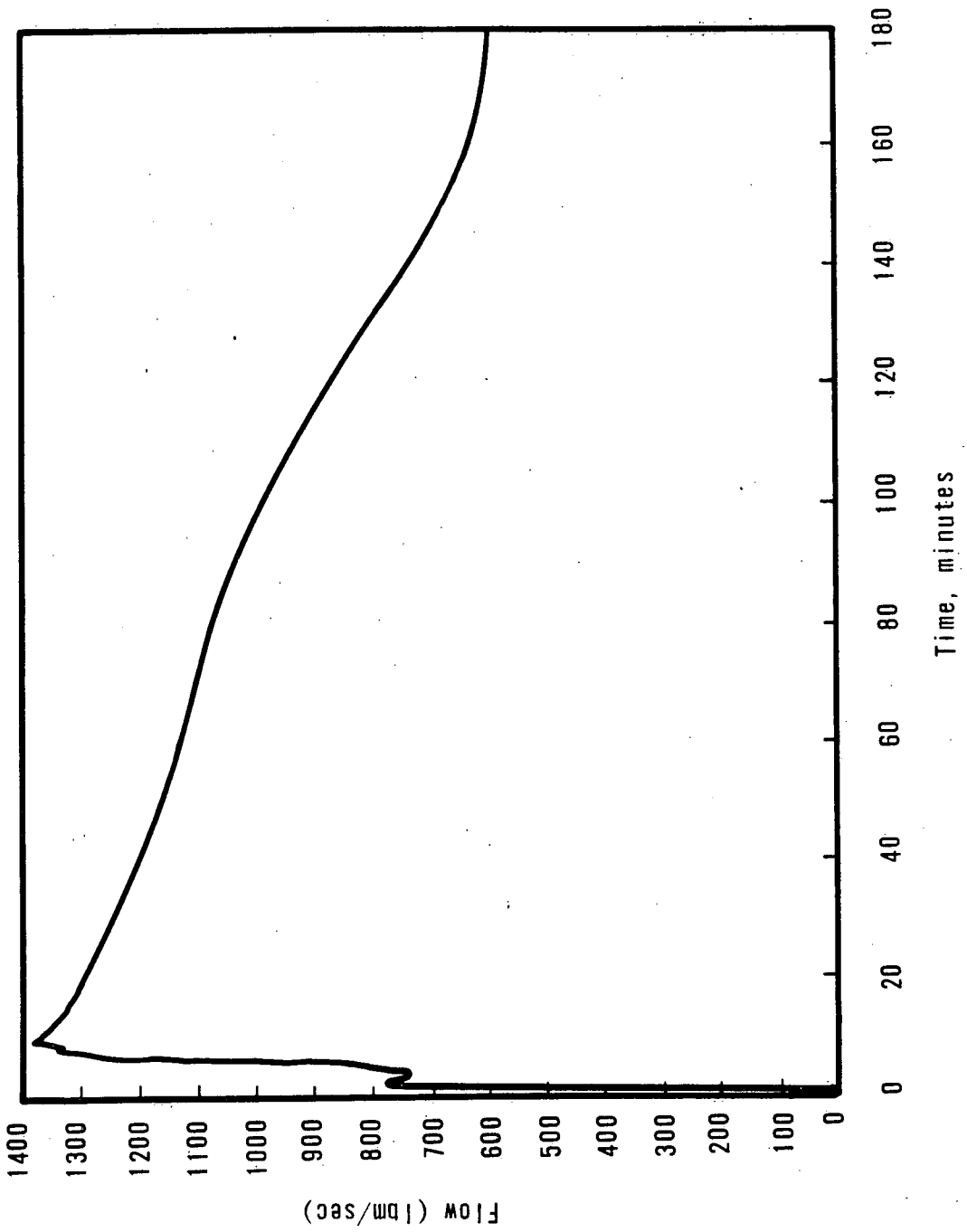

Figure 3.3-7

SBLOCA Simulation Results

Core Outlet Temperature and Subcooling Margin

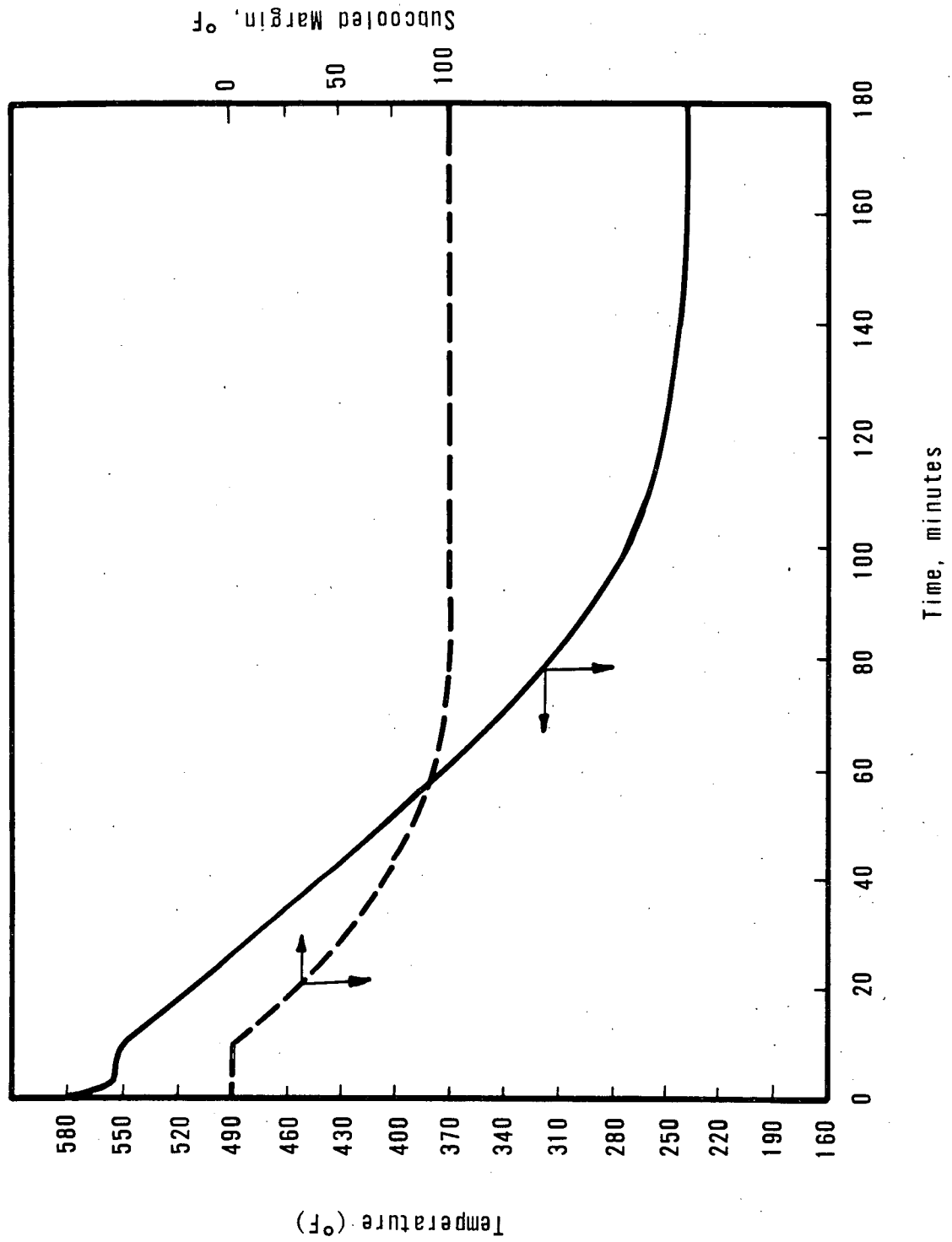

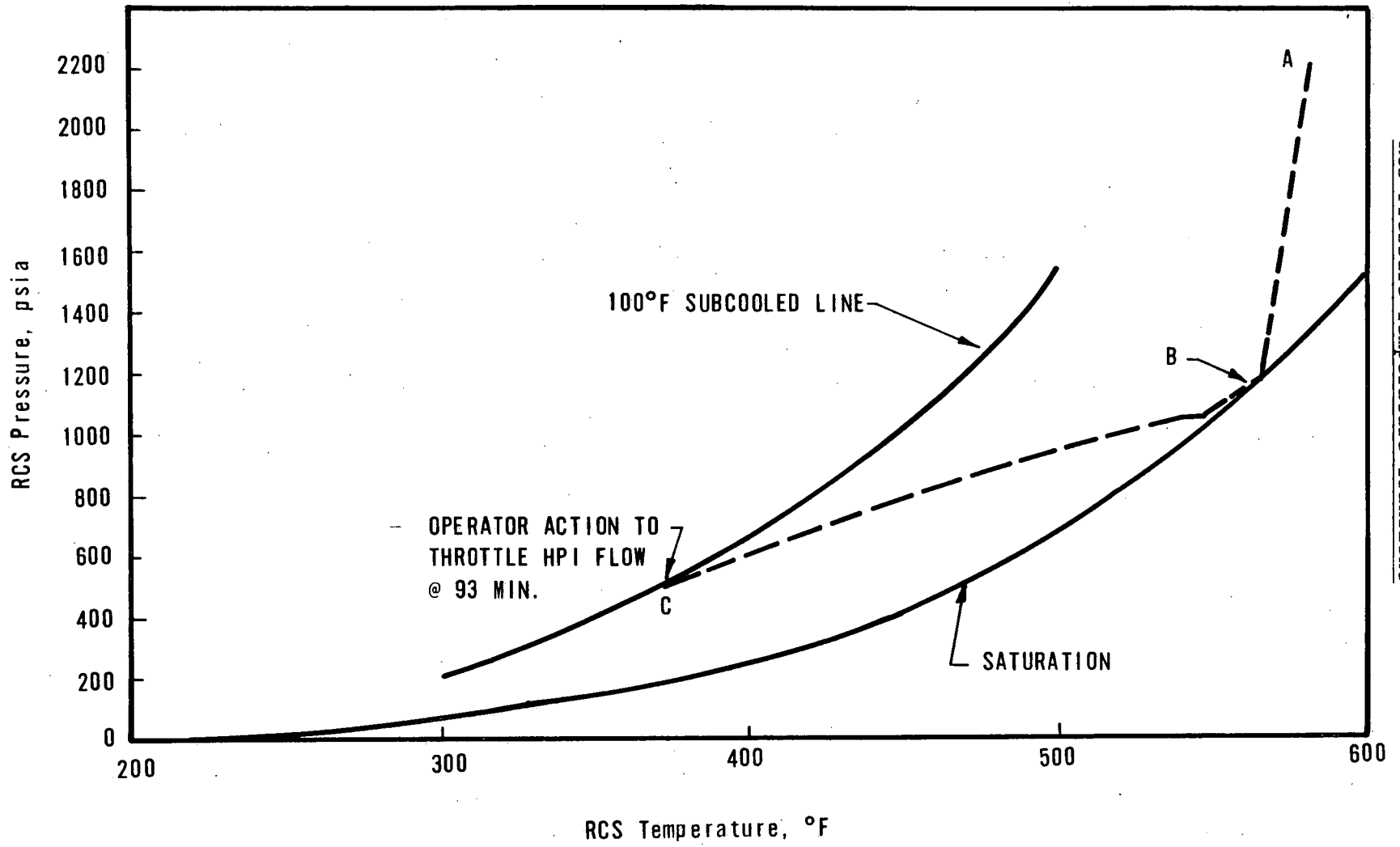

Figure 3.3-8

SBLOCA Simulation Results

RCS Pressure-Temperature Transient

4.0 FLUID MIXING IN RCS COLD LEG AND VESSEL DOWNCOMER

4.0 FLUID MIXING IN RCS COLD LEG AND VESSEL DOWNCOMER

4.1 Introduction

The results of the vessel stress analyses are dependent upon both the irradiation effect on the specific vessel materials, which will be discussed in Chapters 6.0 and 7.0 and vessel wall thermal gradient. For secondary system overcooling transients, full mixing is assumed and the vessel thermal gradient is governed by the bulk fluid temperatures. For SBLOCA events, the thermal gradient will be governed largely by the extent to which the cold HPI fluid and hot vent valve fluid are mixed and there is no cold leg flow.

In this case, the fluid entering the downcomer could be cold HPI fluid were it not mixed with the hot vent valve fluid. To evaluate and understand this mixing process, two different studies were undertaken. The ultimate output from both evaluations was the fluid temperature next to the RV wall which determined the vessel azimuthal temperature profile. The geometry of the vessel cold leg and vent valves required multi-dimensional analysis. Since natural circulation exists after RC pump coastdown for a period of time, gravity effects and turbulent exchange models needed to be included to effectively model any mixing that might occur. Forced and free convection heat transfer models were applied to calculate the maximum wall film heat transfer coefficient during natural or forced circulation.

4.2 Turbulent Jet Mixing Model

4.2.1 Discussion

Using turbulent jet theory, a conservative model was developed to predict the fluid temperatures in the vessel downcomer.

A turbulent jet mixing analytical model provided a simple approach to representing the flow of the cold HPI fluid into the vessel downcomer. Figure 4.2-1 shows the geometry of the jet flow as applied to mixing in the downcomer. As is shown in the figure, the conservative model assumed as a boundary condition a constant temperature for the cold fluid over the entire width of the cold leg nozzle. The cold fluid was assumed to flow into the downcomer as a jet and mix with the surrounding hot vent valve fluid. As this jet flow occurred, any spreading of the cold fluid would result in it being heated by the surrounding fluid. Since the longitudinal welds in the Oconee 1 vessel are outside the width of the cold leg nozzle and 5 to 10 feet below the nozzle, the colder fluid would be heated before it reached these welds. Details of the jet model are described in the following paragraphs.

The flow entering the the downcomer was considered to comprise a developing mixing layer and a fully-developed jet. The mixing layer was assumed to extend about five orifice diameters below the cold leg nozzle. Beyond that distance, a fully-developed jet flow configuration was applied. Reichardt, as quoted in Schlichling,[6] presented the following relationship for the developing mixing layer:

$$U = \left[\frac{U_1 + U_2}{2}\right]\left[1 + \left(\frac{U_1 - U_2}{U_1 + U_2}\right) \text{erf } \xi\right] \qquad (1)$$

$$\xi = \frac{13.5\ X}{Z} \qquad (2)$$

where

U_1 = original velocity of the jet, ft/sec

U_2 = original velocity of the surrounding fluid, ft/sec

U = fluid velocity at any point (X, Z) ft/sec

Since the surrounding fluid velocity was assumed to be zero, then $U_2 = 0$. Therefore, to compare with jet formulas where $U_2 = 0$, a relative velocity was defined:

$$U_{JET} = U_1 - U_2 \qquad (3)$$

When equation (3) is substituted in equation (1), it becomes

$$U = \frac{U_{JET}}{2} (1 + \text{erf } \xi) \tag{4}$$

For a fully developed jet, Reichardt gave the following relationship for the local jet velocity.

$$U = U_j \left(\frac{S}{Z}\right)^{1/2} (1 - \tanh^2 \xi) \tag{5}$$

$$\xi = \frac{7.67\ X}{Z} \tag{6}$$

U = local velocity, ft/sec

U_j = original jet velocity

S = characteristic dimension, ft

tanh = hyperbolic tangent

In order for the jet centerline velocity in equation (5) to be equal to U_j when Z/d equals 5, the characteristic dimension was chosen to be 5d. Since $1-\tanh^2\xi$ is identical to $\text{sech}^2\xi$, equation (5) can be written as:

$$u = u_j \left(\frac{5d}{Z}\right)^{1/2} \text{sech}^2 \xi \tag{7}$$

Therefore, equation (4) was used for the local velocity when Z is less than 5d, and equation (7) was used for Z greater than 5d.

Reichardt also showed that the temperature distribution was related to the velocity distribution in the following manner

$$\frac{T}{T_{max}} = \left(\frac{U}{u_{max}}\right)^{A\tau/aq} \tag{8}$$

The subscript "max" refers to the maximum difference in temperature and velocity. Also, the axes for u and T must be arranged so the relative temperatures and velocity difference approach zero at the same point. The ratio $A\tau/Aq$ is the quotient of the coefficients for momentum transfer and heat transfer. Experimental results for the two dimensional jet and wake show good agreement when $A\tau/Aq$ equals one half.

Since the highest temperature is the vent valve temperature (T_{vv}) and the lowest is that of the HPI fluid (T_{HPI}) then equation (8) becomes

$$\frac{T - T_{vv}}{T_{HPI} - T_{vv}} = \left(\frac{U}{U_{max}}\right)^{1/2} \qquad (9)$$

Rearranging equation (9) the downcomer fluid bulk temperature distribution becomes

$$T = T_{vv} - (T_{vv} - T_{HPI})\left(\frac{U}{U_j}\right)^{1/2} \qquad (10)$$

where:

$$U/U_j = \left(\frac{5d}{Z}\right)^{1/2} \text{sech}^2\xi \text{ for } Z \geq 5d$$

$$U/U_j = \left(\frac{1 + \text{erf } \xi}{2}\right) \text{ for } Z < 5d$$

d = ID. of cold leg (28")

It was noted that this model was derived for boundary free flows whereas the application was to flow along the vessel wall. Grella and Faeth[7] compared measurements of a 2-D thermal plume along a vertical wall with predictions based on a free plume (a boundary free shear flow) and concluded that the wall plume spread less rapidly than a free plume. Thus the model as presented should be conservative.

4.2.2 Jet Mixing Model Results

Using the SBLOCA transient data as input to the turbulent jet mixing model, the vessel downcomer azimuthal bulk fluid temperature profile was obtained. The azimuthal temperature profile was determined for that area below the vessel inlet nozzle spanning 62 inches azimuthally and extending 140 inches below the centerline of the inlet nozzle. The mixing below the inlet nozzle is illustrated in Figure 4.2-2. The cold fluid plume was assumed to exit the inlet nozzle and widen as it mixed with the hot fluid from the internal vent valves. The temperature profiles for two locations below the inlet nozzle, at 600 and 3600

seconds into the SBLOCA transient, are shown in Figure 4.2-3. The object in using such a mixing model was to approximate the aximuthal temperature profile below the vessel inlet nozzle. Since there are longitudinal welds in the vessel within 20 inches of the centerline of the nozzle, it was important that the temperature profile across these welds be known. In Figure 4.2-3, the temperature profile is shown to increase steeply within the span (arc length) corresponding to the radius of the inlet nozzle. It is also apparent that the plume has spread very little at 65 inches below the centerline of the nozzle.

At 135 inches below the nozzle, however, the plume has spread substantially, encompassing the longitudinal weld nearest to the centerline of the nozzle. The mixing between the cold HPI water exiting the nozzle and the much hotter vent valve flow raises the temperature of the fluid at this weld significantly above the HPI temperature. This mixing continues throughout the transient. At 3600 seconds, all temperatures outside the nozzle projection are colder than at 600 seconds, because the vent valve fluid temperature and the core outlet temperature decrease with time as shown in Figure 3.3-7. The temperature below the centerline of the cold leg nozzle is seen to increase slightly due to mixing occurring as the fluid travels down the downcomer of the vessel.

The bulk temperature profile was used in the thermal model, as discussed in Chapter 5.0, to obtain the vessel wall temperature and thermal gradients through the vessel wall for the SBLOCA transient.

4.2.3 Qualification of the Jet Mixing Model

Data have recently become available from mixing tests performed upon a facility representative of the B&W plant geometry, using conditions similar to those considered in these analyses.

The test data were presented in the EPRI Preliminary Report[8] of testing completed in September 1981 at CREARE on a transparent 1/5 scale test facility. This test program provided flow visualization records of the mixing and flow regimes, and temperature measurements were made in the

downcomer of the model. These data were used for a comparison between this 1/5 scale model and the analysis of the Oconee Unit 1 vessel. Test 24 in the CREARE series matched closely the density differences, vent valve flows, and HPI flows predicted in the analyzed SBLOCA transient. The test temperatures and geometry of the model were different from those in the plant analyses. Consequently, the comparison was done in terms of dimensionless parameters. A dimensionless temperature was defined as

$$T_D = \frac{T - T_c}{T_H - T_c}$$

where T = vessel downcomer temperature

T_c = temperature at exit of cold leg

T_H = vent valve temperature

Using equal values of Z/D the test elevations of 7 and 8.8 inches were equivalent to elevations of 31.3 and 44 inches below the nozzle in the model. For equal values of X/D the model dimensions of 0, 4.37 and 7.68 inches from the centerline translated to 0, 21.7 and 38.26 inches for the prototype.

The comparison shown in Figure 4.2-4 indicates the turbulent jet mixing model predicted the temperature profile conservatively when compared to the CREARE test data. For locations within the projected nozzle diameter, the test data shows significantly more mixing than predicted by the analysis. For locations equal to or greater than the diameter of the nozzle the test data compares extremely well with the jet mixing model.

The extent of fluid mixing inferred from the jet model was also compared to the results obtained in the FLOW 2-D studies described in Section 4.3. Those studies predicted significant mixing in the cold leg and, hence, much higher fluid temperatures than those extracted from the jet model. Therefore, by comparison to both the test data and the FLOW 2-D results, it was concluded that the turbulent jet mixing model conservatively predicted the mixing phenomenon in the vessel downcomer.

4.3 2-D Digital Code Turbulent Fluid Simulation

A second analytical model was also used to evaluate the mixing processes in the upper-vessel and vessel inlet piping. The FLOW 2-D[9] program, derived from SOLA-VOF[10], was applied by Flow Science, Inc., to perform studies of the mixing behavior using two-dimensional computing regions. These studies were concentrated upon analysis of fluid mixing expected to occur in the vessel inlet piping between HPI injection point and the inlet nozzle. The FLOW 2-D analyses confirmed that a significant flow of vent-valve fluid would penetrate the cold leg and would mix with the high energy HPI stream near the injection site. The calculations showed that the cooler mixed fluid would flow to the vessel, countercurrent to the vent valve fluid at the top of the pipe, with additional temperature diffusion between the two streams. Scoping studies were performed to isolate the effects of gravitational and turbulent exchange terms. The most significant conclusion drawn from the FLOW 2-D studies was that the fluid mixing processes in the vessel inlet piping will be sufficient to raise the temperatures of flows into the vessel substantially above the HPI temperature.

4.3.1 FLOW-2D Mixing Model

FLOW-2D is an extension of the SOLA-VOF solution algorithm which has performed well for a wide class of fluid dynamics problems. FLOW-2D was developed to solve time-dependent, incompressible flow of a Navier-Stokes fluid containing free surfaces or involving flow of two immiscible fluids. For this application one fluid was the cold water and the other was the hot water. The method used for interface treatment is referred to as the volume of fluid method. The method utilizes a function whose value is unity in a cell filled with fluid number 1 (cold water) and zero in a cell filled with fluid number 2 (hot water). The average value of this function F in a cell then represents the fractional volume of the cell occupied by cold water. To avoid numerical smoothing of F, a special advection algorithm is used.

The governing differential equations for the fluid dynamics are the Navier-Stokes momentum equations,

$$\frac{\partial u}{\partial t} + u\frac{\partial u}{\partial x} + v\frac{\partial u}{\partial y} = -\frac{1}{\rho}\frac{\partial p}{\partial x} + g_x + \nu\left[\frac{\partial^2 u}{\partial x^2} + \frac{\partial^2 u}{\partial y^2} + \xi\left(\frac{1}{x}\frac{\partial u}{\partial x} - \frac{u}{x^2}\right)\right]$$

and

$$\frac{\partial v}{\partial t} + u\frac{\partial v}{\partial x} + v\frac{\partial v}{\partial y} = -\frac{1}{\rho}\frac{\partial p}{\partial y} + g_y + \nu\left[\frac{\partial^2 v}{\partial x^2} + \frac{\partial^2 v}{\partial y^2} + \frac{\xi}{x}\frac{\partial v}{\partial x}\right] \quad (1)$$

Fluid pressure is denoted by p. Velocity components (u,v) are in the Cartesian coordinate directions (x,y) or axisymmetric coordinate directions (r,z). The choice of coordinate systems is controlled by the value of ξ, where $\xi = 0$ corresponds to Cartesian and $\xi = 1$ to axisymmetric geometry. Body accelerations are denoted by (g_x, g_y), ν is the coefficient of kinematic viscosity, and ρ is the fluid density.

The condition that a fluid parcel has constant density is expressed by the mass continuity equation

$$\frac{\partial u}{\partial x} + \frac{\partial v}{\partial y} + \frac{\xi u}{x} = 0. \quad (2)$$

Equations (1) and (2) are discretized with respect to an Eulerian grid of fixed rectangular cells. Grid cells may have variable sizes, e.g., δx_i for the ith column and δy_j for the jth row, as shown schematically in Figure 4.3-2. Dependent variables are located at the staggered grid locations indicated for a typical cell in Figure 4.3-2. The basic procedure for advancing a solution through one increment in time, δt, consists of three steps:

1. Explicit finite-difference approximations of equation (1) are used to compute first guesses for the new time-level velocities. In this step the initial dependent variable values, or the values from the previous time-level, are used to evaluate all advective, pressure, and viscous accelerations.

2. To satisfy the continuity equation, equation (2), pressures are iteratively adjusted in each cell. As each pressure value is

4.3 2-D Digital Code Turbulent Fluid Simulation

A second analytical model was also used to evaluate the mixing processes in the upper-vessel and vessel inlet piping. The FLOW 2-D[9] program, derived from SOLA-VOF[10], was applied by Flow Science, Inc., to perform studies of the mixing behavior using two-dimensional computing regions. These studies were concentrated upon analysis of fluid mixing expected to occur in the vessel inlet piping between HPI injection point and the inlet nozzle. The FLOW 2-D analyses confirmed that a significant flow of vent-valve fluid would penetrate the cold leg and would mix with the high energy HPI stream near the injection site. The calculations showed that the cooler mixed fluid would flow to the vessel, countercurrent to the vent valve fluid at the top of the pipe, with additional temperature diffusion between the two streams. Scoping studies were performed to isolate the effects of gravitational and turbulent exchange terms. The most significant conclusion drawn from the FLOW 2-D studies was that the fluid mixing processes in the vessel inlet piping will be sufficient to raise the temperatures of flows into the vessel substantially above the HPI temperature.

4.3.1 FLOW-2D Mixing Model

FLOW-2D is an extension of the SOLA-VOF solution algorithm which has performed well for a wide class of fluid dynamics problems. FLOW-2D was developed to solve time-dependent, incompressible flow of a Navier-Stokes fluid containing free surfaces or involving flow of two immiscible fluids. For this application one fluid was the cold water and the other was the hot water. The method used for interface treatment is referred to as the volume of fluid method. The method utilizes a function whose value is unity in a cell filled with fluid number 1 (cold water) and zero in a cell filled with fluid number 2 (hot water). The average value of this function F in a cell then represents the fractional volume of the cell occupied by cold water. To avoid numerical smoothing of F, a special advection algorithm is used.

The governing differential equations for the fluid dynamics are the Navier-Stokes momentum equations,

$$\frac{\partial u}{\partial t} + u\frac{\partial u}{\partial x} + v\frac{\partial u}{\partial y} = -\frac{1}{\rho}\frac{\partial p}{\partial x} + g_x + \nu\left[\frac{\partial^2 u}{\partial x^2} + \frac{\partial^2 u}{\partial y^2} + \xi\left(\frac{1}{x}\frac{\partial u}{\partial x} - \frac{u}{x^2}\right)\right]$$

and

$$\frac{\partial v}{\partial t} + u\frac{\partial v}{\partial x} + v\frac{\partial v}{\partial y} = -\frac{1}{\rho}\frac{\partial p}{\partial y} + g_y + \nu\left[\frac{\partial^2 v}{\partial x^2} + \frac{\partial^2 v}{\partial y^2} + \frac{\xi}{x}\frac{\partial v}{\partial x}\right] \quad (1)$$

Fluid pressure is denoted by p. Velocity components (u,v) are in the Cartesian coordinate directions (x,y) or axisymmetric coordinate directions (r,z). The choice of coordinate systems is controlled by the value of ξ, where $\xi = 0$ corresponds to Cartesian and $\xi = 1$ to axisymmetric geometry. Body accelerations are denoted by (g_x, g_y), ν is the coefficient of kinematic viscosity, and ρ is the fluid density.

The condition that a fluid parcel has constant density is expressed by the mass continuity equation

$$\frac{\partial u}{\partial x} + \frac{\partial v}{\partial y} + \frac{\xi u}{x} = 0. \quad (2)$$

Equations (1) and (2) are discretized with respect to an Eulerian grid of fixed rectangular cells. Grid cells may have variable sizes, e.g., δx_i for the ith column and δy_j for the jth row, as shown schematically in Figure 4.3-2. Dependent variables are located at the staggered grid locations indicated for a typical cell in Figure 4.3-2. The basic procedure for advancing a solution through one increment in time, δt, consists of three steps:

1. Explicit finite-difference approximations of equation (1) are used to compute first guesses for the new time-level velocities. In this step the initial dependent variable values, or the values from the previous time-level, are used to evaluate all advective, pressure, and viscous accelerations.

2. To satisfy the continuity equation, equation (2), pressures are iteratively adjusted in each cell. As each pressure value is

4.3 2-D Digital Code Turbulent Fluid Simulation

A second analytical model was also used to evaluate the mixing processes in the upper-vessel and vessel inlet piping. The FLOW 2-D[9] program, derived from SOLA-VOF[10], was applied by Flow Science, Inc., to perform studies of the mixing behavior using two-dimensional computing regions. These studies were concentrated upon analysis of fluid mixing expected to occur in the vessel inlet piping between HPI injection point and the inlet nozzle. The FLOW 2-D analyses confirmed that a significant flow of vent-valve fluid would penetrate the cold leg and would mix with the high energy HPI stream near the injection site. The calculations showed that the cooler mixed fluid would flow to the vessel, countercurrent to the vent valve fluid at the top of the pipe, with additional temperature diffusion between the two streams. Scoping studies were performed to isolate the effects of gravitational and turbulent exchange terms. The most significant conclusion drawn from the FLOW 2-D studies was that the fluid mixing processes in the vessel inlet piping will be sufficient to raise the temperatures of flows into the vessel substantially above the HPI temperature.

4.3.1 FLOW-2D Mixing Model

FLOW-2D is an extension of the SOLA-VOF solution algorithm which has performed well for a wide class of fluid dynamics problems. FLOW-2D was developed to solve time-dependent, incompressible flow of a Navier-Stokes fluid containing free surfaces or involving flow of two immiscible fluids. For this application one fluid was the cold water and the other was the hot water. The method used for interface treatment is referred to as the volume of fluid method. The method utilizes a function whose value is unity in a cell filled with fluid number 1 (cold water) and zero in a cell filled with fluid number 2 (hot water). The average value of this function F in a cell then represents the fractional volume of the cell occupied by cold water. To avoid numerical smoothing of F, a special advection algorithm is used.

The governing differential equations for the fluid dynamics are the Navier-Stokes momentum equations,

$$\frac{\partial u}{\partial t} + u\frac{\partial u}{\partial x} + v\frac{\partial u}{\partial y} = -\frac{1}{\rho}\frac{\partial p}{\partial x} + g_x + \nu\left[\frac{\partial^2 u}{\partial x^2} + \frac{\partial^2 u}{\partial y^2} + \xi\left(\frac{1}{x}\frac{\partial u}{\partial x} - \frac{u}{x^2}\right)\right]$$

and

$$\frac{\partial v}{\partial t} + u\frac{\partial v}{\partial x} + v\frac{\partial v}{\partial y} = -\frac{1}{\rho}\frac{\partial p}{\partial y} + g_y + \nu\left[\frac{\partial^2 v}{\partial x^2} + \frac{\partial^2 v}{\partial y^2} + \frac{\xi}{x}\frac{\partial v}{\partial x}\right] \quad (1)$$

Fluid pressure is denoted by p. Velocity components (u,v) are in the Cartesian coordinate directions (x,y) or axisymmetric coordinate directions (r,z). The choice of coordinate systems is controlled by the value of ξ, where $\xi = 0$ corresponds to Cartesian and $\xi = 1$ to axisymmetric geometry. Body accelerations are denoted by (g_x, g_y), ν is the coefficient of kinematic viscosity, and ρ is the fluid density.

The condition that a fluid parcel has constant density is expressed by the mass continuity equation

$$\frac{\partial u}{\partial x} + \frac{\partial v}{\partial y} + \frac{\xi u}{x} = 0. \quad (2)$$

Equations (1) and (2) are discretized with respect to an Eulerian grid of fixed rectangular cells. Grid cells may have variable sizes, e.g., δx_i for the ith column and δy_j for the jth row, as shown schematically in Figure 4.3-2. Dependent variables are located at the staggered grid locations indicated for a typical cell in Figure 4.3-2. The basic procedure for advancing a solution through one increment in time, δt, consists of three steps:

1. Explicit finite-difference approximations of equation (1) are used to compute first guesses for the new time-level velocities. In this step the initial dependent variable values, or the values from the previous time-level, are used to evaluate all advective, pressure, and viscous accelerations.

2. To satisfy the continuity equation, equation (2), pressures are iteratively adjusted in each cell. As each pressure value is

changed the velocities dependent on this pressure are also changed. This pressure iteration is continued until equation (2) is satisfied to a prespecified level of accuracy.

3. Finally, the F function [see equation (3)] defining fluid regions is updated to give the new fluid configuration. After all necessary bookkeeping adjustments are completed, including data output, this three-step process can be restarted for the next time-level calculation. At each step, of course, suitable boundary conditions must be imposed at all boundaries.

The actual finite-difference approximations used in FLOW-2D for equations (1) and (2) are not a crucial part of the algorithm. That is, various approximations could be used without affecting the basic solution procedure. The particular approximations used are essentially those contained in SOLA-VOF. This flexibility does not apply, however, to the way the F distribution is advanced in time. Because F is a scalar quantity fixed in the fluid, its evolution is governed by pure advection in the absence of turbulence.

$$\frac{\partial F}{\partial t} + \frac{1}{r}\frac{\partial rFu}{\partial x} + \frac{\partial Fv}{\partial y} = 0. \qquad (3)$$

where $r = x$ when $\xi = 1$ and $r = 1$ when $\xi = 0$.

FLOW-2D employs a type of donor-acceptor fluxing to advance the values of F in each cell. The amount of F crossing a cell boundary depends on the distribution of F in the donor cell. Generally, the donor cell distribution is established from a surface orientation algorithm. However, if the acceptor cell is empty of F or if the cell upstream of the donor cell is empty, then the acceptor cell determines the donor cell distribution regardless of the surface orientation. This means that a donor cell must fill before any F fluid can enter a downstream empty cell.

To calculate the effects of turbulent mass diffusion, equation (3) becomes

$$\frac{\partial F}{\partial t} + \frac{1}{r}\frac{\partial rFu}{\partial x} + \frac{\partial Fv}{\partial y} = \frac{1}{r}\frac{\partial}{\partial x}\left(r\nu\frac{\partial F}{\partial x}\right)+\left(\frac{\partial}{\partial y}\ \nu\ \frac{\partial F}{\partial y}\right)$$

where ν is the turbulent kinematic viscosity, which is assumed to have the same value for mass and momentum diffusion.

4.3.2 FLOW 2-D Mixing Model Results

Using the FLOW 2-D code on the vessel inlet cold leg configuration shown in Figure 4.3-3, and with the flow conditions existing in the SBLOCA transient, results with and without gravitational effects were obtained. These conditions consisted of HPI flow only, since natural circulation as modeled by the computational mesh shown in Figure 4.3-4 gave the following results for the SBLOCA transient. Without gravitational effects there is no force acting to move the lower density hot water up the cold leg piping over the higher density, cold HPI water. The velocity field, Figure 4.3-5, shows no penetration of the hot water into the cold leg piping and no mixing of the vent and HPI flow streams in the case of no gravitational effects.

However, when buoyant forces are allowed to act, the flow is very different, and both experimental and theoretical investigations have demonstrated that the hot water will penetrate the inlet pipe. Using the same computational mesh, with both gravitational effects and turbulent mixing allowed to occur in the cold leg piping, the velocity field of Figure 4.3-6 and temperature contours of Figure 4.3-7 result. The velocity field clearly shows that the vent valve hot water flows up the cold leg piping, indeed it flows to the point of injection early in the transient. At this point, 20 minutes into the SBLOCA transient, due to the high turbulence at the point of injection the flow is no longer stratified but is well mixed. The temperature contours, Figures 4.3-7 and 4.3-8, show the mixing effectiveness obtained when gravitational effects are considered and turbulent mixing as a result of the HPI flow injection is modeled. The HPI fluid is injected into the cold leg piping 150 inches upstream of the vessel downcomer. This substantiates that

the cold HPI fluid does not flow into and down the reactor vessel wall. The temperature results, Figure 4.3-8, at 20 minutes into the SBLOCA transient, show the fluid entering the downcomer of the reactor vessel to be greater than 286°F. This analysis was repeated at 90 and 180 minutes into the SBLOCA transient. While the density difference between the hot vent valve fluid and the cold HPI fluid decreases from 20% at 20 minutes to 5.2% at 280 minutes, and the hot vent valve fluid is not driven as far into the cold leg piping at 180 minutes into the transient, the turbulent mixing that occurs assures that the cold HPI does not directly enter the downcomer of the vessel. The bulk fluid temperatures at the inlet to the vessel downcomer, Point A in Figure 4.3-8, and 8 inches down into the downcomer, Point B in Figure 4.3-8, are shown in Figure 4.3-9 for 90 and 180 minutes of the SBLOCA transient. From Figure 4.3-9, the mitigation of vessel downcomer temperature versus time is evident when compared to the conservative assumptions of 50°F used in past thermal shock analysis.

These results have been used in the evaluation of the vessel inlet nozzle in this report. Since the availability of the FLOW-2D results did not coincide with the time that the vessel LEFM analysis was being done, the conservative Jet Turbulent mixing model results of Section 4.1 were used for the evaluation of all vessel welds and base metal.

4.4 Overcooling Transient Mixing

During the overcooling transient analysis various plant conditions were simulated. This simulation considered that RC pumps were either running or tripped by the operator during the transient. If the pumps were tripped, then natural circulation continued in all cases except when zero decay heat had been assumed. Therefore, the thermal analysis assumed complete mixing of the HPI flow with the forced RC pump flow or with the natural circulation flow. It has been shown in the past that for a case with no decay heat, the RC system will come to equilibrium at some temperature and remain there. However, it is impossible to get into this situation in the actual plant operations because if any appreciable power level is obtained, a decay heat level significantly above the assumption of zero decay heat will be present in the core.

Figure 4.2–1 TURBULENT JET MODEL

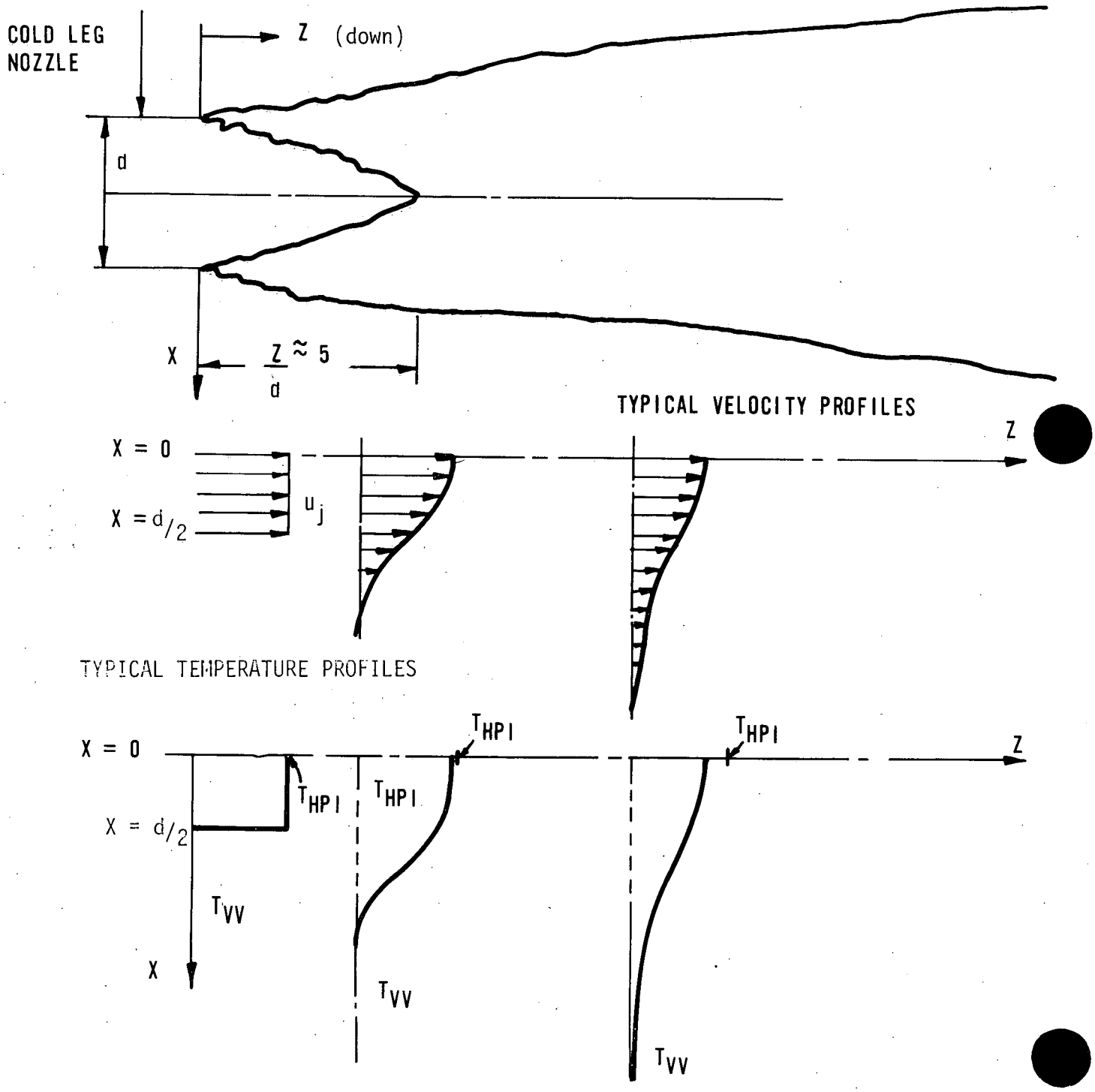

Figure 4.2–2 MIXING OCCURRING BELOW VESSEL INLET NOZZLE

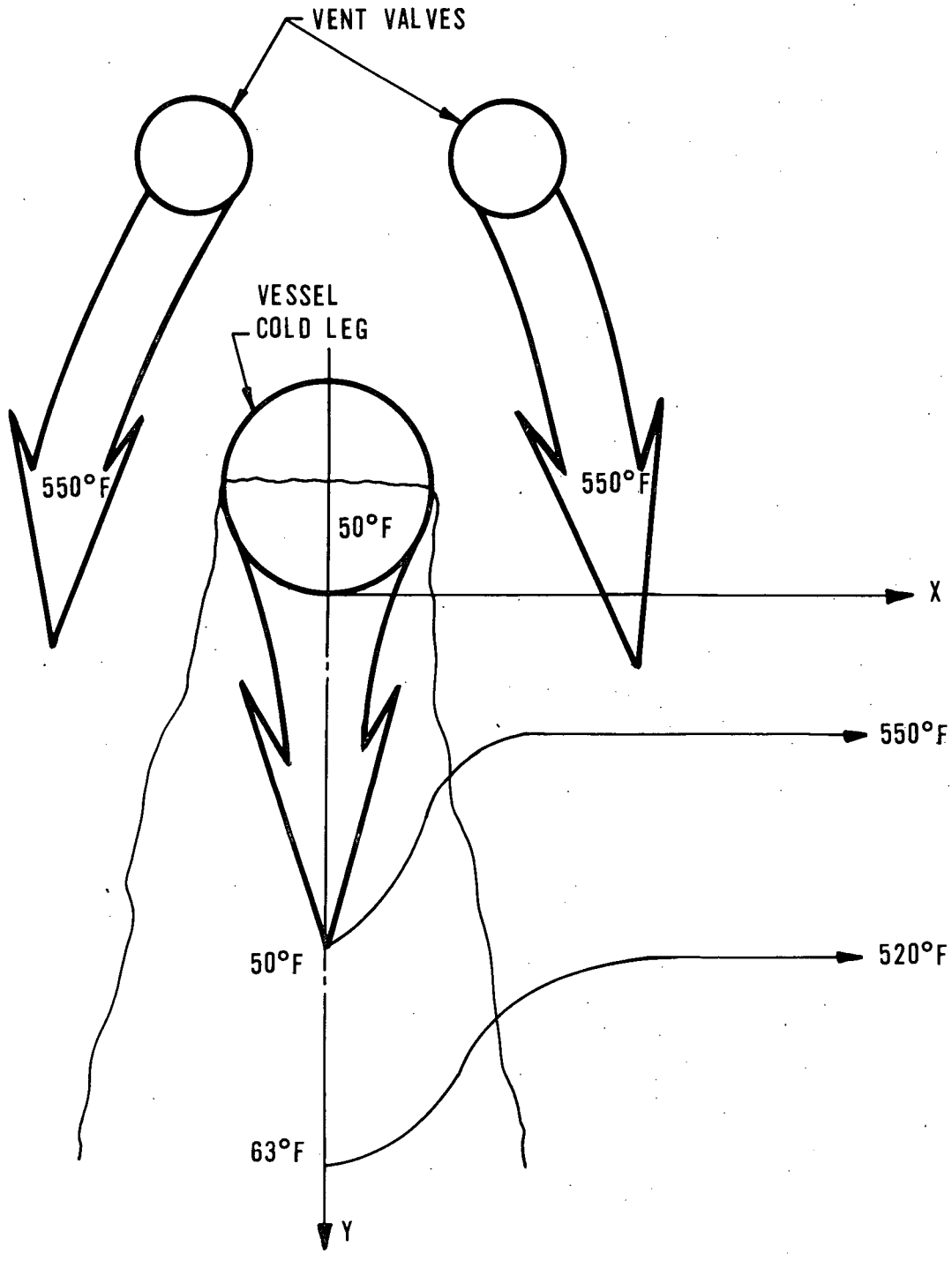

Figure 4.2–3 VESSEL AZIMUTHAL FLUID TEMPERATURE PROFILE VS TIME

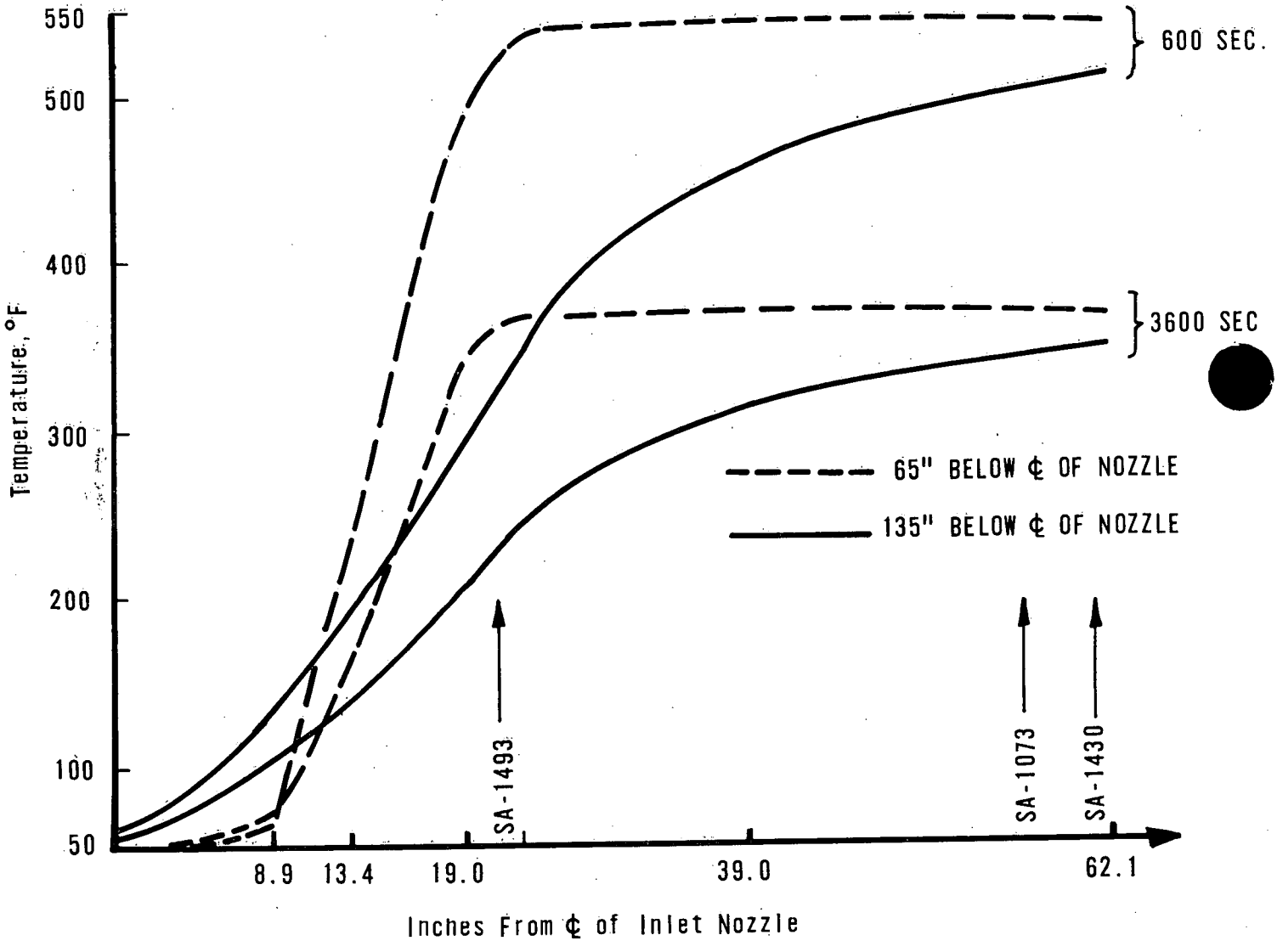

Figure 4.2–4 COMPARISON OF CREARE 1/5 - SCALE MODEL DATA WITH TURBULENT JET ANALYSIS

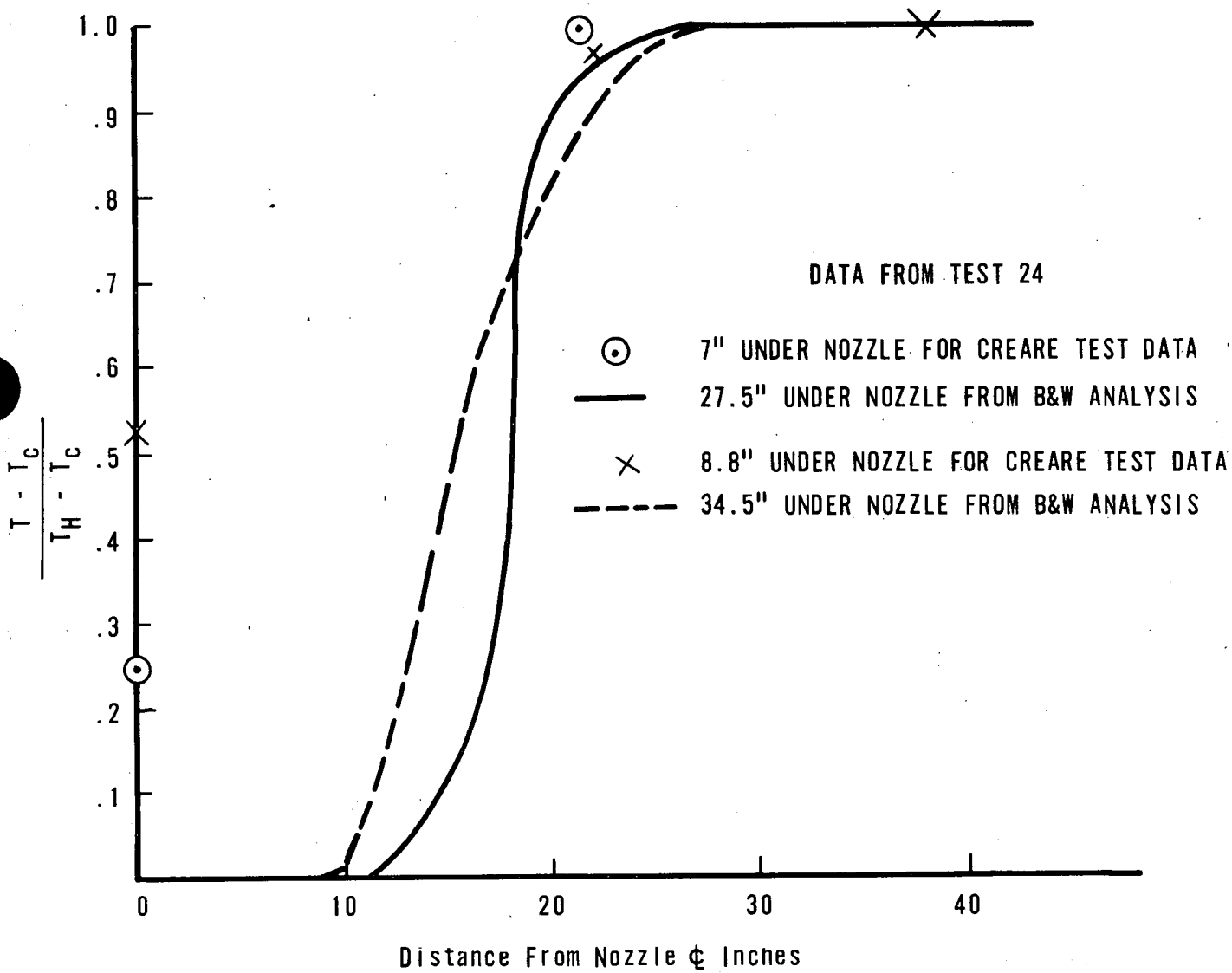

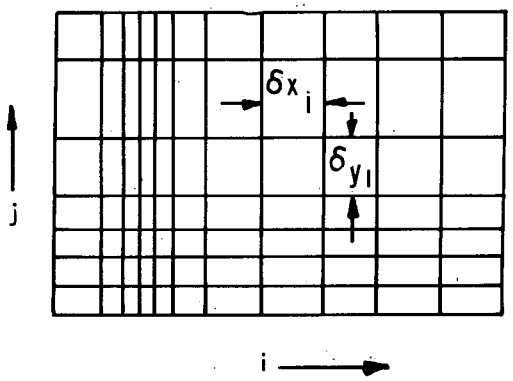

Figure 4.3–1 FINITE-DIFFERENCE MESH WITH VARIABLE RECTANGULAR CELLS

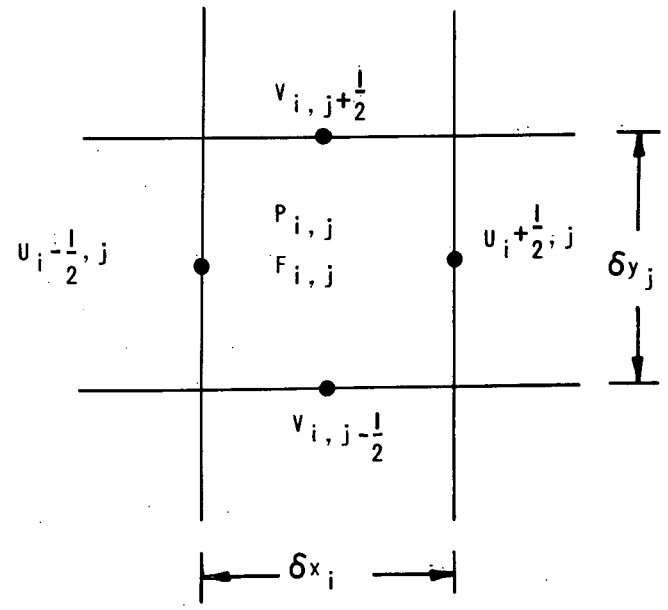

Figure 4.3–2 LOCATION OF VARIABLES IN A TYPICAL MESH CELL

Figure 4.3–3 COLD LEG INLET PIPE-TO-VESSEL GEOMETRY

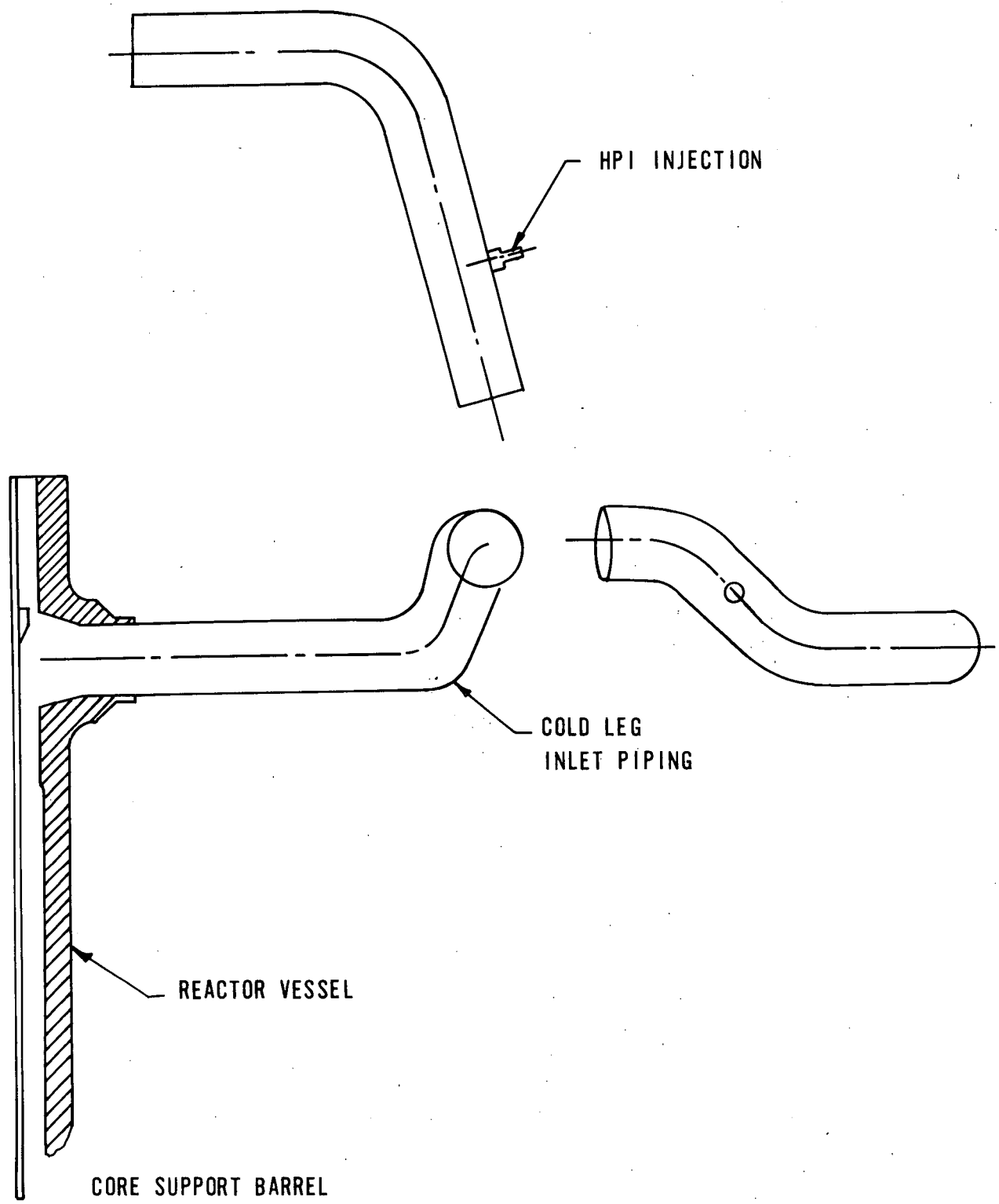

Figure 4.3–4 FLOW-2D COMPUTATIONAL MESH FOR COLD LEG INLET PIPING (150 IN.) REGION

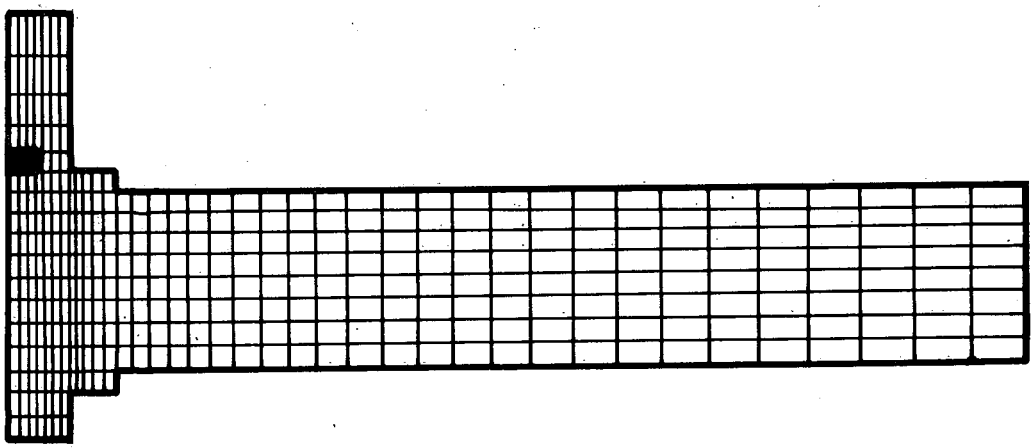

Figure 4.3–5 VELOCITY FIELD AND INTERFACE BETWEEN THE VENT VALVE AND HPI STREAMS IN THE ABSENCE OF GRAVITATIONAL (BUOYANCY) EFFECTS AND NATURAL CIRCULATION.

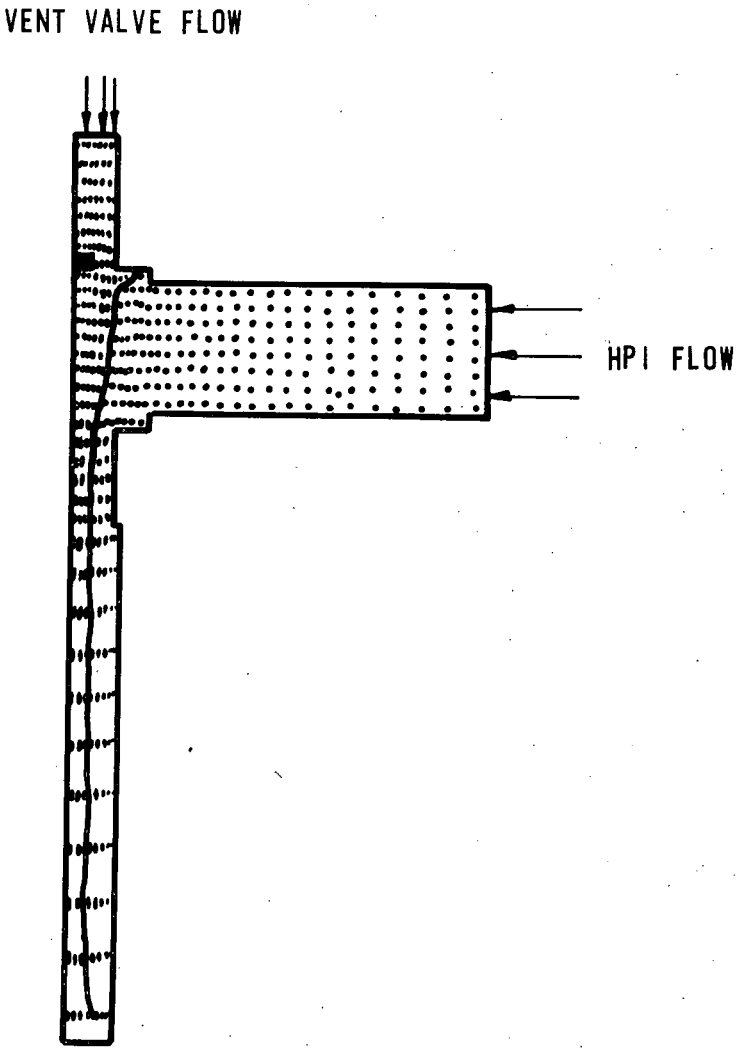

Figure 4.3–6 VELOCITY FIELDS WITH GRAVITATIONAL EFFECTS AND TURBULENCE

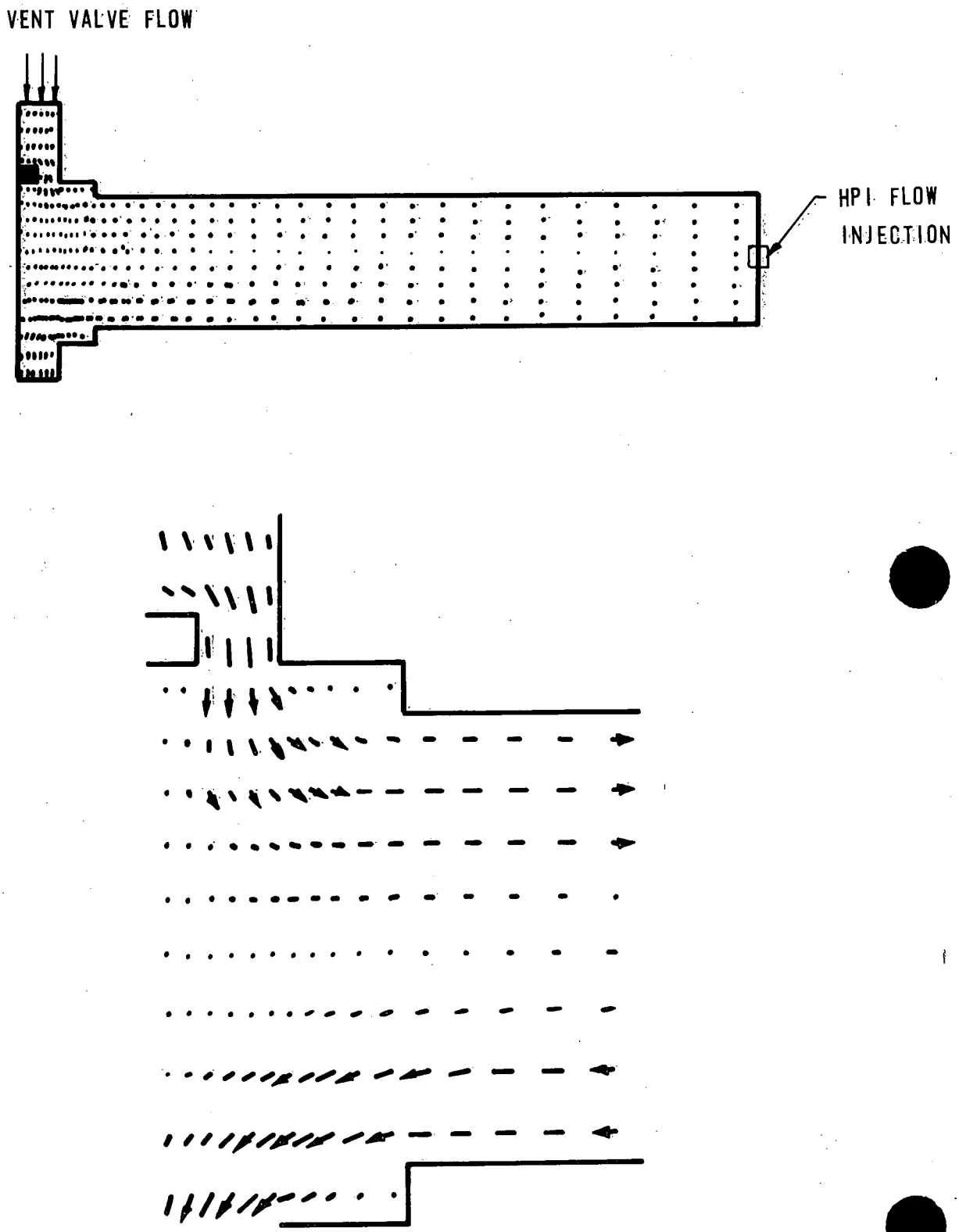

Figure 4.3–7 TEMPERATURE CONTOURS ASSOCIATED WITH THE VELOCITY FIELD IN FIGURE 4.3–6

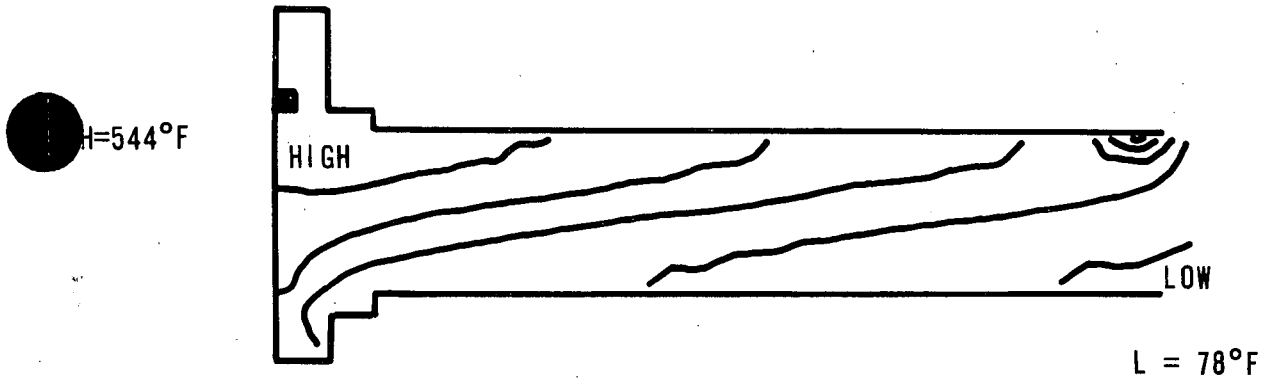

Figure 4.3–8 TEMPERATURE CONTOURS ACROSS THE DOWNCOMER AT THE LOWER LIP OF THE INLET PIPE.

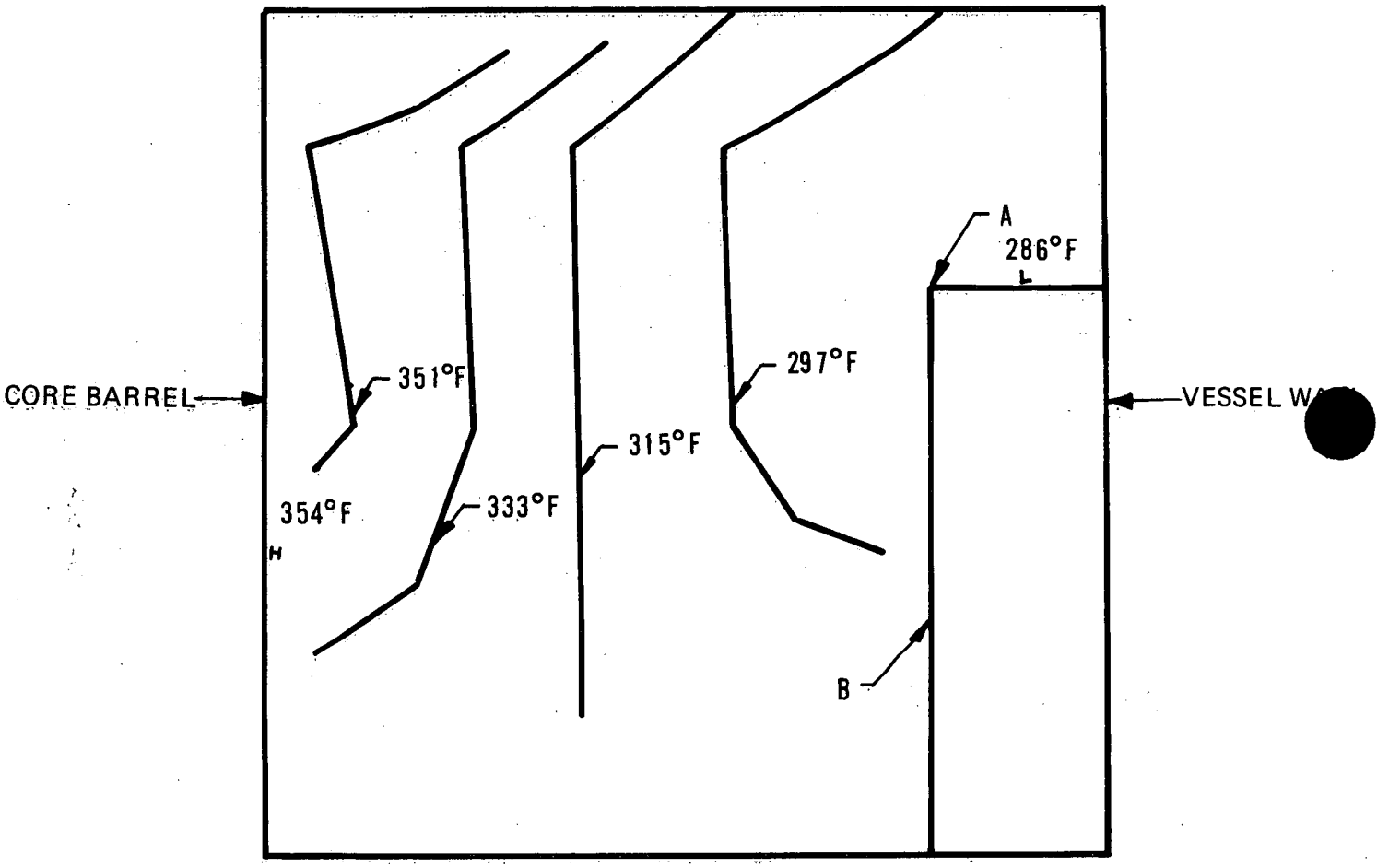

(20 minutes into the SBLOCA transient)

Figure 4.3–9 BULK FLUID TEMPERATURE FROM FLOW 2-D MIXING MODEL FOR SB LOCA TRANSIENT

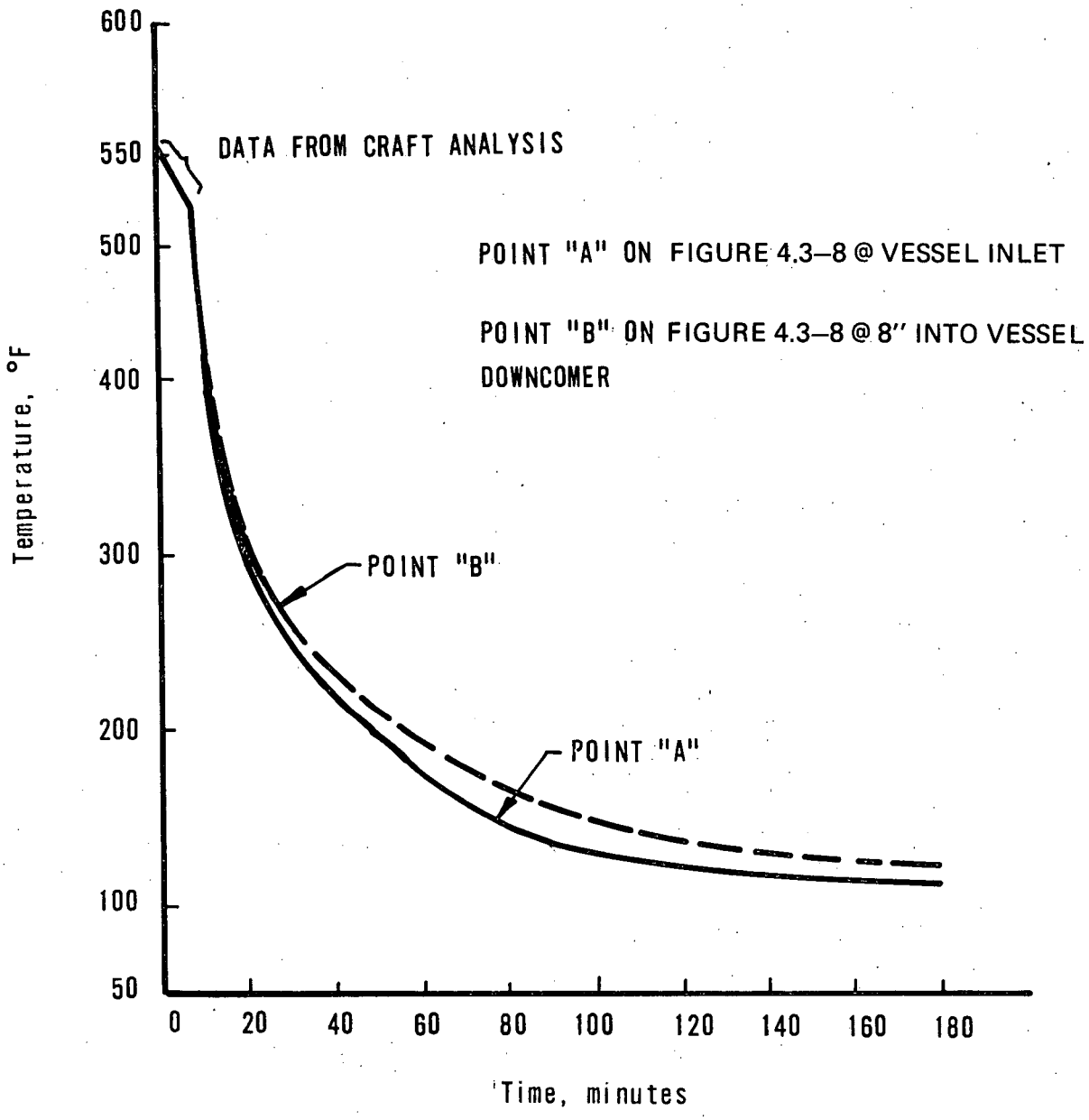

5.0 VESSEL WALL THERMAL ANALYSIS

5.0 VESSEL WALL THERMAL ANALYSIS

5.1 Introduction

Transient analyses for use in the fracture mechanics analysis have been performed for overcooling transients (Chapter 2.0) and small break LOCAs (Chapter 3.0). For the small break transients, which have zero loop flow, detailed mixing analyses were performed as discussed in Chapter 4.0 (Fluid Mixing). In order to determine the temperature dependent properties of the vessel, vessel wall temperature profiles are calculated. An illustration of the thermal gradient in the reactor vessel is shown in Figure 5.1-1.

The determination of the fluid-to-vessel wall heat transfer coefficient (HTC) is described in Section 5.2. The determination of vessel wall thermal gradients is described in Section 5.3.

5.2 Fluid-to-Base Metal Heat Transfer Coefficient (Film & Cladding) and Azimuthal Temperature Distribution

The overall HTC consists of the wall film coefficient determined as the larger of forced (turbulent) or free convection plus the clad metal conduction coefficient. This definition of the overall heat transfer coefficient allows the calculation of the azimuthal temperature profile at the vessel base metal. This is an input requirement for the finite element model used in the vessel wall thermal gradient analysis for the SBLOCA analysis. The HTC for the overcooling/repressurization transients consists of only the film coefficient since the model used to calculate the vessel gradient for these overcooling transients included cladding.

5.2.1 Forced and Free Convection Heat Transfer Coefficients

Selection of an appropriate convection heat transfer coefficient must consider that the surface heat transfer may be via forced convection,

free convection, or by some combination of the two modes. The dominant mode of convection heat transfer at the vessel wall will depend upon local conditions which may vary considerably. Because of the uncertainty associated with accurate determination of the local heat transfer regime, a conservative approach was taken. Heat transfer coefficients applicable to forced convection and to free convection for turbulent flows were calculated at each location on the vessel wall. The higher of the two coefficients was used to calculate the surface heat flux.

The heat transfer coefficient for forced convection was determined by the Dittus-Boelter[11] equation.

$$h_{forced} = 0.023\ K/D\ Re^{0.8}\ Pr^{0.43}\ (BTU/h - ft^2 - F)$$

where K = fluid thermal conductivity, Btu/h-ft^2-F,
D = hydraulic diameter, ft (D$\sim$2W where W = downcomer width),
Re = Reynolds number, the ratio of internal to viscous forces, $Re = VD/\nu$
V = fluid velocity, fps,
ν = kinematic viscosity, ft^2/s,
Pr = Prandtl number, the ratio of storage to conduction energy transfer, $Pr = C_p\mu/K$
C_p = specific heat, Btu/lbm-F,
μ = dynamic viscosity, lbm/h-ft.

The free (or natural) convective HTC[12] is given by:

$$h_{free} = 0.094\ K/L\ (Gr\ Pr)^{1/3}$$

where L = heated length, ft,
Gr = Grashof number, the ratio of buoyant to inertial force, $Gr = g\beta\Delta TL^3/\nu^2$
g = gravitational acceleration, 32 ft/s^2,
β = fluid thermal expansivity, $\beta = 1/\rho\ \partial\rho/\partial T\ (1/F)$,
ΔT = governing temperature difference, wall to fluid, F

It is noteworthy that the HTC for turbulent free convection is independent of heated length.

The film HTC is calculated for the entire region below the vessel inlet nozzle as shown in Figure 5.2-1. The HTC at each mesh point may switch from forced convection to free convection at any time in the transient. However, the variation in the magnitudes of the coefficients among the different locations is not great at any given time. The data shown in Figure 5.2-2 are typical of all mesh points.

The SBLOCA heat transfer coefficient data for the bottom of the longitudinal weld (SA-1493) in the Oconee 1 vessel is shown in Figure 5.2-2. It is evident from the figure that free convection governs the heat transfer over all but the first two minutes of the SBLOCA transient.

The resultant film HTC used for the overcooling transient with RC pumps running (Case 9 of Section 2.4.3) is 3000 BTU/h-ft^2-F for the entire transient. The resultant film HTC for the overcooling transient (Case 10 of Section 2.4.3) which consists of all turbine bypass valves failing open on reactor trip and the main feedwater system continuing to feed the steam generators at 100% flow until the high level limit in steam generators is reached, is shown in Figure 5.2-3. This transient has the RC pumps tripped but maintains natural circulation in the primary loops. Since loop flow is maintained at all times, the heat transfer rate to the vessel is controlled by the forced heat convection coefficient.

The film HTC for the vessel inlet nozzle was determined as the larger of the two coefficients obtained from a flat plate or circular pipe consideration for the SBLOCA transient. The coefficient varied from $\sim$1500 BTU/h-ft^2-F at two minutes to $\sim$50 BTU/h-ft^2-F at 180 minutes into the transients.

For the overcooling transient (Case 9 of Section 2.4.3), the same HTC as used for the vessel wall analysis was used. Since this transient has forced flow existing at all times a coefficient of 3000 BTU/h-ft^2-F is assumed throughout the entire transient.

5.2.2 Base Metal Azimuthal Temperature Distribution

For the SBLOCA transient only, the HTC was calculated at the vessel base metal to accommodate available 3-D finite-element programs that were used to calculate the through-wall temperature gradients. Using the bulk fluid temperatures determined in Chapter 4.0 (Fluid Mixing) and the fluid-to-cladding HTC determined in Section 5.2.1, the HTC at the surface of the vessel base metal is defined as:

$$h_{\substack{\text{base}\\\text{metal}}} = \frac{1}{1/h_{\text{fluid}} + \dfrac{\Delta X_{\text{clad}}}{k_{\text{clad}}}}$$

where: h_{FLUID} is obtained from Section 5.1.1.
ΔX_{CLAD} = Thickness of cladding (assumed 1/8", nominal value 3/16")
K_{CLAD} = Clad thermal conductivity, BTU/h-ft^2-F

The base metal azimuthal temperature profile at the location of the SA-1229 weld (65 inches below the nozzle outlet) at 12 and 52 minutes into the SBLOCA transient is shown in Figure 5.2-4.

To show the differences in cooldown rates at various locations, the base metal temperature profile versus time for the longitudinal weld (SA-1493) and circumferential weld (SA-1229) are compared to the SBLOCA transient core outlet temperature distribution in Figure 5.2-5. The longitudinal weld is seen to experience a linear cooldown ramp of 3.0°F/min for the first 1.5 hours of the transient. This compares with an approximate 3.1°F/min cooldown rate for the core outlet temperature from the SBLOCA transient analysis. The circumferential weld which passes beneath the nozzle and therefore experiences the coldest fluid exhibits the largest cooldown rate ∿ 30°F/min for the first 12 minutes and a second rate of 0.7°F/min that continues for the duration of the transient. The location of both welds are shown on Figure 5.2-1.

For the overcooling transients of Chapter 2.0, homogeneous mixing in the vessel downcomer was used with the coldest inlet temperature determined from the overcooling transient analysis. The homogeneous flow results

in all locations below the vessel inlet nozzle being at the same temperature and therefore, no azimuthal temperature profile exists as in the SBLOCA transient.

Even though the 2-D finite element codes used to determine the through-wall temperature gradients for the overcooling transient contained the clad in the model, the vessel base metal wall temperature distribution versus time is shown in Figure 5.2-6 for Case 10 Section 2.4.3 and is consistent with the SBLOCA data. The cooldown rate for the vessel base metal surface is 9.5°F/min as compared to the vessel inlet temperature cooldown rate of 12.8°F/min for the first 20 minutes of the transient. After 20 minutes, the vessel inner surface essentially remains constant for the duration of the transient.

5.2.3 Vessel Inlet Nozzle Inner Surface Profile

The FLOW 2-D results, described in Section 4.3, were used to evaluate the thermal conditions existing in the vessel inlet nozzle during the SBLOCA transient. The resulting nozzle base metal temperature versus time for the "knee" of the nozzle is shown in Figure 5.2-7. The FLOW-2D bulk fluid temperature at the nozzle wall, used as input to the finite element program to generate the thermal profiles, is shown for comparison.

For the overcooling transient (Case 9, Section 2.4.3), homogeneous mixing using the coldest inlet temperature determined from the overcooling transient analysis was used for the nozzle thermal calculations. This is the same data used for evaluation of the vessel wall welds during this overcooling transient.

5.3 Wall Thermal Gradient Determination

5.3.1 SBLOCA Transient

When no cold leg flow exists, normal mixing of the cold HPI flow with the hot fluid flowing in the cold leg of the RCS occurs by a different process. When this situation exists for extended periods of time,

it has been assumed in previous studies that the cold HPI fluid would begin to flow down the vessel wall thereby causing a drastic reduction in the vessel wall temperature below the cold leg nozzle. The results from Chapter 4.0 (Fluid Mixing) and Section 5.2 were used to evaluate the actual mixing under these conditions and to determine the base metal wall azimuthal temperature distribution versus time for the specific SBLOCA transient. Since there exists large gradients in the surface of the base metal and small vessel welds are located at varying distances below and to the side of the cold leg nozzle, a 3-D finite element model was constructed to accurately determine the temperature gradient through the vessel wall as a function of time at the various weld locations. The 3-D heat transfer analysis, using the ANSYS[13] code determines nodal temperatures through the vessel wall with additional nodes that coincide with the critical pressure evaluation nodes of 1/40T to 16/40T. In the axial and azimuthal directions, the nodes coincide with the location of all longitudinal and circumferential welds within the beltline region of the Oconee 1 vessel, as shown on Figures 5.2-1 and 5.3-1.

The wall temperature profiles for the location of the longitudinal weld (SA-1493) and the circumferential weld (SA-1229) are shown in Figures 5.3-2 and 5.3-3 respectively. Due to their respective location in comparison to the vessel inlet nozzle, the longitudinal weld exhibits the smaller vessel gradient of the two welds. However, the circumferential weld experiences the larger gradient earlier in the transient than does the longitudinal weld. Both conditions result in the circumferential weld becoming the limiting weld. When the mixing analysis discussed in Section 4.3 is used in the thermal analysis, the vessel gradients at all welds will approach those in Figure 5.3-2.

5.3.2 Overcooling Transients

The wall thermal gradients for the overcooling transients of Chapter 2.0 were calculated in a manner similar to those for the SBLOCA analysis discussed in Section 5.3.1 except that a 2-D axisymmetric heat transfer model and appropriate film heat transfer coefficient were used as explained in

Section 5.2.1. Since the overcooling transients were analyzed with RC pumps running and tripped, the film coefficient chosen was considerably different. The point of injection is highly turbulent and the flow enters the downcomer of the vessel as equilibrium or homogeneous flow. Since the flow is not stratified but equal to the bulk fluid temperature at all azimuthal weld locations, a 2-D axisymmetric heat transfer analysis, using the ANSYS code, was used to determine the thermal gradient through the vessel wall. Node points through the wall were selected to correspond to the critical pressure evaluation nodes.

The wall temperature profile for the worst case overcooling transient analyzed is shown in Figure 5.3-4. It is obvious that large wall thermal gradients are induced in the vessel but not as large as in the SBLOCA transient profile shown in Figure 5.3-3. As discussed in Section 5.3.1, when the 2-D mixing analysis results are used on the SBLOCA transient it is likely it will then become less severe than this overcooling transient.

An additional difference in the transient is that the vessel inner and outer walls experience only cooling in the SBLOCA transient whereas in the overcooling transient they cool and then begin a heatup and repressurization as the transient continues.

5.4 Inlet Nozzle Temperature Gradient Determination

Since the cooldown rates are higher than design basis, a single check was made on the inlet nozzle to determine the thermal gradient through the "knee" of the nozzle. To determine the temperature gradient through the thickness of the inlet nozzle, the procedure was to use a 2-D axisymmetric finite element model, shown in Figure 5.4-1, using the ANSYS profile. The stress profile due to pressure through the "knee" of the nozzle is used in conjunction with the BIGIF[14] code to generate a stress intensity factor, SIF, due to pressure.

The vessel inlet nozzle temperature profiles, at the nozzle "knee", are shown in Figure 5.4-2 for various times during the SBLOCA transient. Large thermal gradients through the nozzle wall are experienced during the SBLOCA transient with the maximum ΔT existing at 25 minutes into the transient. These large thermal gradients exist for about an hour, beginning around 20 minutes and decreasing rapidly at about 90 minutes into the transient.

For the overcooling transient (Case 9, Section 2.4.3), the same homogeneous mixing data obtained from the overcooling transient analysis for the vessel wall was used in the evaluation of the nozzle analysis. The nozzle temperature profiles, at the "knee", are shown in Figure 5.4-3 for various times during the overcooling transient. The nozzle temperature profiles when compared to the vessel wall temperature profile exhibit similar trends but with larger temperature gradients. The inner surface in both cases reaches a minimum temperature in approximately 30 minutes and then began increasing due to a characteristic of this overcooling transient. The transient, as simulated, begins re-pressurization at approximately six minutes and heatup at approximately 20 minutes into the transient. Therefore, the inner surface temperature begins increasing while the outer surface is still cooling. This causes a rapidly decreasing temperature gradient through the nozzle wall at this time.

Figure 5.1–1 THERMAL GRADIENT IN REACTOR VESSEL DURING NORMAL AND ABNORMAL CONDITIONS

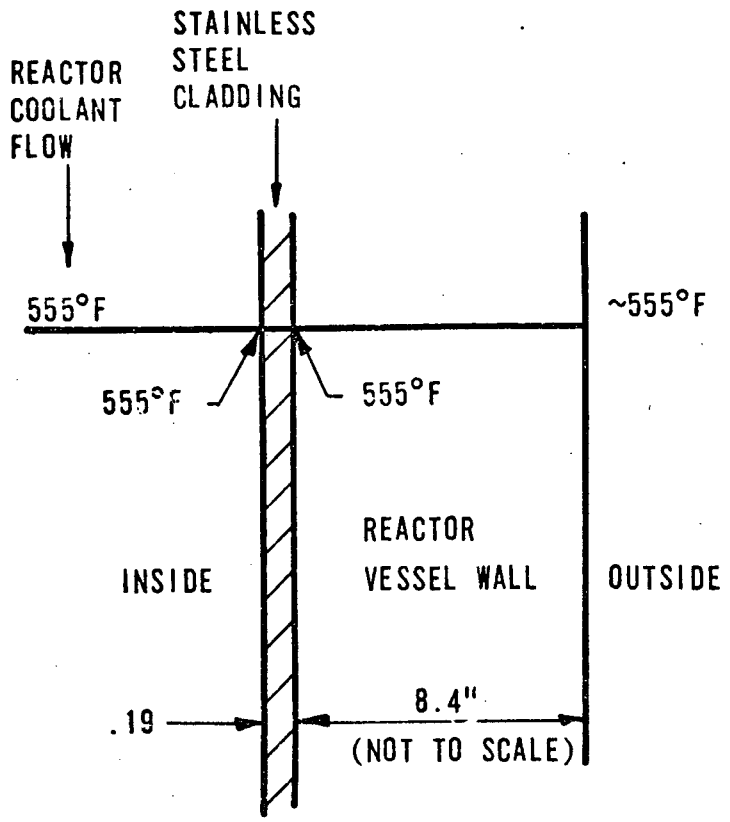

NORMAL TEMPERATURE DISTRIBUTION, STEADY STATE

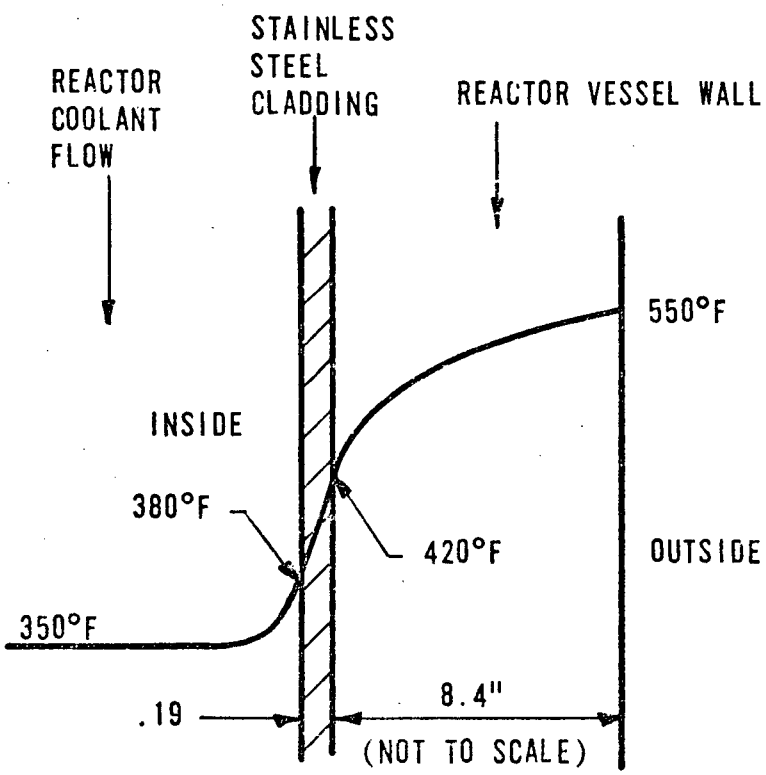

ABNORMAL TEMPERATURE DISTRIBUTION EXISTING DURING OVERCOOLING TRANSIENT

Figure 5.2–1 LOCATION OF OCONEE I VESSEL WELDS IN θ, Z CO-ORDINATES FOR SB LOCA TRANSIENT

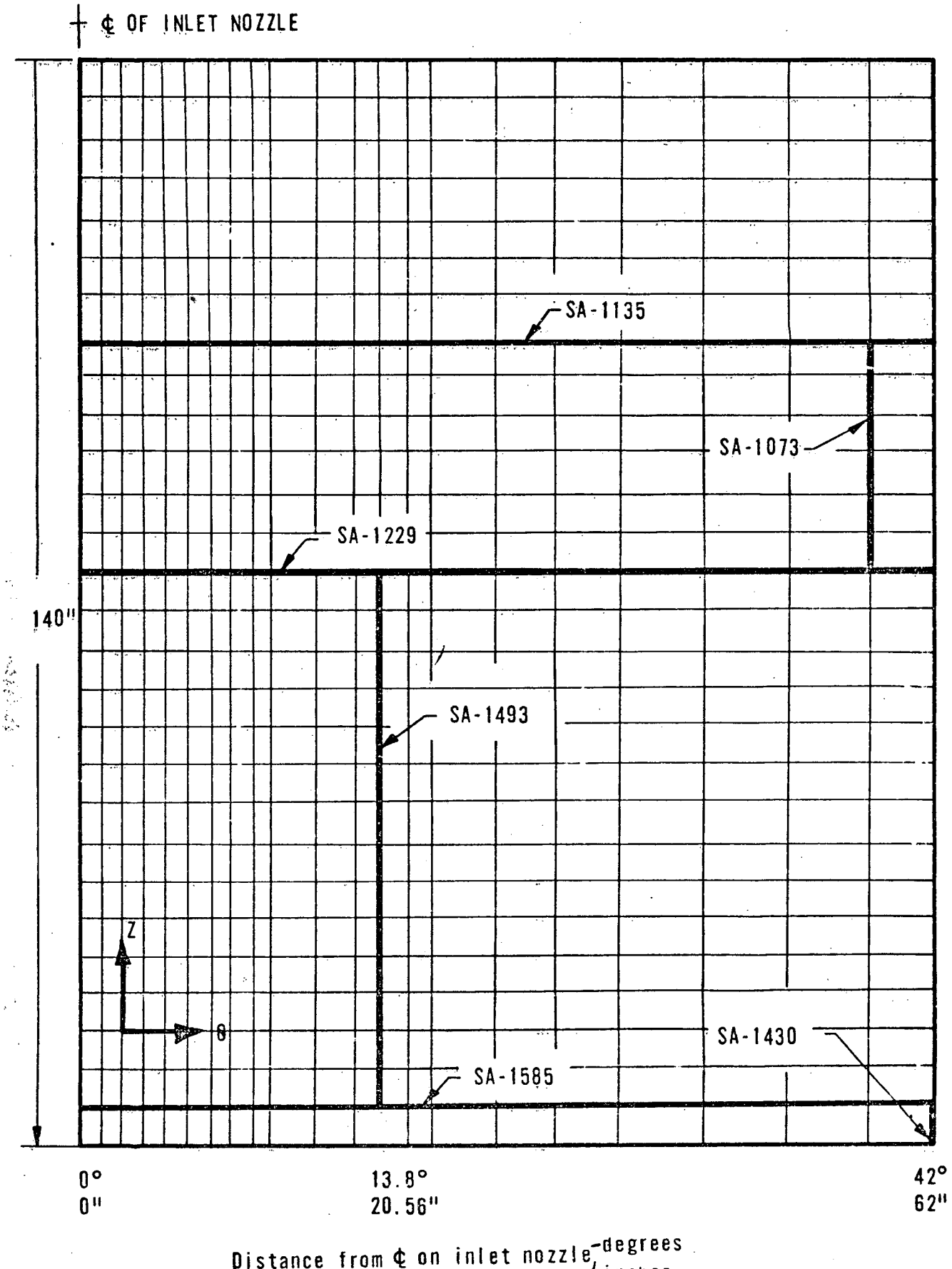

Figure 5.2–2 WALL CONVECTIVE HEAT TRANFER COEFFICIENT VERSUS TRANSIENT TIME FOR SB LOCA TRANSIENT

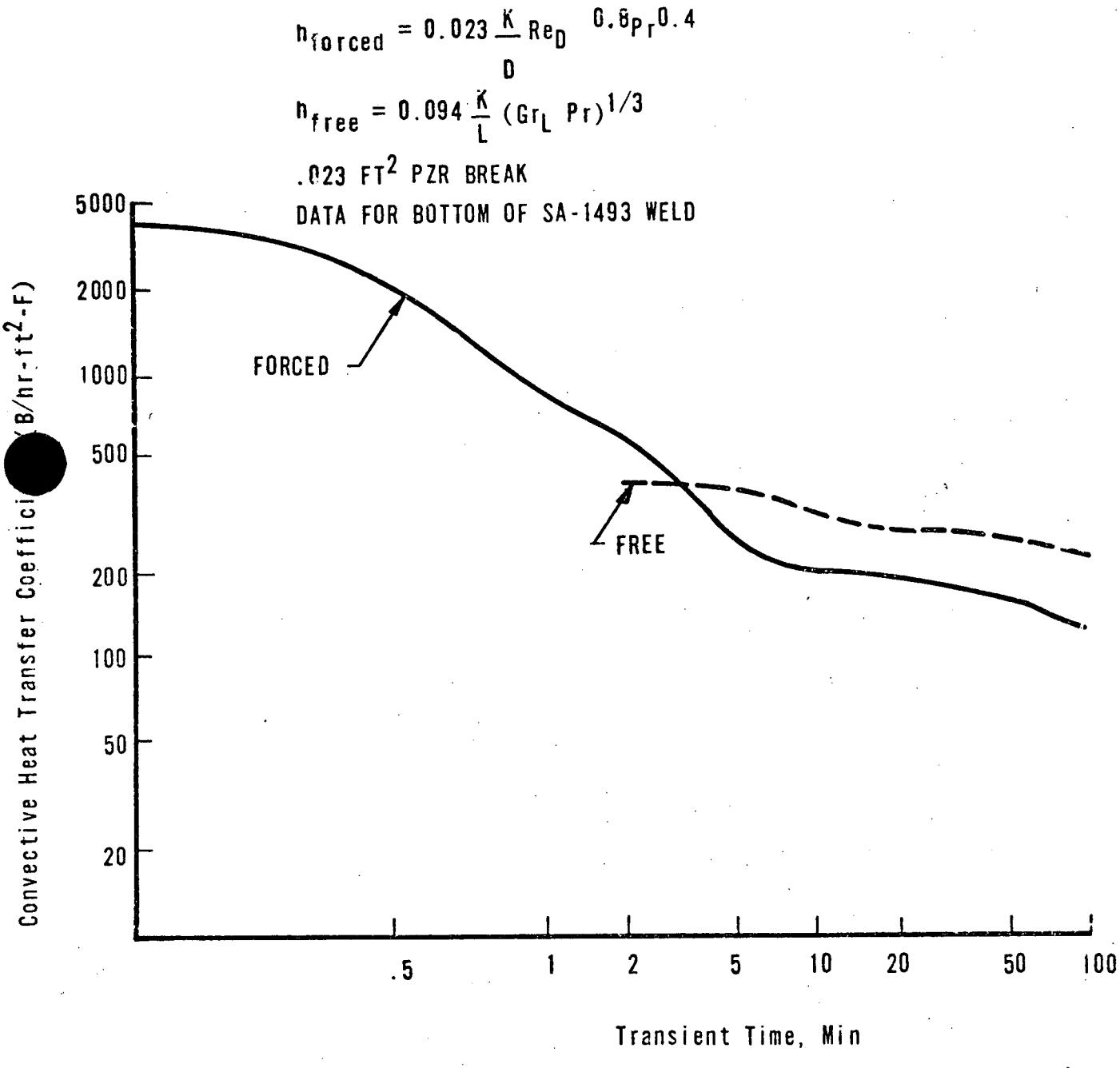

Figure 5.2–3 WALL CONVECTIVE HEAT TRANFER COEFFICIENT VS TIME FOR OVERCOOLING TRANSIENT, CASE 10

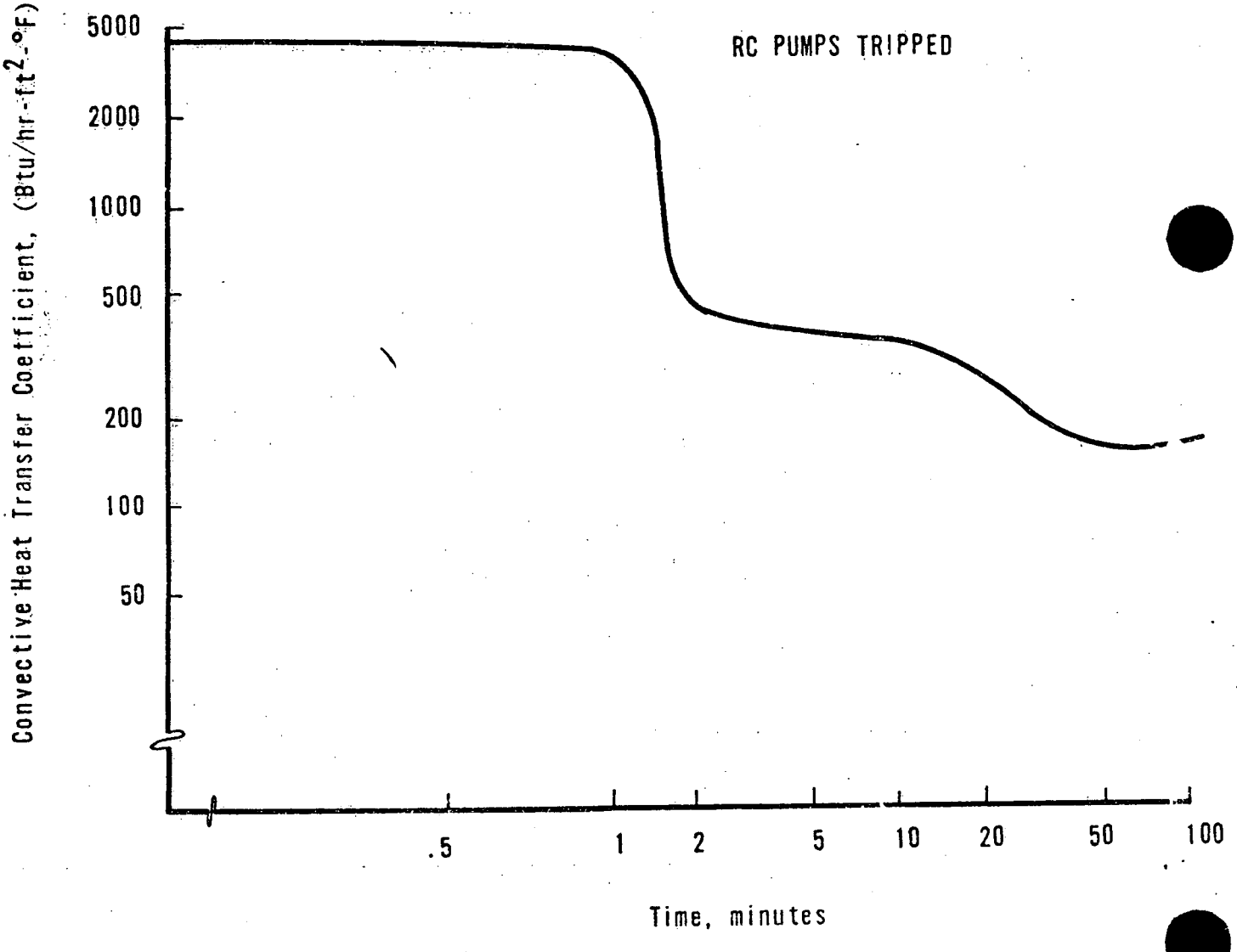

Figure 5.2–4 BASE METAL AZIMUTHAL TEMPERATURE PROFILE FOR SA-1229 WELD LOCATION AT VARIOUS TIMES FOR SB LOCA TRANSIENT

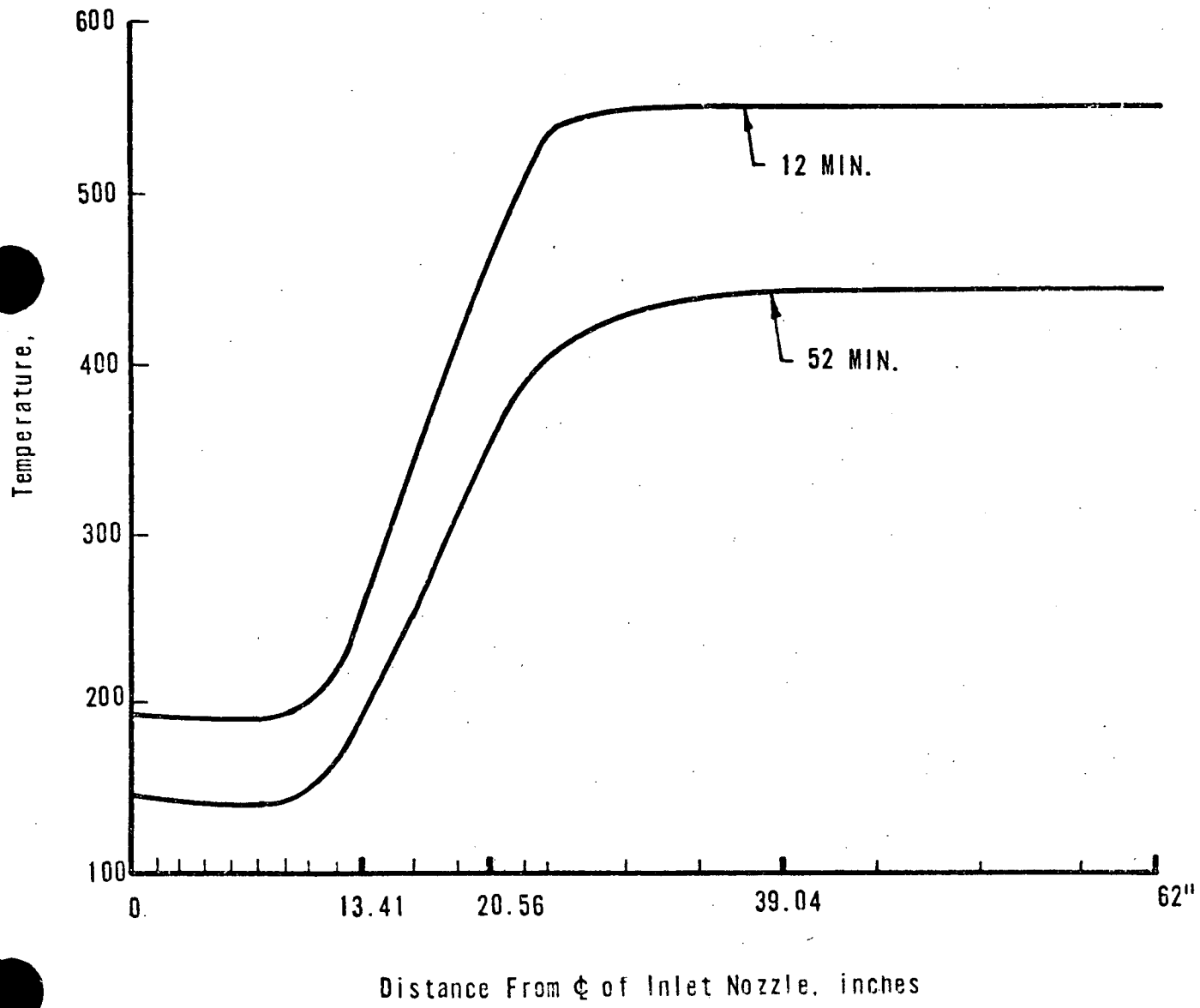

Figure 5.2–5 BASE METAL TEMPERATURE PROFILE VS TIME FOR SB LOCA TRANSIENT AT LOCATION OF SA-1493 AND SA-1229 WELDS

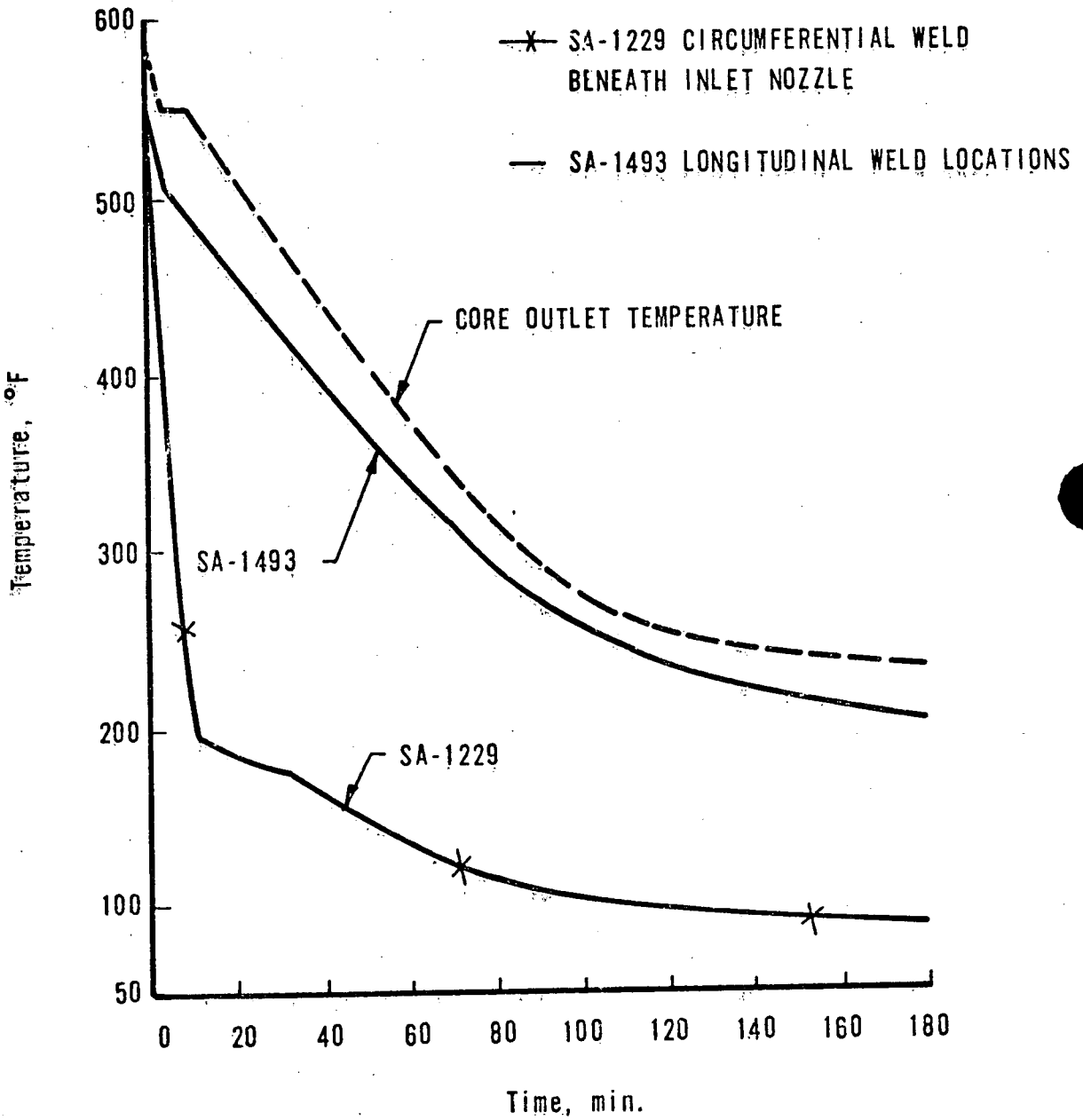

Figure 5.2–6 BASE METAL TEMPERATURE PROFILE VS TIME FOR OVERCOOLING TRANSIENT CASE 10

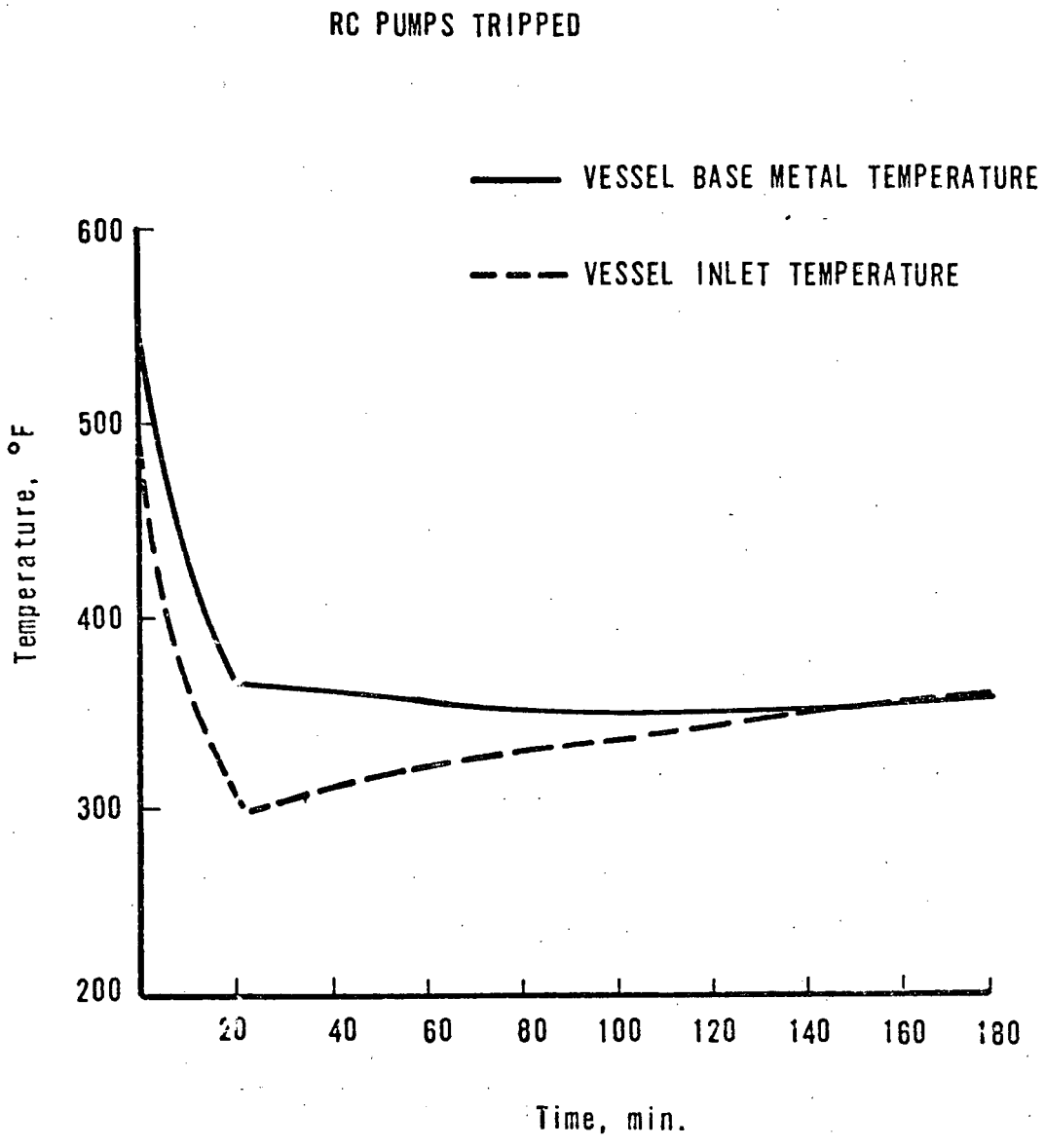

Figure 5.2–7 VESSEL INLET NOZZLE BASE METAL TEMPERATURE VS TIME FOR SBLOCA TRANSIENT AT "KNEE" OF NOZZLE

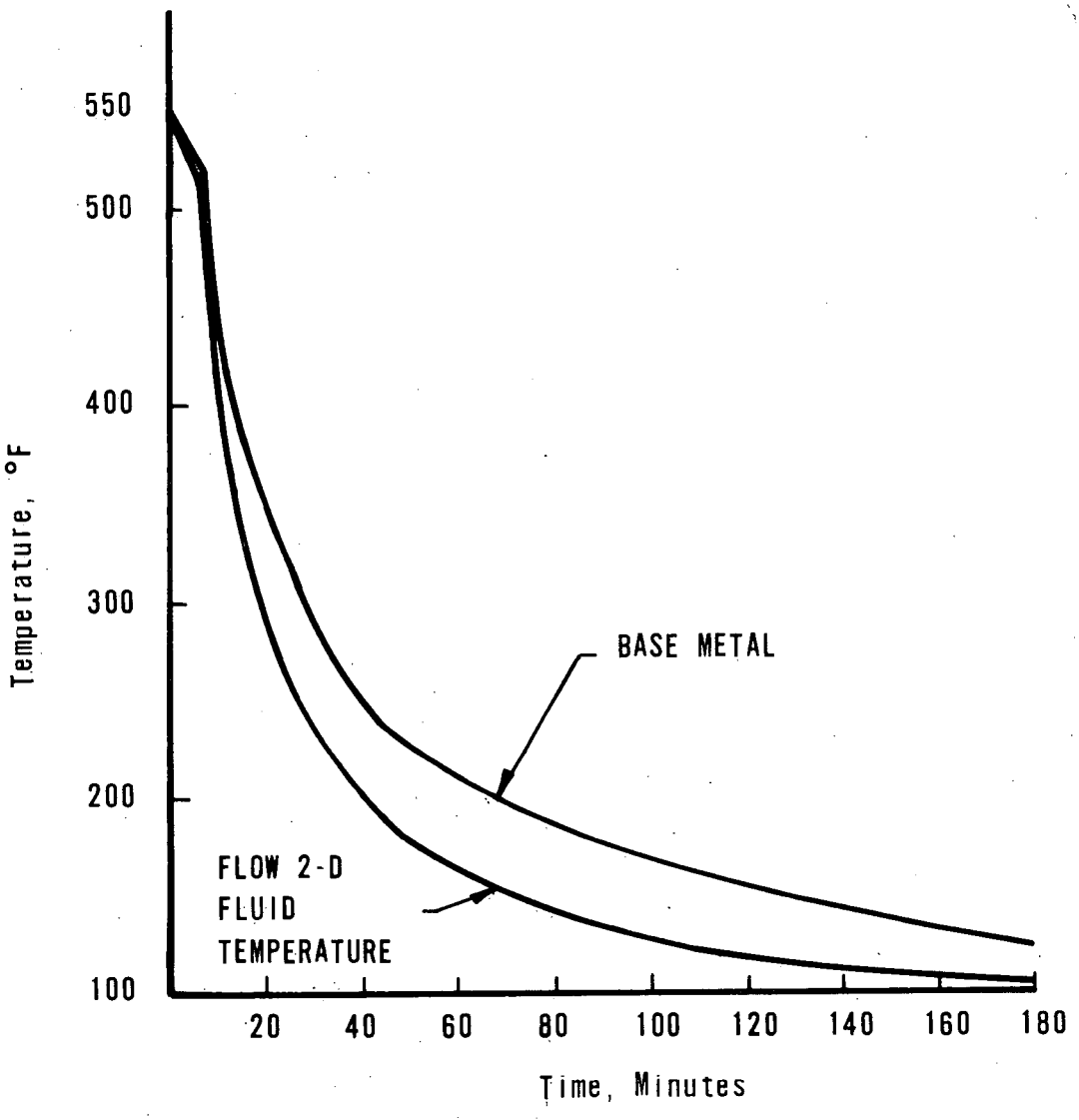

Figure 5.3–1 OCONEE I INSIDE SURFACE OF REACTOR VESSEL WELD LOCATIONS

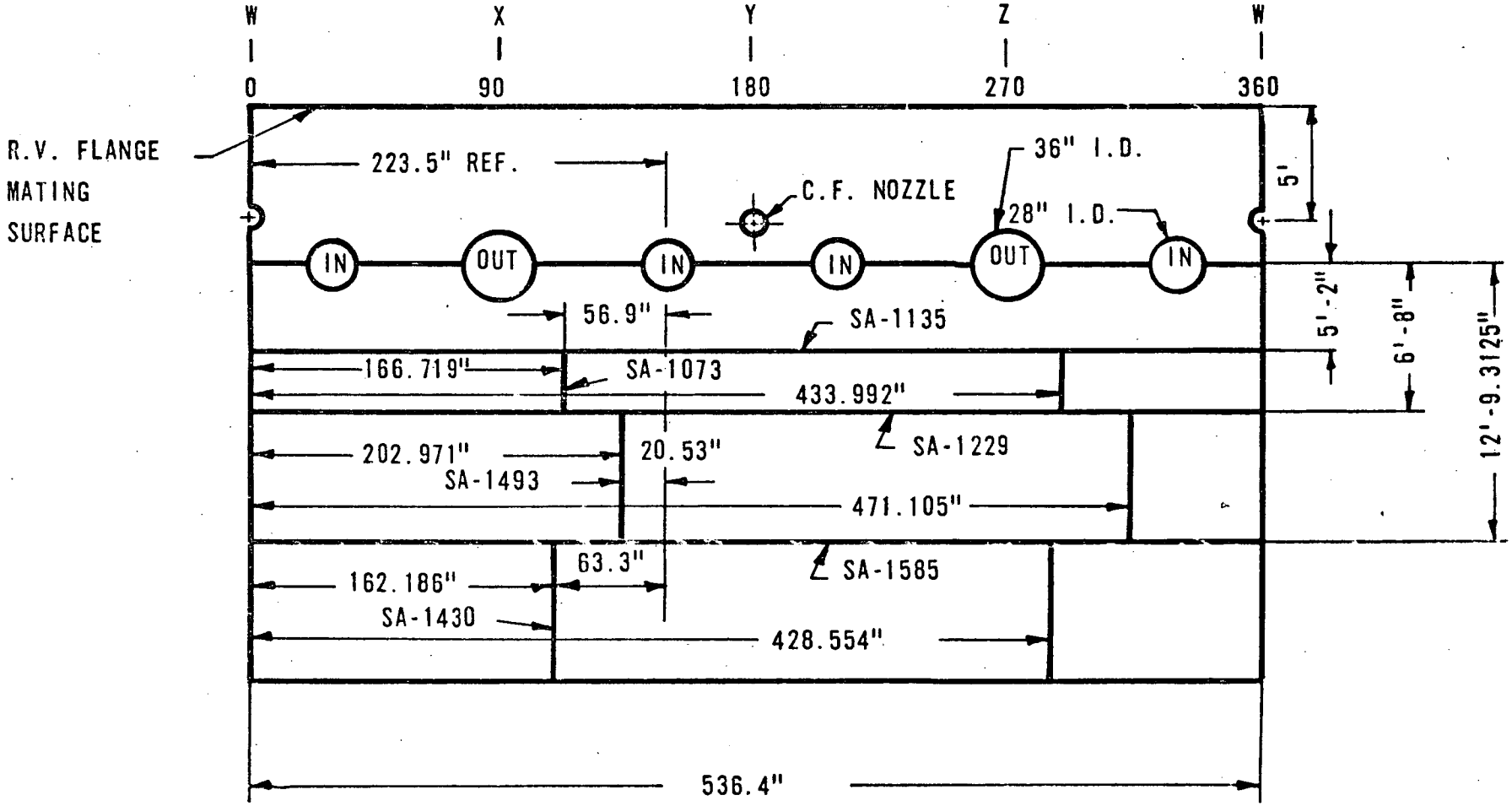

Figure 5.3–2 SB LOCA TRANSIENT WALL TEMPERATURE PROFILES
FOR LOCATION OF SA-1493 WELD

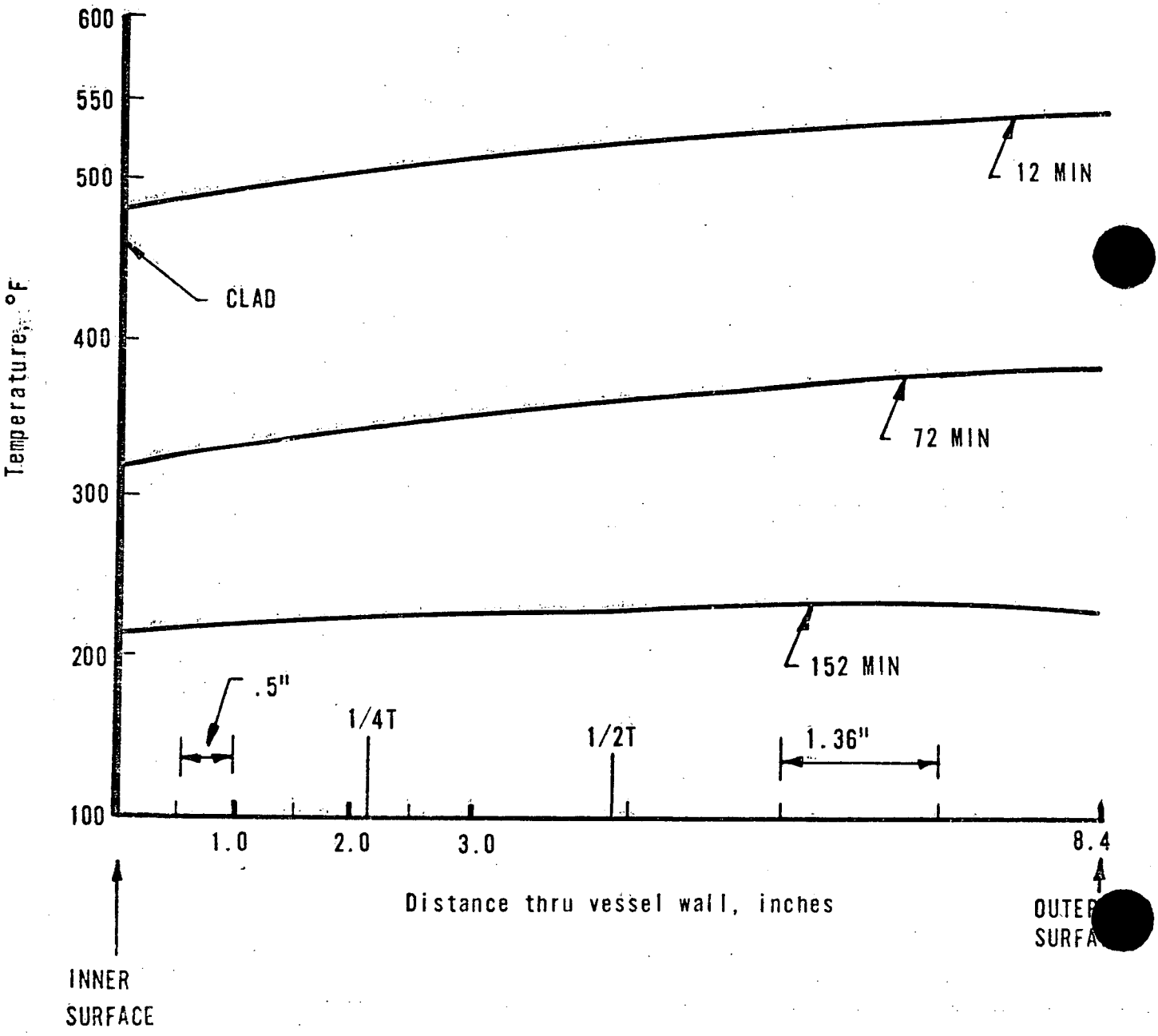

Figure 5.3–3 SB LOCA TRANSIENT WALL TEMPERATURE PROFILES FOR LOCATION OF SA-1229 WELD

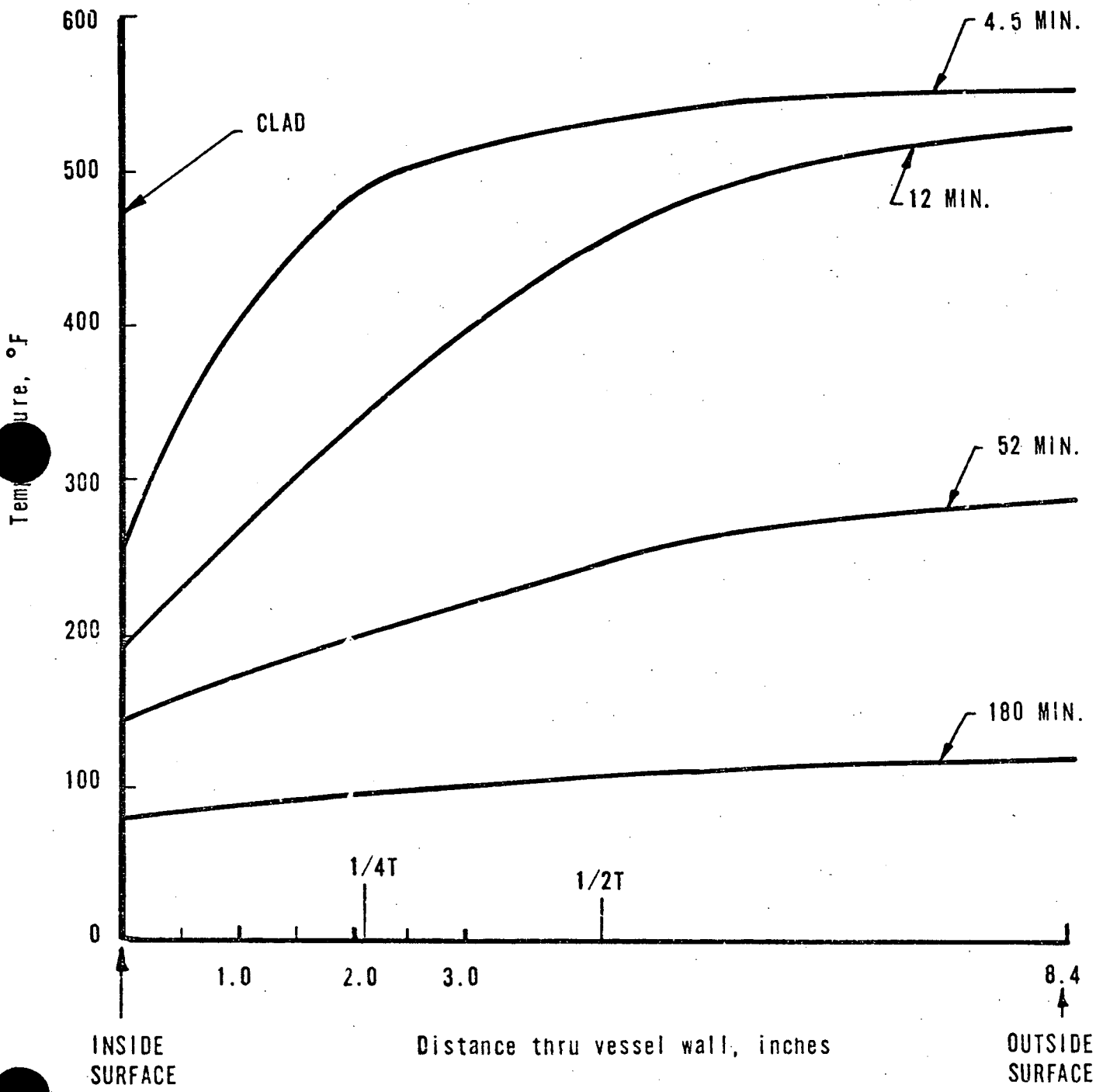

Figure 5.3–4 CASE 9, WALL TEMPERATURE PROFILE VERSUS TIME FOR OVERCOOLING TRANSIENT

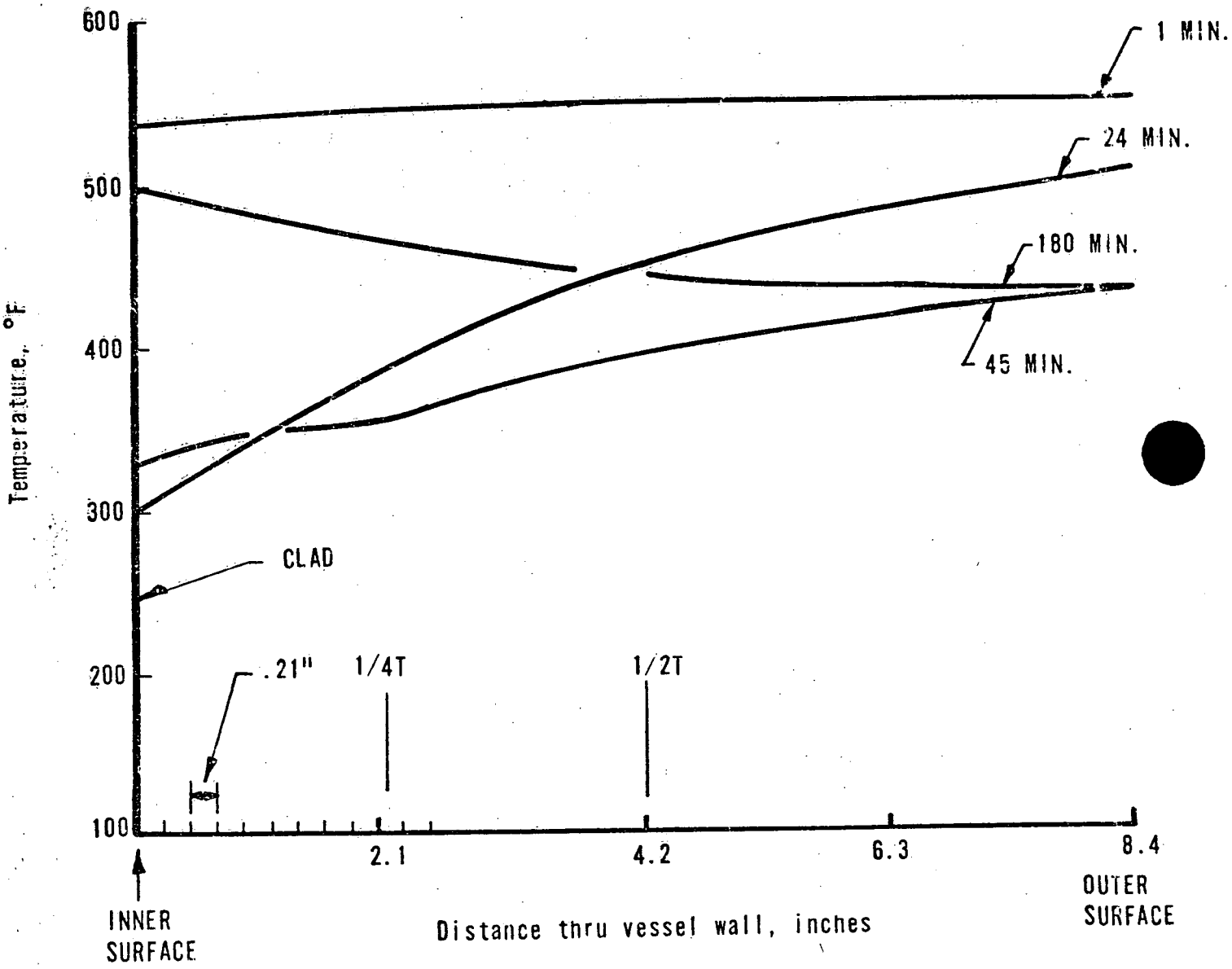

Figure 5.4—1 VESSEL INLET NOZZLE FINITE ELEMENT MODEL

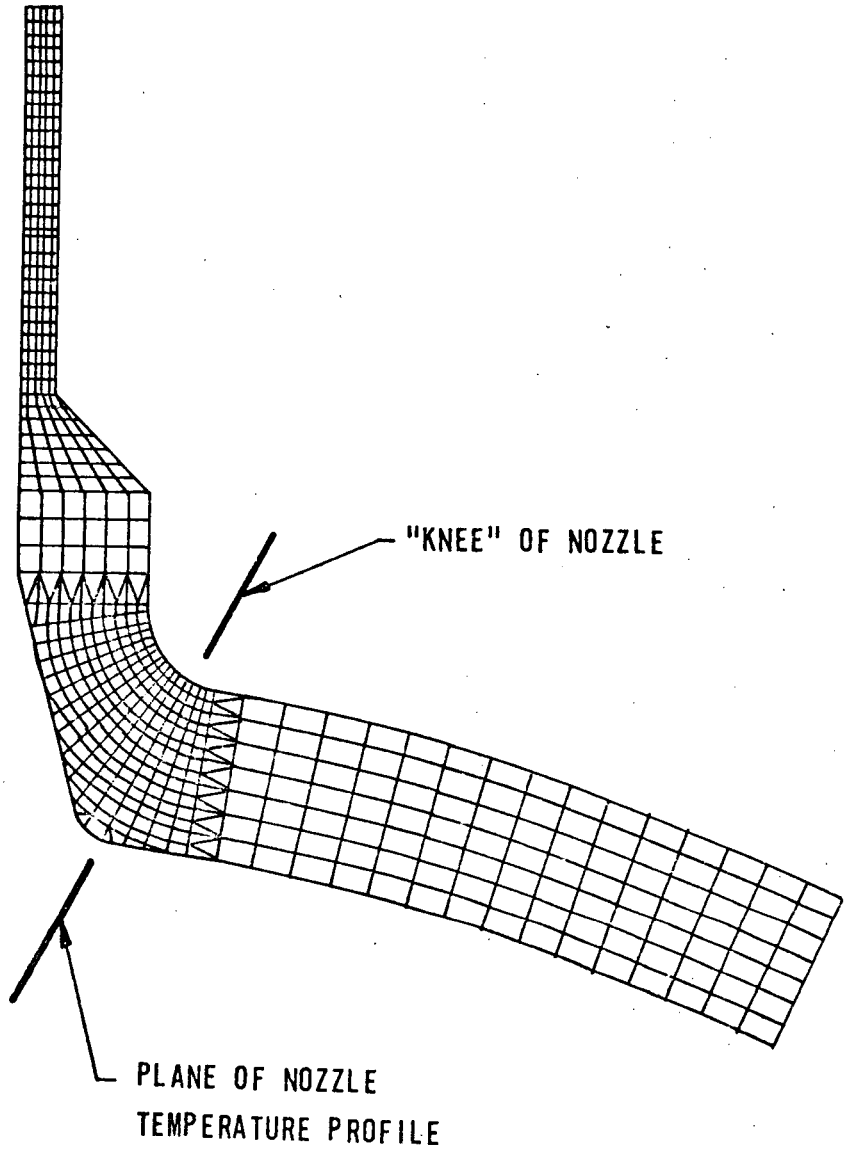

Figure 5.4–2 SBLOCA TRANSIENT INLET NOZZLE TEMPERATURE PROFILES @ THE PLANE OF THE NOZZLE "KNEE"

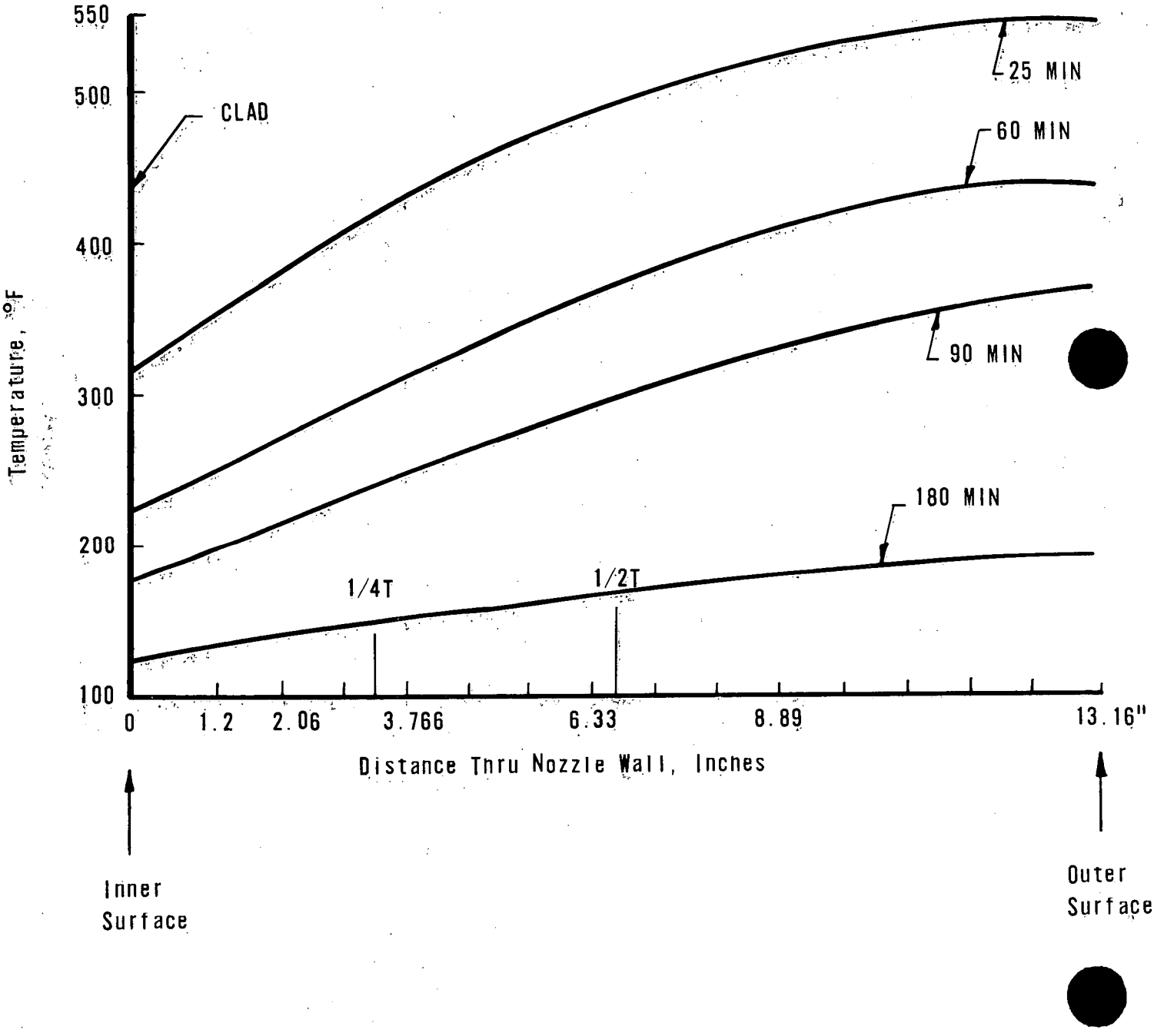

Figure 5.4–3 VESSEL INLET NOZZLE BASE METAL TEMPERATURE PROFILE VS TIME @ "KNEE" OF NOZZLE OVERCOOLING TRANSIENT, CASE 9

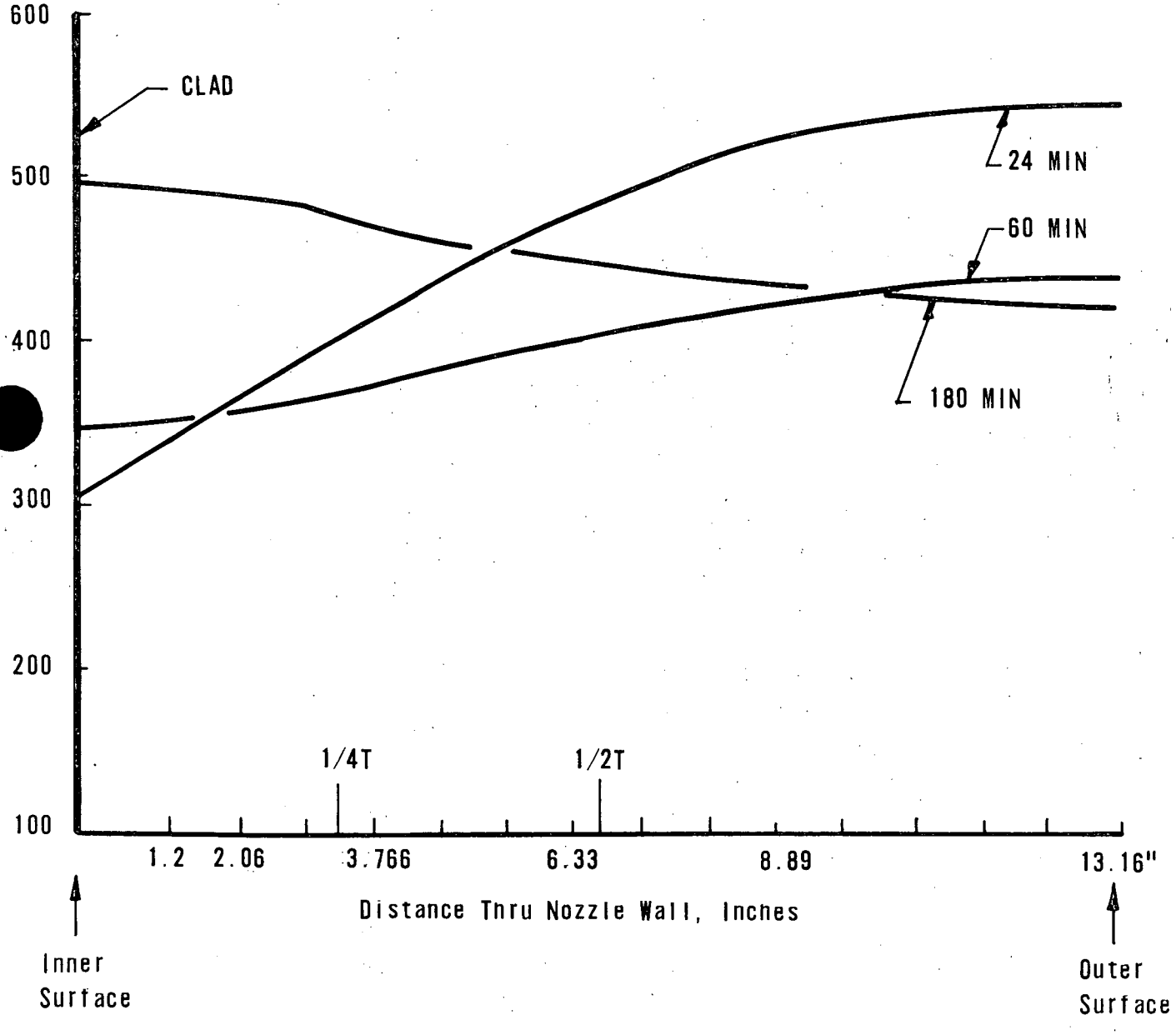

6.0 VESSEL MATERIAL PROPERTIES

6.0 VESSEL MATERIAL PROPERTIES

6.1 Introduction

In order to realistically determine the service life of a reactor vessel for selected transient conditions, a fracture mechanics analysis is conducted, using as input the vessel wall temperature distribution (Chapter 5.0), the material properties of the vessel, and the fluence distribution (Chapter 7.0). This chapter describes the method for determination of vessel specific material properties.

6.2 Determination of Vessel Specific Material Properties for Input to Linear Elastic Fracture Mechanic (LEFM) Analysis

The material properties used as input to the LEFM analysis are based on the material certification and weld metal qualification records where available. These properties and data are available in BAW-1436,[15] which reports the results of the last capsule removed and tested for Oconee 1. For those cases where the properties were not available, because they were not required at the time the Oconee reactor vessel was fabricated, the properties were established in accordance with the requirements of BAW-10046A, Rev. 1.[16] There are two exceptions to the above procedures, and because of their importance to this analysis, they are discussed separately.

6.2.1 Copper and Phosphorus Content of Welds

The true copper and phosphorus contents of the weld metals were not determined as part of the weld metal qualification procedure and subsequently a detailed study was made to ascertain the representative chemical composition of all core region weld metals of 177-FA vessels. This study established the chemical composition as well as the copper and phosphorus contents of the deposited weld metals. These values published in BAW-1511P[1] were used to establish the copper and phosphorus values used in the LEFM analysis.

6.2.2 Fluence at Weld Locations

The fluence at the weld location determines the radiation damage that the specific weld metal exhibits. Thus, it is important that each weld metal be identified as to the specific fluence it will experience for a given service period. The fluence is related to the location of the weld metal relative to the core region and must take into account the azimuthal and axial relationship of the weld metal. Since the longitudinal weld exists in the axial flux plane, the highest flux over the weld is used in the analysis. The values used to determine the relative fluence for each material used in this analysis were obtained from BAW-1485.[17] These geometry factors are applied to the peak fluence calculation for the specific vessel as described in Chapter 7.0.

6.3 Adjustment of RT_{NDT}

The adjustments in the RT_{NDT} of the reactor vessel materials to account for the effect of irradiation damage to both the base metal and the weld metals were performed in accordance with Regulatory Guide 1.99, Revision 1, using the chemistry as described in Section 6.2.1 and the fluence values developed as described in Section 6.2.2. No adjustment was made to the RT_{NDT} of the vessel inlet nozzle materials because the predicted EOL fluence is less than the threshold for radiation damage as defined in 10CFR50 Appendix H Paragraph II.A.

6.4 Upper Shelf Requirement for LEFM Analysis

Definition of the upper shelf fracture toughness values for LEFM analysis is required because the ASME Code does not define an upper shelf value for the K_R curve. For consistency with the previous analysis contained in BAW-1648, an upper shelf value of 200 ksi $\sqrt{in.}$ was established for B&W analysis.

6.5 Assumptions and Conservatisms in Analysis

The assumptions used to develop the data base are included in the reference documents and no additional assumptions were made during development of the data for these analyses.

The conservatisms in the input data used in this analysis are many. The copper and phosphorus contents are believed to be realistic and the variations in chemistry that may exist are believed to be minor. The variations in chemical content will have only a negligible impact on the predicted value of the shift in RT_{NDT}. Likewise, the fluence value is believed to be conservative and any additional refinement will have a positive impact on the overall margin of the analysis. Furthermore, the use of Regulatory Guide 1.99 to predict the change of RT_{NDT} as a function of chemistry and fluence has proven to be conservative as demonstrated by comparing measured irradiated properties data from twelve surveillance capsules with the predictions based on Regulatory Guide 1.99. Although a detailed qualitative evaluation of conservatism for these data has not been made because of insufficient data on a quantitative basis, it is reasonable to assume that an overall evaluation of the input data would demonstrate that it is conservative.

6.6 Results

The results of this materials determination of vessel specific material properties are given in BAW-1436 and BAW-1511P. The properties for all base metal and welds in the beltline region of the vessel used in the LEFM analysis are given in Table 6.6-1. The properties for the vessel inlet nozzle forging used in the LEFM analysis are given in Table 6.6-2. The predicted fluence for the inlet nozzle at 32 EFPY is calculated to be less than 1.0×10^{16} n/cm^2. Since the fluence is below the threshold for analysis as defined by 10CFR50 Appendix H, minimal irradiation damage occurs and therefore no adjustment of the initial RT_{NDT} is calculated for this analysis. The chemistry of the nozzle forging was not determined in the same manner as the vessel beltline materials were determined. However, since the accumulated fluence is extremely low at this position,

negligible irradiation damage is expected to occur during the life of the vessel. The result of the beltline region materials evaluations are conservative and the materials are expected to continue to behave in a predictable manner as demonstrated by the results from the two reactor vessel materials surveillance capsules evaluated to date for Oconee 1. Because the capsules are irradiated at fluence levels greater than that being experienced by the reactor vessel, the material behavior of the capsule leads that of the actual reactor vessel wall. This assures advanced knowledge of the behavior of the material properties in the reactor vessel, and in the unlikely event that an abnormal material behavior is observed, adequate time will exist to evaluate the impact of such property changes on reactor vessel integrity. The materials behavior of the Oconee 1 reactor vessel will continue to be monitored by the future evaluation of surveillance capsules as scheduled.

In addition, the results from the Integrated Reactor Vessel Materials Surveillance Programs for all B&W operating plants and other materials research programs will be available to evaluate and predict the future behavior of the Oconee 1 materials as affected by its service environment.

Table 6.6-1

MATERIAL PROPERTIES USED IN THE LEFM ANALYSIS

OF THE OCONEE UNIT 1 REACTOR VESSEL 32 EFPY

MATERIAL IDENTIFICATION[3]			CHEMISTRY[1]		NEUTRON FLUENCE (Inside Surface)	INITIAL[2] RD_{NDT}
Weld or Heat Number	Type	Location	Cu wt. %	P wt. %	n/cm^2	°F
AHR-54	SA508,CL2	Nozzle Belt Forging	0.16	.006	1.97E18	(+60)
SA-1135	circumferential weld	Nozzle Belt/ Upper Shell	-	-	1.97E18	(+20)
C2197	SA302B	Upper Shell	0.15	0.008	9.35E18	(+40)
SA-1073	longitudinal weld	Upper Shell	-	-	7.38E18	(+20)
SA-1229	circumferential weld	Upper Circumferential (61% I.D.)	-	-	9.35E18	(+20)
SA-1493	longitudinal weld	Middle Shell	-	-	8.98E18	(+20)
C3278-1	SA-302B	Middle Shell	0.12	0.010	1.23E19	(+40)
SA-1585	circumferential weld	Middle Shell	-	-	1.23E19	(+20)
C2800-1	SA-302B	Lower Shell	0.11	0.012	1.23E19	(+40)
SA-1430	longitudinal weld	Lower Shell	-	-	1.09E19	(+20)

(1) Chemistry per BAW-1511P, October 1980. (Weld data is proprietary.)

(2) Estimated RT_{NDT} values per BAW-10046A, Rev. 1, March 1976.

(3) Per BAW-1436, September 1977.

Table 6.6-2

MATERIAL PROPERTIES FOR OCONEE UNIT 1

REACTOR VESSEL INLET NOZZLE

MATERIAL IDENTIFICATION

Type	Location	Chemistry (2)	Neutron Fluence n/cm^2 (1)	Initial RT_{NDT} °F (3)
Forging, SA508 Class 2	Cold Leg Nozzle	N/A	$<1.0E16$	+60

(1) Predicted EOL fluence for vessel inlet nozzle.

(2) Since EOL fluence is $<10^{16}$ n/cm^2, no chemistry was used in analyses of nozzle material.

(3) Estimated RT_{NDT} values per BAW-10046A, Rev. 1, March 1976.

7.0 VESSEL AND WELD FLUENCE DETERMINATION

7.0 VESSEL AND WELD FLUENCE DETERMINATION

7.1 Introduction

Fluence analysis as a part of the ongoing reactor vessel surveillance program has three primary objectives:

a. Determination of maximum fluence in the reactor vessel as a function of reactor operation
b. Prediction of reactor vessel fluence in the future
c. Determination of the test specimen fluence within the surveillance capsule.

Vessel fluence data are used to evaluate changes in reference transition temperature and upper shelf energy levels. Fluence data along with vessel wall temperature distributions and material properties are used to calculate the allowable service life for selected transients.

7.2 Analytical Procedure for Fluence Determination

Vessel fluence as a function of time was determined by first calculating the fluence for an irradiation period for which surveillance capsule dosimetry are available and then extrapolation of that result to future operational conditions. Weld fluence can then be obtained from axial and azimuthal shape factors that relate weld location to relative variations in fast flux ($E > 1$ MeV). Data from the Oconee I-E capsule fluence calculation are presented in BAW-1436 and analytical procedures for both vessel and weld fluence calculations are described in BAW-1485.

Oconee 1 vessel fluence for Cycles 1 and 2 was calculated with an analytical model which was normalized to the capsule dosimeter measurements. The measured to calculated normalization factor from BAW-1436 was 1.10. Vessel fluence at the end of Cycle 5 was obtained from the proportionality of excore fluence to fast flux escaping the core. Core escape flux data are obtained from fuel management PDQ calculations which are performed

for all reload cores. Thus, an average fast flux for Cycles 3, 4, and 5 at the maximum fluence location on the vessel inner surface was calculated to be 1.68×10^{10} n/cm^2-s; the corresponding fluence at the end of Cycle 5 is 2.14×10^{18} n/cm^2.

For Cycle 6, a reload core design was initiated to establish an 18-month Lumped Burnable Poison (LBP) fuel cycle. This new fuel cycle management results in a significant decrease in the peripheral fuel assembly's power, with a corresponding decrease in core leakage flux and fluence at the vessel wall. This approach utilizes once-burned fuel assemblies on the periphery of the core. The fresh fuel assemblies with burnable poison rods are loaded throughout the remainder of the core in checker-board fashion. After Cycle 5, vessel flux was calculated to be 1.21×10^{10} n/cm^2-s based on proportionality with core leakage flux. The corresponding maximum fluence accumulation rate is $.037 \times 10^{19}$ n/cm^2/EFPY. The location of maximum fluence in the vessel, shown in Figure 7.2-1, is the inside surface of the base metal at an azimiuthal position of $\sim 12°$ from a major axis and near the core midplane in elevation.

Vessel fluence as a function of wall penetration (Figure 7.2-2) is obtained from the analytical model described in BAW-1485. From a plot of fast flux versus wall thickness, lead factors are obtained which represent the ratios of surface flux to flux at T/4, T/2, 3T/4, and T positions where T is the thickness of the pressure vessel, $\sim$ 8.6 inches. The corresponding flux ratios at the above wall locations are 1.8, 3.7, 7.7, and 21, respectively. These data are considered to be independent of azimuthal and axial location.

Shape factors for converting maximum vessel fluence to a weld location are obtained from RΘ and RZ reactor model calculations of flux distribution in the pressure vessel using the DOT35 transport code. An RΘ model produced relative factors for azimuthal displacement as a function of angular deviation from 12° off a major axis (angular position of maximum fluence), and an RZ model was used for axial displacement as a function of distance from core midplane. The relative azimuthal flux produced by the RΘ model for a typical 177 FA plant is shown in Figure 7.2-1. Because

of symmetry in the power distribution in the azimuthal direction, only 1/8 core data is shown. The longitudinal weld in the Oconee 1 vessel with the highest fluence was determined to be SA-1430 located at 19° off the major axis. Vertically, the SA-1430 weld passes through the peak location in the axial fluence profile. Thus, shape factors for the SA-1430 weld are F_θ = .89 for the 19° location and F_Z = 1.0 for an axial location near the core midplane. Existing longitudinal welds in the Oconee 1 vessel are located relative to the maximum fluence as shown in Figure 7.2-1 and 7.2-3. However, the limiting weld, when material properties, fluence and thermal environment are taken into account, will be determined by the fracture mechanics analysis discussed in Chapter 8.0.

7.3 Assumptions

The principal assumptions used in the determination of vessel and weld fluences are:

1. The point of location of maximum flux (azimuthal and axial) is invariant from cycle to cycle.

2. The azimuthal shape of fast flux does not vary significantly from cycle to cycle.

3. Ex-core flux (E > 1 MeV) is proportional to core leakage flux (E > 1.8 MeV) as determined from cycle dependent power distribution calculations.

4. For cycles with equivalent designs, i.e., (out-in versus in-out-in shuffle schemes), relative core escape fluxes (cycle to cycle) are essentially the same for all 177FA reactors.

5. The axial shape of fast flux for all cycles can be represented by an "equilibrium" cycle power distribution.

6. Structural configuration, materials, and coolant conditions are sufficiently similar between 177FA reactors that core power distribution is the only input parameter that significantly affects ex-core fast flux distribution with respect to a specific reactor.

The procedure used to establish the calculational model for the analytical determination of fast fluence in the pressure vessel has been benchmarked through participation in the "Blind Test" Phase of the Light Water Reactor Pressure Vessel Dosimetry Improvement Program (LWRPVDIP). In addition, the "measured" fluence at the end of cycle 2 in the Oconee 1 capsule, OCI-E (to which analytical flux data were normalized) was verified by HEDL under another phase of LWRPVDIP to within 1% of the B&W value (HEDL-SA 2546).[19] Confidence in the overall fluence calculational procedure has been achieved from the analysis of 12 surveillance capsules from eight B&W 177 FA reactors participating in the integrated vessel material surveillance program. Comparison between calculated and measured dosimeter activities has consistently been within 10%.

Uncertainty limits have been estimated for reported fluence in the reactor vessel - ±15% for time periods corresponding to concurrent in-reactor surveillance capsule irradiation and ±18% for reactors without capsules (i.e., dosimeter to benchmark analysis). For extended time periods, this uncertainty limit is ±21% for reactors without capsules. The uncertainty limit for welds is somewhat greater and is a function of location. However, at no time can the upper limit on the uncertainty of a weld fluence exceed the upper limit on the uncertainty of maximum vessel fluence.

7.4 Oconee 1 Fluence Results

Oconee 1 has completed 6 fuel cycles which corresponds to 5.1 EFPY and a neutron fluence of 2.55×10^{18} n/cm^2 at the peak location. With conversion to the low leakage 18-month LBP fuel cycles, the fluence accumulation rate at the peak location in the vessel has decreased from $.054 \times 10^{19}$ n/cm^2/EFPY (for first 4 EFPY) to $.037 \times 10^{19}$ n/cm^2/EFPY. This has reduced the projected life fluence at the peak location from 1.73×10^{19} to

1.25 x 10^{19} n/cm^2 (about 28%). This peak value also applies to the circumferential weld SA-1585. For the longitudinal weld, SA-1430, a corresponding decrease occurred in the fluence accumulated from .046 x 10^{19} to .033 x 10^{19} n/cm^2/EFPY. The location of the longitudinal welds and the peak neutron fluences at the vessel inner surface is illustrated in Figure 7.2-3 and the location of all beltline region welds is shown in Figure 7.4-1.

Figure 7.2–1 TYPICAL AZIMUTHAL FLUX PROFILE NORMALIZED TO PEAK FLUX LOCATION

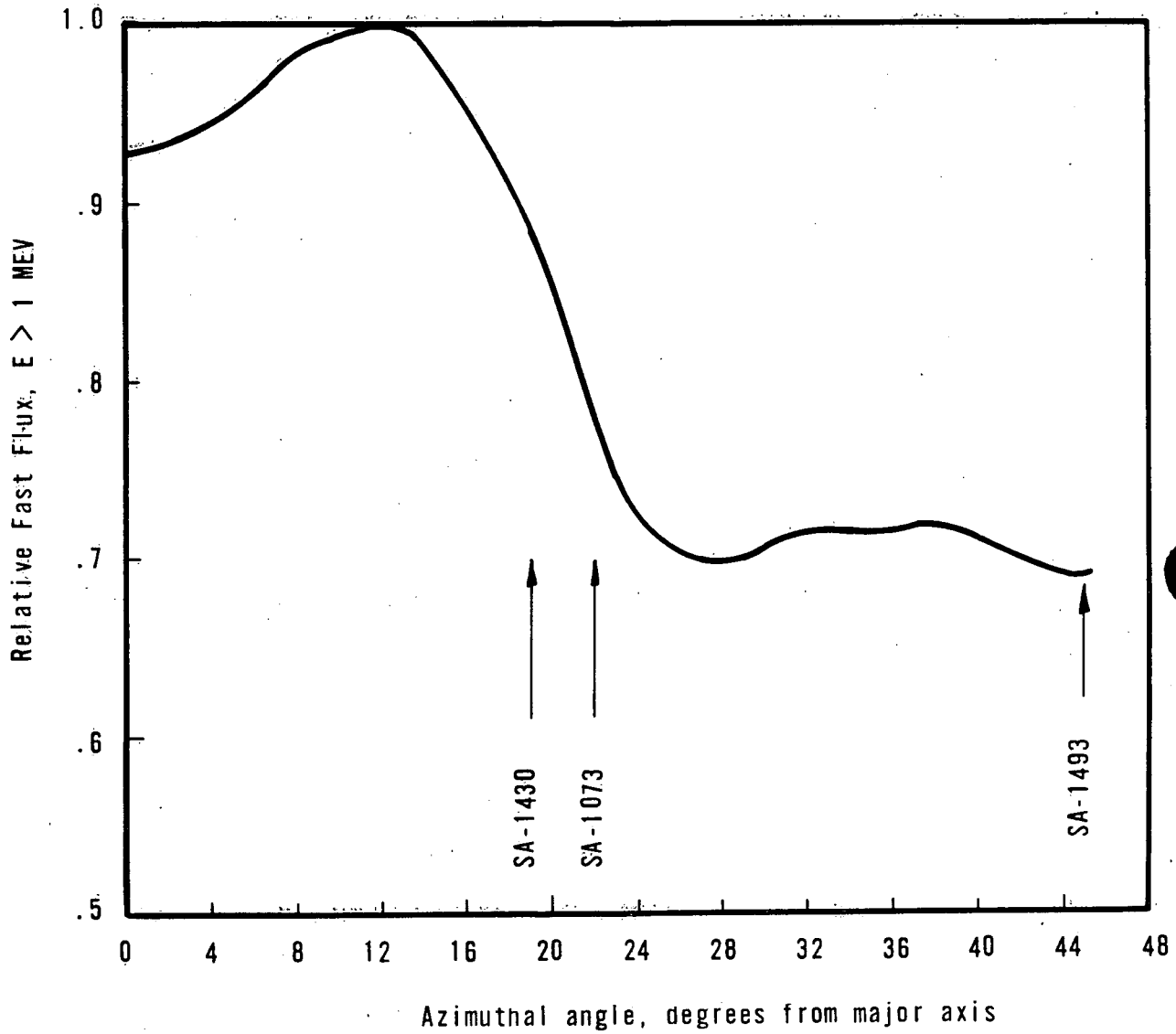

Figure 7.2–2 FAST FLUX ATTENUATION THROUGH PRESSURE VESSEL WALL

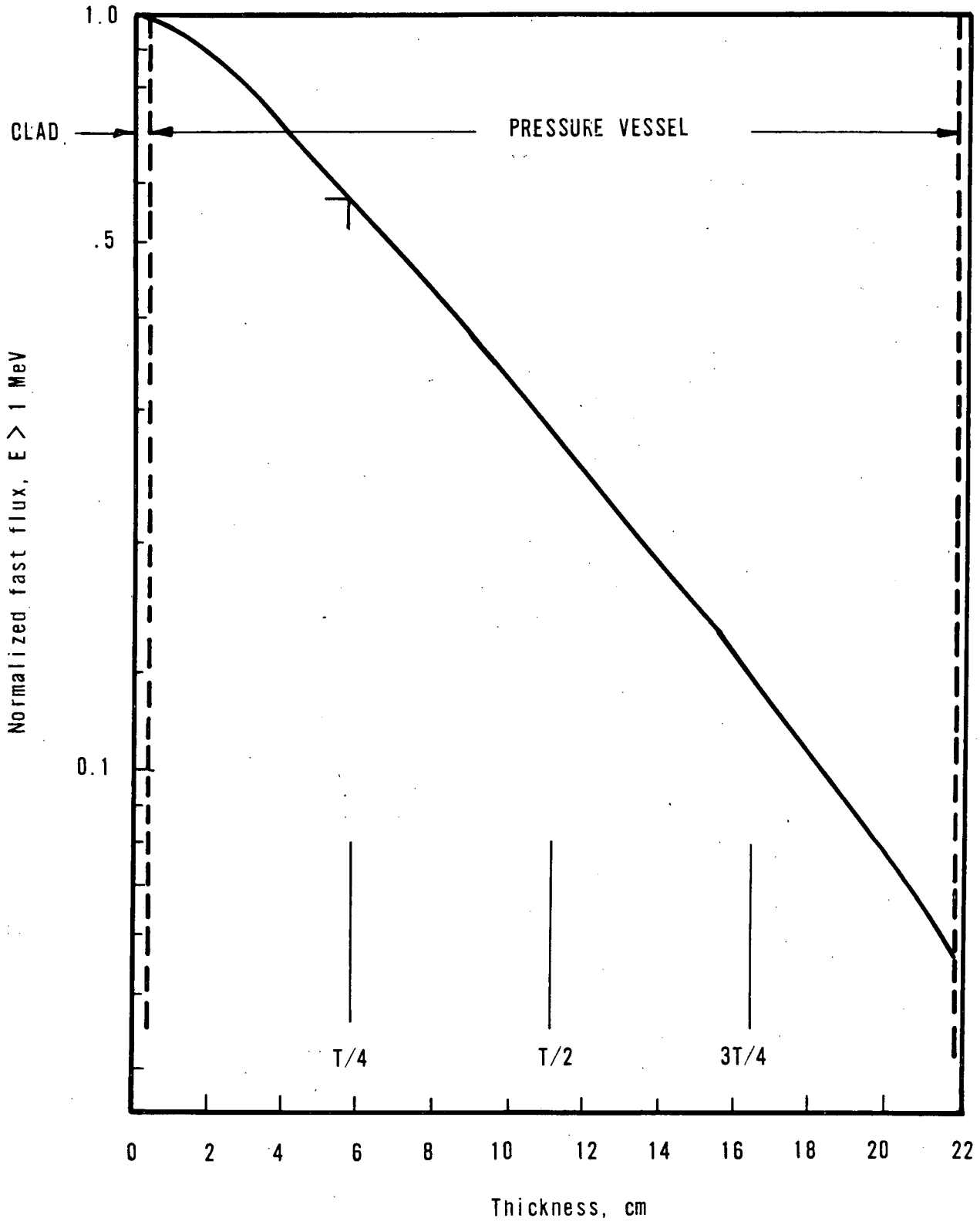

Figure 7.2–3 LONGITUDINAL WELD LOCATIONS TO AZIMUTHAL FLUENCE PROFILE

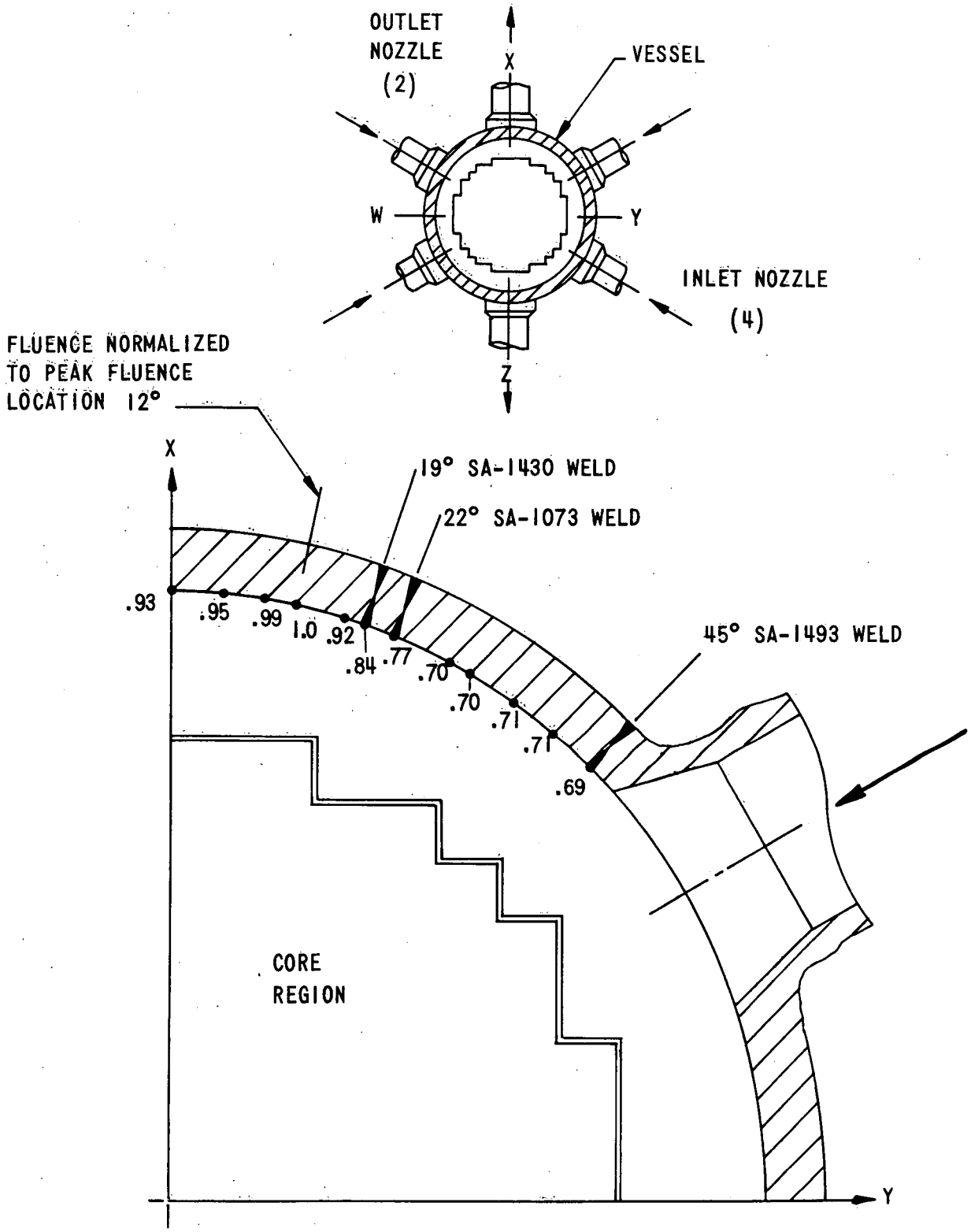

Figure 7.4–1 Location and Identification of Materials Used in Fabrication of Oconee Unit 1 Reactor Pressure Vessel

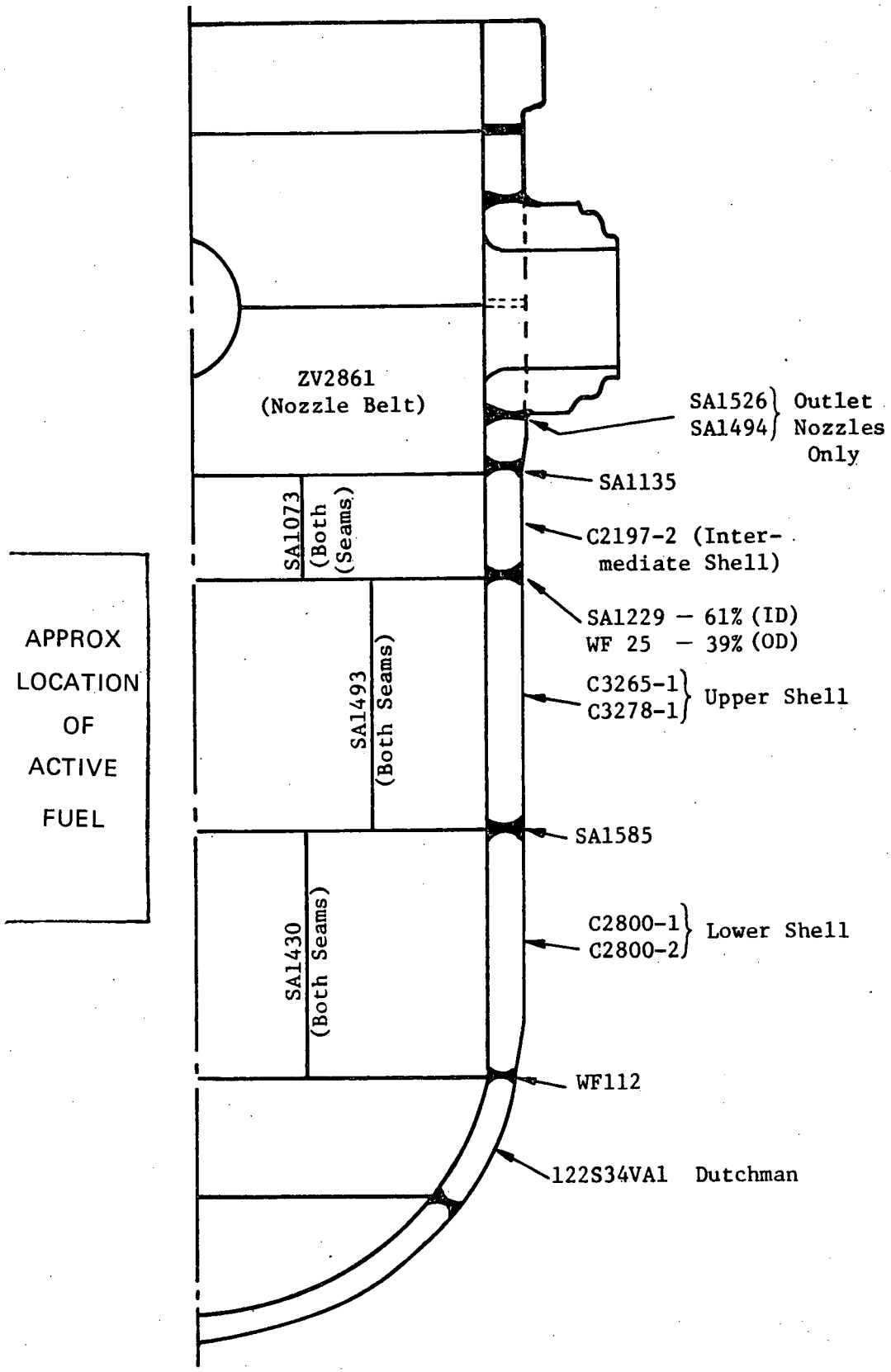

8.0 VESSEL FRACTURE MECHANICS ANALYSIS

8.0 VESSEL FRACTURE MECHANICS ANALYSES

8.1 Introduction

Over the lifetime of an operating reactor, the reactor vessel is subjected to a variety of transients that were not part of the initial design basis; however, all these transients would satisfy the stress criteria of ASME Section III for unflawed vessels. However, if a flaw were postulated to exist in a vessel undergoing a severe transient it becomes necessary to evaluate the structural integrity of the pressure vessel to determine if the flaw would grow during the transient. The transients defined in Chapter 2.0 and 3.0 were evaluated using ASME Section XI, Appendix A, Linear Elastic Fracture Mechanics (LEFM) techniques to determine whether crack initiation is predicted and, if so, that crack arrest occurs within 1/4T.

The LEFM analysis uses an input various vessel material properties and neutron fluences on the vessel wall to evaluate the integrity of a specific reactor vessel. The plant specific material properties (base metal and weld metal) such as copper and phosphorus content, RT_{NDT} shift and fracture toughness are described in Chapter 6.0 (Vessel Material Properties). The plant specific vessel neutron fluence is obtained per the procedure outlined in Chapter 7.0 (Vessel and Weld Fluence Determination). The copper and phosphorus content in the welds and the accumulating fast neutron fluence on the vessel as a result of continued operation, results in lowering the vessel toughness and hence, lower resistance to fracture.

The plant overcooling transients selected for fracture mechanics analysis were obtained from Chapter 2.0. The SBLOCA plant transient data selected for fracture mechanic analysis was obtained from Chapter 3.0. The thermal analysis for all transients was performed as outlined in Chapters 4.0 and 5.0. The LEFM evaluations described here determine the maximum life that a vessel can withstand and maintain crack arrest within 1/4T for the severe transients considering the decreasing fracture

toughness of the vessel. For the thermal shock concern, various regions within the vessel were evaluated. LEFM analyses were performed on the vessel's beltline region longitudinal and circumferential welds, the base metal and a vessel inlet nozzle.

8.2 Analytical Model

8.2.1 Vessel Beltline Region

Based on LEFM techniques from ASME Code Section XI, Appendix A, the computer code PCRIT[20] determines the critical pressure as a function of time using the plant specific vessel weld chemistry, the weld location, the flaw tip (vessel gradient) temperature as a function of time and the material properties as a function of EFPY (fluence) and fluence attenuation through the vessel wall. The flaw shown in Figure 8.2-1a is evaluated as a semi-elliptic flaw with a 6:1 aspect ratio. Flaw sizes from 1/40T to 16/40T in 1/40T increments and to 20/40T are evaluated at various time steps throughout the transient for an input set of operating histories (EFPY). The procedure is the same for evaluation of the vessels' longitudinal weld, circumferential weld, and base metal.

8.2.2 Vessel Inlet Nozzle

The output from the 2-D axisymmetric finite element model (Section 5.3) consisting of a detailed pressure and thermal stress profile is used in conjunction with the BIGIF code to determine the K versus a through the "knee" section of the nozzle (Figure 8.2-1b). From the pressure stress results, a plot of the stress intensity factor (SIF) versus a/t for flaws in the nozzle material can be made. The SIF for the inlet nozzle was determined here using the BIGIF computer code in lieu of those provided in the Welding Research Council Bulletin-175[21] because the Bulletin has been shown to be overly conservative for small flaw sizes, that is flaw sizes less than $a/r_n < .15$. The flaw geometry shown in Figure 8.2-1b is assumed in the evaluation of thermal shock in the "knee" of the vessel inlet nozzle.

Using the flaw size, fracture toughness and flaw tip temperature, the critical pressure can then be determined as a function of time using the SIF. The critical pressure is then compared to the actual transient pressure. These evaluations are iterative to determine the maximum vessel lifetime in EFPY, for the transient being considered.

8.2.3 Warm Prestressing

Warm prestressing (WPS) is the term applied to a phenomenon which can limit the extent of total crack growth during certain overcooling transients. The conditions under which WPS has been demonstrated to occur is when a crack in a structure is loaded to a maximum K_I level at some elevated temperature which may exceed the critical K_{IC} value for the material at a lower temperature and then follow this maximum K_I level by a decreasing K_I field. Crack growth has been shown not to occur even if the stress intensity factor K_I reaches the K_{IC} value at the lower temperature. Since the unloading results in a decrease in strain at the crack tip, this eliminates a necessary condition for fracture. These conditions will occur in any overcooling transient where the temperature and pressure profiles continue to decrease, as in LOCA and most SBLOCA transients. However, in the case where the system repressurizes, as with no break in the primary system and the HPI not throttled, the WPS phenomenon is not applicable for use as a fracture mechanics method to predict crack growth. WPS is used in this analysis for evaluation of the SBLOCA welds. WPS phenomenon has been demonstrated in laboratory tests[23] with small specimens and in a large thick-walled cylinder during an unpressurized thermal shock experiment.

8.2.4 Criteria for Acceptability

For LEFM analysis, several criteria were considered in judging whether a particular analysis gave an acceptable result for vessel life. Each criterion was judged on its intent and what conservatisms it provides in the final evaluation of a particular set of fracture mechanics results. For the LEFM analysis evaluation of the thermal shock concern two criteria for acceptability were considered:

1. No crack initiation during transient.
2. Crack initiation with arrest within 1/4T.

The first criterion has the intent of preventing crack initiation at all times; therefore, maximum conservatism exists, but it is overly conservative in that it may restrict plant useful lifetime unnecessarily.

The second criterion allows credit to be taken for possible small existing flaws that may run to slightly larger flaws and arrest. This allows additional service life for the reactor vessel with only a slight reduction in the conservatism. This criterion follows the philosophy of Section III of the ASME code for plant design analysis and is the one selected for use in the LEFM analysis of the thermal shock concern.

The criterion used to judge the acceptability of the Warm Prestressing (WPS) results was that crack arrest would occur within 1/2T.

The Warm Prestressing methodology used to evaluate the SBLOCA transient affects on vessel integrity proceeds as follows:

Using the results of the PCRIT fracture mechanics program, a plotting routine draws the WPS line through the $K_I$max points for various flaw sizes on a flaw size (a/w) versus time (t) plot as shown in the following illustration. If the WPS conditions are satisfied, i.e., decreasing K_I and temperature fields, then WPS concludes that any crack initiated will not propagate across this WPS line as shown in the illustration.

8.3 Assumptions and Conservatisms

The use of LEFM technique implies certain basic assumptions per the ASME Code being made. Other major assumptions or changes to the basic ASME Code, Section XI, Appendix A, are as follows:

A. Flaw Description

The aspect ratio for the initial flaw, Figure 8-1, was assumed to be 6:1 as recommended by Section III, Appendix G, of the ASME Code.

B. Material Fracture Toughness

The material reference temperature, RT_{NDT}, is adjusted to account for the radiation embrittlement effects. The amount of adjustment (see Chapter 6.0) is computed using Regulatory Guide 1.99 and is a function of fluence and chemistry (i.e., copper and phospherous).

C. Upper Shelf Toughness

A limit of 200 KSI $\sqrt{in.}$ is used as the upper limit for the material toughness (see Chapter 6.0).

D. Cladding

The effects of the cladding have been taken into consideration in developing the SIF(s) due to the thermal stress but were excluded from the SIF due to pressure. The cladding effects were also included in the determination of the heat transfer film coefficients for the inner surface of the 3-D vessel and nozzle models.

E. Material Properties

Material properties are taken from the ASME Boiler and Pressure Vessel Code Appendices, 1980 Edition. The vessel clad is stainless steel. Clad thickness of 1/8" is used for conservatism; the nominal thickness is 3/16". The vessel base metal is Mn-Mo.

8.4 Discussion of Fracture Mechanics Results

8.4.1 Critical Pressure Versus Time Histories

Critical pressure curves were determined for each longitudinal and circumferential weld, the vessel base metal and the vessel inlet nozzle for both overcooling plant transients (Chapter 2.0) and SBLOCA (Chapter 3.0). A typical critical pressure curve is compared to the actual transient pressure versus transient time in Figures 8.4-1 and 8.4-2. Comparison of Figures 8.4-1 and 8.4-2 illustrates how the welds were determined to be acceptable. Figure 8.4-1 shows an acceptable weld at 24 EFPY but fails the acceptance criterion at 25 EFPY. This is evident by the intersection of the critical pressure curve with the actual transient pressure curve in Figure 8.4-2. The PCRIT program also determines the flaw size that exists, what flaw size becomes critical or does not arrest and at what time in the transient this occurs.

These allowable-versus-actual pressure comparison curves are similar for all welds and transients evaluated.

8.4.2 Overcooling Transients

Four overcooling transients as described in Chapter 2.0 (case numbers 9, 10, 11 and 12) were selected for fracture mechanics analyses. The bases of this selection are provided in Chapter 2.0. WPS was judged not to be applicable on these overcooling transients due to the repressurization that occurred during the transients. The LEFM results for each overcooling transient are as follows in terms of EFPY, using acceptance criterion 2.

Case 9	EFPY
Vessel Inlet Nozzle	32
Limiting Longitudinal Weld	25
Limiting Circumferential Weld	>32
Vessel Base Metal	>32

Case 10	EFPY
Vessel Inlet Nozzle	See Note Table 8.4-1
Limiting Longitudinal Weld	>32
Limiting Circumferential Weld	<32
Vessel Base Metal	>32

Case 11	EFPY
Vessel Inlet Nozzle	See Note Table 8.4-1
Limiting Longitudinal Weld	>32
Limiting Circumferential Weld	>32
Vessel Base Metal	>32

Case 12	EFPY
Vessel Inlet Nozzle	See Note Table 8.4-1
Limiting Longitudinal Weld	>32
Limiting Circumferential Weld	>32
Vessel Base Metal	>32

All LEFM analysis results for the above overcooling transients are listed in Table 8.4-1.

8.4.3 SBLOCA Transient

Not all evaluations of Oconee 1 reactor vessel's welds, base metal, and inlet nozzle materials using jet mixing in the downcomer and LEFM methodology met the criteria of crack initiation with arrest within 1/4T, at 32 EFPY's.

The base metal, longitudinal welds, and inlet nozzle did provide integrity for the vessel for the entire 32 EFPY. However, circumferential welds SA-1229 and SA-1585 were acceptable for 16 and 24 EFPY respectively using LEFM analysis. The circumferential welds proved limiting due to the large thermal gradients (see Figure 5.3-3) across the vessel wall. The jet mixing model used in the analysis is conservative in its prediction of the temperature directly below the cold leg nozzle. Preliminary mixing analysis program results, as discussed in Chapter 4.0,

and the comparison to the 1/5 scale CREARE Test Facility data have shown that FLOW 2-D and COMMIX mixing analyses have a much higher mixed temperature below the inlet nozzle than is used in this analysis.

The inlet nozzle was evaluated using the FLOW 2-D mixing results since the data was available when the nozzle analysis was begun. The nozzle temperature profile is shown in Figure 5.2-7. Since the nozzle was found to be acceptable for 32 EFPY using this data no additional analysis will need to be performed in the future for the SBLOCA transient.

The LEFM results for the SBLOCA transient shows the following in terms of EFPY's, using acceptance criterion 2, without WPS.

	EFPY
Vessel Inlet Nozzle	32
Limiting Longitudinal Weld	>32
Limiting Circumferential Weld	
(SA-1229)	>16
(SA-1585)	>24
Vessel Base Metal	>32

The use of WPS on the above limiting circumferential welds resulted in the following vessel integrity in terms of EFPY.

	EFPY
Limiting Circumferential Welds	
SA-1229	32
SA-1585	32

All LEFM and WPS analysis results for SBLOCA transient are listed in Table 8.4-1.

8.4.4 SMUD Transient

The SMUD "Lightbulb" transient of March 20, 1978 was analyzed using Oconee 1 vessel specific fluence and material properties to evaluate the

results of that transient if it had occurred on the Oconee 1 vessel. Since this transient had received much attention and has been declared the worst overcooling transient that has occurred in a PWR to date by the NRC, the transient was analyzed for comparison purposes.

The LEFM results for the transient shows the following in terms of EFPY:

	EFPY
Vessel Inlet Nozzle	32
Limiting Longitudinal Weld	>25
Limiting Circumferential Weld	>32
Vessel Base Metal	>32

Therefore, if the SMUD event were to occur on the Oconee 1 vessel, it would be greater than 25 EFPY before any concern over vessel integrity would need to be addressed. All LEFM results for this event are given in Table 8.4-1.

8.5 Correlation of LEFM Results with Oconee 1 Reactor Vessel 10 Year ISI

The LEFM analysis assumes that all flaws which initiate must be arrested within 1/4T. This evaluation looks at flaws ranging from 1/40T to 10/40T in increments of 1/40T. For the thermal shock evaluation it is usually the very shallow flaws, i.e., 1/40T, 2/40T or 3/40T which initiate without arrest due to the steep thermal gradients at the inner surface of the vessel. Results of the recent Oconee 1 ISI were that no indications of concern were found. It is, therefore, very conservative to make a prediction of safe EFPY based on postulated flaws which are not likely to be present in the Oconee 1 vessel.

Table 8.4-1

LEFM RESULTS FOR THERMAL SHOCK ANALYSES OF OCONEE 1 REACTOR VESSEL(1)

WELD I.D.(2) OR HEAT	TRANSIENT					
	SMUD EVENT	SBLOCA	OVERCOOLING CASE 9	10	11	12
AHR 54	32	32	32	32	32	32
SA-1135	32	32	32	32	32	32
C2197-2	32	32	32	32	32	32
SA-1073	30	32	30	32	32	32
SA-1229	32	32(3)	32	32	32	32
SA-1493	30	32	31	32	32	32
C3278-1	32	32	32	32	32	32
SA-1585	32	32(3)	32	32	32	32
C2800-1	32	32	32	32	32	32
SA-1430	25	32	25	32	32	32
Vessel Inlet Nozzle	32	32	32	*	*	NA

(1) Acceptance criteria is crack arrest within 1/4T and no credit for WPS, except where otherwise noted.

(2) Refer to Tables 6.6-1 and 6.6-2 for location.

(3) Results using warm prestressing (acceptance criteria is crack arrest within 1/2T).

* Since Case 9 has a larger vessel temperature gradient and lower flow tip temperature, it is judged that Case 9 sounds Cases 10 and 11.

NA Not analyzed.

Figure 8.2–1 FLAW GEOMETRY USED IN VESSEL THERMAL SHOCK ANALYSIS

Figure 8.2–1a ASSUMED FLAW GEOMETRY IN VESSEL

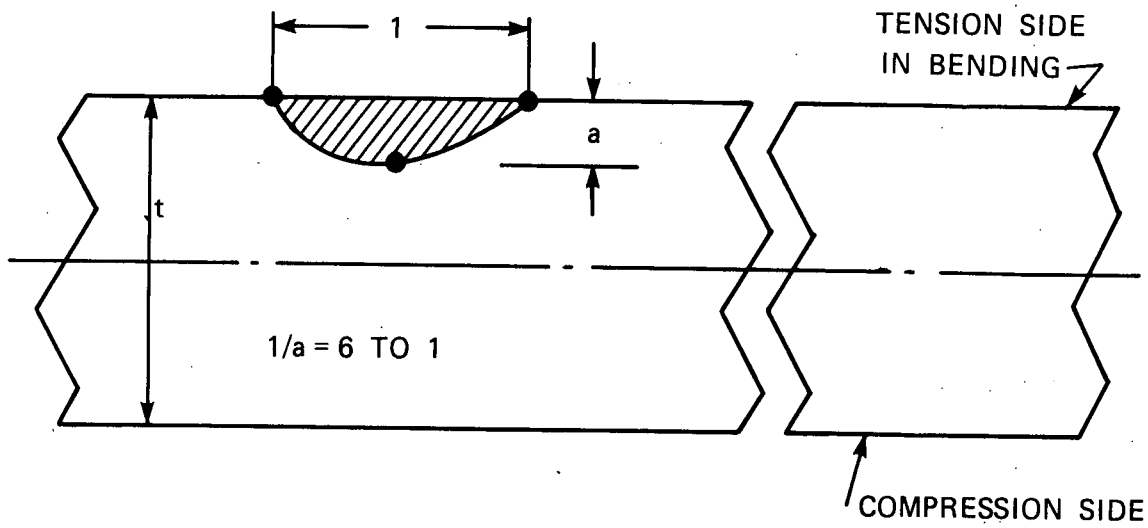

SURFACE FLAW
(t = SECTION THICKNESS)

Figure 8.2–1b ASSUMED FLAW GEOMETRY IN VESSEL INLET NOZZLE

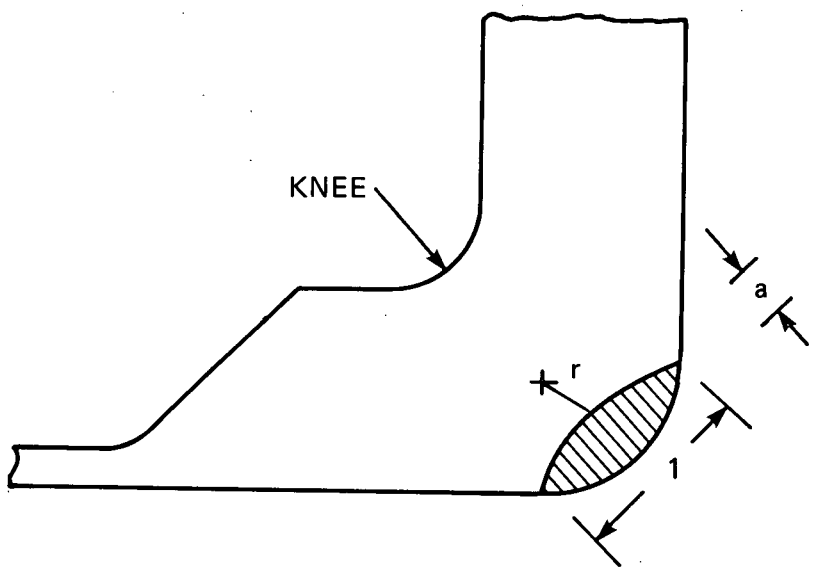

Figure 8.4–1 PRESSURE HISTORY FOR SB LOCA TRANSIENT, SA–1585 WELD @ 24 EFPY

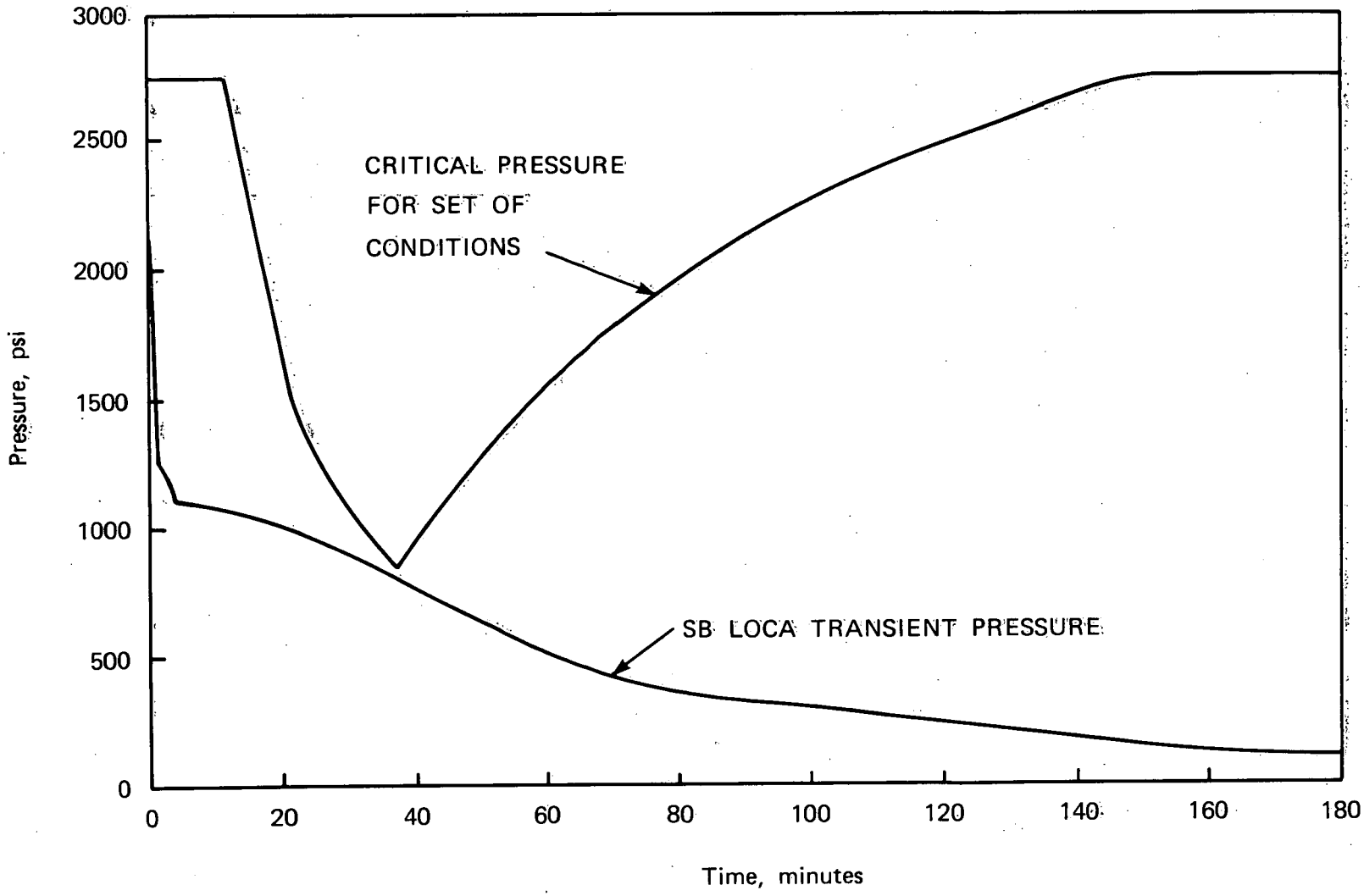

Figure 8.4–2 PRESSURE HISTORY FOR SB LOCA TRANSIENT, SA–1585 WELD @ 25 EFPY

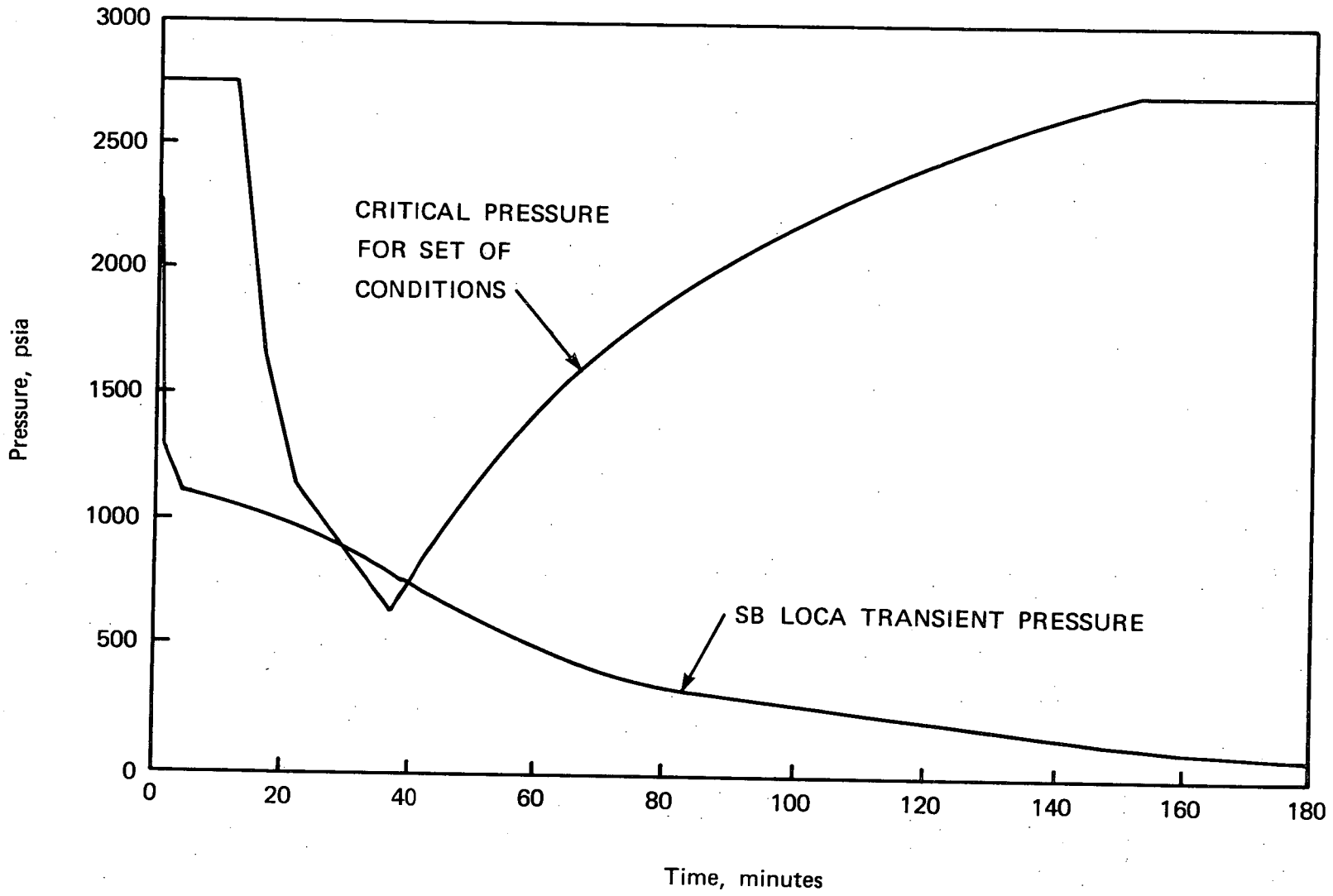

9.0 ANALYSIS OF FREQUENCY OF OCCURRENCE OF REACTOR VESSEL THERMAL SHOCK EVENTS

9.0 ANALYSIS OF FREQUENCY OF OCCURRENCE OF REACTOR VESSEL THERMAL SHOCK EVENTS

9.1 Introduction

Previous chapters of this report dealt with the identification and characterization of transient events with potential for reactor vessel thermal shock. The results of fracture mechanics analyses of these transients presented in Chapter 8.0 indicate the available lifetime of the vessel satisfying the applicable criteria on crack initiation, propagation and arrest. It is obvious that if a transient more severe than the ones analyzed in Chapters 2.0 and 3.0 were to occur, the available lifetime of the vessel would be lower than that calculated in Chapter 8.0. Therefore, it is useful to estimate the frequency of thermal shock events more severe than those considered in Chapters 2.0, 3.0, and 8.0.

The frequency of vessel failure due to an event that causes vessel thermal shock can be expressed as the product of the following two factors:

$$\phi_i(F) = \phi(E_i) \cdot P(F/E_i),$$

where $\phi(E_i)$ is the frequency of the specific thermal shock event E_i, and

$P(F/E_i)$ is the probability of vessel failure conditional on occurrence of event E_i.

The calculation of $P(F/E_i)$ entails a detailed evaluation of the thermal-hydraulic behavior of the event, coupled with a probabilistic fracture mechanics analysis for these thermal-hydraulic conditions. Further, in order to assess the ability to maintain core cooling following occurrence of the vessel failure, a prediction of the size and location of the resulting crack is needed.

The purpose of this investigation is to provide an estimate for the first of these factors, the frequencies of the thermal shock events of interest. These frequencies can be useful in establishing a priority for addressing the more complex problems associated with the conditional failure probabilities, and can help to eliminate from further consideration sequences determined to be of sufficiently low frequency. Finally, calculating these sequence frequencies is a necessary step in assessing the contribution of vessel failure to risk.

9.2 Approach

It is clearly not practicable to calculate either of the above factors for every conceivable sequence of events. However, it is possible, to obtain estimates of thermal shock sequence frequencies by grouping events similar in system response and consequences into classes. By calculating frequencies for each of these more general classes of sequences, a fairly complete spectrum of events is included.

The calculation of the frequencies of sequences resulting in thermal shock requires an estimate of the frequencies of the initiating events of interest, together with the failure probabilities of plant systems in response to these events. The evaluation of the likelihood of operator intervention, either to correct or to exacerbate the problem, must be examined. Where available, Oconee-specific data and logic models were used in this evaluation. Although the models were developed for Oconee 3 (based on the Oconee 3 PRA model[24]), they were reviewed to verify applicability to Oconee 1 and 2 as well. In addition, although the factor $P(F/E_i)$ is strongly a function of time due to the effects of neutron fluence on the vessel materials properties, the thermal shock event frequencies were assumed to be time-independent. Finally, an estimate of the degree of confidence in the results was made to permit comparison to frequencies calculated by other studies.

9.3 Definition of Event Sequences

Three general categories of events have at various times been identified to be of concern with respect to the thermal shock issue: large-break loss-of-coolant accidents (LBLOCAs); small-break loss-of-coolant accidents (SBLOCAs); and severe overcooling transients caused by secondary system failures, followed by repressurization of the reactor coolant system (RCS) by high pressure injection (HPI) flow. Each of these three categories represents a somewhat different threat to vessel integrity.

The LBLOCA exhibits a very rapid initial cooldown, followed by injection of fairly cold (40°-90°F) water. The resulting thermal gradient across the vessel wall can induce stresses large enough to cause assumed pre-existing flaws of the proper size and orientation to grow into cracks. Although this is the most severe event in terms of the rate cooldown, arrest of any crack growth is likely to occur because the RCS remains at low pressure.

The larger range of the SBLOCA spectrum exhibits similar system response with respect to thermal shock. Since RCS pressure decreases rapidly relative to vessel wall temperature and remains low, critical pressure is never achieved. Since no mitigating actions are available or required for these events, no further definition or quantification of the LBLOCA or larger SBLOCA event sequences is necessary.

Of more interest from a sequence frequency standpoint are events that require some operator action or that are adversely affected by additional system failures. These sequences include smaller SBLOCAs and sustained overcooling events. The SBLOCAs of interest are those that cause the RCS to depressurize very slowly or repressurize, requiring operator action to throttle HPI to avoid undesirable pressure/temperature combinations; this range is represented earlier in this report by the stuck-open pressurizer safety relief valve. The overcooling sequences result from secondary system failures, and in general require operator intervention to terminate the

excessive heat removal. The frequencies of these event sequences are evaluated in the following sections.

9.3.1 SBLOCA Event Sequences

The concern associated with the SBLOCA is that if the relatively cold HPI water is not mixed sufficiently before entering the reactor vessel, it will cause rapid cooling of the vessel wall. This can result in pressurized thermal shock if the operator does not take the action to throttle HPI when an adequate subcooling margin is regained. For the case of the stuck-open pressurizer safety valve, this time is approximately 1-1/2 hours after the break occurs. For smaller breaks subcooling would be regained more quickly due to the slower depressurization, but the diminished break flow and reduced HPI flow also result in slower cooling of the reactor vessel. On the other hand, breaks somewhat larger than the relief valve cause more rapid cooldown of the vessel, but also require a longer period for the pressurization effects to become important. Therefore, 1-1/2 hours is assumed to be a representative time for operator action to throttle HPI flow.

A SBLOCA can occur as an initiating event or as a consequence of a transient that causes RCS pressure to increase to the point that the pressurizer pilot-operated relief valve (PORV) or safety relief valves (SRVs) are challenged. These transients include loss of heat removal via the steam generators, pressure control system failures, and events other than LOCAs that cause HPI to be actuated. These sequences can be obtained from the logical development shown in fault-tree format in Figure 9.3-1. The failure to throttle HPI in time to avoid severe thermal shock conditions is represented by event H_1 . The development under gate Q03 represents a stuck-open relief valve resulting from loss of RCS heat removal via the steam generators. It is assumed that if main feedwater (MFW) flow is lost and emergency feedwater fails to respond automatically, RCS pressure will increase to the PORV setpoint. If the PORV fails to open, or if feedwater is not recovered within 10 minutes, pressure will increase to the SRV setpoint. Note that because the SRVs

may be less reliable after having relieved liquid flow than after steam, these states are discriminated in the logic.

Gate Q04 includes the development for sequences in which HPI is actuated, leading to high RCS pressure. The events included are spurious actuation of engineered safeguards (ES), denoted as initiating event T_8, and low RCS pressure caused by failure of the pressurizer spray, denoted as event T_{10}. Note that actuation of HPI due to overcooling events is not included. This is because these events are considered separately with respect to thermal shock. In fact, for these events a stuck-open relief valve can actually be beneficial in limiting the pressurization effects.

The third way in which a transient-induced SBLOCA can occur is included as gate Q05. The initiating event in this case is a spurious low RCS pressure signal, a pressure control system failure that causes the pressurizer spray to remain off while the pressurizer heaters energize. Without operator action to turn off the heaters pressure can increase to the relief valve setpoint. However, the initiating event also causes the PORV to remain closed, resulting in a challenge to the SRVs.

The sequences obtained in this manner are listed below in boolean form. For ease of reference, an abbreviated expression is also listed for event sequences E_2 and E_3.

$$E_1 = S \cdot H_1$$

(SBLOCA with failure of the operator to throttle HPI)

$$E_2 = [(T_1 \cdot M_1 + T_2 + T_3 + T_4 + T_5 + T_6) \cdot L_1 \cdot (PORVC \cdot H_3 + PORVO \cdot SRVSC + R_1 \cdot SRVLC) + T_3 \cdot L_1 \cdot (SRVSC + R_1 \cdot SRVLC)] \cdot H_1$$

or $$E_2 = T\ M\ L_1\ Q_1\ H_1$$

(transient resulting in total loss of feedwater, followed by failure of the PORV or SRV to reclose, with failure of the operator to throttle HPI; T_1 denotes a turbine trip)

$$E_3 = [T_8 \cdot PORVC \cdot H_3 + (T_8 \cdot PORVO + T_{10} \cdot H_4) \cdot (SRVSC + SRVLC \cdot H_5)] \cdot H_1$$

or $E_3 = T\ Q_2\ H_1$

(transient causing actuation of HPI, with RCS pressure increasing to relief valve setpoint, followed by failure of the valve to reclose and failure of the operator to throttle HPI)

$$E_4 = T_9 \cdot SRVSC \cdot H_1 \cdot H_2$$

(failure of the pressurizer pressure control system, leading to a challenge to the SRVs with one sticking open, followed by failure to reclose and failure of the operator to throttle HPI).

9.3.2 Overcooling Transients

The non-LOCA transient event sequences of concern with respect to thermal shock are primarily those that cause severe, sustained overcooling of the RCS. These overcooling events cause shrinkage of the reactor coolant, and consequently depressurization to the HPI setpoint. The HPI flow arrests or retards the depressurization and restores the RCS to a subcooled state. Without operator action to throttle or terminate HPI, RCS pressure can increase to the pressurizer relief valve setpoints for most transients. Although the number of sequences of potential interest is large, they can, in general, be adequately represented by three classes: large breaks on the secondary side of the steam generators, small steamline breaks, and excessive feedwater events. These classes of events are outlined in Figure 9.3-2.

Large steamline breaks cause the most rapid cooling of the RCS. If feedwater flow to the affected steam generator is not isolated, the overcooling can be sustained for a sufficient duration to cause concern for the integrity of the reactor vessel. Large feedwater line breaks downstream from the isolation check valves produce similar effects, although the blowdown is slower. Also, the broken steam generator is effectively isolated from MFW flow, but EFW flow is likely to be actuated and can

still provide sufficient flow to be of concern. These events will cause actuation of HPI on low RCS pressure. Because the operator is instructed to trip the RCPs under these conditions, the severe shrinkage may cause stagnation of the RCS. In order to assure that the pressurized thermal shock to the reactor vessel is not excessive, it may also be necessary for the RCPs to be restarted. This is called for by procedure when an adequate subcooling margin is regained.

Small steamline breaks have similar effects, but cause slower, less severe cooldown of the RCS. The time available for corrective operator action is therefore longer. On the other hand, because the RCS shrinkage is less than for large breaks, repressurization may occur more rapidly. The sequences illustrated by Figure 9.3-2 include the small steamline break as an initiating event, as well as events with similar effects, including main steam relief valve (MSRV) and turbine bypass valve (TBV) failures following a turbine trip. In the case of the TBV failure, an additional operator section is available, since the overcooling can be terminated by closure of the TBV block valves.

Excessive feedwater events can result from failure to control MFW or EFW properly. Excessive MFW events can occur initially because an overfeed condition leads to a reactor trip or because the Integrated Control System (ICS) fails to run back MFW flow properly following a reactor or turbine trip. However, in order for the overcooling to persist, additional control failures are necessary, and the high steam generator level trip of the MFW pumps must fail. In reality, this event may not be credible, in light of the amount of condensate available to the MFW pumps and the likelihood of losing the steam supply to the MFW pump turbines. Nevertheless, the frequencies of the potential control system failures were calculated as a point of comparison to the estimates of other studies. The EFW system is capable of supplying only a much smaller rate of flow to the steam generators. Severe overcooling has been postulated to occur for excessive EFW events only in conjunction with failures in

the main steam pressure control system. These sequences are reflected in Figure 9.3-2. The sequences obtained from Figure 9.3-2 are listed below:

$E_5 = (B_1 + B_3) \cdot (H_1 + H_2)$

(large secondary line break with failure to isolate broken steam generator or to restart RCPs)

$E_6 = (B_2 + T_n : MSRVC) \cdot H_3$

(small steamline break or MSRV failure with failure to isolate broken steam generator)

$E_7 = [T_5 + (T_1 + T_2 + T_7 + T_8 + T_9 + T_{10}) \cdot H_4] \cdot B_4 \cdot H_3$

(turbine bypass valve failure following reactor trip, with failure to close block valves and failure to isolate feedwater)

$E_8 = [(T_1 + T_8 + T_9 + T_{10}) \cdot M_2 + T_7] : M_3 \cdot H_5$

(failure to control main feedwater flow, with failure of MFW pumps to trip on high steam generator level or by operator action)

$E_9 = \{(T_1 \cdot M_1 + T_2) \cdot [(B_{5a} + MSRVAC) \cdot L_{2a} + B_{5b} + MSRVBC) \cdot L_{2b}]$
$+ (T_3 + T_4 + T_5 + T_6) \cdot (MSRVAC \cdot L_{2a} + MSRVBC : L_{2b})\} \cdot H_6$

or $E_9 = T\ M\ L_2\ H_6$

(excessive EFW flow with failure of steam pressure control and failure of the operator to throttle EFW)

It is pointed out that for these overcooling transients no credit is taken for throttling the HPI to control the RCS pressure. This represents a major conservatism in this analysis.

9.4 System Failure Analyses

9.4.1 Main Feedwater System

The MFWS supplies feedwater to the steam generators during power operation, and during startup and shutdown conditions. The MFWS consists of two turbine-driven pumps, with suction flow provided from the condensate system by electric motor-driven hotwell and condensate booster pumps. At low power and decay heat conditions, flow to the steam generators is controlled by the air-operated startup control valves. At higher power levels the main control valves regulate flow. Control is provided automatically by the ICS, unless the operator assumes manual control. After a reactor trip, the ICS runs back MFW by limiting flow through the control valves and reducing the pump speed. The ICS then controls MFW to maintain a minimum level in the steam generators, unless the RCPs are tripped, in which case flow is redirected to a higher injection point in the steam generators and level is controlled to 50% to promote natural circulation.

The MFWS is of interest with respect to pressurized thermal shock because its loss, with additional failures, can lead to a SBLOCA due to a stuck-open pressurizer relief valve, and because overcooling can result from failure to control MFW properly following a reactor trip.

Loss of main feedwater can occur directly as a result of an initiating event or because of failures following a turbine/reactor trip. The initiating events loss of condenser vacuum, loss of offsite power, loss of instrument air and loss of ICS power all lead to loss of main feedwater. In addition, the likelihood of losing MFW following a turbine trip was obtained by evaluation of the fault tree included as Figure 9.4-1. An independent solution of this fault tree yields a mean unavailability of 5.5×10^{-2} following a reactor trip. This value is supported by plant operating data.

Failure of MFW to run back following a reactor trip can lead to significant overcooling only if excessive MFW flow is sustained. This requires that, in addition to failure of the ICS to control steam generator level, the BTU and high level limiters must fail to function. Also, at least one MFW pump must fail to trip when the high steam generator level setpoint is reached. Failure to control MFW flow following a trip, including failure of the BTU and high level limiters, was assessed by solution of the fault tree included as Figure 9.4-2. The mean probability of this event, denoted in Figure 9.3-2 as Event M_2, was found to be 3.9×10^{-2}. Event M_3, the probability that at least one MFW pump would fail to trip on high level was found to be 2.5×10^{-3}. The fault tree logic for this event is depicted in Figure 9.4-3.

9.4.2 Steam Pressure Control

Following a turbine trip, main steam pressure control is provided by the turbine bypass valves (TBVs) and the main steam relief valves (MSRVs). The TBVs provide relief for 25% of full steam flow. They modulate to maintain constant steam generator pressure until cooldown of the reactor is initiated or the turbine is placed on line. The eight MSRVs on each steam generator provide the additional relief capacity needed immediately following a turbine trip, and also provide overpressure protection in the event the TBVs are unavailable.

The two TBVs per steam generator receive steam generator pressure signals from the ICS. Each pair of TBVs is downstream from a motor-operated block valve that can be closed by remote manual action should either TBV fail to reclose. The fault tree development for failure of the TBVs to reclose following a turbine trip is illustrated by Figure 9.4-4. Event B_4, failure of all four TBVs to reclose following a reactor trip, was calculated to have a mean probability of 1.9×10^{-3}. Failure of at least one TBV on steam generator A or steam generator B to reclose, events B_{5a} and B_{5b}, respectively, was estimated to have a mean probability of 9.5×10^{-3} (for either generator).

The MSRVs are calibrated so that two per steam generator open at each of four settings. Because the reactor trips directly on a turbine trip, it is unlikely that all 16 valves will be demanded to open for most events. However, because it is difficult to determine how many valves would open, it was assumed that all 16 could fail to reclose. The probability that two or more would fail to reclose can be found from the following:

$$\alpha\ (\text{MSRVC}) = \frac{16!}{(16 - 2)\ !2!}\ (5 \times 10^{-3})^2 = 3 \times 10^{-3}$$

The probability that one or more of eight MSRVs would fail open is then:

$$\alpha\ (\text{MSRVAC}) = \alpha\ (\text{MSRVBC}) = 8\ (5 \times 10^{-3}) = 4 \times 10^{-2}$$

Note that these values are quite conservative in light of Oconee operating experience, since there have been no failures of MSRVs to reclose in 186 reactor trips.

9.4.3 Emergency Feedwater System

The EFWS provides flow to the steam generators in the event MFW flow is lost. The EFWS consists of three pumps, two motor-driven and one turbine-driven, that take suction initially from the upper surge tanks, and subsequently by operator action from the condenser hotwell. The system is actuated automatically on low pressure at the discharge of the MFW pumps or when the MFW pumps are tripped. EFW flow is then controlled by a steam generator level control system. The actuation and control circuitry is independent of the ICS. Flow from any of the three pumps is sufficient for decay heat removal. Failure of the EFWS to supply flow upon loss of the MFWS was developed by the fault tree shown in Figure 9.4-5. The mean unavailability on demand, denoted as Event L_1, was found to be 6.6×10^{-4}.

Flow to each steam generator is controlled independently by the steam generator level control system. An air-operated valve in the discharge line to each steam generator provides flow modulation. The likelihood that excessive EFW flow will be supplied to a steam generator due to control system or valve hardware failures was evaluated by construction of the fault tree included as Figure 9.4-6. The mean value obtained by solution for Event L_{2a} or for Event L_{2b} was found to be 6.7×10^{-4} for events other than loss of instrument air, and 3.7×10^{-3} following loss of instrument air.

9.4.4 Pressurizer Pressure Control System

The events of interest with respect to pressurizer pressure control are those related to failures of the PORV and safety relief valves to operate. The probability that the PORV would fail to open on demand (Event PORVO), including the likelihood that the PORV block valve is initially closed, was found to have a mean probability of 4.2×10^{-2}. The probability for Event PORVC, failure of the PORV to reclose, was found to have a mean value of 1.1×10^{-2}.

The logic for occurrence of a transient-induced SBLOCA included discrimination for the state of the fluid being relieved by the SRVs if they should open, since there have been some indications that they may be damaged while cycling with liquid relief. The mean probability that either of the two SRVs would fail to reclose following steam relief. Event SRVSC, is (2) (4.8×10^{-3}); or 9.6×10^{-3}. The probability of failure following liquid relief, Event SRVLC, is estimated to be a factor of 10 greater, or 0.1 per demand.

9.5 Sequence Quantification

The severe thermal shock sequences of interest were defined in qualitative terms in Section 9.3, and the necessary system unavailabilities were obtained in Section 9.4. In this section frequencies are obtained for each of the nine event sequences, after first estimating the probabilities for the operator error events. As a point of reference, frequencies are also provided for the transient cases for which thermal-hydraulic calculations were performed, reported in Chapter 2.0.

In general, the system failures are treated as independent events. This was done only after reviewing the important cut sets for each events to assure that the assumption of independence was acceptable. An exception to this assumption was the solution for event sequence E_9, where the interdependencies between the TBV failures for each steam generator necessitated a coupled solution of the TBV and EFWS control system fault trees.

9.5.1 Sequence-Dependent Operator Error Probabilities

The reliability of the operator in preventing or mitigating the effects of the pressurized thermal shock sequences was assessed subjectively for each sequence within the context of the Oconee PRA human reliability analysis, using a somewhat modified version of the techniques developed by Swain.[25]

Sequence E_1 represents a SBLOCA with failure of the operator to throttle HPI. Because operator action is not required until 1-1/2 hours into the event, substantial time is available for diagnosis and determination of appropriate actions. On the other hand, since the operator is faced to some extent with a conflict in priorities between assuring adequate core heat removal is maintained and protecting the integrity of the reactor vessel, an extremely low unreliability is inappropriate. Therefore, a moderately low probability of failure of 5×10^{-2} was selected for event H_1.

Sequences E_2, E_3 and E_4 are all transient-induced SBLOCAs. Because there is no rationale to distinguish them from sequence E_1 with aspect to long-term actions to throttle HPI, the same value of 5×10^{-2} was selected for event H_1 for each sequence. For sequences E_2 and E_3, the operator may terminate the SBLOCA by closing the PORV block valve. Although substantial training has been provided in this area and clear indications are available that the PORV is open, fairly quick operator response is required, and attention may be directed to correcting other concurrent failures. Therefore, a high failure probability of 0.3 is chosen for event H_3 for sequences E_2 and E_3. Sequence E_2 also includes event R_1, failure to recover steam generator feedwater before the pressurizer becomes water-solid, which occurs about 10 minutes into the event. In general, several recovery actions are available from the control room but a high probability of failure of 0.3 was estimated for this event as well in light of the relatively short time available and the possibility that local actions may be required. In sequence E_3, events H_4 and H_5 represent operator actions to block a stuck-open pressurizer spray valve before HPI is actuated and to throttle HPI before the pressurizer is filled, respectively. A time frame of about 10 to 20 minutes is available for the operator to act. No credit was taken for throttling HPI before reaching the PORV setpoint, an action that must be taken in a much shorter time. Because adequate indications are available (i.e., increasing pressure, subcooling margin and pressurizer level), but fairly early diagnosis is necessary, a moderately high probability of 0.1 was assigned to event H_5, failure to throttle HPI to prevent liquid flow through the SRVs. This value is also appropriate for combined event $H_4 \cdot H_5$. For event H_4 independent of H_5, a higher probability of failure of 0.3 was chosen in light of the potential for confusion due to similarities between a stuck-open spray valve and a SBLOCA.

For sequence E_4, the operator may terminate the pressurization before the SRV setpoint is reached by securing the heaters or initiating spray flow. However, because this event includes an initial runback of MFW (before the reactor trip), attention may tend to be focused on the secondary systems. In addition, a fairly short time is available for action (about

5 minutes). Therefore, a high probability of 0.3 was assigned to event H_2 in sequence E_4.

Failure of the operator to isolate the affected steam generator following a large break results in the sustained overcooling sequence E_5. For the large steamline break, operator response is required within about 5 minutes. While this is a short time frame, the indications of rapidly falling steam pressure with the indications of overcooling provide fairly unambiguous direction to the operator. The feedwater line break permits additional time for operator action, and is actually somewhat self-limiting, since the condensate supply will be depleted without prompt isolation. However, restarting the RCPs may also be required to avoid thermal shock concerns. A somewhat longer time is available to the operator, but restarting the RCPs also has a somewhat lower priority in terms of providing adequate core heat removal. Therefore a moderately high value of 0.1 was assigned to the combined event $H_1 + H_2$ for sequence E_5.

The small steamline breaks represented by sequences E_6 and E_7 result in slower depressurization, with additional time for isolation of the broken steam generators. A more optimistic value of 1×10^{-2} for event H_3 was selected for sequence E_1. For sequence E_7 the additional (and more effective) action of isolating the TBVs is available to terminate the overcooling. Therefore, the same value of 1×10^{-2} was assigned to event H_4, failure to close the block valves. Because substantial credit is given for this action, a high probability of failure to control feedwater of 0.3 was chosen for event H_3 for this sequence. For loss-of-offsite power sequences, the TBV block valve motors are load-shed, and the only operator action available in the short-term is to limit the cooldown by throttling EFW. Because of the possibility of attendant confusion, a higher probability for event H_3 is appropriate here than for sequence E_6, and a valve of 3×10^{-2} was chosen.

Sequences E_8 and E_9 represent excessive feedwater events. Event H_5 is the failure of the operator to terminate excessive MFW flow. Adequate time is available for diagnosis of the event, and a moderately low

probability of 5×10^{-2} was selected for this event. Because of the lower amount of flow available from the EFWS, a significantly longer period for operator response is available for sequence E_9, and a low probability of failure of 1×10^{-2} was assigned to event H_6.

9.5.2 Calculation of Event Sequence Frequencies

The final step necessary is obtaining the frequencies for the thermal shock sequences is an identification of the initiating event frequencies. These frequencies, taken from the Oconee PRA are listed in Table 9.5-1.

The frequencies for the sequences are calculated below:

$$E_1 = S \cdot H_1$$
$$\phi(E_1) = (3 \times 10^{-3})(5 \times 10^{-2})$$
$$\phi(E_1) = 1.5 \times 10^{-4}/yr$$

$$E_2 = [(T_1 \cdot M_1 + T_2 + T_3 + T_4 + T_5 + T_6) \cdot L_1 \cdot (PORVC \cdot H_3 + PORVO \cdot SRVSC + R_1\ SRVLC) + T_3 \cdot L_1 \cdot (SRVSC + R_1 \cdot SRVLC)] \cdot H_1$$
$$\phi(E_2) = \{[(4.94)(5.5 \times 10^{-2}) + 0.67 + 0.02 + 0.21 + 0.17 + 0.17](6.6 \times 10^{-4})[1.1 \times 10^{-2})(0.3) + (4.2 \times 10^{-2})(9.6 \times 10^{-3}) + (0.3)(0.1)] + (0.02)(6.6 \times 10^{-4})[9.6 \times 10^{-3} + (0.3)(0.1)]\}(5 \times 10^{-2})$$
$$\phi(E_2) = 1.7 \times 10^{-6}/yr$$

$$E_3 = [T_8 \cdot PORVC \cdot H_3 + (T_8 \cdot PORVO + T_{10} \cdot H_4) \cdot (SRVSC + SRVLC \cdot H_5)] \cdot H_1$$
$$\phi(E_3) = \{(0.01)(1.1 \times 10^{-2})(0.3) + (0.01)(4.2 \times 10^{-2})[9.6 \times 10^{-3} + (0.1)(0.1)] + (8.5 \times 10^{-3})[(0.3)(9.6 \times 10^{-3}) + (0.1)(0.1)]\}(5 \times 10^{-2})$$
$$\phi(E_3) = 7.5 \times 10^{-6}/yr$$

$$E_4 = T_9 \cdot SRVSC \cdot H_1 \cdot H_2$$

$$\phi(E_4) = (0.044)\ (9.6 \times 10^{-3})\ (5 \times 10^{-2})\ (0.3)$$

$$\phi(E_4) = 6.3 \times 10^{-6}/yr$$

$$E_5 = (B_1 + B_2) \cdot (H_1 + H_2)$$

$$\phi(E_5) = (9.3 \times 10^{-4} + 9.3 \times 10^{-5})\ (0.1)$$

$$\phi(E_5) = 1.0 \times 10^{-4}/yr$$

$$E_6 = (B_2 + T_n \cdot MSRVC) \cdot H_3$$

$$\phi(E_6) = [3 \times 10^{-3} + (6.3)\ (3 \times 10^{-3})]\ (1 \times 10^{-2})$$

$$\phi(E_6) = 2.2 \times 10^{-4}/yr$$

$$E_7 = [T_5 + (T_1 + T_2 + T_7 + T_8 + T_9 + T_{10}) \cdot H_4] \cdot B_4 \cdot H_3$$

$$\phi(E_7) = [(0.17)\ (5 \times 10^{-2}) + (4.94 + 0.67 + 0.092 + 0.01 + 0.044 + 8.5 \times 10^{-3})\ (1 \times 10^{-2})\ (0.3)]\ (1.9 \times 10^{-3})$$

$$\phi(E_7) = 4.9 \times 10^{-5}/yr$$

$$E_8 = [(T_1 + T_8 + T_{10}) \cdot M_2 + T_7] \cdot M_3 \cdot H_5$$

$$\phi(E_8) = [(4.94 + 0.01 + 8.5 \times 10^{-3})\ (3.9 \times 10^{-2}) + (0.092)]\ (2.5 \times 10^{-3})\ (0.05)$$

$$\phi(E_8) = 3.6 \times 10^{-5}/yr$$

$$E_9 = \{(T_1 \cdot M_1 + T_2) \cdot [(B_{5a} + MSRVAC) \cdot L_{2a} + (B_{5b} + MSRVBC) \cdot L_{2b}] + (T_3 + T_4 + T_5 + T_6) \cdot (MSRVAC \cdot L_{2_a} + MSRVBC \cdot L_{2_b})\} \cdot H_6$$

$$\phi(E_9) = \{[(4.94)\ (5.5 \times 10^{-2}) + 0.67]\ [(2)\ (4 \times 10^{-2})\ (6.7 \times 10^{-4}) + 1.2 \times 10^{-5}] + (2)\ (4 \times 10^{-2})\ [(0.02 + 0.21 + 0.17)\ (6.7 \times 10^{-4}) + (0.17)\ (3.7 \times 10^{-3})]\}\ (1 \times 10^{-2})$$

$$\phi(E_9) = 1.3 \times 10^{-6}/yr$$

9.5.3 Estimated Frequencies for Sequences Selected for Analysis

Twelve cases of overcooling sequences were selected for thermal-hydraulic analyses, as described in Chapter 2.0. As a point of reference, the frequencies of these sequences were estimated using the results of Sections 9.4, 9.5.2 and 9.5.3. For each of the twelve cases, the frequency of the system failures leading to overcooling was calculated. The sequences that included some operator error were then modified by the appropriate human reliability value.

Case 1: This sequence is a failure of MFW to run back following a reactor trip, followed by tripping of the MFW pumps on high steam generator level and subsequent failure of the EFW control systems such that excessive flow is provided to at least one steam generator. The sequence can be expressed as the following:

$$\phi = \frac{(T_1 \cdot M_2 + T_7) \cdot (L_{2a} + L_{2b})}{[(4.94)\ (0.039) + 0.092]\ (8.4 \times 10^{-4}) = 2.4 \times 10^{-4}/yr}$$

Case 2: This sequence is similar to that in case 1, except that the reactor is initially in hot shutdown. Many of the cut sets for event M_2 are applicable, yielding a failure rate for high MFW flow of 1.7×10^{-5}/hr. Assuming the unit is at hot shutdown for 120 hr/yr (5 shutdowns at 24 hr per shutdown), the frequency for MFW failing high is 2×10^{-3}/yr. The frequency of this event followed by failure of EFW control is then the following:

$$\phi = (2 \times 10^{-3})\ (8.4 \times 10^{-4}) = 1.7 \times 10^{-6}/yr$$

Case 3: This is an excessive MFW event, similar to sequence E_8 except that the operator successfully trips the pumps. The frequency is then found from the following:

$$\phi = \frac{[(T_1 + T_8 + T_{10}) \cdot M_2 + T_7] \cdot M_3 \cdot \bar{H}_5}{[(4.94 + 0.01 + 8.5 \times 10^{-3})\ (3.9 \times 10^{-2}) + (0.092)]\ (2.5 \times 10^{-3}) = 7.1 \times 10^{-4}/yr}$$

Case 4: The failure of both TBVs on either steam generator to reclose required a reevaluation of the fault tree in Figure 9.4-4, yielding a failure probability of 3.0×10^{-3} and a sequence frequency of:

$$\phi = (4.94)\ (3.0 \times 10^{-3}) = 1.5 \times 10^{-2}/\text{yr}$$

Case 5: This event includes a combination of TBV and EFW control system failures, with no operator action, and is neary identical to sequence E_9. The frequency of the system failures alone was found to be the following:

$$\{(T_1 \cdot M_1 + T_2) \cdot [(B_{5a} + \text{MSRVAC}) \cdot L_{2a} + (B_{5b} + \text{MSRVBC}) \cdot L_{2b}] + (T_3 + T_4 + T_5 + T_6) \cdot (\text{MSRVAC} \cdot L_{2_a} + \text{MSRVBC} \cdot L_{2_b})\} \cdot H_6$$

$$\phi = \{[(4.94)\ (5.5 \times 10^{-2}) + 0.67]\ [(2)\ (4 \times 10^{-2})\ (6.7 \times 10^{-4}) + 1.2 \times 10^{-5}] + (2)\ (4 \times 10^{-2})\ [(0.02 + 0.21 + 0.17)\ (6.7 \times 10^{-4}) + (0.17)\ (3.7 \times 10^{-3})]\}$$

$$\phi = 1.3 \times 10^{-4}/\text{yr}$$

The frequency for the full sequence, including failure of the operator to respond, is that of sequence E_9, 1.3×10^{-6}/yr.

Cases 6 & 7:

These sequences are both equivalent to sequence E_7, failure of the TBVs to reclose following a trip. The frequency for the system failures alone was found from the following:

$$\phi = (T_1 + T_2 + T_5 + T_7 + T_8 + T_9 + T_{10}) \cdot B_4$$

$$\phi = (4.94 + 0.67 + 0.17 + 0.092 + 0.01 + 0.044 + 8.5 \times 10^{-3})\ (1.9 \times 10^{-3}) = 1.1 \times 10^{-2}/\text{yr}$$

The frequency for the full sequencies, including failure of the operator to act, is the same as for sequence E_7, 4.9×10^{-5}/yr.

Case 8: A reevaluation of the TBV fault tree yields a failure rate of 5.5×10^{-7}/hr for all four valves opening spuriously while at hot shutdown. This yields a frequency of

$$(120)\ (5.5 \times 10^{-7}) = 6.6 \times 10^{-5}/\text{yr}$$

Cases 9 & 10:

These cases both include failure of the TBVs to reclose in conjunction with failure of MFW to run back. The sequence is equivalent to the following:

$$(T_1 \cdot M_2 + T_7) \cdot B_4$$

$$\phi = [(4.94)\ (0.039) + 0.092]\ (1.9 \times 10^{-3}) = 5.4 \times 10^{-4}/\text{yr}$$

Cases 11 & 12:

Both cases are steam line breaks with proper operator response. The frequency for either is equivalent to the frequency of the initiating event, 9.3×10^{-4}/yr.

Case 13: This sequence is a steam line break coincident with failure of the ICS to run back MFW flow. The frequency is therefore given by the following:

$$\phi = (B_1 \cdot M_2) = (9.3 \times 10^{-4})\ (0.039) = 3.6 \times 10^{-5}/\text{yr}$$

9.6 Summary of Results

The frequencies calculated above are believed to represent realistic estimates for the sequences of interest. The thermal shock events represented by sequences E_1 through E_9 were found to be low to very low in frequency. In order to provide a point of comparison to estimates made by others, and since other studies have in general presented median frequencies, a subjective estimate of the uncertainty was obtained here by assuming that the probability distributions for the frequencies are

lognormal with a range factor of 10, a typical level of confidence in such estimates. The results are provided in Table 9.6-1.

Although probabilistic fracture mechanics analyses were not performed to provide an estimate of the conditional probability of vessel failure given occurrence of these thermal shock sequences, some preliminary estimates have been obtained that indicate that the factor $P(F/E_i)$ has an upper bound of 10^{-2} to 10^{-3} for the most severe events.[26] The likelihood that the failure will be a catastrophic one such that the ability to maintain core cooling will be lost is even smaller. Therefore, it can be seen that the contribution of vessel failure due to pressurized thermal shock sequences to the overall frequency of core damage is very small, and it is not a significant contributor to risk.

Table 9.5-1

INITIATING EVENT REQUENCIES

	Event	Mean Frequency (yr^{-1})
S	small-break LOCA	3×10^{-3}
B_1	large steamline break	9.3×10^{-4}
B_2	small steamline break	3×10^{-3}
B_3	large feedwater line break inside containment	9.3×10^{-5}
T_1	turbine/reactor trip	4.94
T_2	loss of main feedwater	0.67
T_3	loss of ICS power	0.02
T_4	loss of condenser vacuum	0.21
T_5	loss of offsite power	0.17
T_6	loss of instrument air	0.17
T_7	excessive main feedwater	0.092
T_8	spurious HPI actuation	0.01
T_9	spurious low pzr pressure signal	0.044
T_{10}	pressurizer spray fails on	8.5×10^{-3}

Table 9.6-1

SUMMARY OF THERMAL SHOCK EVENT FREQUENCIES

	Frequency (yr^{-1})			
		Assumed Distribution		
Event	mean	median	95% tile	5% tile
E_1	1.5×10^{-4}	5.6×10^{-5}	5.6×10^{-4}	5.6×10^{-6}
E_2	1.7×10^{-6}	6.4×10^{-7}	6.4×10^{-6}	6.4×10^{-8}
E_3	7.5×10^{-6}	2.8×10^{-6}	2.8×10^{-5}	2.8×10^{-7}
E_4	6.3×10^{-6}	2.4×10^{-6}	2.4×10^{-5}	2.4×10^{-7}
E_5	1.0×10^{-4}	3.8×10^{-5}	3.8×10^{-4}	3.8×10^{-6}
E_6	2.2×10^{-4}	8.3×10^{-5}	8.3×10^{-4}	8.3×10^{-6}
E_7	4.9×10^{-5}	1.8×10^{-5}	1.8×10^{-4}	1.8×10^{-6}
E_8	3.6×10^{-5}	1.4×10^{-5}	1.4×10^{-4}	1.4×10^{-6}
E_9	1.3×10^{-6}	4.9×10^{-7}	4.9×10^{-6}	4.9×10^{-8}

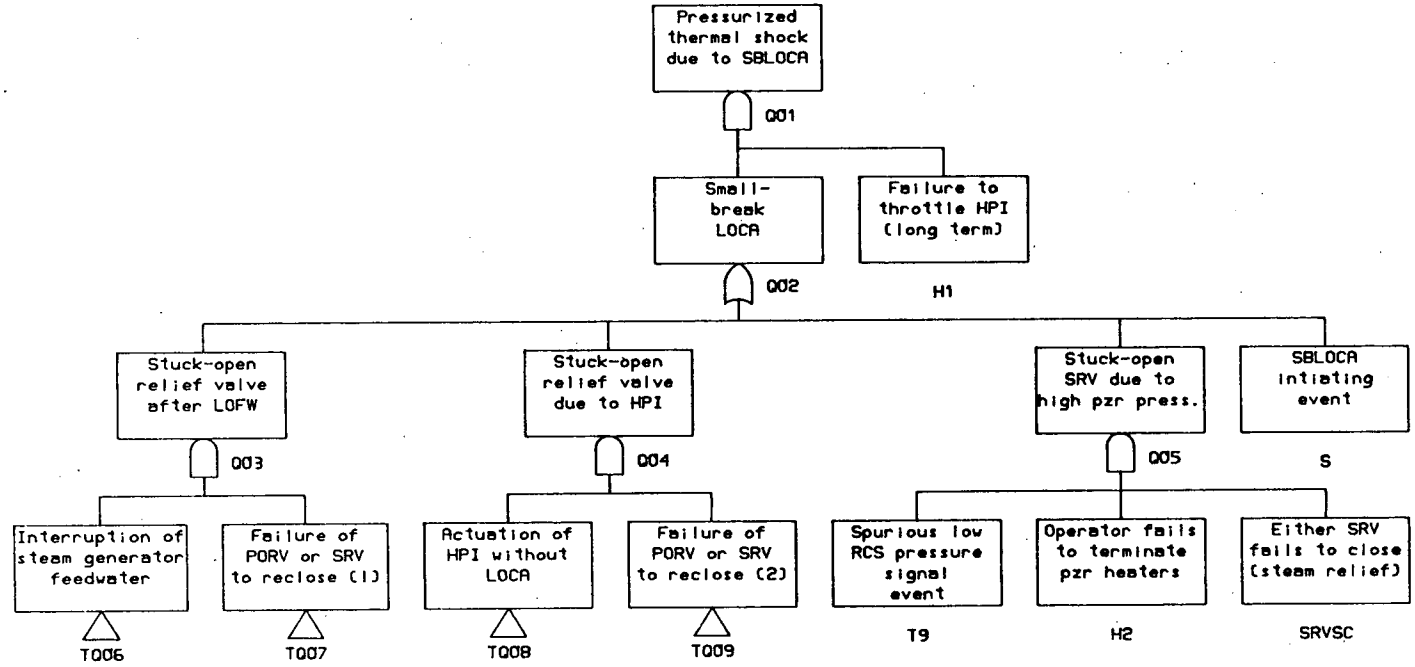

FIGURE 9.3-1. SEQUENCE DEVELOPMENT FOR PRESSURIZED THERMAL SHOCK DUE TO SBLOCA EVENTS

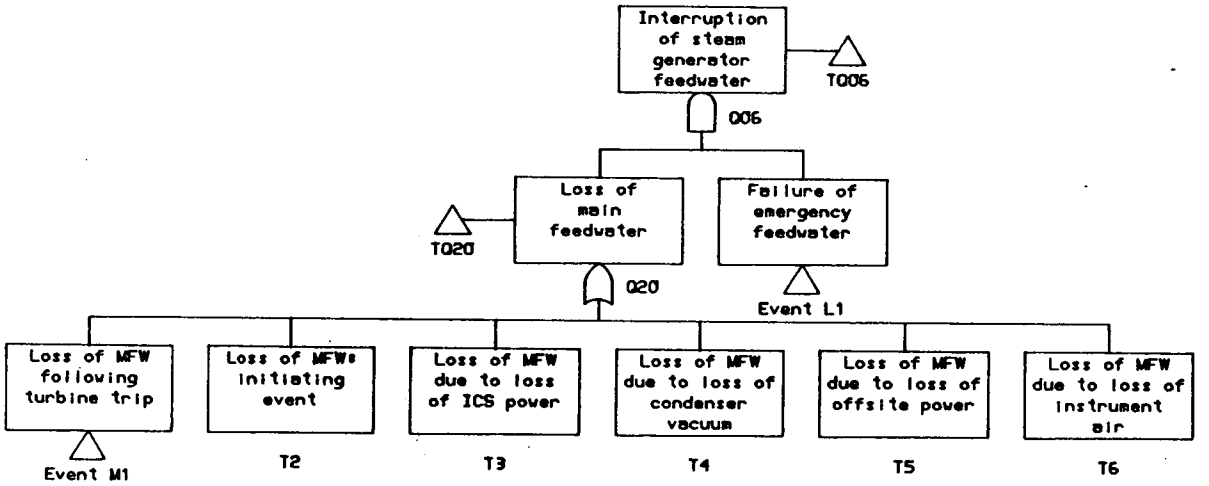

FIGURE 9.3-1. (CONTINUED)

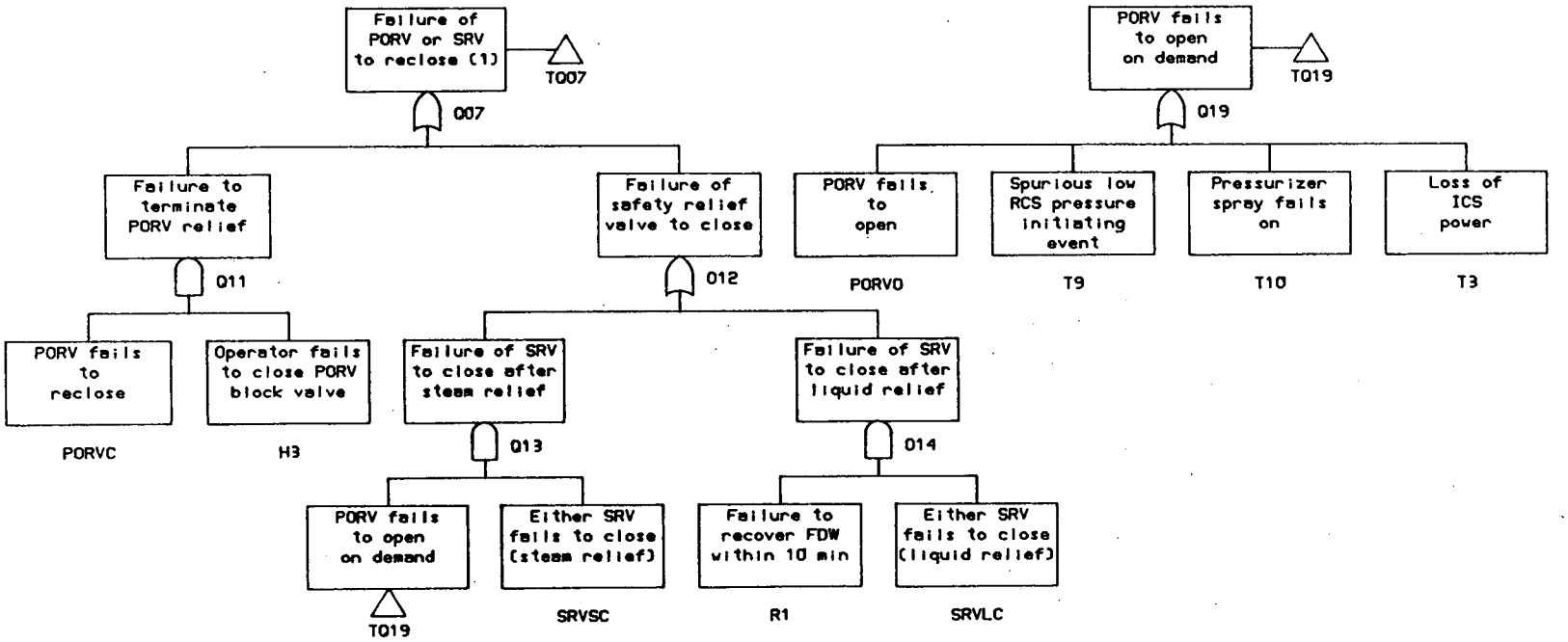

FIGURE 9.3-1. (CONTINUED)

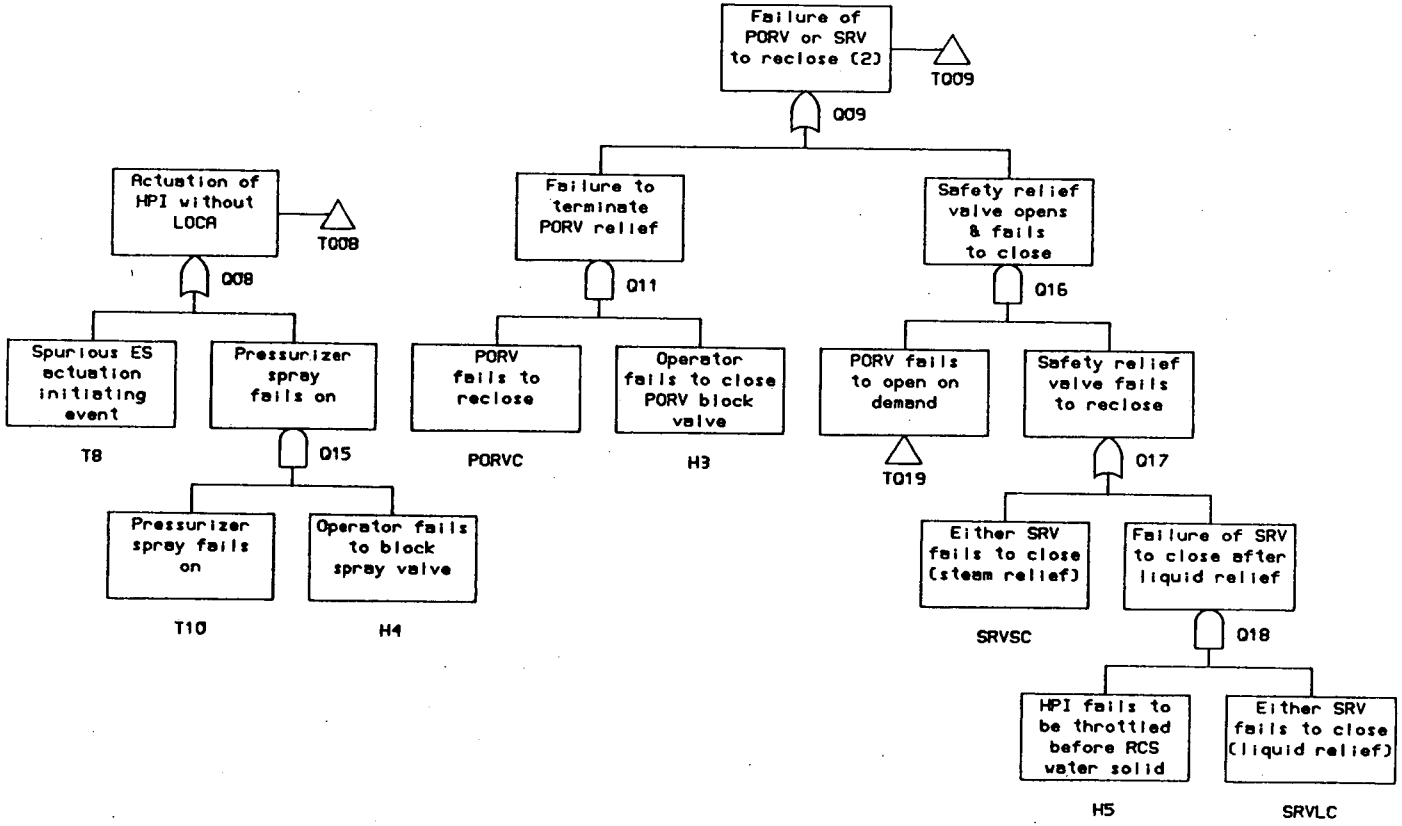

FIGURE 9.3-1. (CONTINUED)

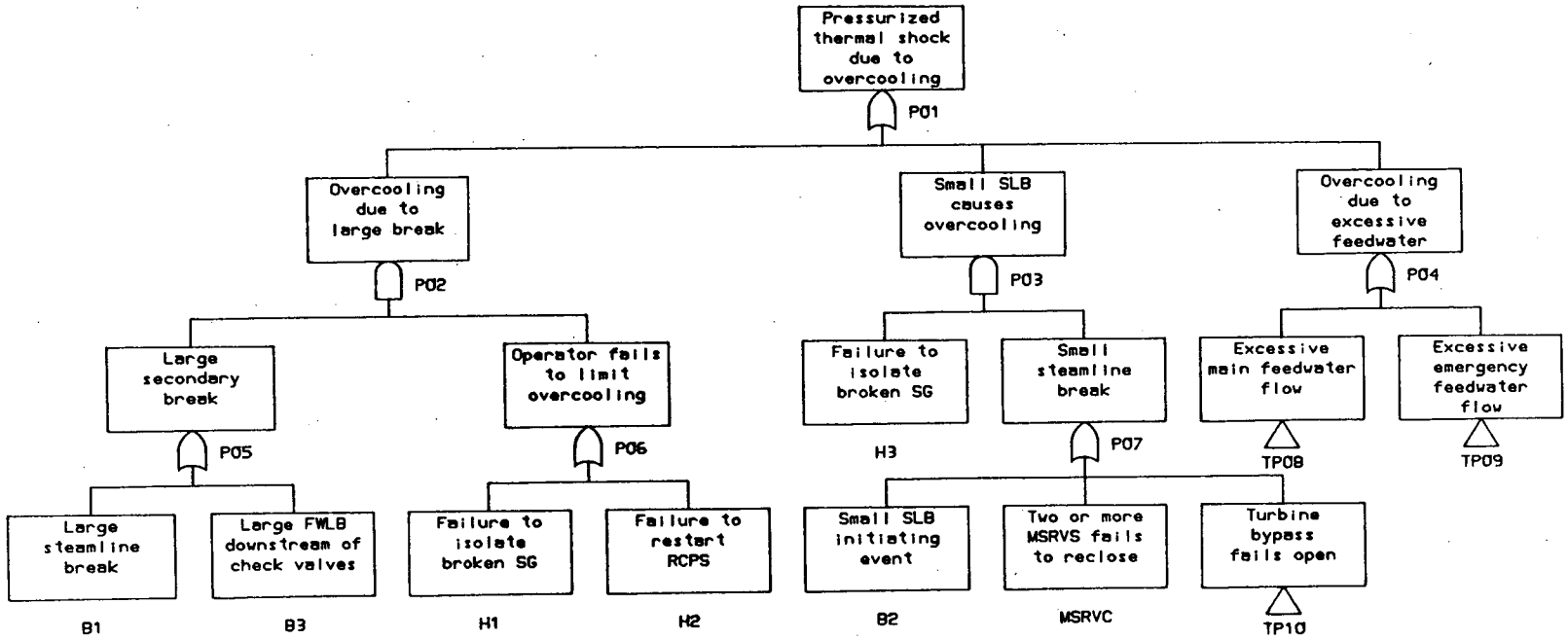

FIGURE 9.3-2. SEQUENCE DEVELOPMENT FOR PRESSURIZED THERMAL SHOCK DUE TO OVERCOOLING TRANSIENTS.

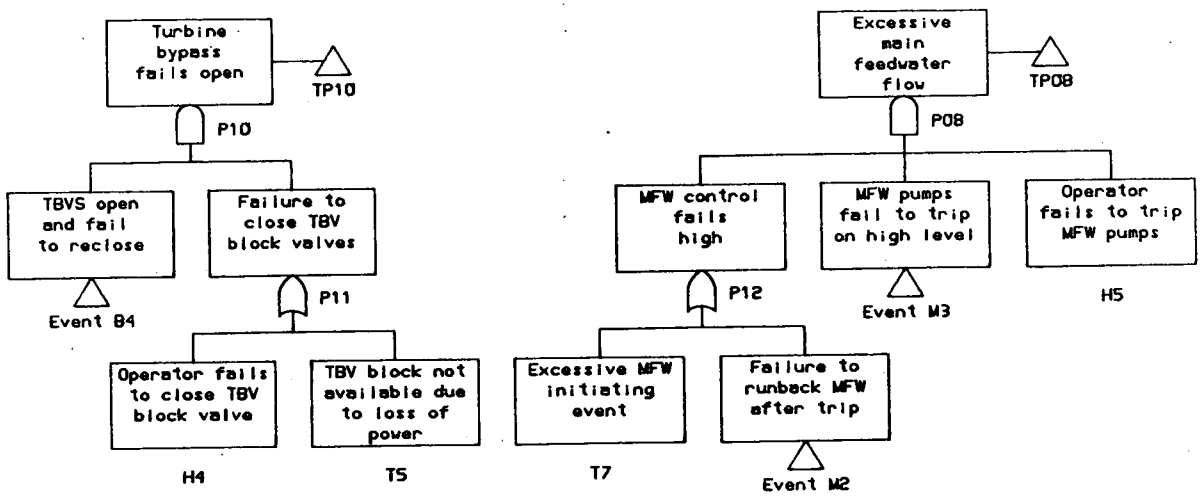

FIGURE 9.3-2. (CONTINUED)

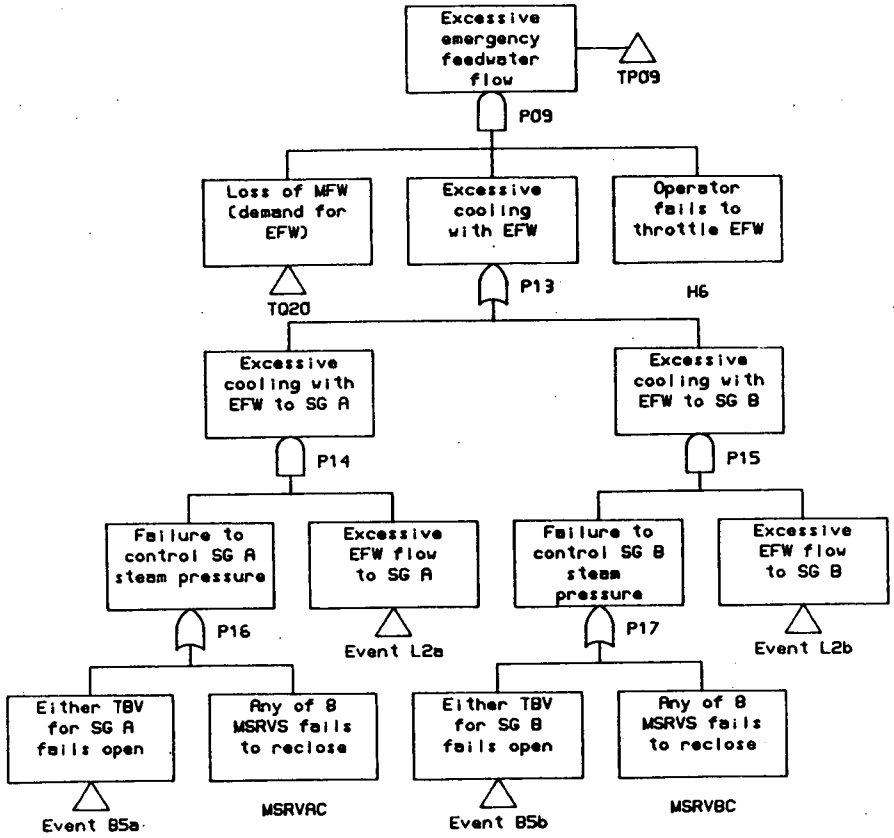

FIGURE 9.3-2. (CONTINUED)

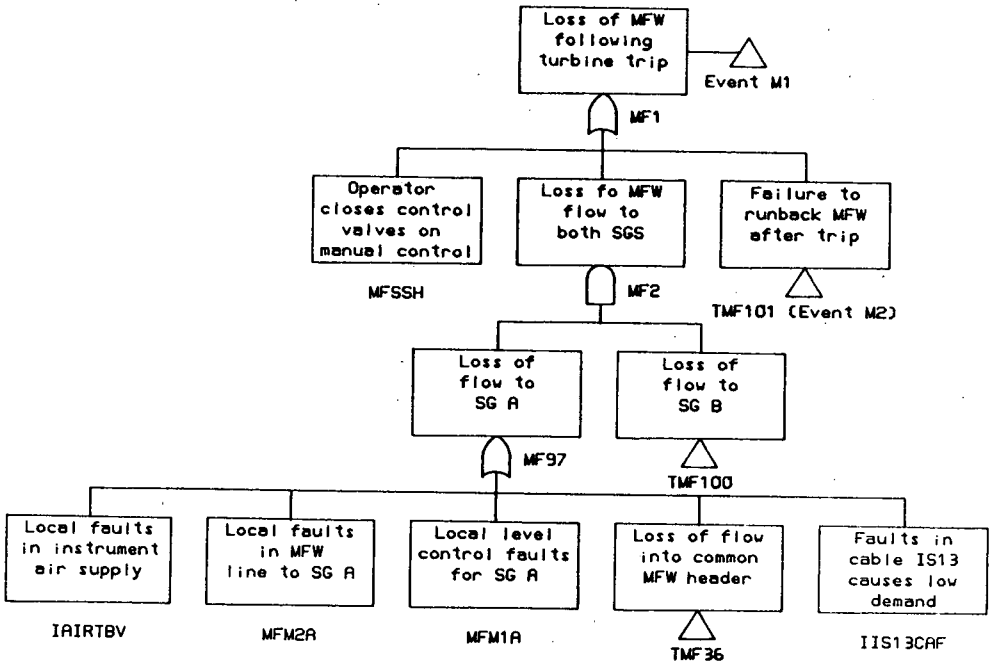

FIGURE 9.4-1. FAULT TREE DEVELOPMENT FOR LOSS OF MAIN FEEDWATER FLOW FOLLOWING TURBINE TRIP.

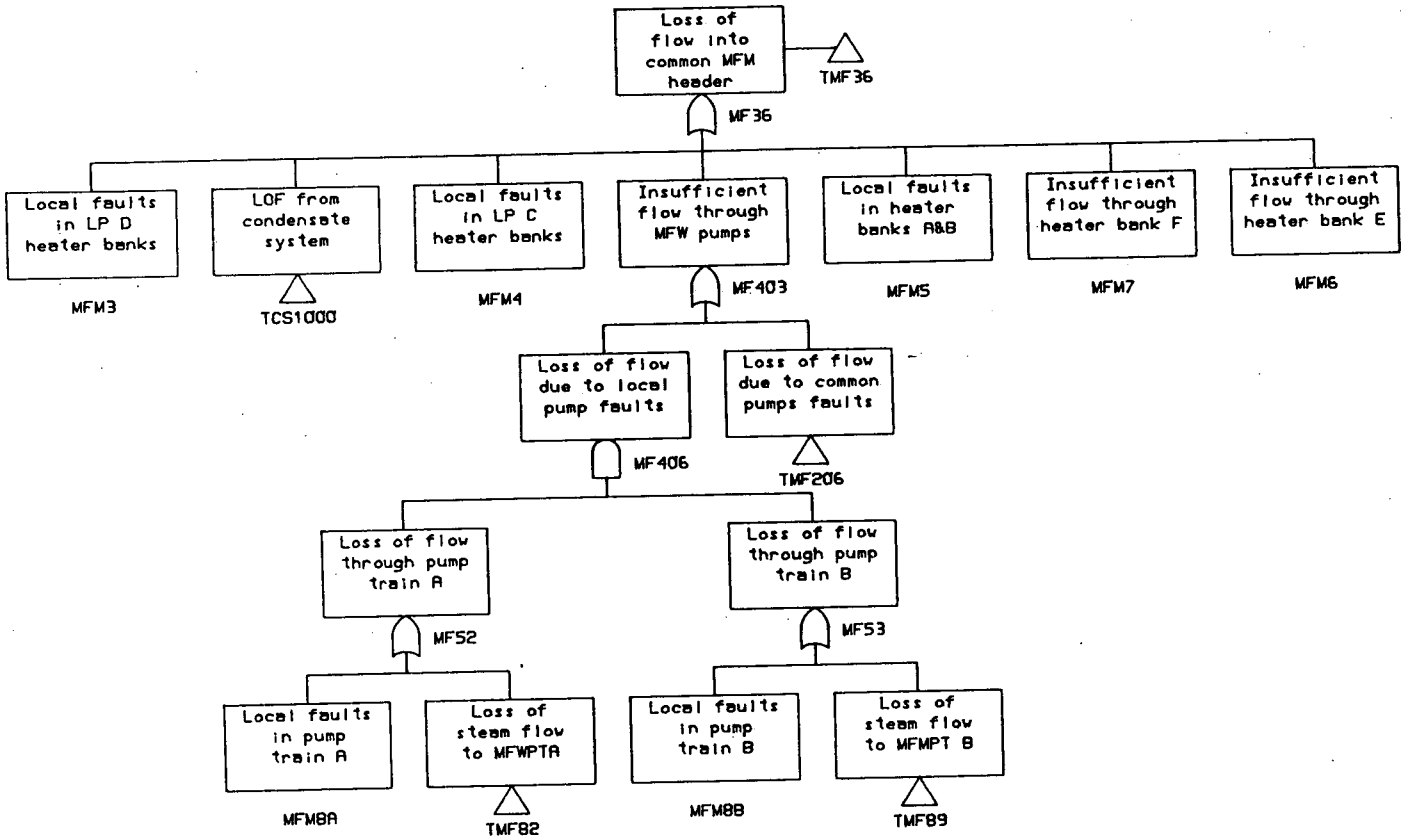

FIGURE 9.4-1. (CONTINUED)

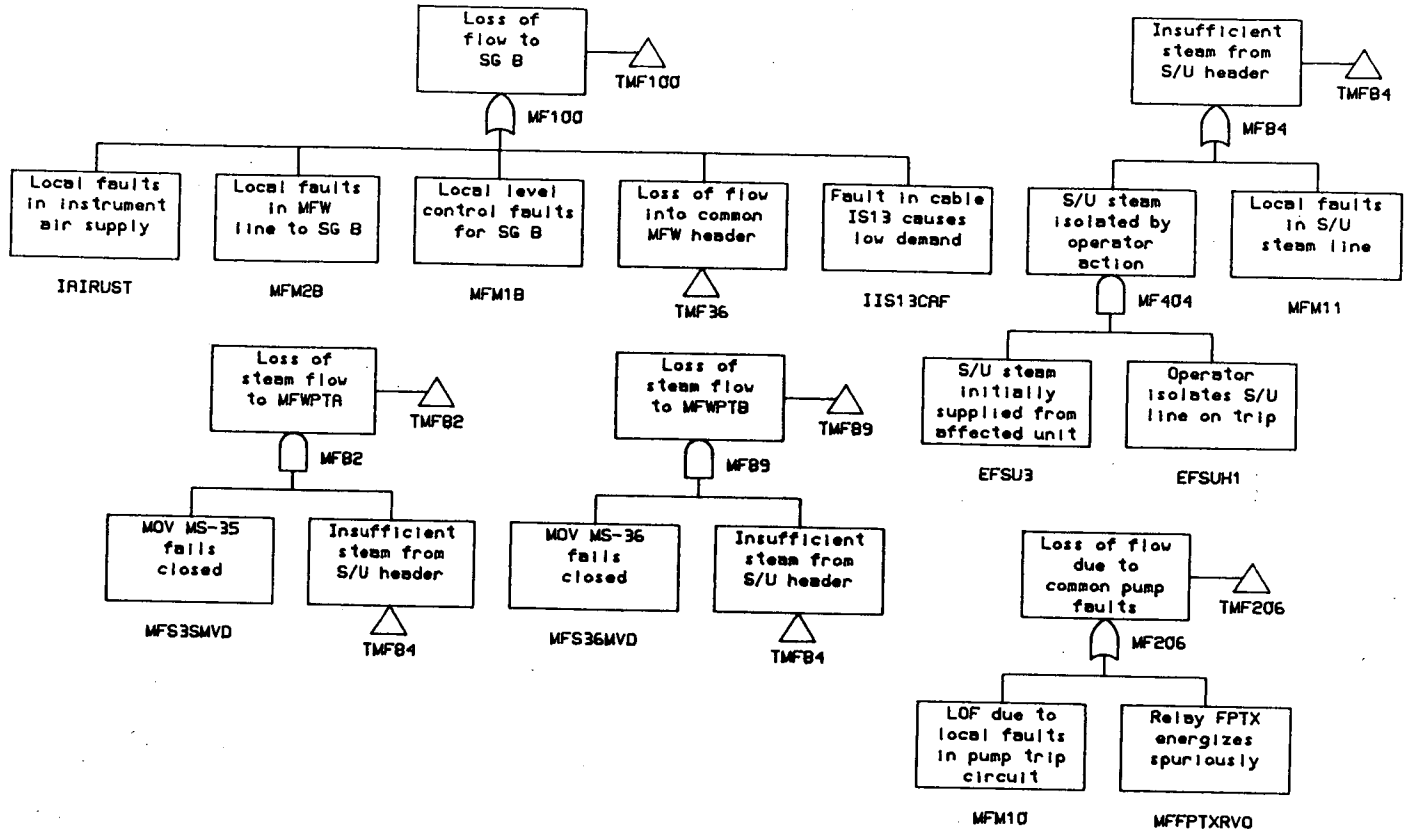

FIGURE 9.4-1. (CONTINUED)

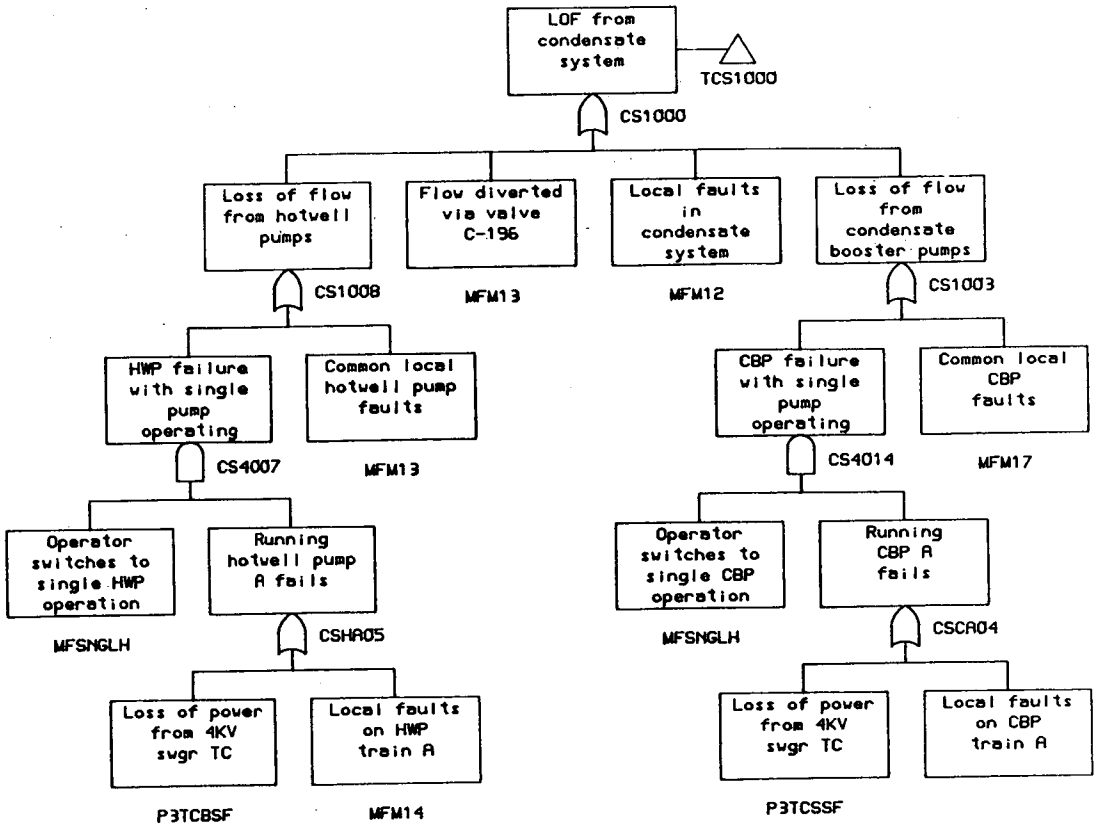

FIGURE 9.4-1. (CONTINUED)

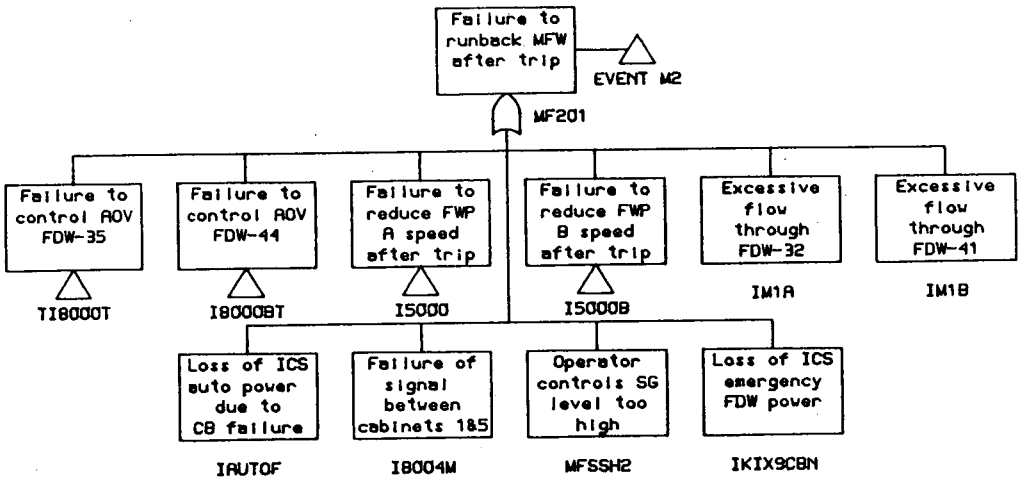

FIGURE 9.4-2. FAULT TREE DEVELOPMENT FOR FAILURE TO RUN BACK MFW FLOW FOLLOWING A REACTOR TRIP.

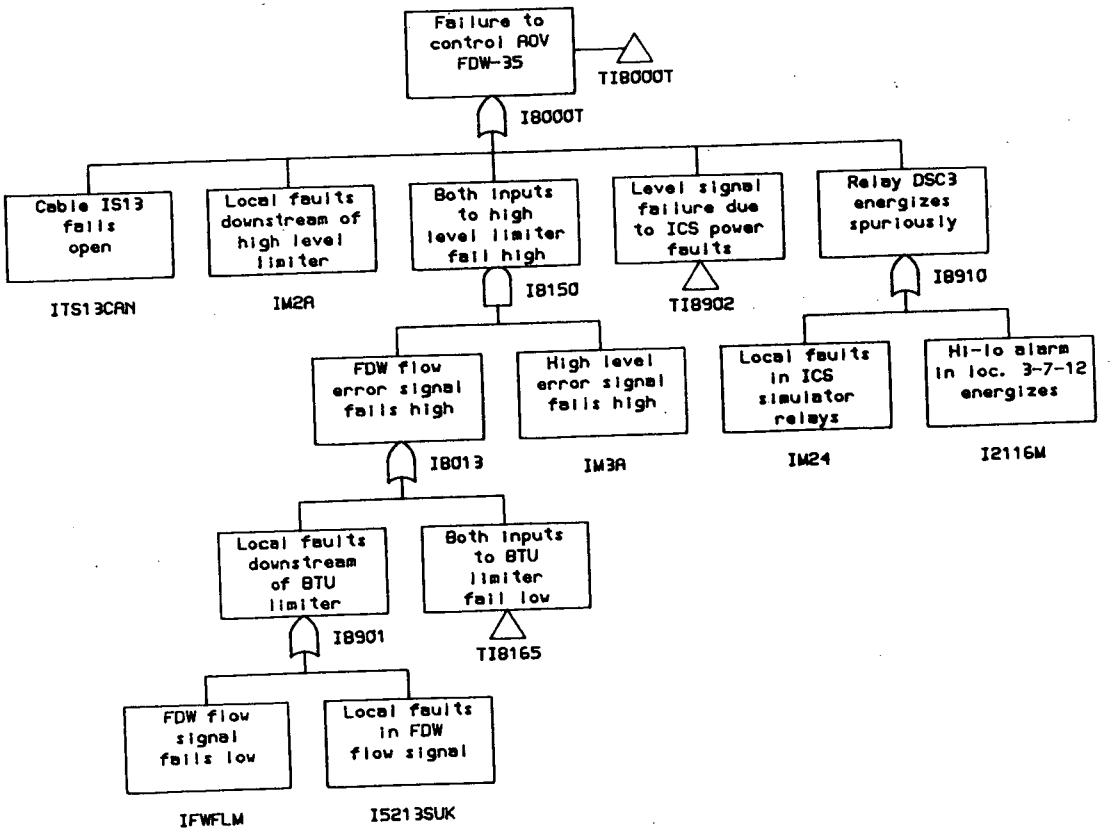

FIGURE 9.4-2 (CONTINUED)

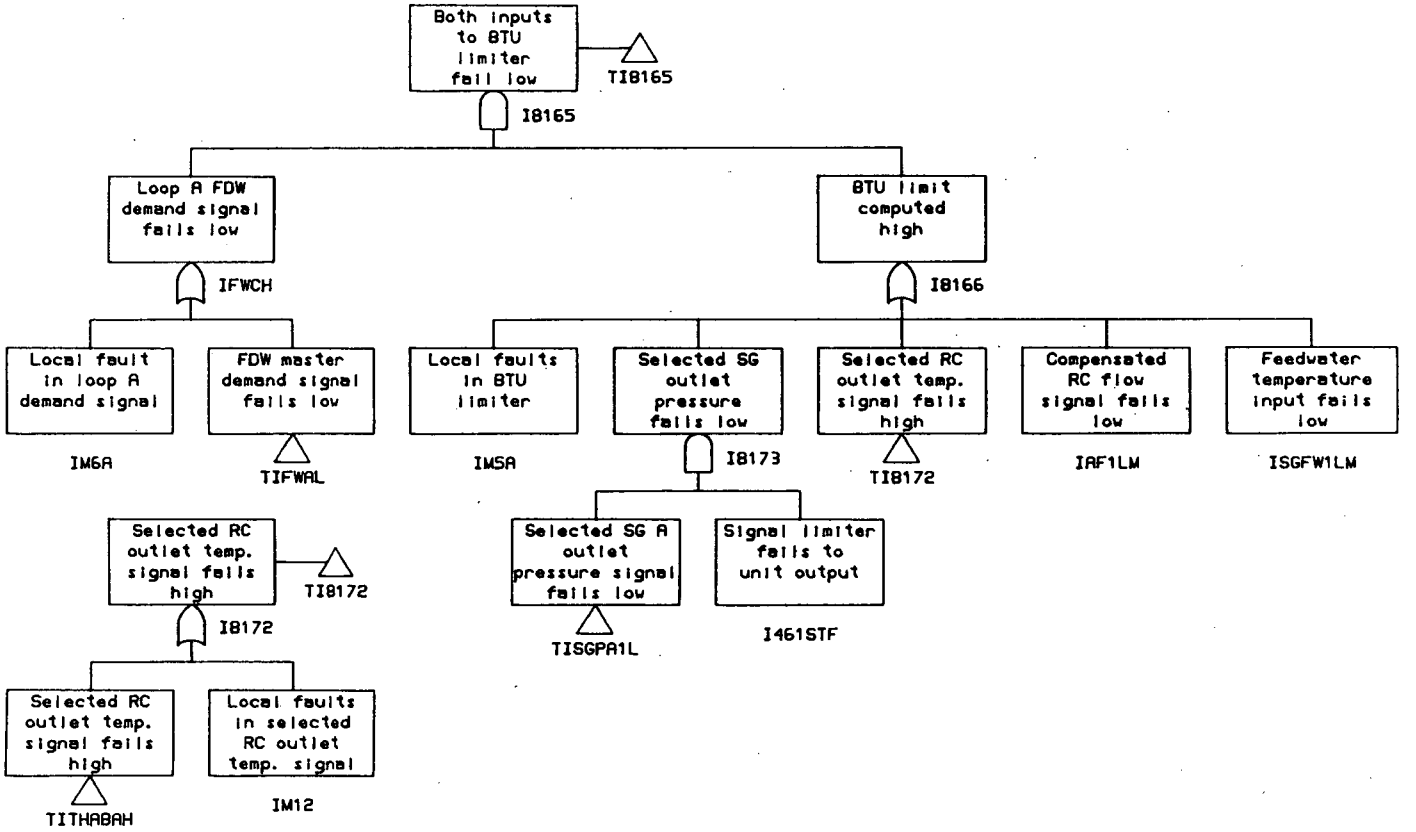

FIGURE 9.4-2 (CONTINUED)

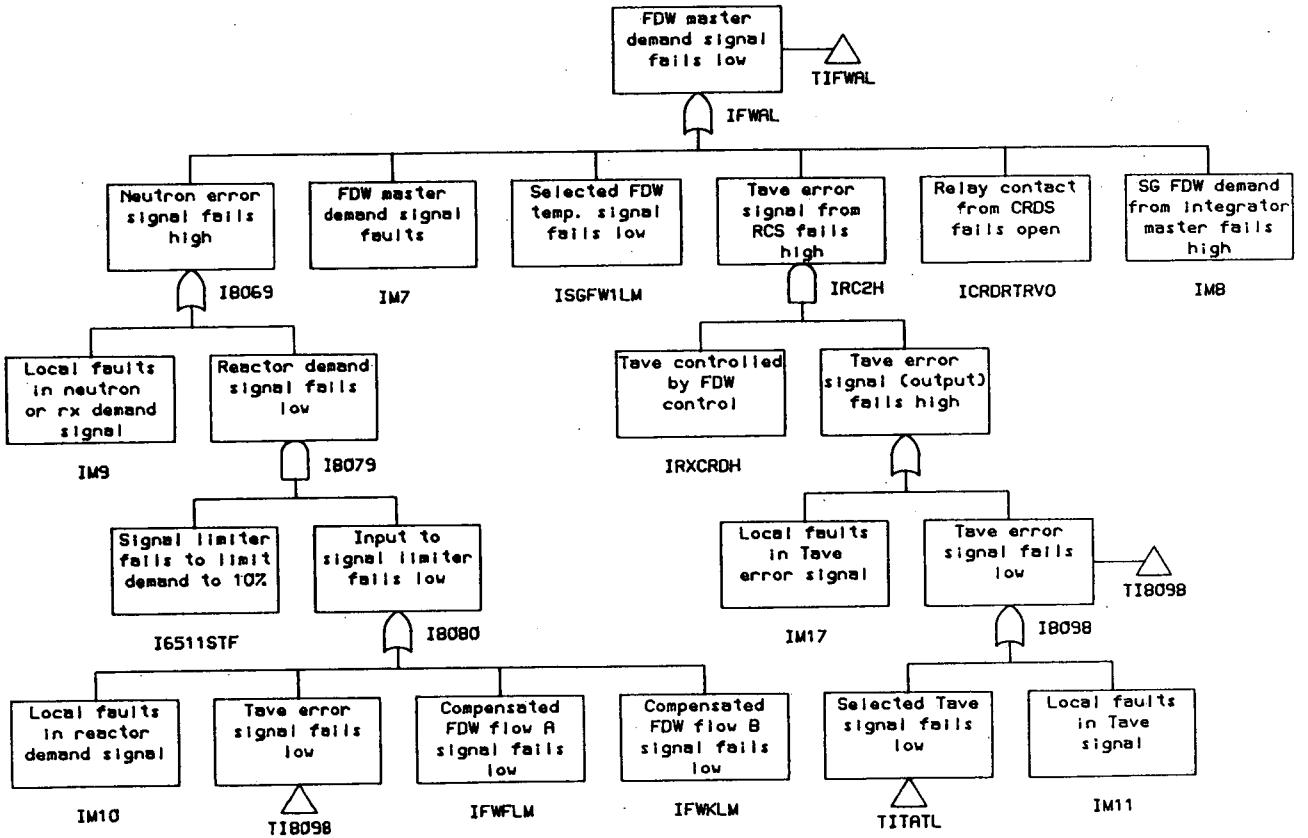

FIGURE 9.4-2 (CONTINUED)

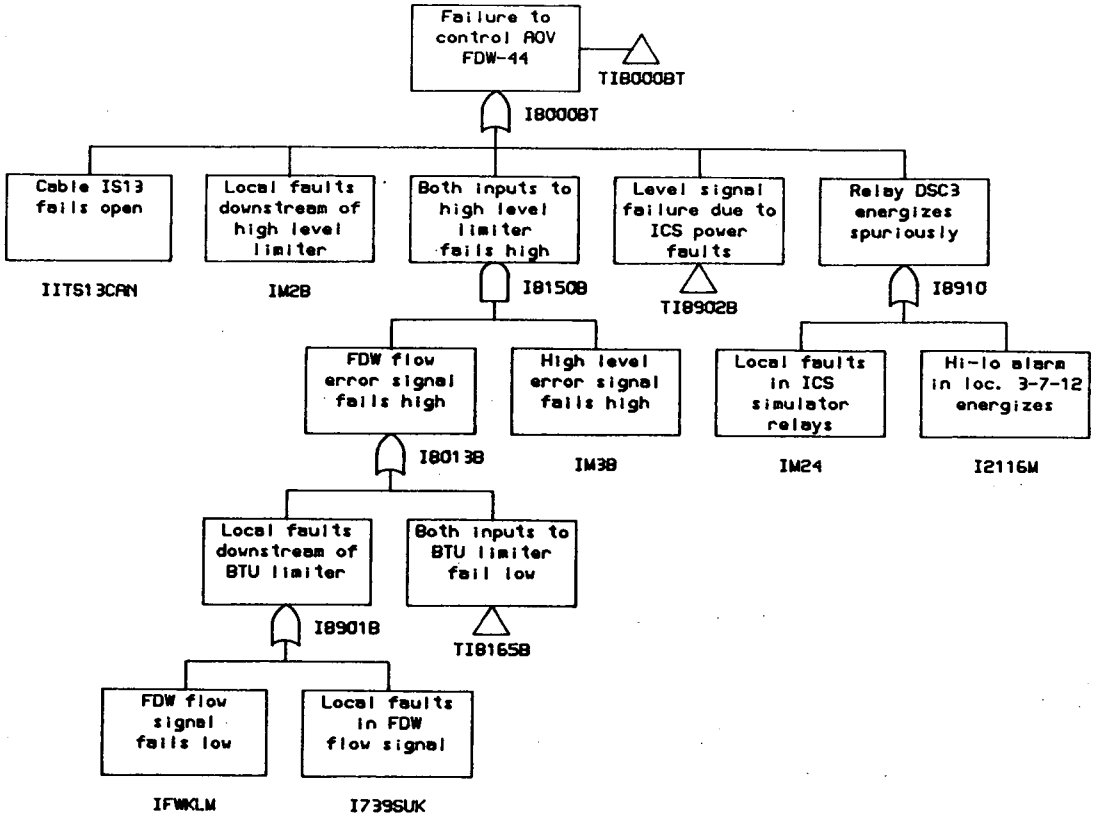

FIGURE 9.4-2 (CONTINUED)

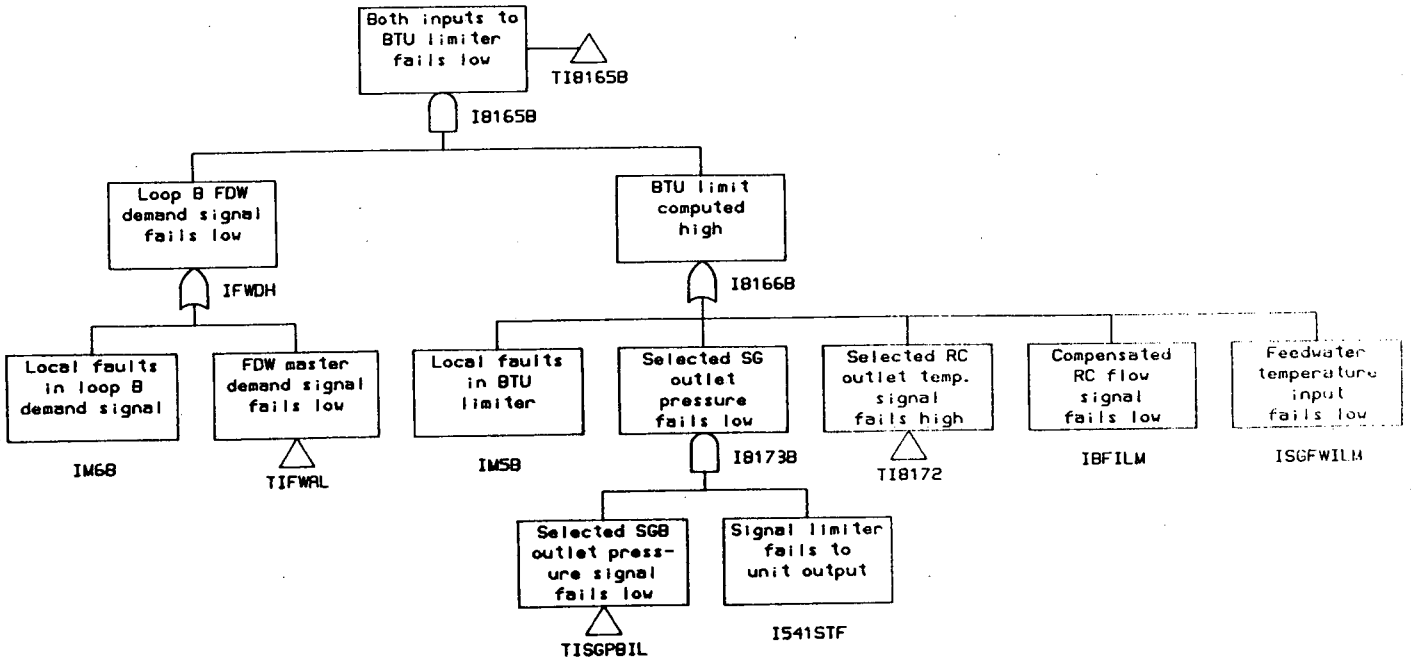

FIGURE 9.4-2. (CONTINUED)

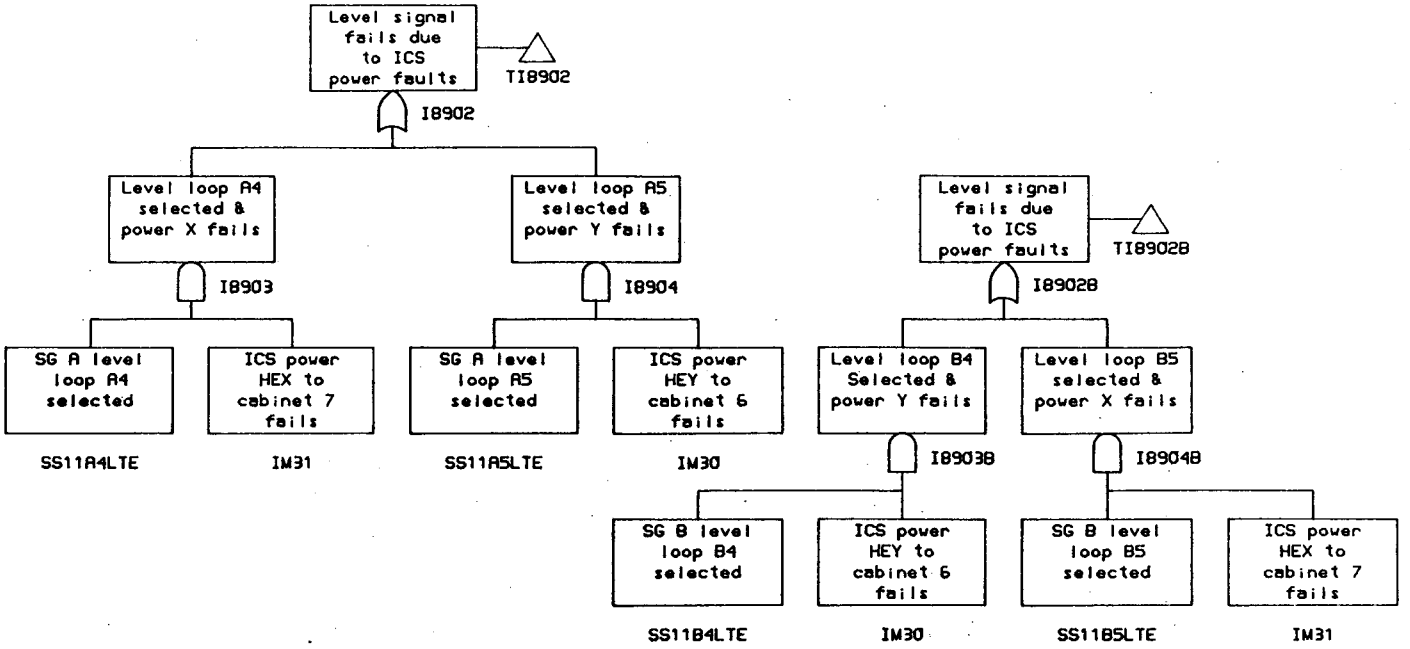

FIGURE 9.4-2. (CONTINUED)

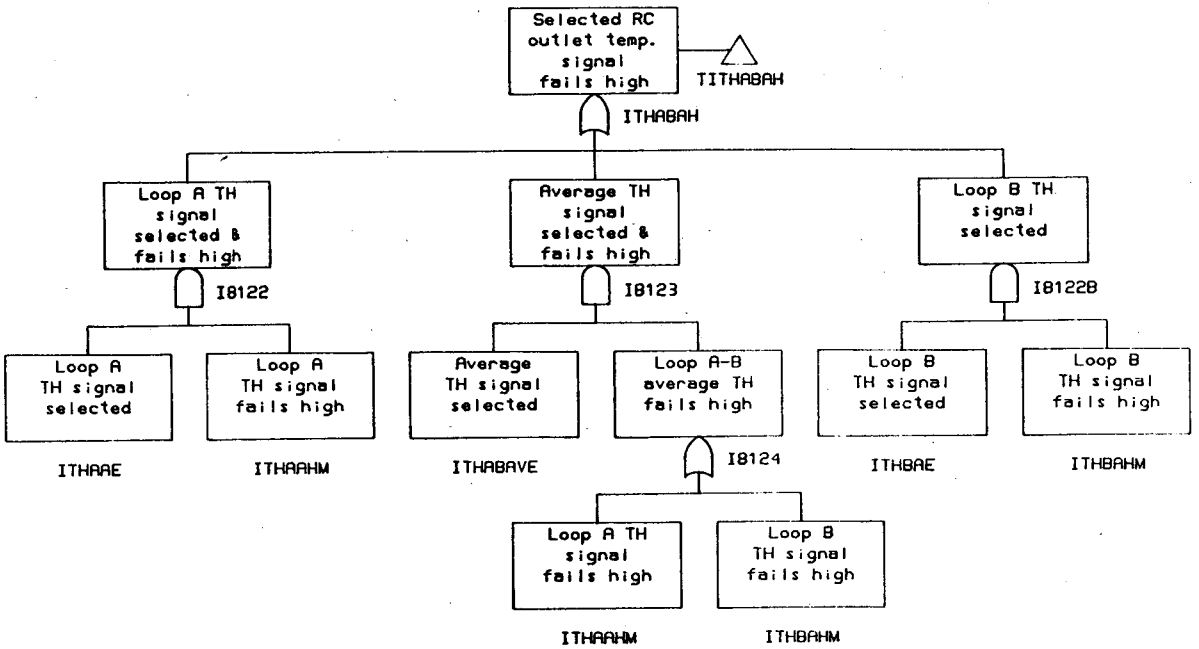

FIGURE 9.4-2. (CONTINUED)

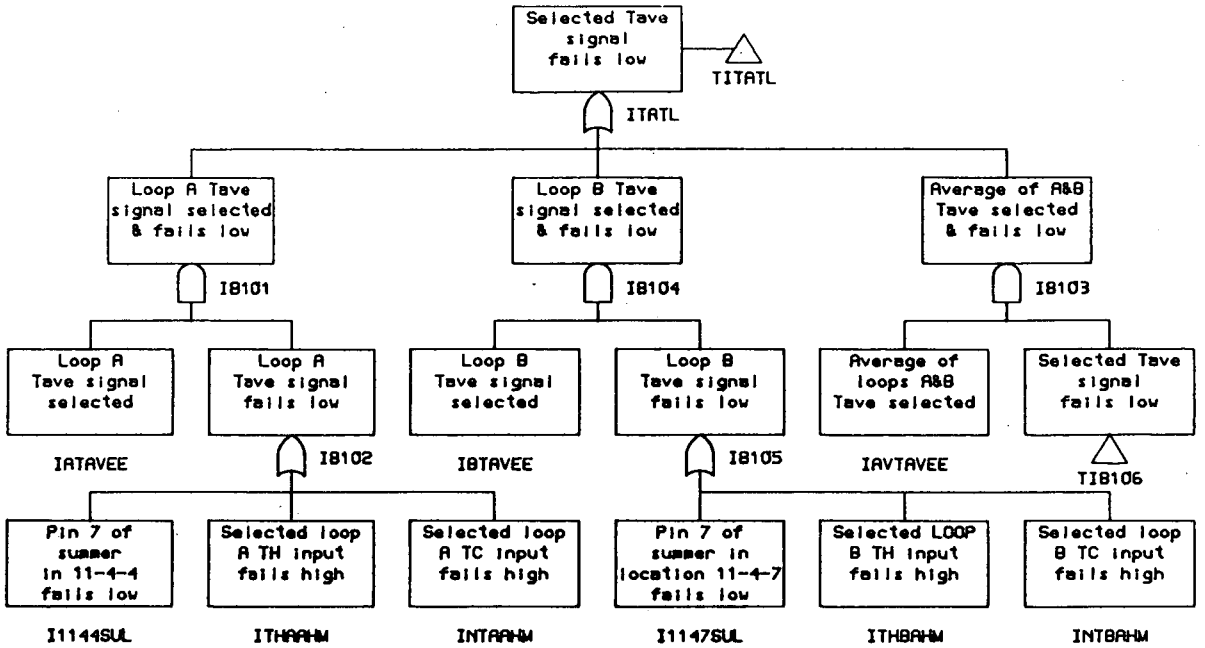

FIGURE 9.4-2 (CONTINUED)

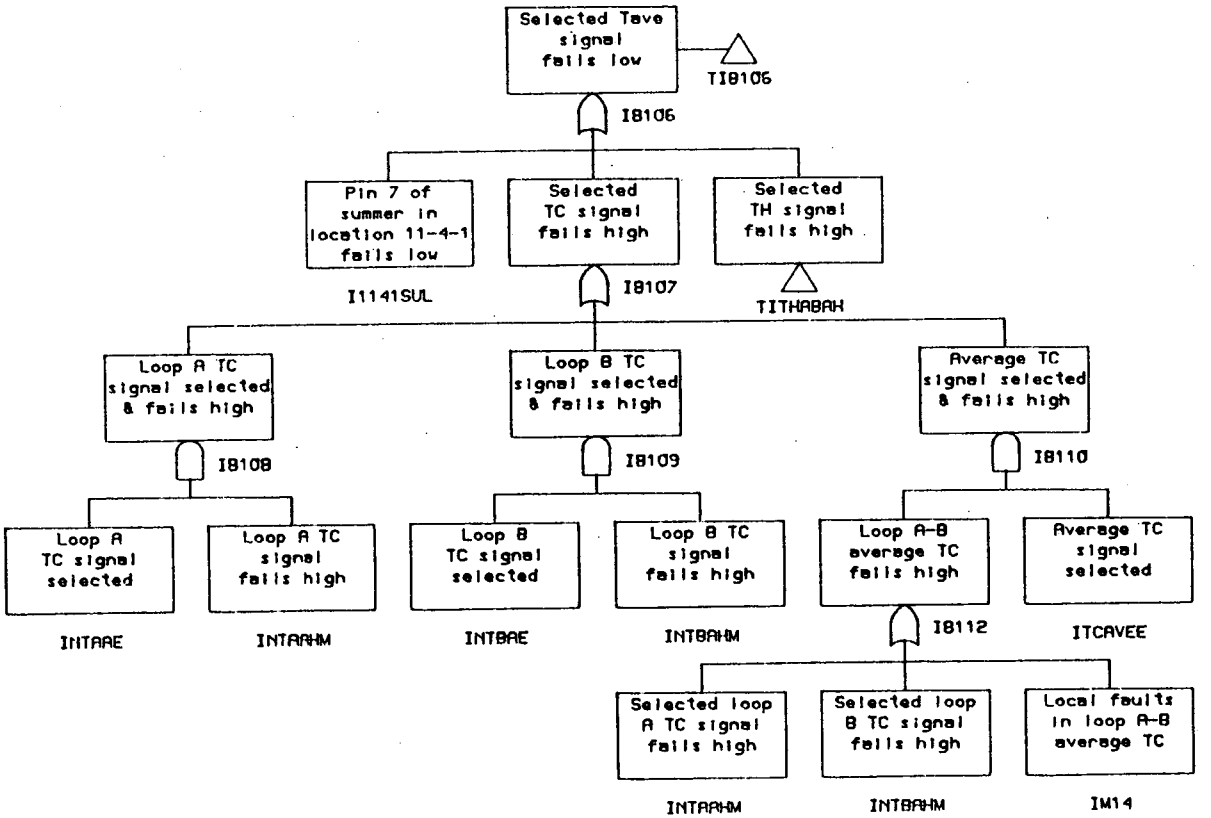

FIGURE 9.4-2 (CONTINUED)

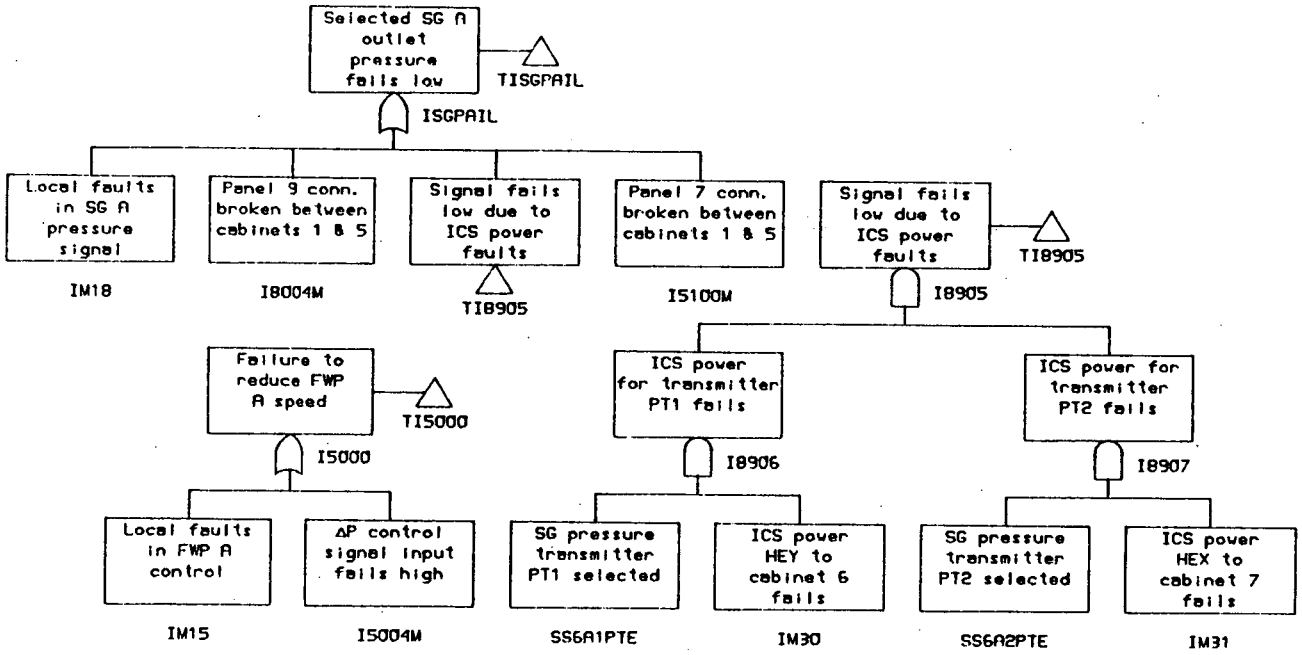

FIGURE 9.4-2. (CONTINUED)

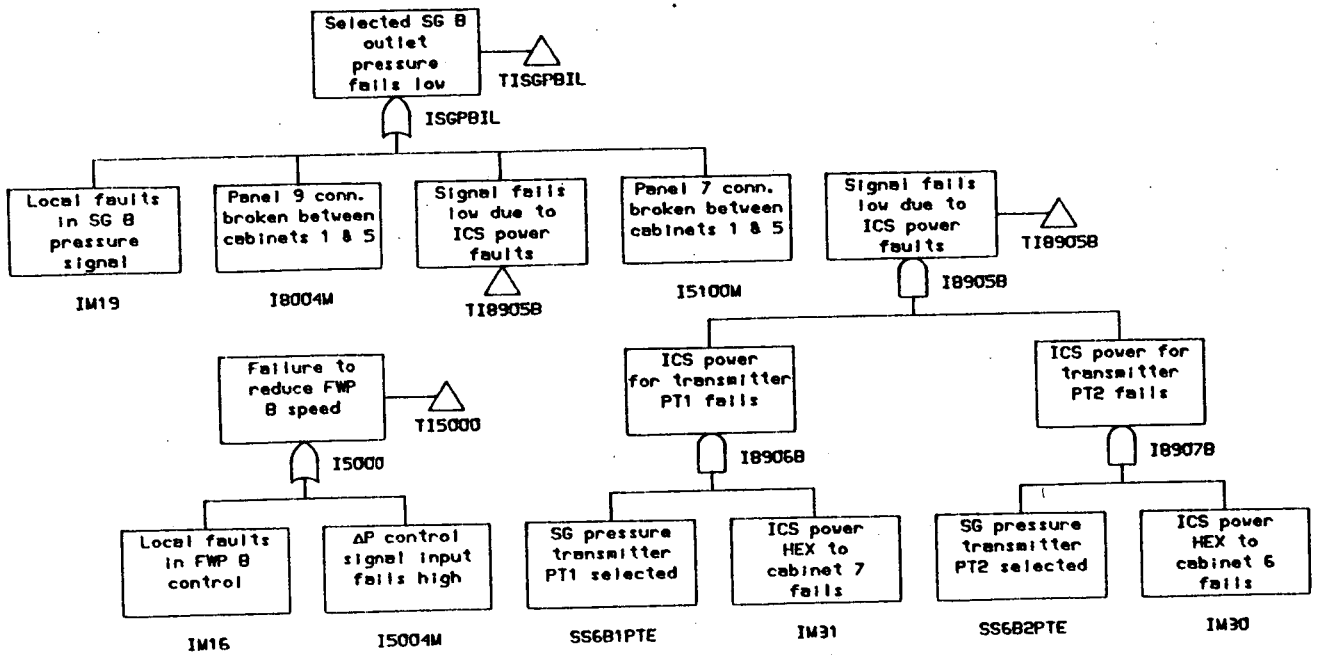

FIGURE 9.4-2 (CONTINUED)

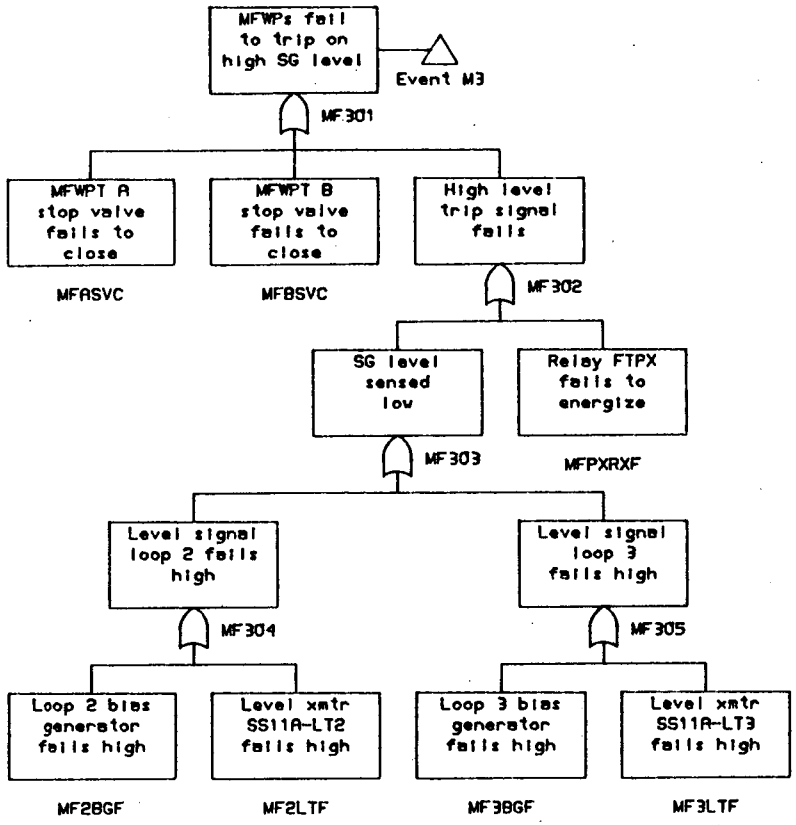

FIGURE 9.4-3 FAULT TREE DEVELOPMENT FOR FAILURE OF MAIN FEEDWATER PUMPS TO TRIP ON HIGH STEAM GENERATOR LEVEL.

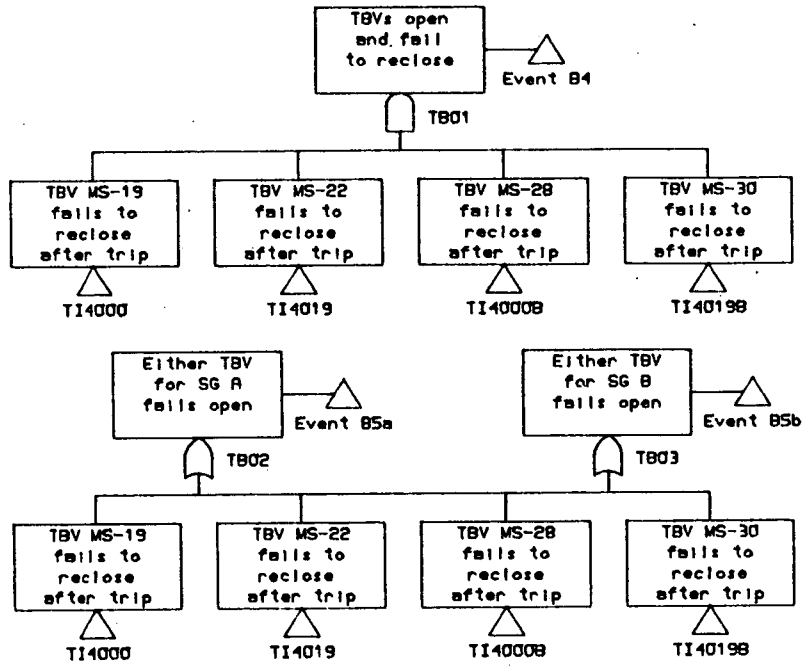

FIGURE 9.4-4 FAULT TREE DEVELOPMENT FOR FAILURE OF TBVs TO RECLOSE

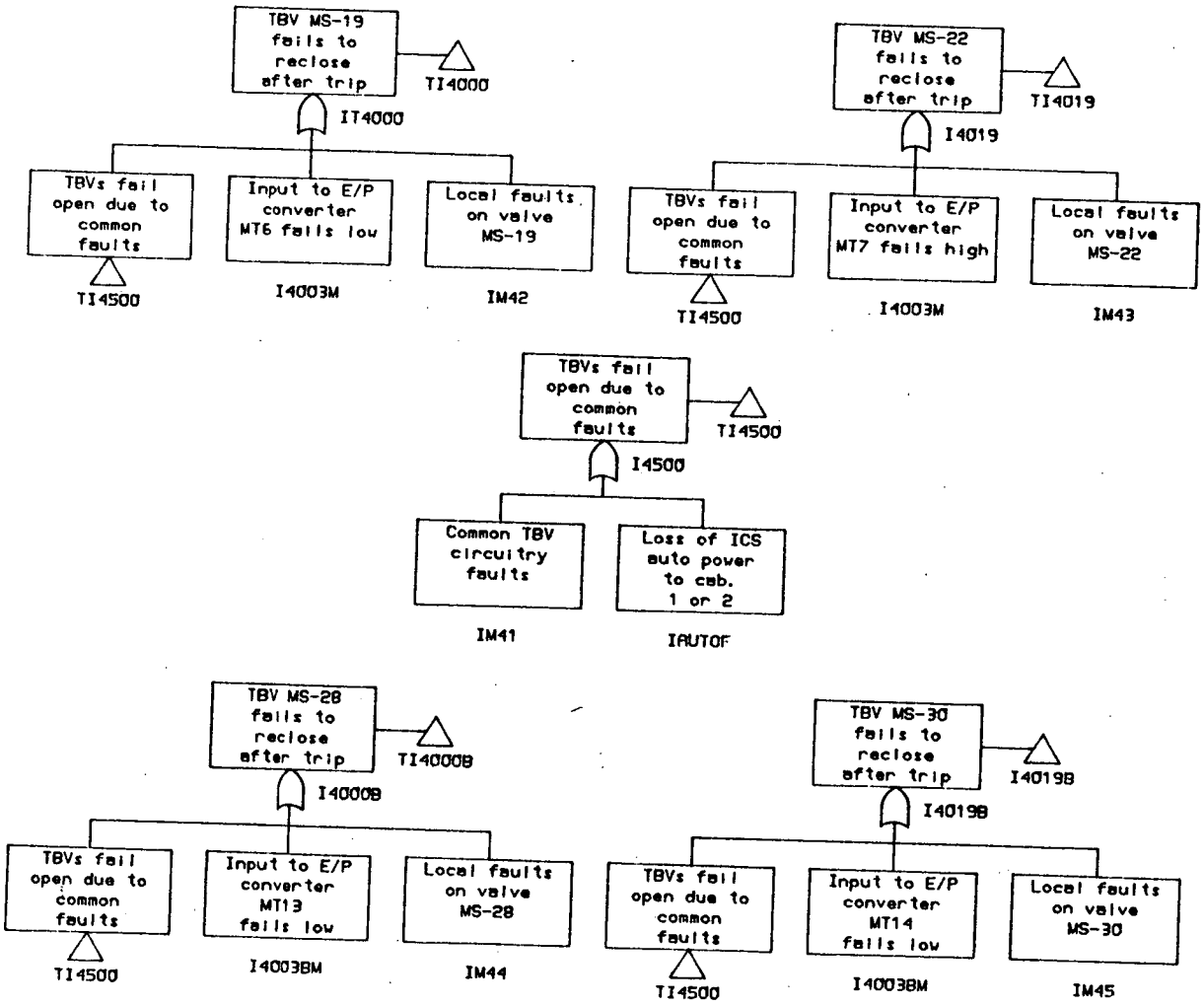

FIGURE 9.4-4 (CONTINUED)

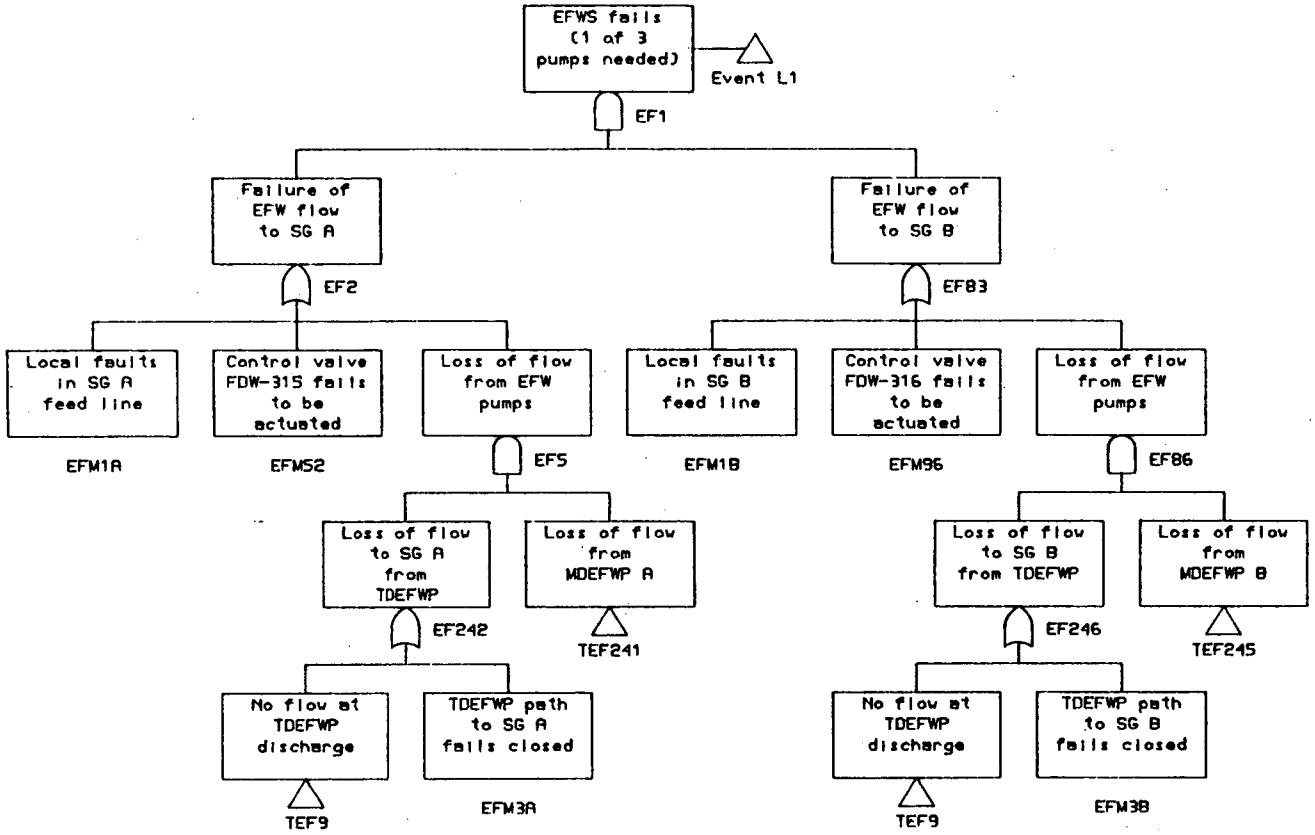

FIGURE 9.4-5 FAULT TREE DEVELOPMENT FOR FAILURE OF EMERGENCY FEEDWATER.

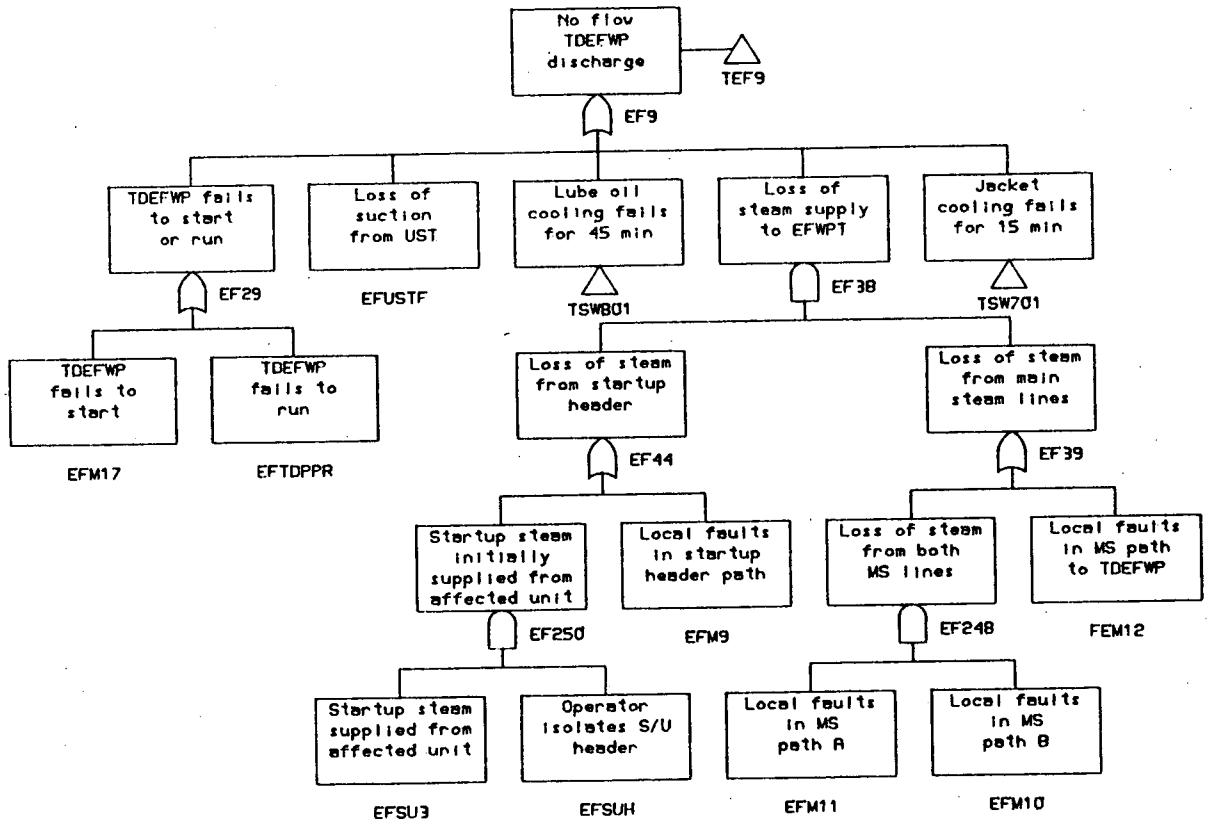

FIGURE 9.4-5 (CONTINUED)

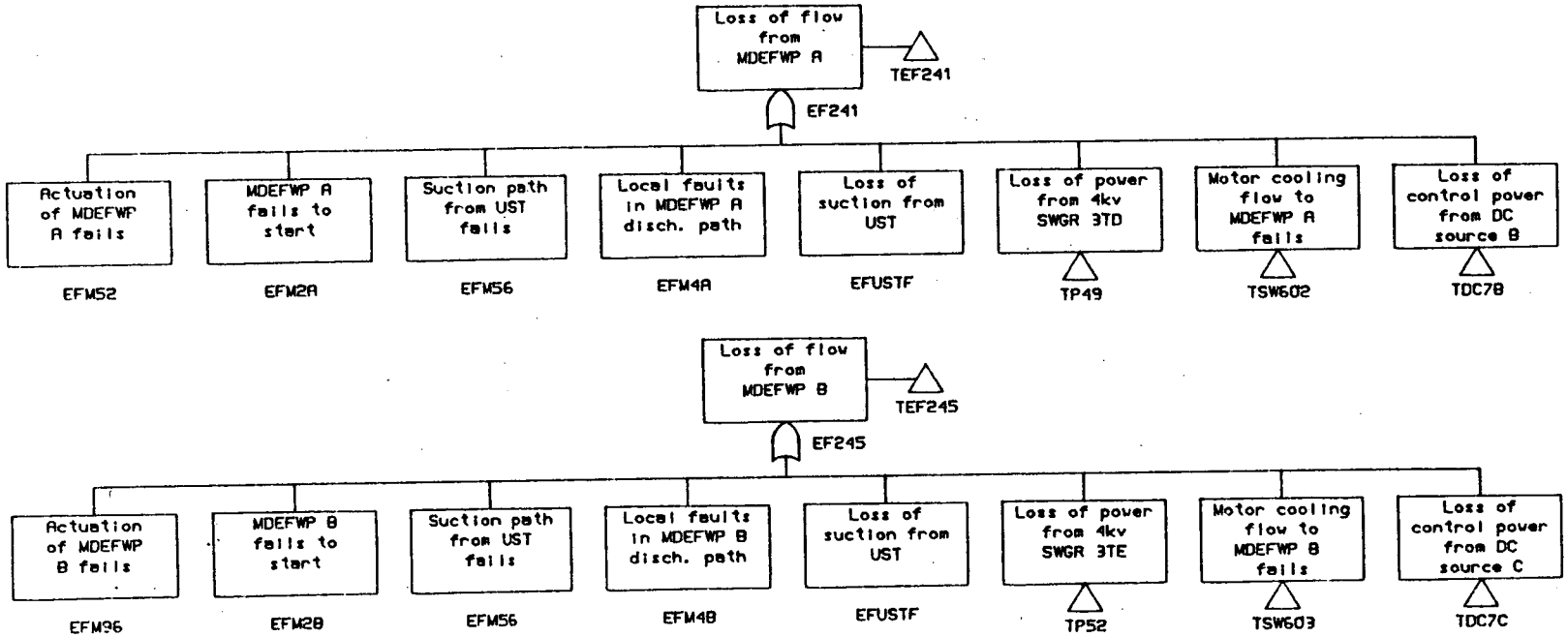

FIGURE 9.4-5 (CONTINUED)

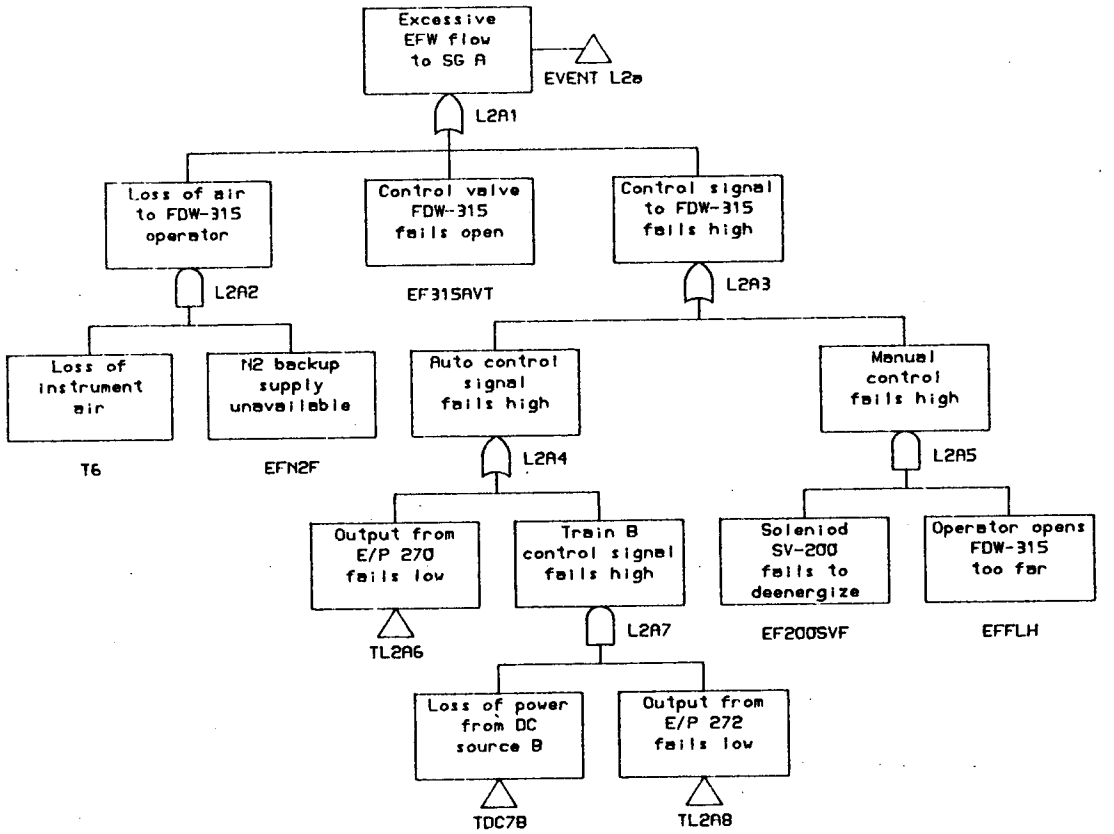

FIGURE 9.4-6 FAULT TREE DEVELOPMENT FOR EXCESSIVE EMERGENCY FEEDWATER FLOW.

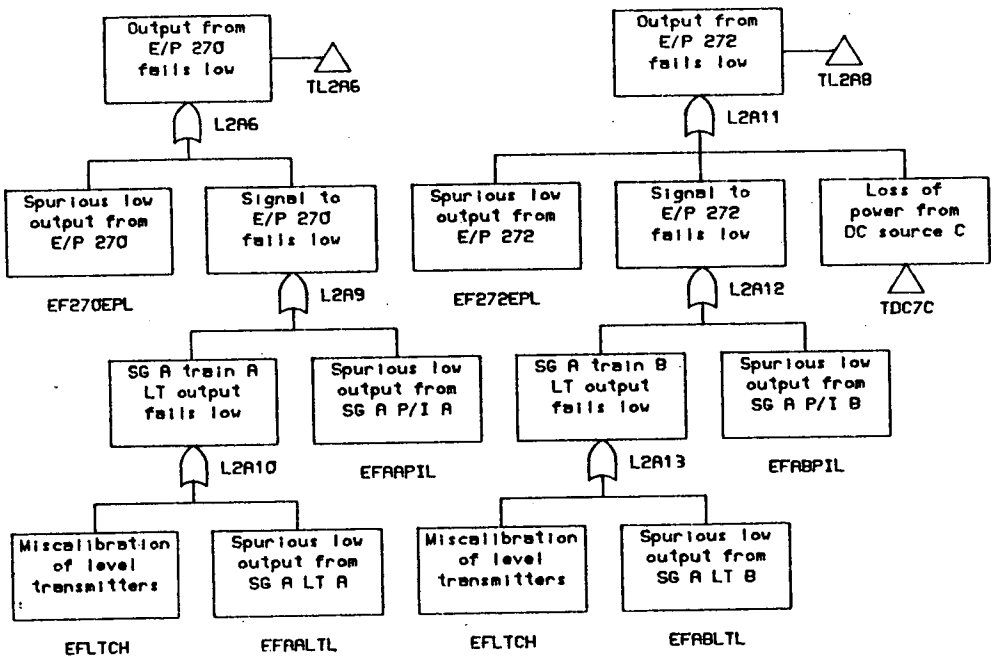

FIGURE 9.4-6 (CONTINUED)

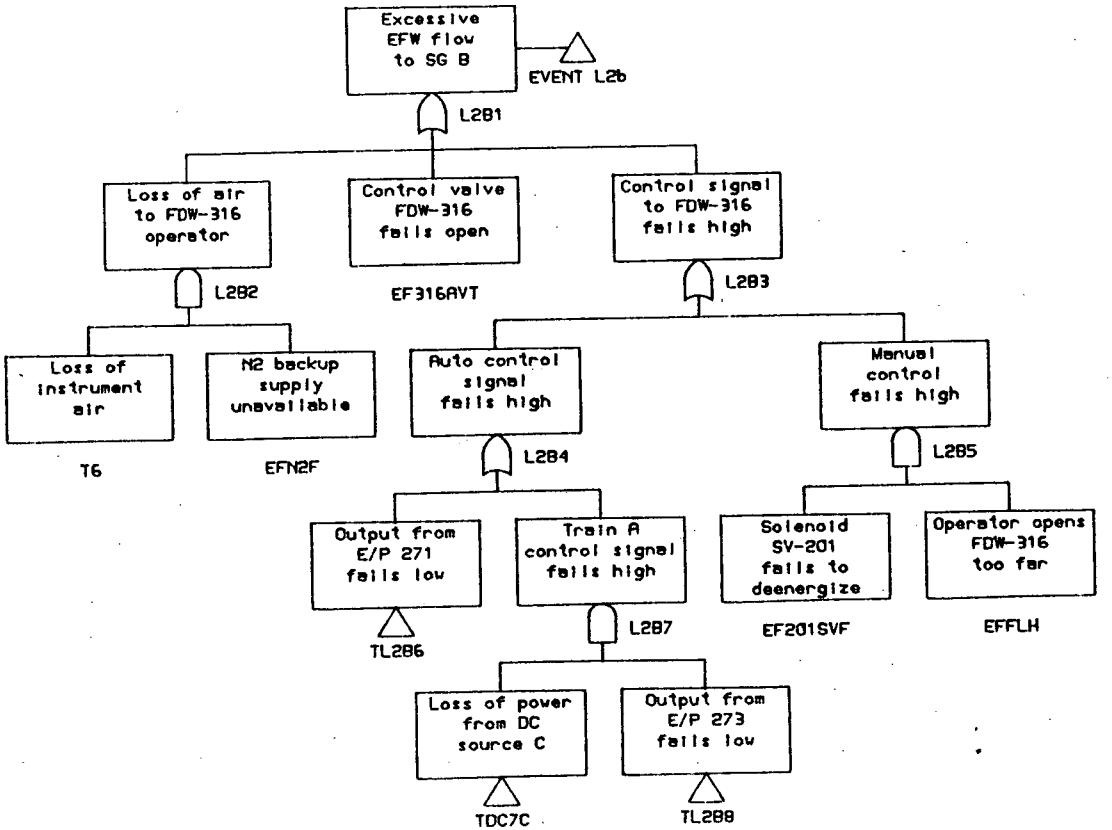

FIGURE 9.4-6 (CONTINUED)

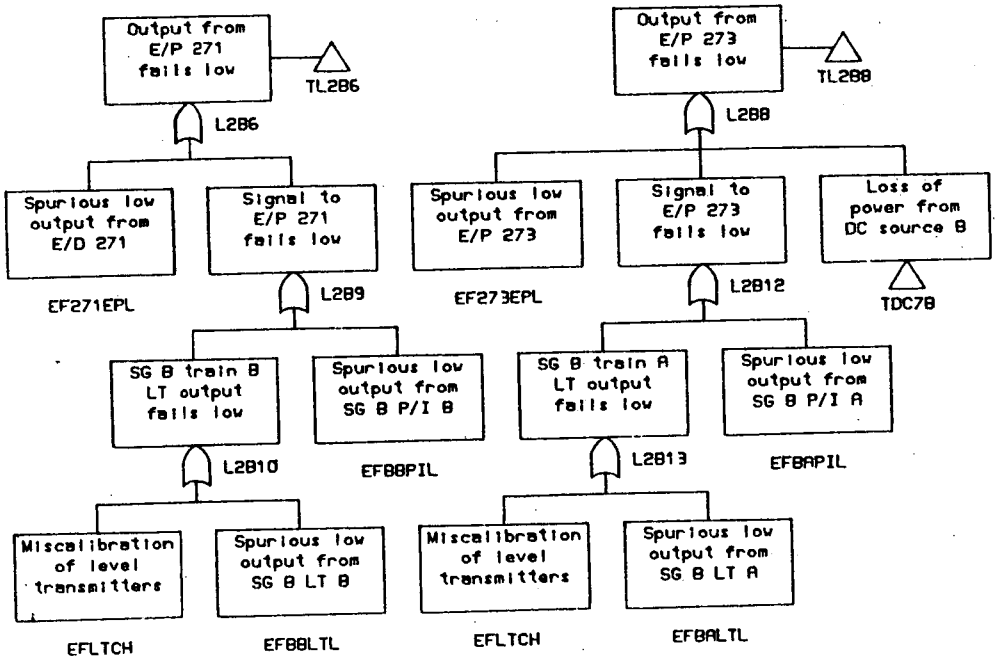

FIGURE 9.4-6 (CONTINUED)

10.0 SUMMARY AND CONCLUSIONS

10.0 SUMMARY AND CONCLUSIONS

10.1 Summary

The investigations and analyses described in this report were performed by Duke Power and Babcock and Wilcox to evaluate the regulatory concern associated with reactor vessel integrity for Oconee 1 following postulated pressurized thermal shock events. This analysis supplements that which was previously conducted in response to NUREG-0737, Item II.K.2.13 and submitted as BAW-1648, January 2, 1981 and is in response to the NRC letters dated August 21 and December 18, 1981.

These analyses were performed using state-of-the-art transient analyses, mixing calculations, material properties determination, and fracture mechanics analyses. In order to reduce the over-conservative nature present in generic calculations, this evaluation utilizes, to a significant degree, plant specific data. This is most evident in the overcooling transient analyses described in Chapter 2.0 and in the vessel material properties and fluence determination presented in Chapters 6.0 and 7.0. These data are realistic yet still conservative for Oconee 1.

The plant specific overcooling transient evaluations were obtained using the computer code RETRAN based specifically on the Oconee design. The plant specific materials data were obtained from the B&W Owners Integrated Reactor Vessel Materials Surveillance Program which was initiated in 1977. This program has provided and will continue to provide vessel materials data to support the adequacy of design of B&W manufactured reactor vessels.

The mixing calculations were based on conservative modeling techniques. The vessel wall thermal analyses utilized bulk fluid temperatures derived from the transient analyses and mixing calculations, and the basic heat transfer correlations to determine vessel wall temperature profiles for the vessel base metal as well as the beltline region welds.

Linear elastic fracture mechanics analyses were conducted utilizing the data obtained from the surveillance program and analytical technqiues based on ASME Code, Section XI, Appendix A. Thus, the results obtained for these severe postulated transients are based on techniques similar to those used for determining normal plant operating limits.

The postulated flaw sizes used in the analyses are conservative based on the 10-year ISI conducted during the summer of 1981 on the Oconee 1 reactor vessel. This examination showed that the existing flaws are smaller than those postulated in these analyses and are not service induced.

Analyses also have been performed on the frequency of severe RV thermal shock events utilizing data on the frequency of initiating events, analysis of system failures, and analysis of possible and necessary operator actions.

10.2 Conclusions

The results of the fracture mechanics analyses for the postulated small break loss of coolant accident indicate that with minimal downcomer mixing, no credit for mixing in the cold leg pipe, and without credit for warm-prestressing, the limiting weld (SA-1229) has an acceptable lifetime of 16 EFPY (1993). When warm-prestressing is used the postulated SBLOCA transient is no longer limiting. That is, an acceptable lifetime of 32 EFPY or greater is available. For overcooling transients due to secondary system upset, the limiting weld (SA-1430) has an acceptable life of 25 EFPY (2007).

Vessel failure is not calculated to result, even in the unlikely event that these postulated transients were to occur at these vessel lifetimes, since the acceptance criterion utilized in the fracture mechanics analysis is crack arrest within 1/4T (1/2T for WPS). Furthermore, the estimated frequency of occurrence of severe reactor vessel thermal shock events is approximately 10^{-4} per reactor year for Oconee. Therefore, the likelihood of reactor vessel failure due to pressurized thermal shock events is acceptably small for Oconee 1.

In order to reaffirm the validity of these results, continued monitoring of reactor vessel materials, as required by 10CFR 50, Appendices G and H is necessary. The B&W Owners Integrated Reactor Vessel Surveillance Program fulfills this need.

In view of these results, plant changes such as an increase in BWST water temperature, additional control systems to reduce thermal shock severity, or additional fuel management changes to further reduce neutron radiation damage, or even in place annealing to recover RPV toughness are not considered to be necessary at this time to assure safe operation of Oconee 1 through the design life of the plant.

REFERENCES

REFERENCES

1. BAW-1511P, "Irradiation-Induced Reduction in Charpy Upper-Shelf Energy of Reactor Vessel Welds," October 1980, submitted by B&W letter dated March 12, 1981 and docketed by Duke letter dated March 23, 1981.

2. BAW-1648, "Thermal-Mechanical Report - Effect of HPI on Vessel Integrity for Small Break LOCA Event with Extended Loss of Feedwater," November 1980, submitted by Duke letter dated January 2, 1981.

3. J. J. Mattimoe (SMUD) letter to H. R. Denton dated May 12, 1981 on behalf of the B&W Owners Group.

4. W. O. Parker letter to H. R. Denton dated May 22, 1981.

5. W. O. Parker letter to H. R. Denton dated December 2, 1981.

6. H. Schlichling; Boundary Layer Theory; Permagon Press; First Edition; 1955.

7. J. J. Grella and G. M. Faeth; "Measurements in a Two-Dimensional Thermal Plume Along a Vertical Adiabatic Wall"; Journal of Fluid Mechanics (1975), Vol. 71.

8. P. H. Rothe, W. D. Marscher, and J. A. Block; Quick Look Data Report Fluid and Thermal Mixing in a Model Cold Leg and Downcomer with Vent Valve Flows; EPRI Project, RP347-1; October 1981.

9. B. D. Nichols, C. W. Hirt, and R. S. Hotchkiss; "SOLA-VOF: A Solution Algorithm for Transient Fluid Flow with Multiple Free Boundaries"; Los Alamos National Laboratory Report LA-8355 (1980).

10. C. W. Hirt and B. D. Nichols; "A computational Method for Free Surface Hydrodynamics"; ASME Pressure Vessels and Piping Conference; San Francisco, CA; August 12-15, 1980; Paper No. 80-C2/PVP-144; Journal of Pressure Vessel Technology, 103, 136 (1981).

11. F. W. Dittus and L. M. K. Boelter; University Publications in Engineering; (University of California); Volume 2, 1930.

12. G. C. Vliet and D. C. Ross; "Turbulent Natural Convection"; ASME Journal of Heat Transfer; November 1975.

13. G. J. De Salvo and J. A. Swanson; ANSYS Computer Code; Swanson Analysis Systems, Inc.; July 1979.

14. BIGIF; Fracture Mechanics Code for Structures; Failure Analysis Associates; December 1980.

15. BAW-1436, "Analysis of Capsule OCI-E, Duke Power Company, Oconee Nuclear Station Unit 1", submitted by Duke letter dated February 21, 1978.

16. BAW-10046A, Rev. 1, "Methods of Compliance with Fracture Toughness and Operational Requirements of 10 CFR 50, Appendix G", March 1976.

17. BAW-1485, "Pressure Vessel Fluence Analysis for 177-FA Reactors," June 1978.

18. Regulatory Guide 1.99, Rev. 1, "Effects of Residual Elements on Predicted Radiation Damage to Reactor Vessel Materials," April 1977.

19. W. N. McElroy, et al.; Surveillance Dosimetry of Operating Power Plants; HEDL-SA2546; October 16, 1981.

20. NPGD-TM-585; "PCRIT, Critical Pressure Calculation Linear Elastic Fracture Mechanics; November 1981.

21. PVRC Recommendations on Toughness Requirements for Ferritic Materials; PVRC Ad Hoc Group on Toughness Requirements; WRC-175; August 1972.

22. Improved Evaluation of Nozzle Corner Cracking; EPRI; NP-339; March 1977.

23. G. D. Whitman and R. H. Bryan; "Heavy-Section Steel Technology Program Quarterly Progress Report for October - November 1980; NUREG/CR-1944.

24. Oconee PRA - to be published in Spring of 1982.

25. A. D. Swain and H. E. Guttman, "Handbook of Human Reliability Analysis with Emphasis on Nuclear Power Plant Applications," NUREG/CR-1278. Sandia Laboratories, April 1980.

26. Personal communication, T. U. Marston, Electric Power Research Institute, January 8, 1982.